WSE 2026

14th – 16th September 2026 – Riga, Latvia

# PROCEEDINGS

## 22nd Annual Meeting of the Northern European Network for Wood Science and Engineering

Riga, Latvia

14th-16th September 2026

WSE 2026

14th – 16th September 2026 – Riga, Latvia

# Proceedings of the 22nd Annual Meeting of the Northern European Network for Wood Science and Engineering (WSE 2026)

14-16 September 2026, Riga, Latvia

**Editors**

Edgars Kuka
Dace Cīrule
Kristīne Meile

**Cover design**

Monta Druviņa

Published with support from SNS – The Nordic Forest Research

SNS Nordic Forest Research

Nordic Council of Ministers

**ISBN**: 978-9934-8769-6-7

**Publisher**: Latvijas Valsts koksnes ķīmijas institūts (Latvian State Institute of Wood Chemistry)

Riga, 2026

**Title**

Proceedings of the 22nd Annual Meeting of the Northern European Network for Wood Science and Engineering (WSE 2026)

14-16 September 2026, Riga, Latvia

**Local organizers**

LATVIAN STATE INSTITUTE OF WOOD CHEMISTRY

Latvian State Institute of Wood Chemistry

RTU

Riga Technical University

**Sponsors and supporters:**

Latvijas Finieris

Latvijas Finieris

am2 arxada

AM2/Arxada

KOPPERS PROTECTING WHAT MATTERS PRESERVING THE FUTURE

Koppers Performance Chemicals

ZAZA TIMBER

ZAZA TIMBER

Latvijas Koks

Latvijas koks

RIGA

Riga Investment and Tourism Agency

## National Coordinators for the Northern European Network for Wood Science & Engineering:

| | |
|---|---|
| Erik Larnøy | Norway |
| Magnus Wålinder | Sweden |
| Tuula Jyske | Finland |
| Jaan Kers | Estonia |
| Edgars Kuka | Latvia |
| Emil Engelund Thybring | Denmark |
| Vaida Jonaitiene | Lithuania |
| Christian Brischke | Northern Germany |
| Dan Ridley-Ellis | Northern UK |
| Bartłomiej Mazela | Poland |

## WSE 2026 organising committee:

| | |
|---|---|
| Kristine Meile (Chair) | Latvian State Institute of Wood Chemistry |
| Edgars Kuka | Latvian State Institute of Wood Chemistry |
| Bruno Andersons | Latvian State Institute of Wood Chemistry |
| Dace Cirule | Latvian State Institute of Wood Chemistry |
| Anda Fridrihsone | Latvian State Institute of Wood Chemistry |
| Daniela Godina | Latvian State Institute of Wood Chemistry |
| Lotars Vasiljevs | Latvian State Institute of Wood Chemistry |
| Monta Druvina | Latvian State Institute of Wood Chemistry |
| Karīna Orlova | Latvian State Institute of Wood Chemistry |
| Uģis Cābulis | Latvian State Institute of Wood Chemistry |
| Liva Pupure | Riga Technical University |
| Laima Barbane | Riga Technical University |

# Preface

Climate change has introduced unexpected events and exposed us to inexperienced circumstances at various levels of our lives. We are in a situation where we must adapt to the new normal. These changes also put pressure on traditionally conservative industries to improve, innovate, and discover new, more efficient, safe, and sustainable ways of working. Those who do not change or adapt promptly will struggle and may not be able to recover. The only way to handle these changes and to adapt is to take action and do it now. This is particularly important for the forestry and wood industry at a time when the use of wood resources is experiencing a renaissance. Everyone, from scientists and enthusiasts to entrepreneurs, practitioners and leaders, has a crucial role to play. Fortunately, most of them are highly motivated and possess in-depth knowledge. However, it is not possible to overcome these climate challenges by yourself. Therefore, communication, networking and the exchange of experiences between truly motivated people are the key for moving forward.

The **22nd Annual Meeting of the Northern European Network for Wood Science and Engineering (WSE 2026)** gathers young and experienced scientists, enthusiasts, entrepreneurs, practitioners, and leaders to communicate, to take action, and to share the latest finding in the field of wood science and technology addressing the pressing challenges of our time. This year's thematic — **The life of wood in an ever-changing world** — is focused on how we can adapt the growth, the use, and the end-of-life of wood to be prepared, to manage, and to mitigate the challenges and unpredictable events introduced by the climate change. The initial stages of wood "life" affects its characteristics (strength, structure, interaction with moisture, quality, etc.), where in the later stages we have to adapt to them or even change them to obtain desired properties (bio-durability, surface properties, moisture resistance, etc.), which can meet the requirements of the current and future service conditions. It is crucial that before the end of "life", the wood is managed according to the principles of the circular bioeconomy (reuse, recycling, etc.) and remains in service as long as possible. However, challenges persist as the wood has accumulated "contributions" from all previous stages of its "life". These are the aspects we all share in this book.

The Northern European Network for Wood Science and Engineering (WSE) was established in 2004 with the vision of fostering collaboration among researchers, institutions, and industry representatives in the fields of wood science and engineering. Over the past two decades, the network has grown into a well-recognized platform for early-career researchers and senior scientists to exchange ideas and present the latest findings. With 21 successful annual meetings hosted across 10 different partner countries, WSE has consistently provided opportunities for advancing knowledge and strengthening connections across Nordic European Countries and beyond.

This year we warmly thank more than 130 participants from 19 countries, the sponsors, the coordinators and the organizers who have made the WSE 2026 possible. Your contributions expressed in 57 oral presentations and 31 posters of excellent research let us believe that WSE remains a growing, vibrant, forward-looking network with committed and enthusiastic people. We hope that the event gave you inspiration for new ideas and collaborations supporting sustainable and manageable future.

**Edgars Kuka**
- Coordinator of Latvia within the WSE Network -

## Contents

# SESSION 1:
# STRUCTURAL MATERIALS

# Bending Performance of Adhesive-Free Dowel-Laminated Timber: A Parametric Study

**Inayat Ullah Khan[1], Mahbube Subhani[2], Kazem Ghabraie[1], Mahmud Ashraf[1]**

[1]School of Engineering, Deakin University, Waurn Ponds, Geelong, VIC 3216, Australia, inayat.khan@deakin.edu.au, k.ghabraie@deakin.edu.au, mahmud.ashraf@deakin.edu.au,
[2]Division of Structural Engineering, Department of Architecture and Civil Engineering, Chalmers University of Technology, Sweden, mahbube@chalmers.se

## Background

Dowel-laminated timber (DLT) is an adhesive-free mass timber system offering recyclability, reusability, and ease of disassembly, making it compatible with circular bioeconomy principles. Load transfer is governed by wooden dowels rather than adhesives or metallic connectors, producing distinct stiffness characteristics, stress distributions, and failure mechanisms that require dedicated assessment (Khan et al. 2025a, 2026a). Although DLT research has predominantly focused on softwood systems, hardwood and hybrid DLT remain largely unexplored (El-Houjeyri et al. 2019; Sotayo et al. 2020). Australian construction relies heavily on plantation softwoods, while abundant hardwood resources remain underutilised in engineered wood products (EWPs) due to processing and bonding challenges. Adhesive-free DLT provides an alternative pathway for incorporating hardwoods, enabling value-added utilisation of low-grade resources while reducing pressure on softwood supply (Khan et al. 2025b). This study investigates the bending behaviour of hybrid softwood-hardwood DLT through advanced finite element modelling in LS-DYNA (MAT-143). Parametric analyses evaluate the effects of timber grade combination, layer arrangement, dowel spacing, dowel diameter, dowel strength, and loading direction. Two configurations are considered: in-plane DLT (IDLT), comprising edgewise-connected laminations, and out-of-plane DLT (ODLT), comprising flatwise-loaded laminations. The study addresses the absence of hybrid DLT research using Australian timber species and the lack of comparative assessment of IDLT and ODLT systems under identical loading conditions, providing insights into efficient utilisation of low-grade hardwood resources in adhesive-free mass timber construction.

**Keywords:** dowel-laminated timber, hybrid timber, bending behaviour, finite element modelling, LS-DYNA, MAT-143.

## Experimental Program and Numerical Modelling

Hybrid DLT beams were manufactured from radiata pine and spotted gum laminations connected using Tasmanian oak dowels. Four-point bending tests were conducted in accordance with AS/NZS 4063.1 (AS/NZS 4063.1 2010). Beams comprised three 30 mm laminations, giving a 90 × 90 mm cross-section, 1700 mm length, and 1500 mm span. The experimental setup is shown in Figure 1a. Material properties of Tasmanian oak dowels, radiata pine, and spotted gum can be found in (Khan et al. 2025c, 2026c, b).
Experimental results were validated using LS-DYNA with MAT-143. Following model calibration, hybrid combinations of F-grade timbers were analysed to establish equivalent GL stress grade limits. Material properties were assigned from F-grade characteristic values specified in AS 1720.1 (AS 1720.1 2010). Parametric analyses evaluated timber grade combination, layer arrangement, dowel spacing, dowel diameter, dowel strength, and

loading direction. To assess the upgrading potential of low-grade resources, F5 timber, characterised by lower stiffness, strength, and dimensional stability, was combined with higher-grade F27 and F34 timber. The numerical model geometry is shown in Figure 1b.

## Results and Discussion

Numerical results (Figure 1c-d) demonstrate the upgrading potential of low-grade F5 timber through hybridisation. F27–F5 and F34–F5 combinations containing up to 50% F5 achieved approximately DL13 stress grade, with MOE and modulus of rupture (MOR) decreasing near-linearly as F5 proportion increased. GL grades are herein designated as DL grades for DLT. F34–F5 hybrids consistently outperformed F27–F5 hybrids due to the higher stiffness and strength of F34 laminations. Although simulations employed clear-wood properties and thus represent upper-bound behaviour, the findings indicate that strategic hybridisation can effectively utilise substantial proportions of low-grade timber while maintaining structural-grade performance in DLT applications.

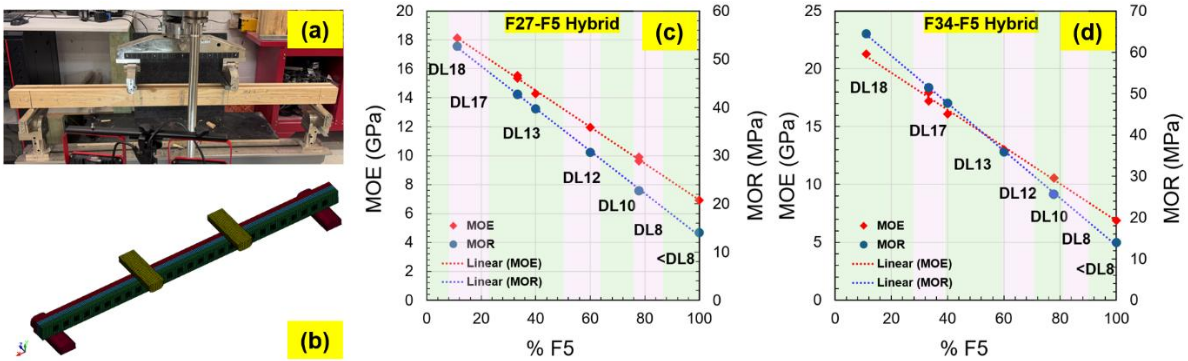


Figure 1. (a) Experimental IDLT bending test setup comprising a radiata pine core lamella and spotted gum side laminations; (b) numerical model geometry; (c) predicted grades of F27–F5 hybrid IDLT; and (d) predicted grades of F34–F5 hybrid IDLT under varying F5 proportions. F5% denotes the percentage of F5 material in the beam, with the remainder comprising F27 or F34. GL grades are herein designated as DL grades for DLT

## Conclusions

Hybrid IDLT demonstrates strong potential for upgrading low-grade F5 timber through load sharing, enabling substantially higher structural grades than individual F5 boards. In contrast, ODLT exhibited significantly lower bending performance due to partial composite action and interlayer slip, with limited improvement from reduced dowel spacing or increased dowel diameter and dowel strength. Ongoing work employs non-local finite element modelling to quantify strength reductions associated with crack initiation and propagation around dowel holes, governed by the low tension-perpendicular-to-grain strength of timber. Durability assessment was beyond the scope of this study and warrants future investigation before establishing the long-term performance of DLT relative to conventional engineered wood products.

**References**

AS 1720.1 (2010) Timber structures Part 1: Design methods

AS/NZS 4063.1 (2010) Characterization of structural timber, Part 1: Test methods

El-Houjeyri I, Thi V-D, Oudjene M, et al (2019) Experimental investigations on adhesive free laminated oak timber beams and timber-to-timber joints assembled using thermo-mechanically compressed wood dowels. Constr Build Mater 222:288–299. https://doi.org/10.1016/j.conbuildmat.2019.05.163

Khan IU, Subhani M, Ghabraie K, Ashraf M (2025a) Experimental and empirical study on the embedment behaviour of wooden and steel dowels in hardwood and softwood. Structures 82:110708. https://doi.org/10.1016/j.istruc.2025.110708

Khan IU, Subhani M, Ghabraie K, Ashraf M (2026a) Analytical framework for predicting stiffness in single wooden dowel timber-to-timber connections. Structures 91:112538. https://doi.org/10.1016/j.istruc.2026.112538

Khan IU, Subhani M, Ghabraie K, Ashraf M (2025b) Mechanical performance and design challenges of wooden fasteners: a critical analysis of evaluation methods and standards. Eur J Wood Wood Prod 83:143. https://doi.org/10.1007/s00107-025-02293-1

Khan IU, Subhani M, Ghabraie K, Ashraf M (2025c) Exploring and refining testing approaches for hardwood dowels under axial and flexural loading: an experimental and numerical study. Wood Mater Sci Eng 0:1–23. https://doi.org/10.1080/17480272.2025.2505135

Khan IU, Subhani M, Ghabraie K, Ashraf M (2026b) Experimental evaluation and theoretical prediction of single hardwood dowel connections in softwood and hardwood. Eng Struct 353:122251. https://doi.org/10.1016/j.engstruct.2026.122251

Khan IU, Subhani M, Ghabraie K, Ashraf M (2026c) Novel approaches for shear testing of wooden dowels parallel to the grain: an experimental and numerical study. Eur J Wood Wood Prod. https://doi.org/10.1007/s00107-025-02373-2

Sotayo A, Bradley DF, Bather M, et al (2020) Development and structural behaviour of adhesive free laminated timber beams and cross laminated panels. Constr Build Mater 259:119821. https://doi.org/10.1016/j.conbuildmat.2020.119821

# Influence of Wood Moisture Content on Coating Adhesion of Pine-Based Interior Building Elements under UV-LED and UV Mercury Curing

**<u>Arturs Dzenis</u>[1,2,3], Ainars Uzuls[1], Uldis Spulle[2,3]**

[1]"Kokpārstrāde 98" Ltd, Latvia;
[2]Institute of Civil Engineering and Woodworking, Latvia;
[3]Latvia University of Life Sciences and Technologies, Latvia.

**Abstract**

The performance and service life of coated wood products are strongly influenced by wood moisture content and the applied curing technology. For pine-based interior building elements, variations in moisture content can affect wood–coating interactions, adhesion quality, and process stability under industrial manufacturing conditions. This study investigates the influence of wood moisture content on coating adhesion by comparing ultraviolet mercury lamp (UV-Hg) curing with ultraviolet light-emitting diode (UV-LED) curing. The results contribute to improving the durability, resource efficiency, and long-term use of coated wood products under variable moisture conditions. Experimental investigations were carried out using profiled Scots pine (*Pinus sylvestris L.*) mouldings representing two macrostructural zones of wood heartwood and sapwood at different moisture content levels. Coating adhesion was evaluated using the cross-cut test method according to ISO 2409. The results demonstrated that the (UV-LED) curing system provides more stable and higher coating adhesion performance across a wider range of wood moisture content compared to the (UV-Hg) curing technology. The best adhesion performance was obtained for sapwood at moisture content of $10 \pm 0.5$ %. Overall, the findings indicate that UV-LED curing has strong potential for achieving reliable coating adhesion and stable surface quality under variable industrial processing conditions.

**Acknowledgements**

This work was supported according to contract No. 1.2.1.2.i.2/1/24/A/CFLA/001 between "Forest Sector Competence Centre of Latvia" Ltd. and the Central Finance and Contracting Agency which dated 05th July of 2024.

# Development of Rotary Peeling Parameters and Preconditioning Temperature for Thick Aspen Veneer Production

**Aleksandr Serebrennikov[1], Heikko Kallakas, Anti Rohumaa, Catherine Kilumets, Ignatius Kristia Adikurnia**

[1]Laboratory of Wood Technology, Department of Material and Environmental Technology, Tallinn University of Technology, Estonia: aleser@taltech.ee, heikko.kallakas@taltech.ee, anti.rohumaa@taltech.ee, catherine.kilumets@taltech.ee, ignatius.adikurnia@taltech.ee

## Background

The veneer industry relies mainly on high-value wood species such as birch (*Betula pendula*) and spruce (*Picea abies*). In contrast, the use of lower-value species remains limited. But rising prices for high-value wood are forcing the use of cheaper wood species. One of such species is the European aspen (*Populus tremula*). It's a pioneer wood species that spreads very quickly and rapidly occupies empty territories and the price is more than 2 times lower than birch (Statistikaamet, 2024). Usually, veneer, regardless of the species, is peeled with a thickness of 1-4 mm (Leggate et al., 2017). The aim of this work was to evaluate the practical possibility of peeling thick aspen veneer with the thickness up to 9 mm. Since it is known that increasing the thickness does not degrade the surface quality of the veneer (Hasan, 2021) and the use of low-temperature preconditioning can improve the surface quality (Tootsi, 2025; Dai and Wong,1996), a hypothesis was proposed that lowering the preconditioning temperature could improve the surface properties of thick aspen veneer. Investigating this area could lead to significant advances in veneer production, offering new opportunities for better utilization of raw materials in veneer-based composites.

**Keywords:** European aspen,  veneer, peeling speed, compression ratio, surface properties, temperature, thickness

## Experimental

The European aspen (*Populus tremula*) logs were used for the work, preconditioned using various temperatures (including snow storage). Parameters for rotary veneer peeling were developed and obtained using a Raute industrial peeling lathe. Experimental peelings were carried out using different preconditioning temperatures, peeling speeds, compression ratios, and veneer thicknesses (3, 6 and 9 mm). Surface roughness and contact angle were measured with Mitutoyo Surftest SJ-210 device with 90˚ 5 µm stylus and DataPhysics OCA 20, deionized water was used.

## Results and Discussion

Lower preconditioning temperature ranges resulted in lower surface roughness values for both the 3 mm (13.1 ± 4.9 compared with 20.0 ± 6.8 µm) and 6 mm (12.8 ± 3.5 compared with 19.1 ± 6.1 µm) veneer thicknesses. Similar trends are likely for the 9 mm thickness, although this still requires repeat peelings during more stable conditioning. Statistical analysis revealed that temperature is the most influential factor in roughness formation, followed by compression ratio and thickness. Two main trends were observed: lower temperatures and compression ratio reduce roughness. In the context of the contact angle, all parameters had an influence, and their influence decreased in the following order:

thickness, temperature, peeling speed, and compression ratio. Increasing the veneer thickness does not significantly alter the surface properties. The results were very similar for all three thicknesses (see Table 1).

Table 1. Comparison of average surface properties for different veneer thicknesses with references

| Type of veneer | **Surface roughness (Ra) [µm]** | **Contact angle 40s [˚]** |
|---|---|---|
| **3 mm aspen veneer in this study** | **16.4 (6.8)** | **75.1 (18.5)** |
| **6 mm aspen veneer in this study** | **15.9 (5.9)** | **65.0 (24.0)** |
| **9 mm aspen veneer in this study** | **16.4 (5.5)** | **81.1 (14.7)** |
| 1.5 mm aspen veneer (Rohumaa et al., 2021) | 23.3 (6.61) | 0.3 |
| 1.5 mm birch veneer (Rohumaa et al., 2021) | 11.1 (3.27) | 43.6 |
| 0.3 mm aspen veneer (Tootsi, 2025) | 8.2 (2.8) | 85.7 (13.0) |

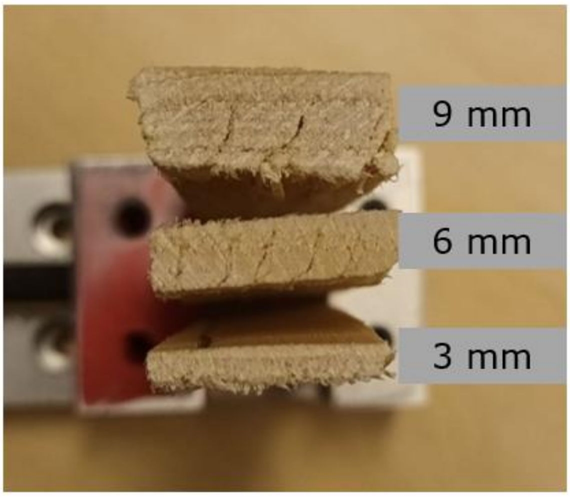


Figure 1. 3 – 6 – 9 mm aspen veneers

## Conclusions

The main outcome of this work is the development of peeling parameters and the actual working ability to peel veneer up to 9 mm. Preconditioning temperature is an important factor influencing the formation of surface properties for thick aspen veneers. Comparison of the average surface properties obtained for all three veneer thicknesses with previous work shows that the properties of the resulting veneer are comparable or better than the reference values. In addition, thick veneer offer potential for the development of new wood-based materials for the wood industry.

## References


Dai C, Wong J (1996) Optimization of peeling of aspen veneer using a 5/8" rotary bar.

Hasan M (2021) Effect of veneer thickness and surface roughness on shear bond strength with different adhesives. Master's thesis, Tallinn University of Technology, Tallinn.

Leggate W, McGavin RL, Bailleres H (eds) (2017) A guide to manufacturing rotary veneer and products from small logs. Australian Centre for International Agricultural Research, Canberra, ACT.

Rohumaa A, Kallakas H, Mäetalu M, Savest N, Kers J (2021) The effect of surface properties on bond strength of birch, black alder, grey alder and aspen veneers. *International Journal of Adhesion and Adhesives* 110: 102945.

Statistikaamet (2024) Development of the forestry, environmental subsidies and ecosystem accounts. Methodological report. Tallinn.

Tootsi K (2025) Enhancement of Thin Aspen Veneer Quality in Rotary Peeling. Master's thesis, Tallinn University of Technology, Tallinn.

# Shear Behaviour of Adhesive and Mechanical CLT-GLT Connections in Ribbed Timber Panels

**Elza Briuka**[1, 2], **Dmitrijs Serdjuks**[2], **Jānis Šliseris**[3]

[1]CLT Profi SIA, Jelgava, Latvia, elza@cltprofi.com, [2,3]Institute of Civil Engineering, Riga Technical University, Riga, Latvia, elza.briuka@rtu.lv, Dmitrijs.Serdjuks@rtu.lv, Janis.Sliseris@rtu.lv

## Background

Ribbed cross-laminated timber (CLT) panels, combining a CLT flange with glued-laminated timber (GLT) ribs, offer a high strength-to-weight ratio and reduced material use compared with solid CLT panels, and are a promising basis for future timber-concrete composite (TCC) ribbed floors. Their performance depends strongly on the flange-to-web connection, which must transfer shear forces so the panel acts as a composite member.
Connections can be realised mechanically, using metal plates and screws, or adhesively, using structural polyurethane adhesives. Mechanical connectors are ductile and practical to assemble but transfer load through localised contact, limiting stiffness; adhesive joints distribute stress over the full bonded area, giving higher stiffness but a more brittle failure.
Previous work has shown the need for reliable connection data and numerical modelling (Kleinhenz et al. 2023; Briuka et al. 2024; Serdjuks et al. 2025; Hull et al. 2024), but a validated comparison of adhesive and mechanical flange-to-web connections is still missing. This paper addresses that gap for ribbed CLT and future TCC panels.

**Keywords:** Cross-laminated timber, connection, FEM, timber-concrete composite, hybrid systems.

## Experimental

Fifteen ribbed CLT-GLT specimens were prepared in five groups of three, each a CLT flange (three or five layers, 600 × 600 × 100 mm) with a GLT rib (GL24h, 600 × 600 × 100 mm). One group used a Rothoblaas SHARP501200 steel plate and screws (ETA-24/0058); the rest used LOCTITE HB or LOCTITE HB XE polyurethane adhesive with structural timber screws, fastened from either the CLT flange or GLT rib side. Specimens were tested at the Latvian University of Biosciences and Technology on a FORM+TEST Alpha 10-3000 machine under concentrated loading until failure or a 15 mm displacement limit.

## Numerical modelling

Detailed non-linear finite element (FE) models of all groups were developed in Verisim4D.
Model results were compared with the experimental load-displacement curves and maximum load-carrying capacities to assess the ability of the FE approach to predict connection response.

## Results and Discussion

Table 1 illustrates experimental mean load bearing capacity reached in each specimen group.

Table 1. Summary of specimen groups and mean load-carrying capacities

| Group | Connection system/ screw direction | Collapse load, kN |
|---|---|---|
| SHARP501200 | Rothoblaas steel plate, screws from CLT side | 39.35 |
| LOCTITE HB 1 | Polyurethane adhesive, screws from CLT side | 187.77 |
| LOCTITE HB 2 | Polyurethane adhesive, screws from GLT side | 198.89 |
| LOCTITE HB XE 1 | Polyurethane adhesive, screws from CLT side | 140.01 |
| LOCTITE HB XE 2 | Polyurethane adhesive, screws from GLT side | 180.01 |

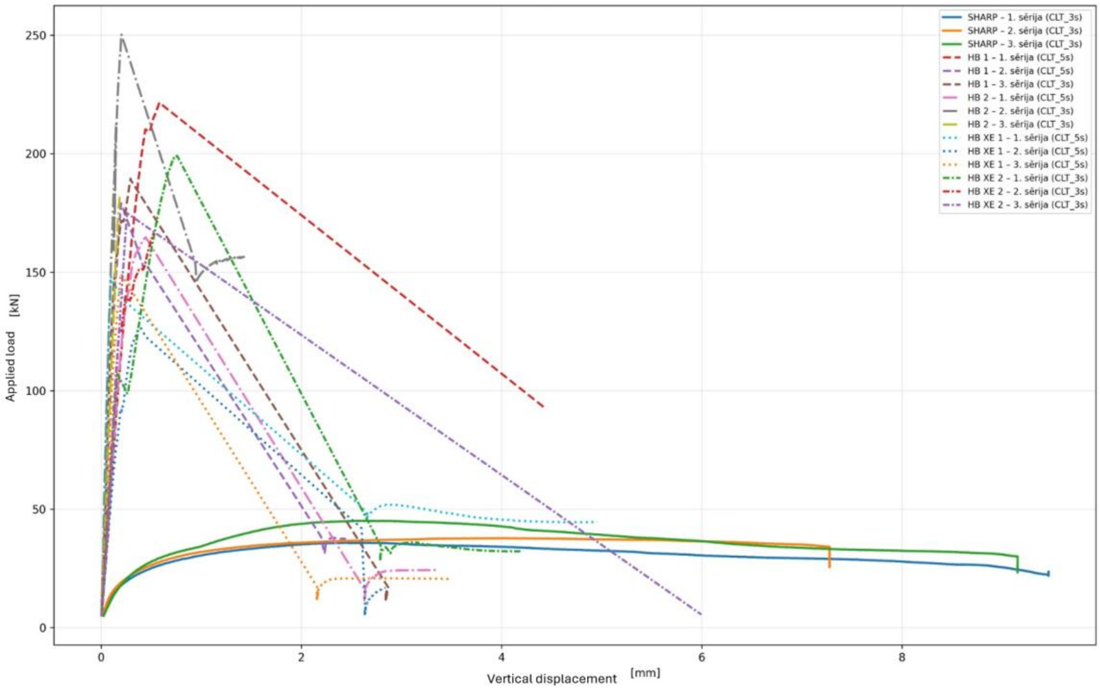


Figure 1. Load-displacement graph for all tested specimens

The highest mean capacity was obtained for LOCTITE HB 2, where screws were installed from the GLT rib side.

## Conclusions

Adhesive CLT-to-GLT flange-to-web connections provided substantially higher shear capacity than the investigated mechanical metal plate connection, while mechanical connection behaviour was more gradual after peak load. Screw installation from the GLT rib side improved performance in the paired adhesive configurations and is relevant for manufacturing and design. The results provide connection data for efficient ribbed CLT panels and a basis for future timber-concrete composite ribbed floor systems.

**References**

Briuka E, Serdjuks D, Akishin P, Sahmenko G, Podkoritovs A, Ozolins R (2024) Behaviour analysis of beam-type timber and timber-concrete composite panels. Applied Sciences 14(16): 7403.

Hull T, Ackerman P, Lacroix D (2024) Development of a glue bonded shear connection aimed for mass timber composites. International Wood Products Journal. https://doi.org/10.1177/20426445241284954.

Kleinhenz M, Viertel M, Demschner T, Frangi A (2023) Determination of the effective width of cross-laminated timber rib panels using digital image correlation. In: Proceedings of the 13th World Conference on Timber Engineering, WCTE 2023: 2416-2425.

Serdjuks D, Rogainis A, Briuka E, Sliseris J, Pakrastins L, Lapkovskis V (2025) Influence of timber-to-concrete connection types on the behaviour of timber-concrete composite structures. Journal of Composites Science 9(11): 593.

# Glue-Free Bamboo Joints Produced by Linear Vibrational Welding

**Ian Vulcanescu[1], Mojgan Vaziri[2]**

[1]KTH Royal Institute of Technology, Sweden, ianv@kth.se
[2]KTH Royal Institute of Technology, Sweden, mojgan.vaziri@ltu.se

## Background

To reduce the use of abiotic components in engineered wood products, this research explores the potential for producing bamboo panels without synthetic adhesives. Wood welding involves joining two wood pieces by applying relative motion between the contact surfaces under pressure. The heat generated by friction leads to thermal degradation of the wood constituents at the interface, followed by the formation of an amorphous bond line upon cooling (Gedara et al. 2021).
This study aims to identify an appropriate set of parameters to improve the bond strength. The quality of the bond line is highly dependent on the welding parameters, including amplitude, frequency, welding pressure and welding time, as well as on the geometry and material properties of the wood (Zhang et al. 2017). A key challenge in the welding process is to achieve uniform heat and friction conditions across the entire welding interface. Melting at the welding interface generates smoke and a slight welding displacement, which may contribute to an uneven joint between the edges and the centre of the contact area (Hahn et al. 2014). The linear vibration welding, being 'linear', introduces different effects to the workpiece on the edges that are perpendicular to the direction of vibration and those that are parallel to it. This paper shows that the effects of these internal asymmetries can be reduced by adjusting the pressure and welding time.

**Keywords:** Linear vibration welding, Moso bamboo, tensile-shear strength

## Experimental

Moso bamboo was used in the form of strips with dimensions of 225 mm × 17 mm × 6 mm. The linear vibration welding machine, type M 624, with a frequency of 240 Hz and an amplitude of 1 mm, was used. A wide range of welding parameters were investigated, as outlined in Table 1. The samples were welded in the longitudinal direction, parallel to the bamboo fibres. Subsequently, an area of 204 mm² was isolated by cutting fine notches right down to the weld line in the middle and close to both ends of the samples. These areas were then subjected to tensile-shear testing based on EN 302-1 to investigate the distribution of bonding strength along the weld line. Five replicate welded joints were prepared for each welding condition.

## Results and Discussion

Effective welding of two wood pieces depends on the uniform melting of the wood constituents across the entire welding interface. In linear vibration welding, the heat generation is initiated at the ends of the samples, where the vibration causes the sharp edge of the end grain to rub successively against the underlying ductile surface. The heat will then propagate inwards as seems to be suggested in Figures 1a and 1b. The early welding that occurs at the ends explains the difference in bonding strength compared to the middle area (Table 1). The results indicate that the welding pressure, $p_{w2}$, plays an important role in achieving a uniformly welded interface. However, the effect of this parameter also depends on the welding time $t_{w2}$. The results of E1 with E2 show that prolonged welding under high pressure leads to char formation, which decreases the shear strength (Vaziri et al. 2012). A welding pressure of 4MPa applied for 3s (D1) resulted in satisfactory and rather uniform bonding strength along the weld line.

Table 1. Welding procedure and mechanical properties of the test pieces. The initial welding pressure, $p_{w1,}$ was applied during the first welding time, $t_{w1}$, followed by the second welding pressure, $p_{w2}$, applied during the effective welding time, $t_{w2}$. The holding pressure, $p_{h,}$ was then applied during the cooling time, $t_h$

| Index | Welding parameters | | Bonding strength | | | |
|---|---|---|---|---|---|---|
| | $t_{w1}$ / $t_{w2}$ / $t_h$ [s] | $p_{w1}$ / $p_{w2}$ / $p_h$ [MPa] | Middle area | | Side areas | |
| | | | Mean [MPa] | SD | Mean [MPa] | SD |
| **A1** | 1.5 / 2 / 10 | | 1.26 | 0.18 | 2.47 | 0.77 |
| **A2** | 1.5 / 3 / 10 | 1.6 / 2.4 / 3.2 | 1.68 | 0.61 | 2.17 | 0.85 |
| **A3** | 1.5 / 4 / 10 | | 1.69 | 0.80 | 2.84 | 0.45 |
| **B1** | 1 / 2 / 10 | | 2.29 | 1.06 | 3.73 | 1.17 |
| **B2** | 1 / 3 / 10 | 2.4 / 3.2 / 3.6 | 3.04 | 1.20 | 4.29 | 0.89 |
| **B3** | 1 / 4 / 10 | | 3.21 | 0.96 | 4.70 | 1.14 |
| **C1** | 0.5 / 2 / 10 | | 2.45 | 0.33 | 3.28 | 0.69 |
| **C2** | 0.5 / 3 / 10 | 2.8 / 3.6 / 3.4 | 4.16 | 2.09 | 5.18 | 1.10 |
| **C3** | 0.5 / 4 / 10 | | 3.83 | 0.40 | 5.24 | 1.26 |
| **D1** | 1 / 3 / 10 | 4.0 / 4.0 / 4.0 | 7.21 | 1.16 | 6.76 | 0.62 |
| **E1** | 1 / 2 / 10 | 4.8 / 4.8 / 4.8 | 6.62 | 1.57 | 10.00 | 0.33 |
| **E2** | 1 / 3 / 10 | | 6.87 | 2.71 | 7.49 | 1.15 |
| **F1** | 1 / 2 / 10 | 5.6 / 5.6 / 5.6 | 10.48 | 1.05 | 9.53 | 0.53 |
| **G1** | 1 / 1 / 10 | 6.4 / 6.4 / 6.4 | 7.71 | 2.38 | 9.72 | 1.22 |

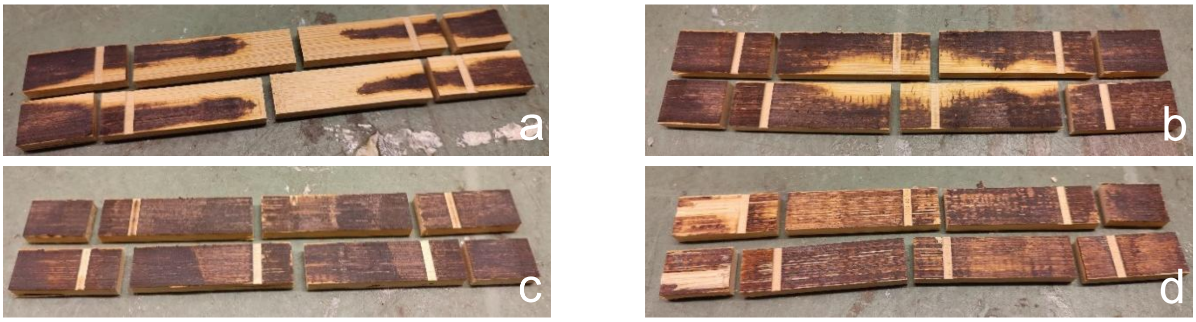


Figure 1. Welded interface (dark area) of four samples produced using welding conditions A3, C2, E2, and G1 corresponding to (a), (b), (c) and (d) respectively. Each specimen contains three isolated welded areas (one in the middle and two near the edges) subjected to tensile-shear testing

## Conclusions

Although the absence of synthetic adhesives favours welding as a joining method for wood components, the technique requires careful selection of welding parameters, such as welding pressure and welding time, respectively around 4MPa and 3s.

**References**

Gedara, A. K. A., Chianella, I., Endrino, J. L., & Zhang, Q. (2021). Adhesive less bonding of wood – A review with a focus on wood welding. BioResources, 16(3), 6448–6470. https://doi.org/10.15376/biores.16.3.Gedara

Hahn, B., Stamm, B., & Weinand, Y. (2014). Linear friction welding of spruce boards: Experimental investigations on scale effects due to humidity evaporation. Wood Science and Technology, 48(4), 855–871. https://doi.org/10.1007/s00226-014-0645-0

Vaziri, M., Berg, S., Sandberg, D., and Tavakoli, I. (2012). Three-dimensional finite element modelling of heat transfer for linear friction welding of Scots pine. Wood Mater. Sci. Eng. 9:102–109.

Zhang, H., Pizzi, A., Zhou, X., Lu, X., & Wang, Z. (2017). The study of linear vibrational welding of moso bamboo. Journal of Adhesion Science and Technology, 32(1), 1–10. https://doi.org/10.1080/01694243.2017.1322767

# Experimental Investigation on the Composite Action of Parallel Glulam Members Mechanically Connected by Double Dovetail Wooden Connectors

**Tianxiang Wang[1], Elis Berg[1], Koen Weijgers[1], Magnus Wålinder[1], and Roberto Crocetti[1]**

[1]Division of Building Materials, Department of Civil and Architectural Engineering, KTH Royal Institute of Technology, tiawan@kth.se, elisberg@kth.se, weijgers@kth.se, magnus.walinder@byv.kth.se, crocetti@kth.se

## Background

In Swedish glulam production, the common width limit in the production line is 215 mm. When large structural cross-sections are required in large-scale timber structures, glulam members are commonly screw-press glued together. This method can provide full composite action, but relies on adhesive bonding and a time-consuming production process. Mechanically connected shear key systems offer a possible alternative, but their finite connector stiffness leads to partial composite action and their structural performance is less established. This study investigates whether parallel glued laminated timber members connected with double dovetail X-fix shear keys can create a satisfactory degree of partial composite action to provide an alternative to screw-glued built-up members.

**Keywords:** double dovetail X-fix wooden connector, shear key, partial composite action.

## Experimental

The X-fix connector used in this study is made of birch plywood. The installation process of the X-fix connector into the timber element is shown in Figure 1.

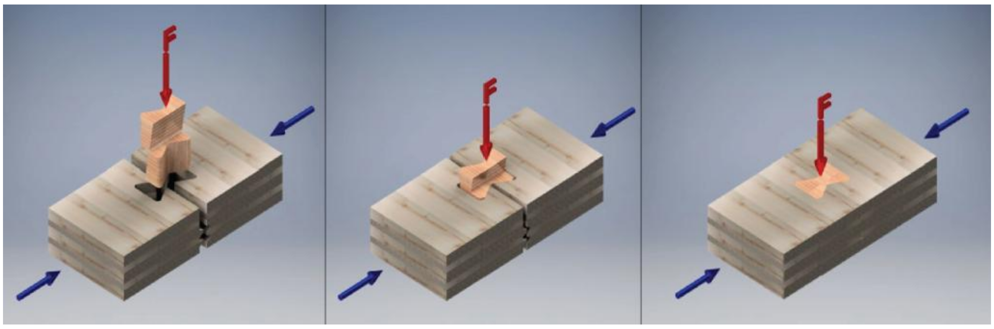


Figure 1. Installation process of one X-fix connector (X-fix wood connector GmbH, 2025)

As can be seen in Figure 1, one X-fix connector is composed of two conical dovetail-shaped wedges that can be hammered into the openings of two adjacent timber elements. This process helps generating clamping force perpendicular to the interface. Moreover, the dovetail-shaped shear key possesses a self-tightening mechanism that it can avoid the risk of separation between the timber elements. While the ordinary shear keys with regular shapes usually need additional screws or other clamping systems to prevent it.
The experimental campaign involves two four-point bending test series with two replicates in each test series. In each test, two parallel glulam beams with dimensions of 90 mm × 270 mm × 6000 mm were connected by X-fix connectors with the embedment depths of 45 mm or 70 mm on both sides of the interface. Therefore, the tested specimens were referred to

as B45A, B45B, B70A, and B70B. The loading rate is 5 mm/min. The configuration and the spacing of the wooden connectors were designed so that the failure of the wooden connector close to the support is expected to take place prior to the global bending failure of the glulam beam. Nevertheless, the experimental tests focused more on the determination of the effective bending stiffness and the degree of partial composite action as these are the critical parameters when calculating the reduction factors for pure flexure buckling of column elements and lateral torsional buckling of beam elements. The bending test setup and the cross-section of the wooden connector are illustrated in Figure 2.

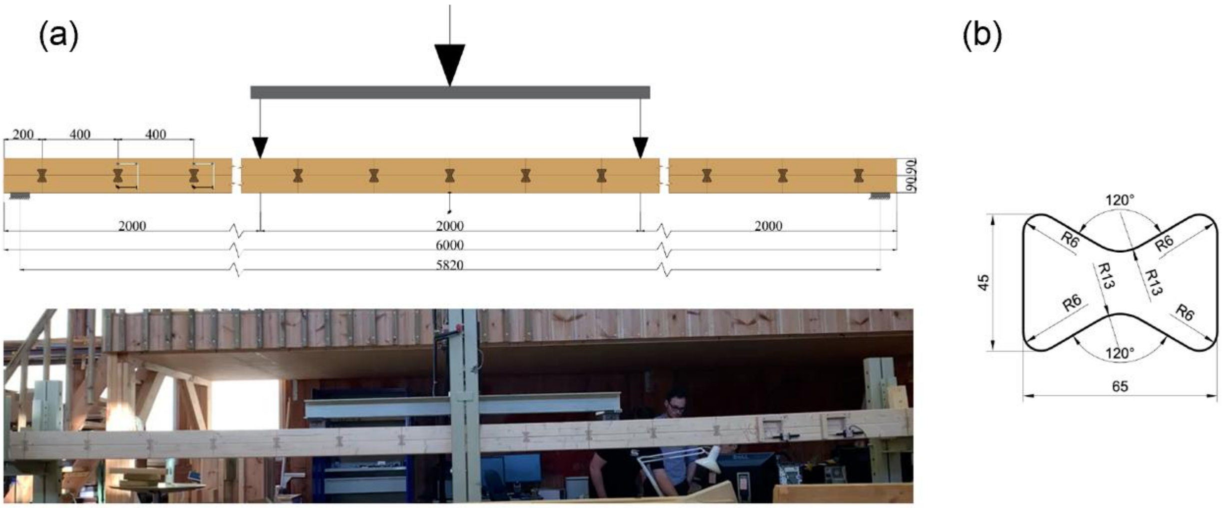


Figure 2. (a) Bending test setup and (b) cross-section of the wooden connector (unit in mm) (Schickhofer, 2025)

### Results and Discussion

The effective bending stiffness can be determined from the measured load-displacement response. The degree of composite action is the ratio of the effective bending stiffness to the bending stiffness in full composite action. The bending stiffness in full composite action (e.g., by screw-gluing) and no composite action (e.g., with no connection) can be determined analytically, which is $1.8\times10^9$ kN*mm$^2$ and $0.45\times10^9$ kN*mm$^2$, respectively.

Table 1. Effective bending stiffness and the degree of composite action of the tested specimens

| Specimen | Bending stiffness [kN*mm$^2$] | Degree of composite action |
|---|---|---|
| B45A | $1.17\times10^9$ | 65% |
| B45B | $0.95\times10^9$ | 58% |
| B70A | $1.42\times10^9$ | 79% |
| B70B | $1.17\times10^9$ | 65% |

The results in Table 1 indicate that the embedment depth of the wooden connectors show positive influence on the bending stiffness. However, the specimen B45A possesses similar bending stiffness to B70B, which is likely due to the imperfection in manufacturing and assembly or variability in the elastic modulus of glulam materials. Overall, the tested specimens can reach approximately 60%-80% partial composite action under the adopted configuration and spacing of the wooden connector.

## Conclusions

This study reveals that it is promising to use double dovetail X-fix wooden connector as an alternative to the screw-gluing method to connect parallel glulam members for structural applications. The tested glulam built-up members show sufficient partial composite action under the adopted configuration and spacing of the wooden connector. Future work might include shear tests to evaluate the slip modulus of the wooden connector, which can serve as an input for the further development of analytical and numerical models to predict the effective bending stiffness under varying geometries and load cases.

## References

Schickhofer G (2025) Prüfergebnisse zum verbindungssystem x-fix-c (45/65/45 mm) in kombination mit 3-schichtigem bsp (60 mm) [Online]. Available: https://x-fix.at/pages/technische-informationen

X-fix wood connector GmbH (2025) X-fix presentation: Projects and technical information.

X-fix wood connector GmbH, Austria, internal company document.

# Free-Form 3D Timber Beams: Research, Prototyping and Manufacturing Challenges

**Tom Svilāns[1], Edgars Rudzītis[1], Miks Peilāns[1], Kristaps Zīverts, Jānis Iejavs, Edvīns Grants**

[1]ZAZA TIMBER Production, Sia, Latvia,
edgars.rudzitis@zazatimber.lv, miks.peilans@zazatimber.lv,
info@zazatimber.lv

**Abstract**

The presentation introduces recent developments in free-form 3D timber beams within ZAZA TIMBER's research and development programme. The research addresses industry trends and key challenges in geometry transfer, adhesive performance and manufacturing constraints. Experimental testing, prototyping and modelling revealed critical issues in shaping accuracy and CNC post-processing. The study resulted in a manufacturable technology concept for structurally reliable free-form beams. Insights from two related publications are summarised, alongside realised pilot projects. The presentation concludes with remaining technological barriers and future research directions.

# Configuring Wood in Hybrid Timber Structures for Low-Carbon and Circular Construction

**Hüseyin Emre Ilgın[1], Markku Karjalainen[1], Teemu Hirvilammi[1], Sami Pajunen[1], Jami Järvinen[1]**

[1]Faculty of Built Environment, Tampere University, Tampere, Finland, emre.ilgin@tuni.fi; markku.karjalainen@tuni.fi; teemu.hirvilammi@tuni.fi; sami.pajunen@tuni.fi; jami.jarvinen@tuni.fi

### Background

Wood is increasingly expected to deliver structural performance and verifiable lifecycle benefits, accelerating hybrid timber systems that combine timber or engineered wood products with concrete, steel, or reinforcement materials. These combinations can overcome stiffness, vibration, fire, acoustic, robustness, and constructability constraints in timber-only solutions, particularly in multi-storey and tall buildings (Pasternack et al. 2022; Abdulmalik et al. 2025). Yet classification by material pair, such as timber-concrete or timber-steel, identifies the materials but not how the structure works. The same pair may provide local reinforcement, form a composite floor, or contribute to a building-scale stability system, with implications for load transfer, stiffness distribution, interface behaviour, material demand, and end-of-life separability (Tannert et al. 2020; Kim and Kim 2022). This matters because neither high timber content nor carbon storage alone guarantees low whole-building impacts or circular recovery (Kumar et al. 2024). This study therefore reframes hybridisation according to wood's position in the load-bearing hierarchy. It develops a transferable three-level framework, locally enhanced timber elements, composite assemblies, and building-level structural systems, and explains how each level affects structural response, carbon-oriented material efficiency, connection reversibility, and design for disassembly.

**Keywords:** hybrid timber systems, structural configuration, load-bearing hierarchy, low-carbon construction, design for disassembly.

### Materials and Methods

The study uses a conceptual and structured synthesis rather than original experiments, quantitative meta-analysis, or a full systematic review. The evidence base comprises scientific and technical sources covering hybrid timber systems, structural and serviceability performance, lifecycle carbon, connection design, reuse, and circular construction. Sources were retained when they examined wood with a complementary material at the element, assembly, or building scale and informed at least one of five analytical dimensions: structural response; subsystem coupling; embodied-carbon performance; regulatory and safety performance; or constructability and lifecycle adaptability. The synthesis proceeded in three stages: classification by integration scale, comparison across the five dimensions, and interpretation of recurring configuration logics. The results express cross-source analytical tendencies, not quantitative design rules or statistically generalisable effects.

## Results and Discussion

The synthesis identifies three distinct structural roles for wood (Figure 1). Moving from element to building scale changes not only the size of the unit being analysed, but also the mechanism through which hybridisation creates performance.

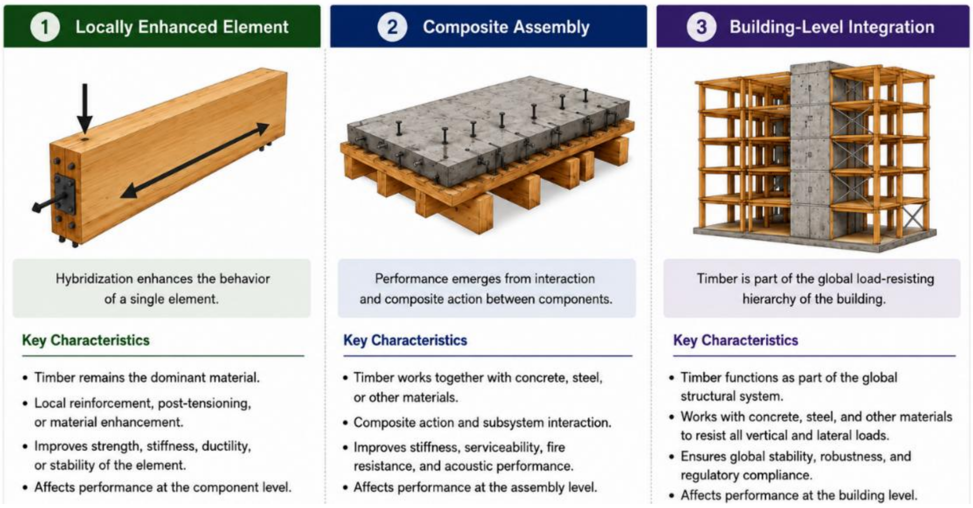


Figure 1. Configuration-based interpretation of hybrid timber systems through three structural roles of wood

**Element level.** Timber remains the dominant load-bearing material, while steel tendons, plates, rods, fibre-reinforced polymers, or bio-based composites address a member-specific limitation in strength, stiffness, ductility, or durability. The global load path remains unchanged. Smaller sections or longer service life may reduce impacts, but bonded or embedded reinforcement can obstruct separation.

**Assembly level.** Performance emerges from interaction between components. Timber-concrete composite floors use interface shear transfer to combine timber's tensile contribution with concrete's compression capacity, mass, fire resistance, and acoustic benefits (Shephard et al. 2021). Timber-steel assemblies use steel for tensile capacity, ductility, or long spans while retaining timber's low self-weight (Loss et al. 2018; Owolabi et al. 2023). Connector stiffness, slip, time-dependent movement, and reversibility govern efficiency, repair, and reuse (Dissanayake et al. 2025).

**Building level.** Hybridisation becomes functional material allocation within the global load-resisting hierarchy. Timber can dominate gravity-load systems, while concrete cores or steel bracing provide lateral stiffness, robustness, fire compartmentation, or transfer capacity (Pan et al. 2021). Brock Commons illustrates how concrete cores can enable a timber-dominant superstructure (Staub-French et al. 2022). The criterion is functional value with minimum whole-building material demand, not timber quantity alone.

**Cross-scale finding.** The comparison does not support a universal ranking in which a higher level is automatically better. Element-level solutions directly address local constraints; assembly-level systems create interface-dependent gains and trade-offs; and building-level integration has the widest leverage over global stability and material intensity.

**Across all three levels, two cross-cutting logics emerge.** Carbon-oriented configuration prioritises functional equivalence, material efficiency, and avoided overdesign rather than maximum timber content. Lifecycle-oriented hybridisation treats adaptability, disassembly, reuse, and recovery as outcomes of connection design, subsystem separation, and material zoning; reusable demountable systems demonstrate the importance of interfaces (Li et al. 2024).

## Conclusions

Hybrid timber construction cannot be evaluated through material selection alone. The structural, carbon, and end-of-life value of wood depends on its role in load paths, subsystem interaction, and interface reversibility. The framework therefore supports performance-oriented material allocation rather than timber-content maximisation. Its tendencies should next be tested through functionally equivalent structural comparisons, lifecycle assessment, and long-term interface evaluation.

## References

Abdulmalik A, Gilbert BP, Guan H, Ngo T, Remennikov A (2025) Advancements in timbersteel hybridisation: a review on techniques, applications, and structural performances. Buildings 15: 2252.

Dissanayake H, Gunawardena T, Mendis P (2025) Adaptation of connection systems for integration with engineered wood products in buildings: A systematic review. Buildings 15:1131.

Kim YM, Kim YM (2022) Classification of hybrid system types of mid and high-rise timber buildings. Journal of the Architectural Institute of Korea 38: 339-348.

Kumar V, Ricco ML, Bergman RD, Nepal P, Poudyal NC (2024) Environmental impact assessment of mass timber, structural steel, and reinforced concrete buildings based on the 2021 international building code provisions. Building and Environment 251: 111195.

Li Z, Tsavdaridis KD, Katenbayeva A (2024) Reusable timber modular buildings, materialcircularity and automation: The role of inter-locking connections. Journal of Building Engineering 98: 110965.

Loss C, Rossi S, Tannert T (2018) In-plane stiffness of hybrid steel-cross-laminated timber floor diaphragms. Journal of Structural Engineering 144: 04018128.

Owolabi D, Loss C, Zhou J (2023) Vibration properties and serviceability performance of a modular cross-laminated timber-steel composite floor system. Journal of Structural Engineering 149: 04023171.

Pan Y, Tannert T, Kaushik K, Xiong H, Ventura CE (2021) Seismic performance of a proposed wood-concrete hybrid system for high-rise buildings. Engineering Structures 238: 112194.

Pasternack R, Wishnie M, Clarke C, et al. (2022) What is the impact of mass timber utilization on climate and forests? Sustainability 14: 758.

Shephard AB, Fischer EC, Barbosa AR, Sinha A (2021) Fundamental behavior of timber-concrete-composite floors in fire. Journal of Structural Engineering 147: 04020340.

Staub-French S, Pilon A, Poirier E, et al. (2022) Construction process innovation on Brock Commons Tallwood House. Construction Innovation 22: 1-22.

Tannert T, Gerber A, Vallee T (2020) Hybrid adhesively bonded timber-concrete-composite floors. International Journal of Adhesion and Adhesives 97: 102490.

# SESSION 2: CLIMATE AND WOOD PROPERTIES

# Influence of the Time of Logging on Moisture Content and Density Variation in Beech Wood (*Fagus sylvatica*)

**Amina Gačo Jež[1], Luka Kopač[2], Miha Humar[3]**

[1,2,3] Biotechnical faculty, University of Ljubljana, Slovenia
amina.gaco.jez@bf.uni-lj.si , miha.humar@bf.uni-lj.si

## Background

Wood is a porous biological material whose hygroscopicity and density strongly influence its properties and applications (Ghorbanian Far et al., 2024; Ma et al., 2022). Wood density is a key indicator of wood quality, as it is closely related to strength, stiffness, durability, workability, and dimensional stability (Chambi-Legoas et al., 2023). In addition, changes in moisture content significantly affect these physical and mechanical properties, influencing wood strength, dimensional stability, and durability (Chambi-Legoas et al., 2023; Dietsch et al., 2015). Previous studies have examined the relationships between phenology, xylogenesis, and environmental drivers such as temperature and water availability (Čufar et al., 2008; Larysch et al., 2021; Tsalagkas et al., 2024; Silvestro idr., 2025). Although several authors have also examined lunar-related fluctuations in tree water dynamics (Zürcher, 2001), the combined effects of logging timing, phenological stages, lunar phases, and storage on wood moisture content and basic density remain insufficiently investigated. This study investigates the influence of harvest time, phenological phases, and lunar phases on the moisture content and wood density of European beech (*Fagus sylvatica* L.) using gravimetric methods and hyperspectral imaging. The findings may improve harvesting strategies, wood quality, and sustainable forest management.

**Keywords:** wood density, wood moisture, European beech, logging, hyperspectral imaging

## Experimental

The study investigated European beech (*Fagus sylvatica* L.) wood from Kočevje, Slovenia. A total of 84 discs were collected during 14 sampling campaigns over approximately two-week intervals. Six trees were sampled each time, including three with red heartwood and three without discoloration. Only defect-free trees with diameters above 20 cm were selected. Samples were analysed using hyperspectral imaging and prepared for analyse. Wood moisture and wood density were determined gravimetrically. The combined methods were used to assess the effects of logging time, phenological stages, and lunar phases on wood moisture content. Statistical analyses were conducted using JASP. To obtain the moisture distribution, we used a model, which we built in Phyton.

## Results and Discussion

The results indicate that phenological phases and harvesting time were more strongly associated with variation in wood density and wood moisture than lunar phases. For both investigated properties, the largest differences were observed among individual harvesting times, whereas the distributions of values across lunar phases largely overlapped.

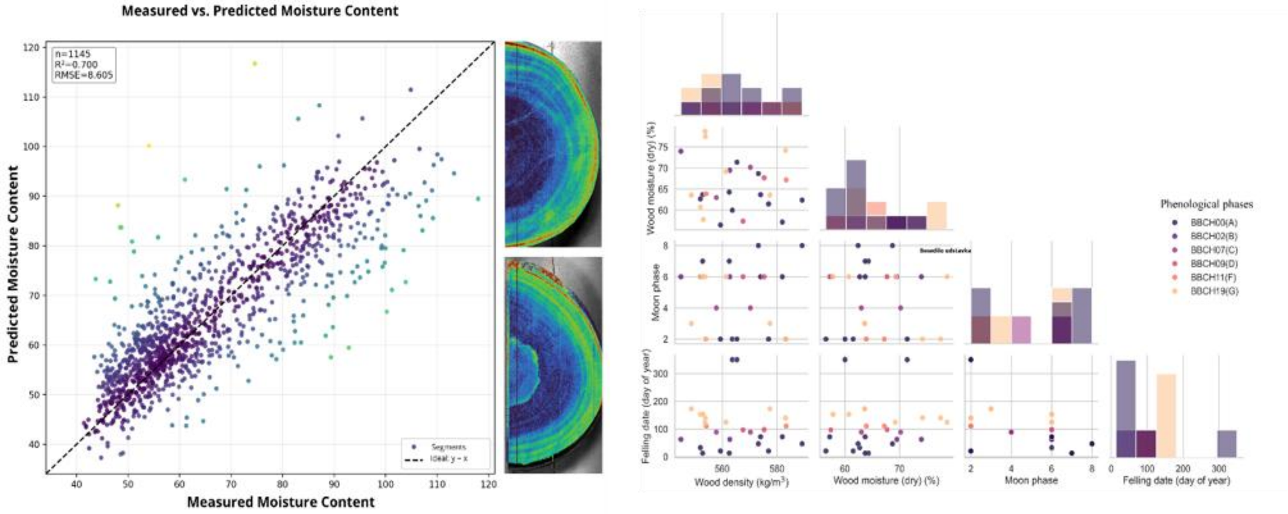


Figure 1. Relationships between wood properties and environmental factors (right), and moisture content mapping of red-heartwood and three without discoloration samples using spectral prediction models (left)

A model for predicting wood moisture was developed using hyperspectral images, standardized spectral data, and reference moisture measurements. The model enables spectral information to be converted into spatial maps of moisture distribution across the wood cross-section. In the sample exhibiting red heartwood, higher moisture content was detected primarily in the central part of the cross-section, whereas in the sample without discoloration, elevated moisture content was more pronounced near the outer edge. These findings demonstrate the potential of hyperspectral imaging as a non-destructive method for assessing and visualizing the spatial distribution of moisture in wood. The comparison between measured and predicted moisture content showed good agreement between the values ($R^2 = 0.700$; RMSE = 8.605%). Most observations were distributed close to the line of perfect agreement, indicating satisfactory predictive performance of the developed model. However, the greater dispersion observed at higher moisture-content values suggests somewhat lower prediction accuracy in the upper moisture range.

## Conclusions

Harvesting time and phenological phases had a greater influence on European beech wood moisture and density than lunar phases. Hyperspectral imaging enabled non-destructive, spatially detailed moisture assessment and visualization across wood samples. Further research should improve prediction accuracy and validate the method under different environmental conditions. These findings may contribute to reducing losses and improving efficiency in the production of high-quality timber.

## References

Chambi-Legoas, R., Tomazello-Filho, M., Vidal, C., & Chaix, G. (2023). Wood density prediction using near-infrared hyperspectral imaging for early selection of Eucalyptus grandis trees. Trees, 37(3), 981–991. https://doi.org/10.1007/s00468-023-02397-2

Čufar, K., Prislan, P., De Luis, M., & Gričar, J. (2008). Tree-ring variation, wood formation and phenology of beech (Fagus sylvatica) from a representative site in Slovenia, SE Central Europe. Trees, 22(6), 749–758. https://doi.org/10.1007/s00468-008-0235-6

Dietsch, P., Franke, S., Franke, B., Gamper, A., & Winter, S. (2015). Methods to determine wood moisture content and their applicability in monitoring concepts. Journal of Civil Structural Health Monitoring, 5(2), 115–127. https://doi.org/10.1007/s13349-014-0082-7

Ghorbanian Far, M., Najafian Ashrafi, M., Shaabani Asrami, H., Amiri Moghadam, Y., Bari, E., Niemz, P., Hosseinpourpia, R., & Ribera, J. (2024). Physical and mechanical properties of different beech wood species grown at various climate conditions: A review. Holzforschung, 78(7), 377–386. https://doi.org/10.1515/hf-2023-0117

Larysch, E., Stangler, D. F., Nazari, M., Seifert, T., & Kahle, H.-P. (2021). Xylem Phenology and Growth Response of European Beech, Silver Fir and Scots Pine along an Elevational Gradient during the Extreme Drought Year 2018. Forests, 12(1), 75. https://doi.org/10.3390/f12010075

Ma, T., Morita, G., Inagaki, T., & Tsuchikawa, S. (2022). Moisture transport dynamics in wood during drying studied by long-wave near-infrared hyperspectral imaging. Cellulose, 29(1), 133–145. https://doi.org/10.1007/s10570-021-04290-y

Silvestro, R., Deslauriers, A., Prislan, P., Rademacher, T., Rezaie, N., Richardson, A. D., Vitasse, Y., & Rossi, S. (2025). From Roots to Leaves: Tree Growth Phenology in Forest Ecosystems. Current Forestry Reports, 11(1), 12. https://doi.org/10.1007/s40725-025-00245-9

Tsalagkas, D., Vavrčík, H., Gryc, V., & Giagli, K. (2024). Age-related phenological and anatomical response of European beech (Fagus sylvatica L.) under severe summer drought conditions. Journal of Forest Science, 70(9), 458–475. https://doi.org/10.17221/16/2024-JFS

Zürcher E. (2001). Lunar rhythms in forestry traditions-lunar-correlated phenomena in tree biology and wood properties. Earth, Moon and Planets, 85-86: 463-478, 2001.

# Mechanical and Physical Properties of Blue Stained Norway Spruce *(Picea abies)*

**Laura Kaljula[1], Triinu Poltimäe[2], Alar Just[3], Siim Pikker[4], Jaan Kers[5]**

[1,2,5]Tallinn University of Technology, Department of Materials and Environmental Technology, Laboratory of Wood Technology, Estonia, laura.kaljula@taltech.ee
[3]Tallinn University of Technology, Department of Civil Engineering and Architecture, Structural Engineering Research Group
[4]Institute of Physics, University of Tartu, W. Ostwaldi 1, 50411 Tartu, Estonia

## Background

An increasing problem of Spruce bark beetle *(Ips typographus)* attacks on softwood, particularly Norway spruce *(Picea abies)* has lead to a situation where there is a large stock of beetle attacked material (Künniger *et al.*, 2024). Bark beetle attack causes the infestation of blue stain fungi, which appears as a blue/grey discoloration on wood. This kind of material is often undesired by the customers as unreliable and anaesthetic.
Nevertheless, beetle attacked wood, when harvested and processed in a comparatively short time (not more than 3 years after attack), has mechanical properties still comparable to a standard material (Jelonek *et al.*, 2020; Künniger *et al.*, 2024).
As the blue stained material is still undesired in our region, this study aims to investigate the basic physical and mechanical properties of blue stained Norway spruce wood, grown in Eastern Estonia. Our results were compared to existing literature with conifers grown in other European regions and additional set of experiments were completed, such as contact angle measurement and scanning electron microscopy on blue stained Norway spruce wood.

**Keywords:** Bark beetle, blue stain, wood properties, Norway spruce**.**

## Experimental

In this study we examined bark beetle attacked and later blue stained Norway spruce lamellae in a size 50x150x3000mm. As a reference there were examined also control samples – defect free Norway spruce lamellae.
There were carried out tests for physical properties – absolute moisture content, oven dry density and contact angle measurement to characterize wettability. Additionally, a scanning electron microscopy *(SEM)* was performed to explore the blue stain fungi growth effect on cell wall structure.
For mechanical properties a four-point bending and compression tests were done, where for compression, some of the samples were tested for accelerated weathering beforehand.

## Results and Discussion

A scanning electron microscopy of blue stained wood samples confirmed a blue stain fungi presence in cell walls and its growth patterns were observed. As the fungi is growing inside the cell walls and spreads to adjacent cells through the openings (pits) only, the cell wall structure seemed not to be affected (figure 1). This also explains why the mechanical properties are also mostly remaining intact, which was the case in our research as well.

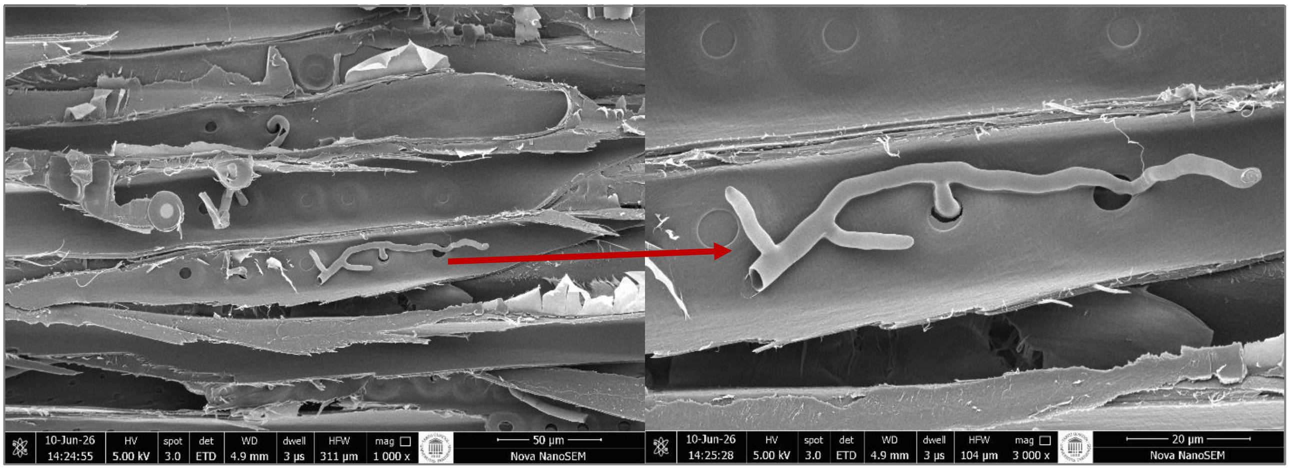


Figure 1. SEM images on blue stained wood radial section

Our initial results show that the blue stain does not significantly decrease physical or mechanical performance of material and is comparable to standard wood. In our case, the mean value of density was even higher than for control, which can be related to amount of specimens tested and the place where sample was taken (blue stain intensity). Summary of density and mechanical properties is given in table 1.

Table 1. Density, modulus of elasticity and modulus of rupture of tested specimens

| **Parameter** | **Control** | **Blue stained Norway spruce** | **Comment** |
|---|---|---|---|
| Density (kg/m$^3$) | *n=36* | *n=120* | *3 cubes per lamella* |
| | 419 ± 59,5 | 435 ± 39,19 | |
| Modulus of Elasticity (kN/mm$^2$) | *n=12* | *n=40* | *1 specimen had 4-5 positions* |
| | 10,48 ± 2,15 | 10,22 ± 1,60 | |
| Modulus of rupture (bending strength)(N/mm$^2$) | *n=6* | *n=8* | |
| | 57,17 ± 11,56 | 55,13 ± 13,55 | - |

Results on wettability characterised by contact angle showed a tendency of room conditioned blue stained spruce samples to be more hydrophilic than the samples which were oven dried before, even though being cut from the same lamella. This suggests that oven drying of blue stained wood decreases wettability and makes surfaces hydrophobic.

## Conclusions

According to current results we can say that blue stain does not significantly decrease the mechanical strength of wood which is also related blue stain fungi growth patterns, where the cell wall still remains intact. However, as the study is in progress and more results will be obtained in near future, strict conclusions cannot be drawn yet.

**References**

Jelonek, T. *et al.* (2020) “Influence of the tree decay duration on mechanical stability of Norway sprucewood (Picea abies (L.) Karst.),” *Forests*, 11(9), pp. 1–13. Available at: https://doi.org/10.3390/f11090980.

Künniger, T. *et al.* (2024) “Mechanical properties of Norway spruce (Picea abies) infested by the bark beetle (Ips typographus),” *Wood Material Science and Engineering*, 19(1), pp. 85–91. Available at: https://doi.org/10.1080/17480272.2023.2226644.

# Estimating Climatic Impact on the Mechanical Properties of Scots Pine

**Tobias Bender[1], Linnea Hesse[2], Alexander Pfriem[3]**

[1]University for Sustainable Development Eberswalde (HNEE), Germany, tobias.bender@hnee.de
[2]Universität Hamburg, Germany,
linnea.hesse@uni-hamburg.de
[3]Technische Universität Dresden, Germany
alexander.pfriem@tu-dresden.de

## Background

Wood is a highly heterogeneous material whose structure and properties are shaped by environmental conditions throughout a tree's lifetime. As climate change is expected to alter these conditions, understanding its impact on wood quality and mechanical performance has become increasingly important.

Scots pine (*Pinus sylvestris* L.) is one of the most widespread and economically important tree species in Europe (e.g. Brichta et al. 2023). This marks the importance to reassess both the species' climate resilience and the quality of the wood it provides.

This case study aims to assess the impact of climate on the mechanical properties of Scots pine wood by integrating dendroecological analyses with standardized material testing. Ultimately, this approach is intended to support the development of predictive models for forecasting changes in wood quality under future climate conditions.

**Keywords:** Climate Change; Wood Growth; Dendroclimatology; Static bending;

## Experimental

Sample-material and climate data were collected from a highly monitored, unmanaged pure Scots pine stand in north-eastern Brandenburg, Germany. For a more detailed site description, see Krause and Sanders (2023).

For the determination of modulus of elasticity (MOE), modulus of rupture (MOR), and density, specimens from the lower trunk of six trees were prepared and tested based on DIN 52-186. In order to reduce the number of tree rings within its cross section, the specimens' size was reduced to 15 x 15 x 280 mm³ (r x t x l). Specimens were dated in order to retrieve their growth-related proxies from adjacent growth profiles. Specimens containing tree rings with a cambial age lower than 15 years were excluded from the sample.

The dendroecological analysis was conducted according to Schröder (2013). Ring-width (RW) latewood-percentage (LWP) and latewood-blue-intensity (LWBI), which according to Rydval et al. (2014) correlates well with maximum latewood density, were measured on growth profiles using the software CooRecorder 9.3.1. The raw time series were standardized in R, using the package “dplr”. For the analysis of climate-growth-relations, a moving-window analysis of the pearson correlation between the respective tree-ring-proxies: LWP and LWBI and the climate data on site: monthly-mean-temperatures and monthly-precipitation-sum, was conducted using the R-package “treeclim”.

## Results and Discussion

LWP shows the strongest correlation to both the mechanical properties (MOR; MOE), as well as the density. LWBI also shares a significant correlation with those parameters. RW on the other hand does not appear to influence the mechanic behaviour at all. However, a small positive trend between RW and LWP can be observed. As seen in the Boxplots, the parameters vary widely between the individual origin trees, indicating a rather strong influence of competition (Figure 1).

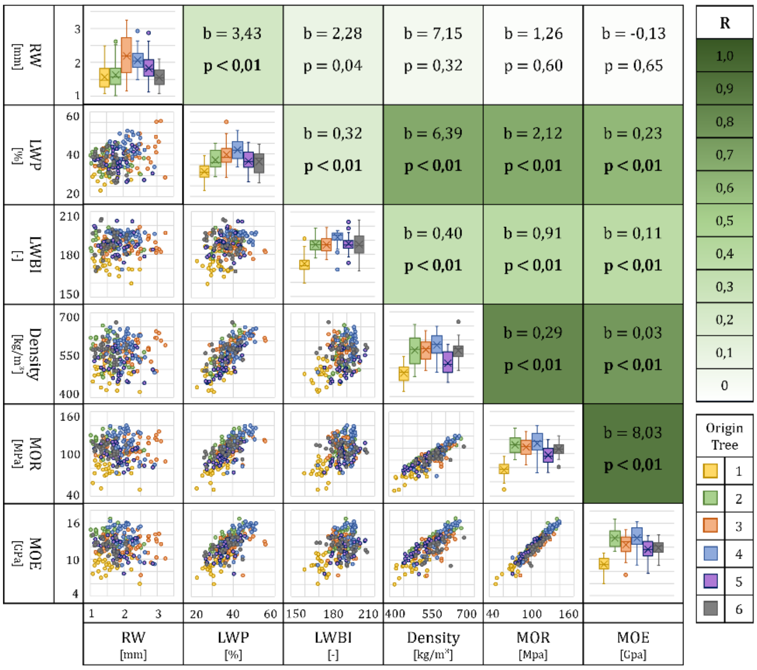


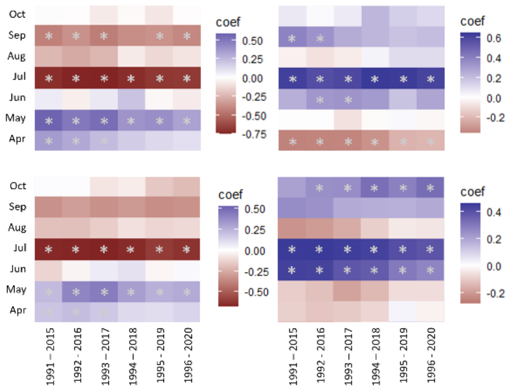


Figure 2. Scatterplot-Matrix on the correlation between the individual parameters (left); Boxplots on the distribution of the individual parameters within the corresponding origin tree (diagonal). Right side: coefficient (b) and p-value (p) of the regression analysis; Heatmap of the corresponding correlation coefficient

Figure 3. Moving window analysis of the correlation between LWP (top) and LWBI (bottom) with mean temperature (left), and precipitation sum (right) of the corresponding months within the vegetation-period. Asterisks mark significant correlations

As seen in Figure 2, both LWP and LWBI show strong negative correlations with summer temperatures, especially in July. At the same time, both parameters share strong positive correlations with July precipitation sum. In the case of LWBI this trend can also be observed for June.

## Conclusions

In our case study, we found that the mechanic behaviour of our specimens was strongly tied to the latewood-share and -density (represented by their respective proxies), rather than ring-width. As seen in the dendroecological analysis, those two parameters are strongly influenced by summer temperature and precipitation.

Based on current climate change scenarios for Brandenburg, summer temperatures tend to rise, while precipitation stays at an unaltered low compared to other regions within Germany (MLUK 2024).

Based on those findings, we come to the conclusion, that climate change could not only affect the quantitative wood growth, but also the mechanical properties of Scots Pine within the region. However, this case study was done on one particular, unmanaged stand, and only included six individual trees. Thus, these results are not necessarily representative for other stand-types.

**References**

Brichta J, Vacek S, Vacek Z, Cukor J, Mikeska M, Bílek L, Šimůnek V, Gallo J, Brabec P (2023): Importance and potential of Scots pine (Pinus sylvestris L.) in 21st century. Central European Forestry Journal, 69 (1), 3–20.

DIN Deutsches Institut für Normung e. V. (Hrsg.): DIN 52186: Prüfung von Holz; Biegeversuch. Ausgabe Juni 1978. Berlin: Beuth Verlag.

Ministerium für Landwirtschaft, Umwelt und Klimaschutz des Landes Brandenburg (2024): Klimareport Brandenburg 2024, Potsdam, 23-28

Krause S, Sanders TGM (2023): Mapping Tree Water Deficit with UAV Thermal Imaging and Meteorological Data. Remote Sensing in Earth Systems Sciences, 6 (3-4), 275–296.

Rydval M, Larsson L-Å, McGlynn L, Gunnarson BE, Loader NJ, Young GH, Wilson R (2014): Blue intensity for dendroclimatology: Should we have the blues? Experiments from Scotland. Dendrochronologia, 32 (3), 191–204.

Schröder J (2013): Zum Einfluss der Witterung auf Wuchsverhalten und Vitalität der Trauben-Eiche. Habilitationsschrift. TU Dresden.

# From Provenance to Performance: Scots Pine Wood Quality in a Changing Environment

**Monika Sołoniewicz**[1], **Aneta Skręta**[1], **Agnieszka Jankowska**[1], **Paweł Kozakiewicz**[1]

[1]Warsaw University of Life Sciences, Institute of Wood Sciences and Furniture
monika_soloniewicz@sggw.edu.pl, aneta_skreta@sggw.edu.pl,
agnieszka_jankowska@sggw.edu.pl, pawel_kozakiewicz@sggw.edu.pl

## Background

Scots pine (*Pinus sylvestris* L.) is one of the most widely distributed and economically important forest tree species in Europe. Its wood is extensively used as a raw material, while considerable variation in wood properties may occur among populations originating from different geographic regions. Understanding the sources of variation in wood quality is important for predicting the technical performance and potential utilization of timber. This is particularly relevant under changing environmental conditions, where the selection of well-adapted and productive forest genetic resources is becoming increasingly important. Although numerous studies have investigated the mechanical properties of Scots pine (Mederski et al., 2015; Krzosek et al., 2020; Kozakiewicz et al., 2020; Regino et al., 2022), relatively little attention has been given to the influence of genetic variation among populations. Moreover, studies conducted under different environmental conditions may confound genetic and environmental effects, making it difficult to distinguish the contribution of provenance to variation in wood properties. Currently, the amount of comprehensive, long-term research that evaluates the mechanical performance of Scots pine wood from different provenances grown under uniform conditions, where genetic factors can be reliably isolated, is limited (Konofalska et al., 2021). This study evaluates selected physical and mechanical properties of Scots pine wood originating from different provenances grown in a comparative trial under uniform environmental conditions. The results will help determine the extent of provenance-related variation in wood quality and may support the identification of provenances with desirable technical properties for future forest management and wood utilization. Key technical terms used throughout the paper include: provenance, referring to the geographic and genetic origin of the tree population studied; modulus of elasticity (MOE), which reflects wood stiffness and resistance to elastic deformation; modulus of rupture (MOR), indicating the wood's strength at failure in bending; compression strength, meaning strength in compression along wood fibres direction.

**Keywords:** Provenance, wood quality, *Pinus sylvestris* L., common garden,

## Experimental

The research material was obtained from the comparative Scots pine (*Pinus sylvestris* L.) plot at the Rogów Forest Experimental Station established in 1966 by the Forest Research Institute. It includes progeny from 16 parent populations from the species' natural range in Poland. Located in central Poland (51°54'29" N, 19°54'46" E) at 160 m ASL, the site offers uniform soil and climate conditions, allowing observed variation to reflect provenance differences and phenotypic plasticity. This study examines nine provenances, with samples collected from 14–19 trees per provenance. From the trunk sections obtained from the basal part of the trunks, below breast height (1.3 m), small beams for static bending strength testing were cut with nominal dimensions of 20×20×300 mm, in accordance with the standard ISO 4471:1982. The beams were marked in relation to the north–south directions and distance from the pith. After the bending tests the samples of nominal dimensions 20x20x60 mm were cut for compression tests. Density determination was carried out in accordance with the standard ISO 13061-2:2014. The static bending strength test (MOR) (according to ISO 13061-2:2014), modulus of elasticity in static bending (MOE) (according to ISO 13061-4:2014) and compression strength (ISO/DIS 13061-17:2014) were performed using a standard INSTRON 3382 testing machine with the Instron Series IX/s Automated Materials Tester – Version 8.32.00 software.

## Results and Discussion

The results indicate significant provenance-related differences among wood samples 4-6 cm from the pith in wood density, bending strength, and modulus of elasticity (MOE), whereas compression strength did not differ significantly among provenances (Table 1). Rospuda had the highest density (589 kg/m³) and MOE (13,914 MPa), while Rogów showed the highest bending strength (151 MPa). Karsko and Starzyna generally exhibited the lowest values for bending strength and MOE. The homogeneous group notation suggests that some differences were statistically significant, particularly for density and MOE, while compression strength remained relatively consistent across all provenances. These results indicate that provenance may contribute to variation in selected technical properties of Scots pine wood, particularly density and stiffness, while compression strength appears to be less sensitive to provenance-related variation under the studied conditions.

Table 1. Homogenous subsets for density, bending strength moduls of elastisity (MOE) and compression strength in wood samples 4-6 cm from the pith in north (N3) and south (S3) directions.

| N3/S3 | Density | | Bending strength | | MOE | | Compression | |
|---|---|---|---|---|---|---|---|---|
| provenance | mean [kg/m3] | group | mean [MPa] | group | mean [MPa] | group | mean [MPa] | group |
| Rogów | 537 | a | 151 | c | 12381 | a | 38,7 | a |
| Bolewice | 559 | ab | 131 | ab | 12712 | ab | 37,3 | a |
| Janów Lubelski | 530 | a | 141 | bc | 11284 | a | 39,4 | a |
| Rospuda | 589 | b | 134 | ab | 13914 | b | 38 | a |
| Spała | 556 | ab | 127 | ab | 12035 | a | 36,5 | a |
| Karsko | 531 | a | 121 | a | 11746 | a | 37,7 | a |
| Starzyna | 535 | a | 119 | a | 11726 | a | 37,1 | a |
| Gubin | 563 | ab | 129 | ab | 12616 | ab | 38,8 | a |
| Tabórz | 538 | a | 129 | ab | 12437 | ab | 39,6 | a |

## Conclusions

Selected physical and mechanical properties of Scots pine wood grown under uniform environmental conditions vary according to parental origin. Identifying such provenance-related phenotypic variation may help select seed material capable of establishing productive stands and producing wood of desirable quality.

**References**

ISO 13061-2. Physical and Mechanical Properties of Wood. Test. Methods for Small Clear Wood Specimens. Part. 2: Determination of Density for Physical and Mechanical Tests; ISO: Geneva, Switzerland, 2014.

ISO 13061-3. Physical and Mechanical Properties of Wood. Test. Methods for Small Clear Wood Specimens. Part. 3: Determination of Ultimate Strength in Static Bending; ISO: Geneva, Switzerland, 2014.

ISO 13061-4. Physical and Mechanical Properties of Wood. Test. Methods for Small Clear Wood Specimens. Part. 4: Determination of Modulus of Elasticity in Static Bending; ISO: Geneva, Switzerland, 2014.

ISO 4471. Wood. Sampling Sample Trees and Logs for Determination of Physical and Mechanical Properties of Wood in Homogeneous Stands; ISO: Geneva, Switzerland, 1982.

ISO/DIS 13061-17:2014 Physical and mechanical properties of wood. Test methods for small clear wood specimens. Part 17: Determination of ultimate stress in compression parallel to grain. International Organization of Standardization, Geneva, Switzerland.

Konofalska, E., Kozakiewicz, P., Buraczyk, W., Szeligowski, H., Lachowicz, H. (2021). The technical quality of the wood of Scots pine (Pinus sylvestris L.) of diverse genetic origin. Forests, 12(5), 619.

Kozakiewicz, P., Jankowska, A., Mamiński, M., Marciszewska, K., Ciurzycki, W., Tulik, M. (2020). The wood of Scots pine (Pinus sylvestris L.) from post-agricultural lands has suitable properties for the timber industry. Forests, 11(10), 1033.

Krzosek, S., Burawska-Kupniewska, I., Mańkowski, P. (2020). The influence of Scots pine log type (Pinus sylvestris L.) on the mechanical properties of lumber. Forests, 11(12), 1257.

Mederski, P. S., Bembenek, M., Karaszewski, Z., Giefing, D. F., Sulima-Olejniczak, E., Rosinska, M., Lacka, A. (2015). Density and mechanical properties of Scots pine (Pinus sylvestris L.) wood from a seedling seed orchard. Drewno. Prace Naukowe. Doniesienia. Komunikaty, 58(195).

Regino, K., Jaak, P., Ahto, K. (2022). Effect of growth conditions on wood properties of Scots pine (Pinus sylvestris L.). Forestry Sudies Tom 75. Zeszyt: 176 – 187.

# Fifty Year Climate Trends of the Wood Decay Hazard in Sweden

**Simon Curling**[1], **Penny Mesa**[1], **Dennis Jones**[2]

[1]BioComposites Centre, Bangor University, Bangor Gwynedd United Kingdom
[2]DJ Timber Consultancy, Neath, United Kingdom

## Background

As climate change proceeds, Europe is becoming on average warmer and wetter. This creates enhanced conditions for wood decay in areas that may traditionally have not had to consider the risk to both construction and heritage assets. Atlantic coast areas of Europe e.g. the United Kingdom (Curling and Ormondroyd 2020) are particularly affected but even in more northern regions, effects will be seen. This paper therefore considers actual historic data from across Sweden to determine the historic risk of wood decay based on the Scheffer climate index (Scheffer 1971). This index is a broad brush approach and does not take into account local microclimates such as in Dose response methods (Marais *et al* 2021). However, the data is valuable as it uses historic data to assess past hazards and projects forward to highlight risks.

**Keywords:** Wood decay, Sweden, Prediction.

## Experimental

Data was obtained from the Swedish meteorological archive with daily temperatures and amounts of precipitation obtained and correlated. These data were used to calculate actual Scheffer Climate indices for decay for the 9 sites using the following equation (Scheffer (1971)

$$SCI = \frac{\sum_{Jan}^{Dec}[(T-2)(D-3)]}{16.7} \qquad \text{\{equation 1\}}$$

Where: SCI = Scheffer Climate Index, T = mean monthly temperature, D = mean number of days in the month with 0.25mm or more of rain. $\sum_{Jan}^{Dec}$ = the sum of the products for each month of the year.
Predicted change in precipitation and average temperature obtained from the Swedish Meteorological Institute were then used to estimate future indices by 2050 and 2100, using the RCP 2-4.5 climate scenario data.

## Results and Discussion

The historic data shows a clear difference in the sites based on latitude (Figure 1), with more southern sites showing higher indices. Over time the historic data also shows a clear increase in decay hazard again especially in the southern sites (Figure 2)

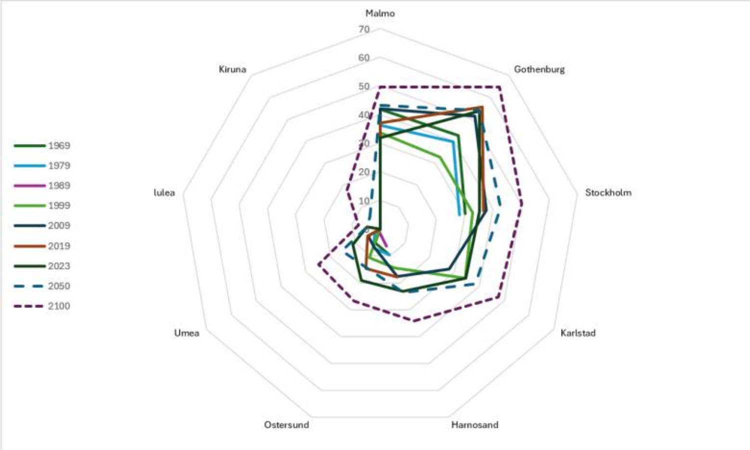


Figure 1. Radar Graph showing actual historic and predicted decay indices for 9 sites in Sweden

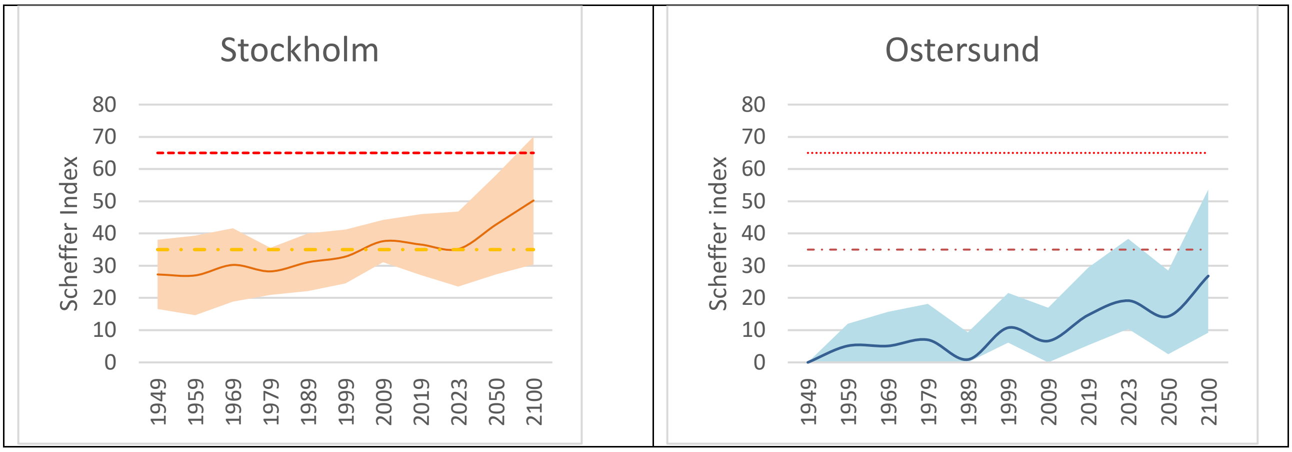


Figure 2. Historic and projected decay indices for Stockholm and Ostersund Mean values are shown with the shaded area denoting confidence range of data and projections. Lines for moderate risk (35) and high risk (65) are also shown

The projections show increased decay hazard with Stockholm moving from low to moderate and even high by 2100. Ostersund has changed from very low hazard to low with a possibility for moderate risk.

## Conclusions

Climate change is having a clear effect on the ability of fungi to grow and decay wood above ground throughout Europe. This data shows that there has been a gradual increase in decay hazard in Sweden over time. This is projected to continue with even the northern latitudes of Sweden having risks for the decay of wood by 2100.

## References

Marais, B.N.; van Niekerk, P.B.; Brischke, C. (2021) Studies into Fungal Decay of Wood in Ground Contact—Part 2: Development of a Dose–Response Model to Predict Decay Rate. *Forests*

Curling, S.F., Ormondroyd, G.A. Observed and projected changes in the climate based decay hazard of timber in the United Kingdom. *Sci Rep* **10**, 16287 (2020).

Scheffer, TC (1971): A climate index for estimating potential for decay in wood structures above ground. *Forest Products Journal* **21**:25-31.

# POSTER SESSION

# Development of Sustainable Bio-Based Materials for 3D Printing Applications from Organic Waste

**Artis Krikovs**[1], **Oskars Platnieks**[1], **Sergejs Gaidukovs**[1]

[1]Institute of Chemistry and Chemical Technology, Riga Technical University, Latvia, artis.krikovs@rtu.lv, oskars.platnieks_1@rtu.lv, sergejs.gaidukovs@rtu.lv.

## Background

Cellulose is a renewable biopolymer and a promising feedstock for replacing petroleum-derived polymers in additive manufacturing, particularly when recovered from wood, agricultural residues, and organic waste. Its high strength, biodegradability, and recyclability make waste-derived cellulose attractive for sustainable 3D-printed materials. However, cellulose cannot be conventionally melted and is poorly soluble in common solvents because of its extensive intra- and intermolecular hydrogen-bonding network. Keratin is another abundant renewable biopolymer, found in waste materials such as wool, hair, and chicken feathers; although its limited solubility and relatively poor mechanical properties present challenges for processing, keratin can be combined with cellulose to produce biodegradable composite materials with potentially improved structural and functional properties. (Acharya et al., 2021; Tran et al., 2016).

Ionic liquids (ILs) have enabled non-derivatizing cellulose and keratin dissolution and regeneration, with solvent-polymer interactions strongly influenced by the anion, water content, crystallinity, and degree of polymerization (Isik et al., 2014; Zhu et al., 2006). Both, dissolved cellulose and keratin have already been demonstrated in 3D printing, although printability depends strongly on viscosity, extrusion conditions, and coagulation (Markstedt et al., 2014; Poluri et al., 2025).

The systematic relationship between diverse waste-derived natural polymer feedstocks, solvent chemistry, dissolution efficiency, and properties required for 3D printing are not sufficiently understood. This study therefore investigates the dissolution of wood cellulose feedstock in combination with wool keratin using selected ILs, with the aim of identifying solvent–feedstock combinations suitable for producing processable, regenerated organic materials and future pellet or filament feedstocks.

**Keywords:** cellulose, wood waste, keratin, ionic liquid, additive manufacturing.

## Experimental

Keratin derived from waste wool, cellulose obtained from wood dust, and the ionic liquid 1-(carboxymethyl)pyridinium chloride were combined at different component ratios. The resulting mixtures were cast into films and characterized for their mechanical and thermal properties. Tensile properties were evaluated using a Tinius Olsen 25ST universal testing machine at a crosshead speed of 1 mm/min. Dynamic mechanical analysis (DMA) was performed using a Mettler Toledo instrument over a temperature range of -70 to 100 ℃ at 3 ℃/min to determine the glass transition temperature (Tg).

## Results and Discussion

Figure 1 shows the cast film samples. Tensile testing demonstrated that increasing the cellulose content improved the mechanical properties of the films. The most pronounced improvement was observed when the cellulose-to-keratin ratio increased from 30:70 to 70:30, resulting in an elastic modulus of 268 MPa and an ultimate tensile strength of 2.58 MPa.

DMA analysis showed that increasing the cellulose content shifted the glass transition temperature (Tg) from approximately -20 ℃ to -30 ℃.

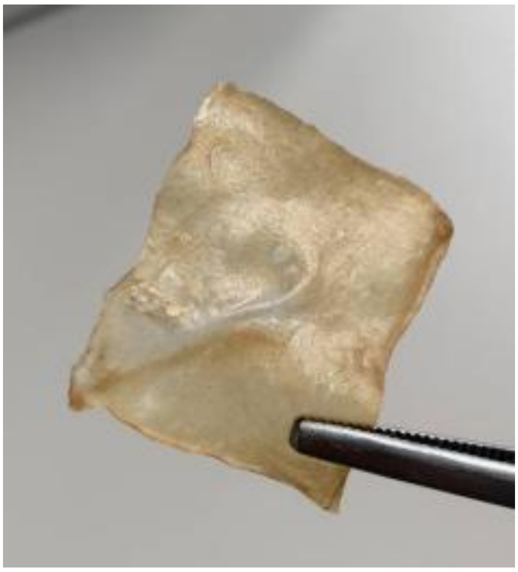

Figure 1. Casted film with 70:30 cellulose-to-keratin ratio

**Conclusions**

This work represents an ongoing study aimed at identifying the optimal ionic liquid and the appropriate cellulose-to-keratin and polymer-to-ionic-liquid ratios. Homogeneous mixtures were successfully prepared and cast into uniform films suitable for mechanical and thermal characterization. Increasing the cellulose content resulted in improved tensile properties, with the highest improvement observed at a cellulose-to-keratin ratio of 70:30.

**Acknowledgments**

This work was supported by the Latvian Council of Science in the famework of FLPP “Valorization of Ionic liquid processed cellulose waste for Optimized Lightweight Engineered Thermoplastics (VIOLET)” (lzp-2025/1-0585)

**References**

Acharya, S., S. Liyanage, P. Parajuli, S. S. Rumi, J. L. Shamshina, and N. Abidi. 2021. "Utilization of Cellulose to Its Full Potential: A Review on Cellulose Dissolution, Regeneration, and Applications." *Polymers (Basel)* 13 (24).

Tran, C. D., F. Prosenc, M. Franko, and G. Benzi. 2016. "Synthesis, structure and antimicrobial property of green composites from cellulose, wool, hair and chicken feather." *Carbohydr Polym* 151:1269-1276.

Isik, M., H. Sardon, and D. Mecerreyes. 2014. "Ionic liquids and cellulose: dissolution, chemical modification and preparation of new cellulosic materials." *Int J Mol Sci* 15 (7):11922-40.

Zhu, Shengdong, Yuanxin Wu, Qiming Chen, Ziniu Yu, Cunwen Wang, Shiwei Jin, Yigang Ding, and Gang Wu. 2006. "Dissolution of cellulose with ionic liquids and its application: a mini-review." *Green Chemistry* 8 (4).

Markstedt, Kajsa, Johan Sundberg, and Paul Gatenholm. 2014. "3D Bioprinting of Cellulose Structures from an Ionic Liquid." *3D Printing and Additive Manufacturing* 1 (3):115-121.

Poluri, N., J. Carter, J. Grasso, W. Miller, M. Leinbach, F. Durant, R. Benbrook, A. John, A. Wang, and X. Hu. 2025. "New Frontiers in 3D Printing Using Biocompatible Polymers." *Int J Mol Sci* 26 (16).

# Sensitivity of Visual Strength Grading to Connection-Derived Hole Patterns in Reclaimed Structural Timber under NS 3691-2025

**Ee Pin Choo[1], Dick Sandberg[2], Magnus Fredriksson[3], Vilma Zubinaite[4]**

[1,2,4] Department of Manufacturing and Civil Engineering, Norwegian University of Science and Technology, Gjøvik, Norway, ee.p.choo@ntnu.no, dick.sandberg@ntnu.no, vilma.zubinaite3@ntnu.no [3] Luleå University of Technology, Department of Engineering Sciences and Mathematics, Solid Mechanics, Sweden, magnus.1.fredriksson@ltu.se

## Background

Reclaimed structural timber carries damage from its previous service, such as holes from past connections, and its reusability depends on the extent of that damage. NS 3691 (NS, 2025a) is among the first standards to formalise the visual grading of reclaimed timber, providing a harmonised basis for reclassification. Prior assessment of reclaimed timber has largely been confined to pilot-scale studies or specific projects (Bergsagel & Heisel, 2023; Llana *et al.*, 2023; Nocetti *et al.*, 2024; Godina *et al.*, 2025; Kauniste *et al.*, 2025), leaving its behaviour over a broader population unexamined. Establishing this empirically would require impractical volumes of testing; simulation instead allows the formalised NS 3691 criteria to be applied across a large sawn-timber population. Simulation using X-ray computed tomography (CT) scanned logs has been used to model timber processing (Sandberg & Johansson, 2006; Fredriksson, 2015), though its application to reclaimed timber remains limited. Because grade depends on both service damage and a timber's natural features, identical damage can produce different grades dependent on the natural features of the sawn timber. This study examined how NS 3691 responds to service-induced damage in combination with natural features, simulated on digitally sawn boards of Norway spruce and Scots pine, characterising the resulting variation in grade and how it differs across damage configurations.

**Keywords:** wood; simulation; modelling, X-ray CT scanning

## Experimental

### Material

Board geometry and natural features (knots) of the sawn timber were drawn from the stem bank dataset (Grönlund *et al.*, 1995), composed of CT-scanned Norway spruce (*Picea abies* L. Karst.) and Scots pine (*Pinus sylvestris* L.) logs. A pool of 6982 digital boards was generated by simulated sawing and graded under the NS-INSTA 142 national standard (NS, 2009). Service-induced defects were modelled as circular holes representing typical floor-joist connections, described by diameter and position, with fastener spacing bounded by Eurocode 5 (CEN, 2004). Two connection classes were applied. The first placed 2 mm holes at fixed intervals (100–400 mm) along the narrow face; being below the standard's single-hole size limit, these affect grade only through their interaction with knots. The second represented end connections on the broad face, varying the concentration and diameter of holes placed vertically across the width of the board, such that at higher concentrations and sizes the grouped defect can exceed the standard's limits independently of the neighbouring features.

### Method

Each board had the service-induced defect data superimposed, then was graded under NS 3691-3 (NS, 2025b), both with and without natural features i.e. knots. The grading assigned one of three outcomes (R-grade) relative to the board's original grade (C-grade): maintain (*e.g.* C24 → R24), downgrade (*e.g.* C24 → R18s), or reject. The two defect classes were varied independently: interval spacing and end-connection configuration. Each class was set to "null" in turn, isolating the effect of each defect type. Without natural features, grading was deterministic (Table 1); with natural features, the same defect configurations produced non-uniform outcomes (Table 2). Comparing the tables isolates the effect of the interaction between service induced defects and natural features.

### Results and Discussion

Table 1. NS 3691-3 grading outcome for sawn timber without natural features (M: Maintain, D: Downgrade, R: Reject)

| Interval spacing (mm) | End connection configurations - No. of holes per connection, diameter (mm) | | | | | | | | | |
|---|---|---|---|---|---|---|---|---|---|---|
| | | 1 | | | 2 | | | 4 | | |
| | Null[1] | 4 mm | 6 mm | 7 mm | 4 mm | 6 mm | 7 mm | 4 mm | 6 mm | 7 mm |
| Null[1] | M | M | M | M | D | D | R | D | D | R |
| 400 | M | M | M | M | D | D | R | D | D | R |
| 300 | M | M | M | M | D | D | R | D | D | R |
| 200 | M | M | M | M | D | D | R | D | D | R |
| 100 | M | M | M | M | D | D | R | D | D | R |

Table 2. NS 3691-3 grading outcome for sawn timber with natural features, as a percentage of the population (n = 6982; 3491 Norway spruce, 3491 Scots pine)

| Interval Spacing (mm) | NS 3691-3 Outcome | End Connection Configurations - No. of holes per connection, diameter (mm) | | | | | | | | | |
|---|---|---|---|---|---|---|---|---|---|---|---|
| | | | 1 | | | 2 | | | 4 | | |
| | | Null[1] | 4 mm | 6 mm | 7 mm | 4 mm | 6 mm | 7 mm | 4 mm | 6 mm | 7 mm |
| Null[1] | Reject | - | - | - | - | 45.2 | 50.6 | 100.0 | 45.2 | 50.6 | 100.0 |
| | Downgrade | - | - | - | - | 54.8 | 49.4 | - | 54.8 | 49.4 | - |
| | Maintain | 100.0 | 100.0 | 100.0 | 100.0 | - | - | - | - | - | - |
| 400 | Reject | 75.6 | 75.6 | 75.6 | 75.6 | 81.1 | 82.7 | 100.0 | 81.1 | 82.7 | 100.0 |
| | Downgrade | 4.4 | 4.4 | 4.4 | 4.4 | 18.9 | 17.3 | - | 18.9 | 17.3 | - |
| | Maintain | 19.9 | 19.9 | 19.9 | 19.9 | - | - | - | - | - | - |
| 300 | Reject | 82.4 | 82.4 | 82.4 | 82.4 | 85.9 | 86.8 | 100.0 | 85.9 | 86.8 | 100.0 |
| | Downgrade | 4.0 | 4.0 | 4.0 | 4.0 | 14.1 | 13.2 | - | 14.1 | 13.2 | - |
| | Maintain | 13.6 | 13.6 | 13.6 | 13.6 | - | - | - | - | - | - |
| 200 | Reject | 89.1 | 89.1 | 89.1 | 89.1 | 90.6 | 91.2 | 100.0 | 90.6 | 91.2 | 100.0 |
| | Downgrade | 2.7 | 2.7 | 2.7 | 2.7 | 9.4 | 8.8 | - | 9.4 | 8.8 | - |
| | Maintain | 8.2 | 8.2 | 8.2 | 8.2 | - | - | - | - | - | - |
| 100 | Reject | 94.1 | 94.1 | 94.1 | 94.1 | 94.6 | 95.0 | 100.0 | 94.6 | 95.0 | 100.0 |
| | Downgrade | 1.5 | 1.5 | 1.5 | 1.5 | 5.4 | 5.0 | - | 5.4 | 5.0 | - |
| | Maintain | 4.3 | 4.3 | 4.3 | 4.3 | - | - | - | - | - | - |

1. Null indicates a defect class is turned off.

Table 1 shows the outcome without natural features i.e. knots: the best grade recoverable under each configuration. The inclusion of knots (Table 2) led to non-uniform outcomes, with identical damage producing different grades within the timber population. Two holes of 7 mm exceeded the grading limit on their own, rejecting every piece of timber regardless of knots. Interval-spaced 2 mm holes, well below the size limit (≤ 7 mm), also rejected most timber. Because such holes cannot fail the grade alone, rejection arises only where a hole coincides with a knot; decreasing the spacing increases the probability of their occurrence, with rejection easing from 94% at 100 mm to 75% at 400 mm as coincidences become less frequent. Identical defect patterns therefore yield different outcomes within the population, dependent on the intrinsic knot distribution of each piece of sawn timber. This raises the question of whether the same knot-driven variation occurs in other connection typologies, and whether it systematically biases the recovery towards certain species or knot structures. Establishing this will require a more detailed study across the reclaimed population.

**References**

Bergsagel, D., & Heisel, F. (2023). Structural design using reclaimed wood – A case study and proposed design procedure. *Journal of Cleaner Production*, *420*, 138316. https://doi.org/10.1016/j.jclepro.2023.138316

CEN (2014). EN 1995-1-1:2004+A2:2014, Eurocode 5: Design of timber structures - Part 1-1: General - Common rules and rules for buildings. *The European Committee for Standardization (CEN), Brussels*

Fredriksson, M. (2015). Optimizing sawing of boards for furniture production using CT log scanning. Journal of Wood Science, 61(5), 474–480. https://doi.org/10.1007/s10086-015-1500-0

Godina, M., Gowler, P., Rose, C. M., Wiegand, E., Mills, H. F., Koronaki, A., Ramage, M. H., & Shah, D. U. (2025). Strategies for salvaging and repurposing timber elements from existing buildings in the UK. *Journal of Cleaner Production*, *489*, 144629. https://doi.org/10.1016/j.jclepro.2024.144629

Grönlund, A., Björklund, L., Grundberg, S., Berggren, G., (1995). Manual för Furustambank [The Scots pine stembank]. Technical Report 1995:19. *Luleå University of Technology. Luleå, Sweden.*

Kauniste, M., Saarelaan, T., Just, A., & Tuhkanen, E. (2025). Assessment of strength and stiffness properties of reclaimed structural timber of Norway spruce. *World Conference on Timber Engineering 2025*, 3484–3493. https://doi.org/10.52202/080513-0427

Llana, D. F., Íñiguez-González, G., Plos, M., & Turk, G. (2023). Grading of recovered Norway spruce (*Picea abies*) timber for structural purposes. *Construction and Building Materials*, *398*, 132440. https://doi.org/10.1016/j.conbuildmat.2023.132440

Nocetti, M., Aminti, G., Vicario, M., & Brunetti, M. (2024). Mechanical properties of ancient wood structural elements assessed by visual and machine strength grading. *Construction and Building Materials*, *411*, 134418. https://doi.org/10.1016/j.conbuildmat.2023.134418

NS (2009). NS-INSTA 142, Nordic visual strength grading rules for timber. *Standards Norway.*

NS (2025a). NS 3691, Evaluation of recycled timber — Parts 1-3. *Standards Norway.*

NS (2025b). NS 3691-3, Evaluation of recycled timber — Part 3: Visual strength grading. *Standards Norway.*

Sandberg, D., & Johansson, J. (2006). Simulation of the yield of knot-free components from Scots pine (*Pinus sylvestris* L.): A comparative study of star-sawing and square-sawing. *Wood Material Science and Engineering*, *1*(3–4), 108–115. https://doi.org/10.1080/17480270601089883

# Tailoring the Hygroscopic Properties of Bio-Based Insulation Materials to Enhance their Moisture Buffering

**Finnja Heidorn[1], Maria Fredriksson[1], Emil Engelund Thybring[2]**

[1]Lund University, Sweden, finnja.heidorn@byggtek.lth.se, maria.fredriksson@byggtek.lth.se, [2]University of Copenhagen, Denmark, eet@ign.ku.dk

## Background

Buildings present the sector with the highest environmental impact in the European Union, accounting for more than 30% of the total environmental footprint, 42% of energy consumption and about one third of material consumption (European Environment Agency 2024). The choice of construction materials is therefore decisive for reducing embodied emissions and operational energy demand. Bio-based insulation materials from renewable sources, such as wood fibres, have lower embodied carbon than conventional materials such as mineral wool (Liljenström et al. 2015, Hill et al. 2018). In addition to their lower embodied carbon, bio-based insulation materials differ from conventional ones in another important aspect: their hygroscopicity, resulting in increased hygrothermal mass. Hygrothermal mass refers to the capacity of hygroscopic materials to store and release energy, in the form of latent heat, through moisture absorption and desorption processes (Kaniotis & Nore 2017). These hygroscopic properties offer two potential benefits for building applications. First, latent heat exchange could potentially reduce heating and cooling demands in buildings (Kaniotis & Nore 2017, Ding et al. 2023). During periods of high humidity and low temperature, such as at nighttime, the material absorbs water vapour, releasing latent heat through the phase change. During the daytime, when temperatures are higher and humidity is lower, the water is desorbed, absorbing heat from the surroundings and creating a cooling effect. Second, hygroscopic materials can regulate moisture migration and accumulation within building envelopes, contributing to moisture safety and ensuring the health and safety of occupants (Verma et al. 2022). Leszmann et al. (2023) showed that modifications to the shape of the sorption isotherm can influence moisture management in building envelopes by shifting moisture uptake towards mould-relevant relative humidity ranges of 60-90% RH. The resulting moisture robustness is therefore influenced by the sorption isotherm, together with other material properties such as vapour diffusion resistance.
Although wood exhibits different moisture sorption properties compared with conventional insulation materials, its heat storage capacity through moisture sorption remains relatively low. To enhance its thermal storage capacity, phase change materials (PCMs), such as coconut oil, have been combined with wood, providing additional heat storage for energy management in buildings (Nazari et al. 2022, Palanti et al. 2022). Alternatively, the hygroscopic properties of wood can be modified directly. Ding et al. (2023) achieved increased hygroscopicity by incorporating calcium chloride ($CaCl_2$) into wood, resulting in improved humidity and temperature regulation. Building on this approach, the greater aim of this research is to tailor the moisture sorption behaviour of bio-based insulation materials for specific applications in different wall assemblies, thereby enhancing both energy and moisture management. This can be realised through three modification strategies: the addition of hygroscopic additives (e.g. salts), chemical modification to increase the number of sorption sites for water uptake, or structural modification by increasing porosity and/or

internal surface area. These strategies aim to alter moisture sorption properties, such as the shape of the sorption isotherm and moisture transport through the material. Coupled with hygrothermal modelling, they can be used to identify favourable moisture sorption properties for different wall assemblies. As a first approach, sodium chloride (NaCl) was incorporated into wood fibres as a hygroscopic additive.

**Keywords:** Bio-Based, Insulation, Modification, Moisture, Sorption, Wood Fibre

## Experimental

Raw wood fibres without additives supplied by Hunton were used as the raw material. To incorporate the salt, the wood fibres were immersed in a saturated NaCl solution for 15 min under vacuum and afterwards for at least 24 h. Sorption isotherms at 20°C were determined using an automated sorption balance (DVS Advantage, Surface Measurement Systems Ltd., London) with a fixed time period for each RH step (see e.g. Williams 1995). The differential enthalpy of mixing during moisture absorption at 20°C was investigated using a new, unpublished design of a sorption calorimeter based on the same principle as that described by Wadsö & Markova (2000, 2002).

## Results and Discussion

The sorption isotherms of wood fibres, NaCl and both components combined are shown in Figure 1.

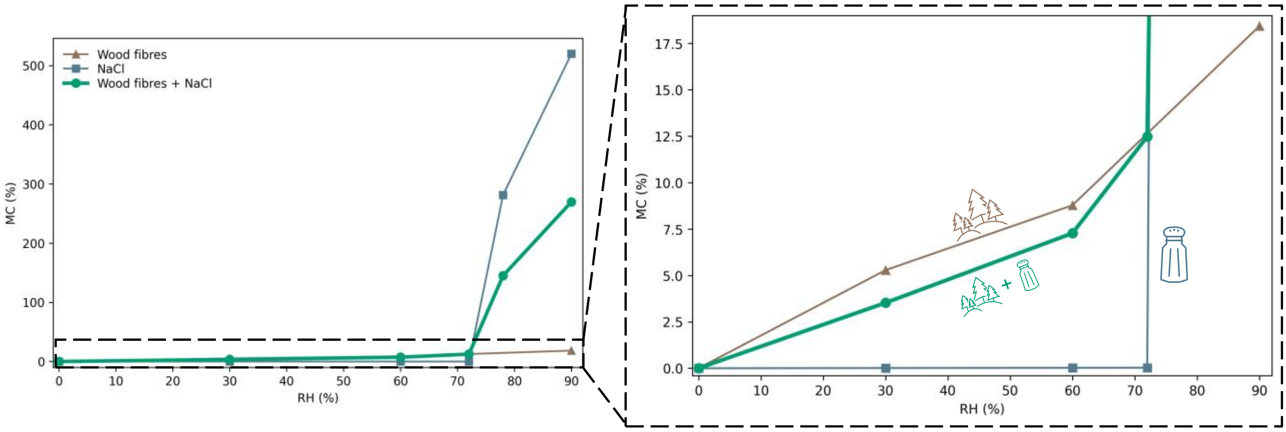


Figure 1. Absorption isotherms of wood fibres, NaCl, and wood fibres with incorporated NaCl at 20°C, showing moisture content (MC) as a function of relative humidity (RH)

The wood fibres show continuous water uptake across the investigated RH range up to 90% RH, while NaCl starts absorbing water around its deliquescence point at approximately 75% RH. The sorption curve of the wood fibres with incorporated NaCl combine the water uptake behaviour of both components. The introduced salt causes a steep change in the slope of the sorption isotherm at its deliquescence point.

## Conclusions

Incorporating NaCl into wood fibres allowed the shape of the sorption isotherm to be modified, demonstrating the feasibility of tailoring the moisture sorption behaviour of raw materials.

**References**

Ding Y, Dreimol CH, Zboray R, Tu K, Stucki S, Keplinger T, Burgert I (2023) Passive climate regulation with transpiring wood for buildings with increased energy efficiency. Materials Horizons 10: 257-267.

European Environment Agency (2024) Addressing the environmental and climate footprint of buildings.

Hill C, Norton A, Dibdiakova J (2018) A comparison of the environmental impacts of different categories of insulation materials. Energy and Buildings 162: 12-20.

Kraniotis D, Nore K (2017) Latent heat phenomena in buildings and potential integration into energy balance. Procedia Environmental Sciences 38: 364-371.

Leszmann AE, Morelli M, Rasmussen TV (2023) Moisture performance requirements for insulation in exterior wood-frame walls without a vapour barrier. Journal of Physics: Conference Series 2654: 012115.

Liljenström C, Malmqvist T, Erlandsson M, Fredén J, Adolfsson I, Larsson G, Brogren M (2015) Byggandets klimatpåverkan: Livscykelberäkning av klimatpåverkan och energianvändning för ett nyproducerat energieffektivt flerbostadshus i betong. Sveriges Byggindustrier.

Nazari M, Jebrane M, Terziev N (2022) Solid wood impregnated with a bio-based phase change material for low temperature energy storage in building application. Journal of Thermal Analysis and Calorimetry 147: 10677-10692.

Palanti S, Temiz A, Köse Demirel G, Hekimoğlu G, Sarı A, Nazari M, Terziev N (2022) Bio-based phase change materials for wooden building applications. Forests 13: 603.

Verma SK, Anand Y, Gupta N, Jindal BB, Tyagi VV, Anand S (2022) Hygrothermal dynamics for developing energy-efficient buildings: Building materials and ventilation system considerations. Energy and Buildings 260: 111932.

Wadsö L, Markova N (2000) A double twin isothermal microcalorimeter. Thermochimica Acta 360: 101-107.

Wadsö L, Markova N (2002) A method to simultaneously determine sorption isotherms and sorption enthalpies with a double twin microcalorimeter. Review of Scientific Instruments 73: 2743-2754.

Williams DR (1995) The characterisation of powders by gravimetric water vapour sorption. International Labmate 20: 40-40.

# Pyrolytic Analysis (PY/GC-MS) of Selected Parts of Common Yew (*Taxus baccata* L.) to Identify Present Compounds

**Grzegorz Mosiej**[1], **Jan Szadkowski**[2]

[1]Faculty of Wood Technology, Warsaw University of Life Sciences, Poland, s221974@sggw.edu.pl
[2]Department of Wood Science and Wood Preservation, Institute of Wood Science and Furniture, Warsaw University of Life Sciences, Poland, jan_szadkowski@sggw.edu.pl

## Background

As a natural material, wood is vulnerable to degradation under the influence of various biotic and abiotic factors. Such degradation can lead to fungal growth, structural damage, and deterioration of the mechanical properties of wood. Some compounds naturally occurring in plants such as terpenes, resins, alkaloids or essential oils have antimicrobial properties contribute to the natural protection of plants against biological degradation. The common yew is a toxic plant having high concentration of these compounds which might be used as wood preservatives. It is known, yew properties are primarily associated with taxine, a complex mixture of pseudoalkaloids. The aim of this study was to examine different anatomical parts of common yew and identify those containing the highest concentrations of toxic compounds, as well as to determine their chemical composition. The scope of the study includes the harvesting of yew wood, preparation of the material for testing by separating individual parts of the plant and grinding them, pyrolytic analysis, and interpretation of the results obtained.

**Keywords:** pyrolysis, wood, yew.

## Experimental

The common yew plant used in the experiment was obtained from the territory of the Warsaw University of Life Sciences. The material was seasoned for three months before testing. The material was separated into five parts: bark, phloem, wood, young branches and needles. Each part was ground in a mill to the same fraction size. Material was dried at low temperatures. The samples were then analyzed using a gas chromatograph coupled with a mass spectrometer and equipped with a Frontier Lab EGA/PY-3030D pyrolyzer. The samples were analyzed using GC/MS Solution version 2.72 with NIST 11a and NIST11b mass spectral libraries.

## Results and Discussion

The average content of toxic compounds across all anatomical parts was estimated at approximately 65%. The highest concentration of toxic compounds, based on the ratio of surface area to peak height, was found in yew phloem. The highest quantity of various toxic compounds was observed in the needles. Figure 1. shows the chromatograms of the PY/GC-MS analysis for the individual compounds of the common yew: first line – wood, second line – branches, third line – needles, fourth line – bark, fifth line – phloem.
The highest peaks were identified for wood, then numbered and the name of the detected compound were determined. The remaining data was handled in the same way. For data clearness, no analogous numbering has been added to subsequent chromatograms.

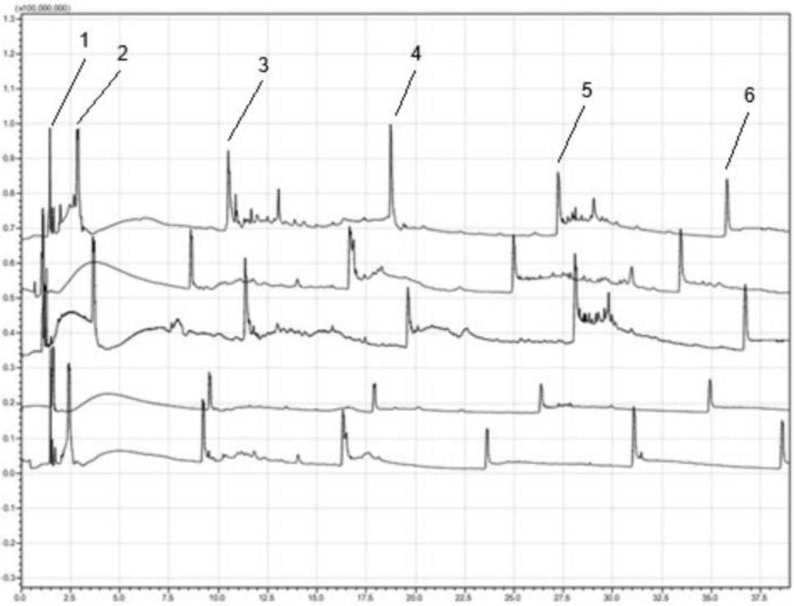


Figure 1. Combined chromatograms from the study (Identification for wood: compound 1 – Dimethylamine; compound 2 - Acetic acid, [(aminocarbonyl)amino]oxo-; compound 3 - Uramil-N, N-diacetic acid; compound 4 - .alpha.-L-Galactopyranoside, methyl 6-deoxy-; compound 5 - cis-1,2-Cyclohexanediol; compound 6 - Uramil-N, N-diacetic acid)

Different wilting peaks were observed for different anatomical parts of common yew wood. These differences result from the content of individual chemical components produced by the plant throughout its life and their storage in cellular organelles. Some chemical compounds are remodeled during the plant's life, transforming into various derivatives. According to available literature, toxic substances are found in all parts of the yew's anatomy. Literature indicates that yew contains toxic substances such as taxines, alkaloids, grayanotoxins, etc. These compounds pose a significant threat to the lives of humans, animals and other organisms.

## Conclusions

In all parts of the yew, protective compounds were found. Phenol and its derivatives were the most common compounds and were present in all parts of the plant. The most significant number of different compounds was found in young branches. The most common groups found in the research were: resins, phenols, carboxylic acids, and their derivatives.

**References**

Appendino G, (1996) Chapter Two Taxine 237-268. Via Giuria 9, 1-10125 Torino, Italy.

Barbero-López A, Akkanen J, Lappalainen R, Peräniemi S, Haapala A, (2021) Bio-based wood preservatives: Their efficiency, leaching and ecotoxicity compared to a commercial wood preservative. ScienceDirect, Science of The Total Environment, Volume 753, 142013, DOI - 10.1016/j.scitotenv.2020.142013.

Betlej I, Andres B, Krajewski K, Kiełtyka-Dadsiewicz A, Boruszewski P, Szadkowska D, Zawadzki J, Radomski A, Borysiuk P, (2023) The effect of Ethanol Extracts and Essential Oils Obtained from Different Varieties of Mint on Wood Molding. Forests 2023, 14(8), 1522, DOI - 10.3390/f14081522.

Hu Z, Chen J, Jiang S, Liu Z, Ge S, Zhang Z, (2019) Chemical components and functions of Taxus chinensis extract. Journal of King Saud University, 32 (2); 1562- 1568, DOI - 10.1016/j.jksus.2019.12.012.

Kirker GT, Hassan B, Mankowski ME, Eller FJ, (2024) Critical Review on the Use of Extractives of Naturally Durable Woods as Natural Wood Protectants. Insects, 15(1), 69, DOI - 10.3390/insects15010069.

Klećkowska-Nawrot J, Nowaczyk R, Chrószcz A, Janeczek M, (2013) Ziołolecznictwo w medycynie weterynaryjnej 217-239. Zakład Anatomii Zwierząt, Katedra Biostruktury i Fizjologii Zwierząt, Wydział Medycyny Weterynaryjnej, Uniwersytet Przyrodniczy we Wrocławiu.

Krajewski A, Witomski P, (2005) Ochrona drewna surowca i materiału, Czynniki powodujące niszczenie drewna. Wydawnictwo SGGW, Warszawa.

Król B, Kiełtyka-Dadasiewicz A, (2015) Wpływ metody suszenia na cechy sensoryczne oraz skład olejku eterycznego tymianku właściwego (*Thymus vulgaris* L.). Żywność. Nauka. Technologia. Jakość, 2015, 4 (101), DOI - 10.15193/ZNTJ/2015/101/064.

Kula K, Rojek S, Klementowicz W, Kłys M, Konopka T, (2009) Analiza alkaloidów cisa pospolitego w materiale biologicznym z zastosowaniem metod chromatograficznych. Katedra i Zakład Medycyny Sądowej UJ CM, Kraków.

Nižnanský Ľ, Osinová D, Kuruc R, Hengerics Szabó A, Szórádová A, Masár M, Nižnanská Ž, (2022) Natural Taxanes: From Plant Composition to Human Pharmacology and Toxicity. International Journal of Molecular Sciences, 23(24), 15619, DOI - 10.3390/ijms232415619.

Suchocka M, (2011) Człowiek i Środowisko 35 (3-4), s. 19-34 Instytut Gospodarki Przestrzennej i Mieszkalnictwa, Warszawa.

Wilson CR, Sauer JM, Hooser SB, (2001) Taxines: a review of the mechanism and toxicity of yew (Taxus spp.) alkaloids. ScienceDirect, Toxicon, Volume 39, Issues 2–3, Pages 175-185, DOI - 10.1016/S0041-0101(00)00146-X.

# Effects of Flame-Retardant Treated Substrates on the Formation of Mycelium-Based Composites

**Jie Li[1], Percy Festus Alao[1], Heikko Kallakas[1], Jaan Kers[1]**

[1]Tallinn University of Technology, Estonia, jie.li@taltech.ee, percy.alao@taltech.ee, heikko.kallakas@taltech.ee, jaan.kers@taltech.ee

## Background

Mycelium-based composites (MBCs) are bio-based materials grown from fungal mycelium on lignocellulosic substrates such as wood-processing residues, and they are gaining increasing attention as sustainable alternatives for building materials (Motamedi et al. 2025). However, fire safety remains one of the main barriers to their wider application in construction (Irbe et al. 2024; Jones et al. 2018). Previous studies have shown that flame-retardant (FR) treatments can improve the fire performance of MBCs, but most existing approaches focus on post-treatment methods after panel formation (Figel et al. 2026), rather than on how FRs interact with fungal growth during composite development. At the same time, limited knowledge exists on how FR-treated substrates affect *Trametes versicolor* growth and MBC formation at the substrate-treatment stage, where biological compatibility and fire-related functionality must be balanced. To address this gap, the present study investigates substrate-level FR treatment as a route for producing fire-safe MBCs, with a focus on fungal compatibility, substrate pH, and preliminary panel formation behavior.

**Keywords:** biomaterials, fire retardant, fungal compatibility, fire safety.

## Experimental

The FRs supplied by our industrial partners are listed in Table 1. Birch substrate, with an initial pH of 5.94 and a particle size of approximately 1 mm, was used in this study. First, the pH of the FR solutions at different FR concentrations (10%, 5% and 1%) was measured using a SevenCompact pH meter S210. Next, the FR-treated substrate was prepared by mixing birch substrate with the FR solution to reach approximately 65% moisture content, followed by sterilization. The treated substrate was then extracted by suspending 1 g of substrate in 20 mL of distilled water for 24 h, and the pH of the supernatant was measured. *T. versicolor* was subsequently used to evaluate fungal compatibility and panel formation through preliminary small-scale MBC trials at different FR concentrations.

Table 1. Basic information of the flame-retardant formulations

| Flame retardant code | Type |
|---|---|
| **CP45** | Ammonium polyphosphate-based liquid FR |
| **CP50** | Inorganic alkaline ammonium-free liquid FR |
| **APP161** | Solid ammonium polyphosphate-based FR |
| **PW620** | Proprietary phosphorus-containing solid mixture |

## Results and Discussion

Figure 1 shows that FR treatment altered the pH of the birch substrate extracts relative to the initial birch substrate pH (5.94). The effect depended on both the FR formulation and concentration. CP45, APP 161, and PW 620 kept the treated substrate extracts within a mildly acidic to near-neutral range, whereas CP50 produced the lowest extract pH values, remaining around pH 5.0-5.8 across the tested concentrations. Although no strictly linear concentration trend was observed, the results clearly indicate that FR loading changes the chemical environment of the substrate, which is the relevant condition for fungal colonization. This suggests that the effect of FR treatment should be evaluated based on the treated substrate rather than the original FR formulation alone.

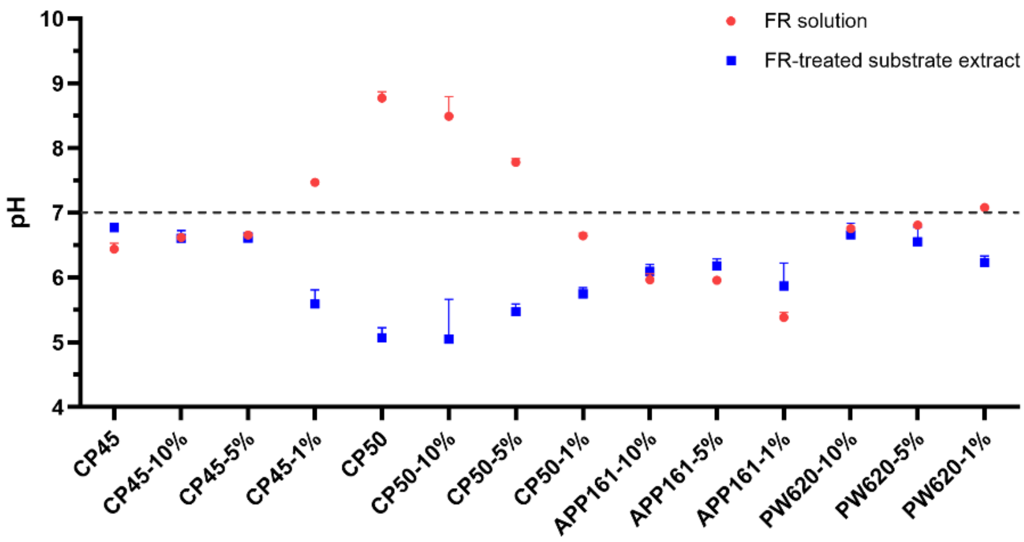


Figure 1. pH of FR solutions and FR-treated birch substrate extracts

The preliminary cultivation trials also revealed a concentration-dependent compatibility window. After 2 weeks of incubation, all 1% FR-treated substrates supported visible colonization by *T. versicolor*, indicating that low FR loading remained compatible with fungal growth under the current conditions. In contrast, 10% treatments were not suitable for reliable panel formation, suggesting that higher FR loading limits the ability of the fungus to establish stable growth. The 5% treatments showed intermediate behaviour and may still be worth further investigation, provided that the panel-production process becomes more stable and reproducible. Plate-based tests also showed that local contact with FR-treated substrate was less inhibitory than direct exposure in FR-containing medium, suggesting that fungal response depends on both FR type and exposure mode.

## Conclusions

Substrate-level flame-retardant treatment appears to be a promising route for producing mycelium-based composites, but its feasibility is limited to a relatively narrow compatibility window. The current results show that 1% FR treatment was the most compatible with *T. versicolor* growth, while 10% was not suitable for stable production under the conditions tested. The 5% level showed intermediate behaviour and may still be worth further investigation once the production process becomes more stable and reproducible. Future work will focus on FTIR characterization of the treated birch substrates to better understand the chemical changes caused by FR treatment, followed by fire-performance testing of the successfully produced panels.

**References**

Figel L, Besserer A, Nicolas B, Vahabi H (2026) Innovative fire-retardant sustainable mycelium composites developed from wood by-products. Available at SSRN 6049364.

Irbe I, Kirpluks M, Kampuss M, Andze L, Milbreta U, Filipova I (2024) Assessing the conformity of mycelium biocomposites for ecological insulation solutions. Materials 17(24): 6111.

Jones M, Bhat T, Huynh T, Kandare E, Yuen R, Wang CH, John S (2018) Waste-derived low-cost mycelium composite construction materials with improved fire safety. Fire and Materials 42(7): 816-25.

Motamedi S, Rousse DR, Promis G (2025) A review of mycelium bio-composites as energy-efficient sustainable building materials. Energies 18(16): 4225.

# A Thorough Insight into the Hyperlignification of Wood

**Kosma Jan Celmer**[1], **Sune Tjalfe Thomsen**[2], **Emil Engelund Thybring**[3]

[1,2,3]University of Copenhagen, Denmark, kjc@ign.ku.dk, stt@ign.ku.dk, eet@ign.ku.dk

## Background

Heterogeneity of technical lignins and their low degree of solubility in water or common solvents has long posed a problem in large-scale utilization of this abundant biogenic resource. However, the inherent protective features of lignin in the natural state of wood have inspired many attempts at using it as a natural protective measure of wood modification. The negative environmental impact of using biocide-based wood treatments, and legislative measures to phase out many of them creates a need for investigation into less harmful methods of protecting wood sourced from local species. Hyperligninfication of wood, a novel method of protective wood treatment using high-concentration lignin solutions developed at the University of Copenhagen is a possible answer to this problem. Previous attempts of treating wood with lignin have provided somewhat positive, but insufficient levels of protection, most often due to low concentrations of applied lignin solutions (Borrega 2022, Chrikova et al. 2011, dos Santos et al. 2012, Gordobil et al. 2017, Herrera et al. 2023, Sanson et al. 2022) or high leaching levels of lignins modified to enable higher solubility (Chrikova et al. 2011). In investigations into hyperlignification performed so far, the ability to create high percentage lignin solutions using simple organic solvents have been demonstrated, as well as treatment of small-scale samples, and hyperlignified wood has been characterized in terms of resistance to fungal decay (Rhodonia placenta, Fomitopsis pinicola), water uptake, penetration by light microscopy. The promising results of aforementioned tests have encouraged the further need for investigation at a larger scale. In-depth chemical analysis of the high lignin concentration fluids and the fluid-wood interactions have to be studied more in depth, to provide further insight into understanding the principles of the process. Moreover, characterization of the material resulting from the wood treatment is necessary. This study aims to define the necessary insights to further the understanding of the process and resulting material, proposing standardized tests and analytical methods, based on the results that have been obtained so far. Chemistry and rheology of the high lignin percentage fluids, wood modification mechanics resulting from hyperlignification, and decay inhibition of hyperlignified wood have to be defined.

**Keywords:** hyperlignification, wood protection, lignin.

## Experimental

Wood samples of a variety of species were used: beech (Fagus sylvatica L.), Scots pine (Pinus sylvestris L.), grand fir (Abies grandis Douglas ex D. Don), either cut into cuboids of dimensions 5 mm x 10 mm x 10 mm (L x H x W) or sticks of dimensions 100 mm x 25 mm x 25 mm (L x H x W). Various types of lignin were used: Kraft lignin (UPM BioPiva™ 100 lignin), Organosolv lignin (Aldrich, Product number: L165), soda lignin (Protobind 1000 and 2600, PLT Innovations, Switzerland). Lignin solutions were prepared using a BOJ (Spain) MC-2000 Thermo Blender. Hyperlignification of wood was performed either by vacuum impregnation in round-bottom flasks, or by vacuum pressure impregnation using a desiccator and Graco (USA) high-pressure tank system. Leaching of samples was performed using a modified EN 84 test. Samples for light microscopy investigations were prepared using a microtome.

**Results and Discussion**

Hyperlignification of cuboid wood samples led to a high mass gain, at 21-82% dry mass gain range after leaching in water, with levels dependent on the wood species and particular lignin fluid being used. In the larger stick samples, the levels remained similar, with an 18-77% dry mass gain range.

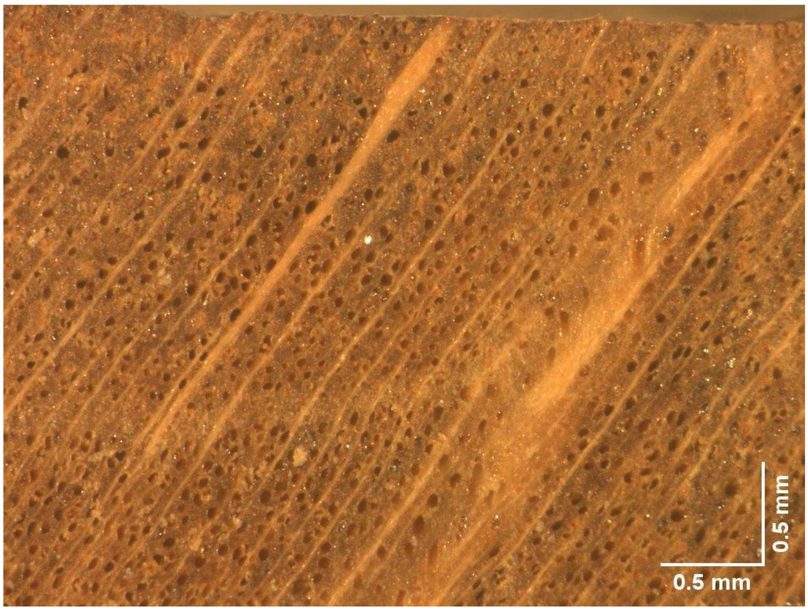


Figure 1. Light microscopy image of a hyperlignified beech sample

Light microscopy images indicate lumen and cell wall penetration of wood by added lignin. Cuboid samples of hyperlignified wood have shown less than 2% of mass loss after 10 weeks of decay by brown rot fungi, compared to a 45-62% range among untreated control samples.

**Conclusions**

Hyperlignification of wood is a promising novel method of wood preservation, which necessitates further investigation to understand the principles behind its functioning. Analytical chemistry of the novel lignin fluids, cell wall bulking and moisture exclusion efficiency tests, standardized fungal decay tests like the EN 113 will be performed.

**References**

Borrega M (2022) Impregnation of pinewood with softwood Kraft lignin, pre-print https://doi.org/10.21203/rs.3.rs-2305655/v1

Chirkova J, Anderson I, Irbe I, Spince B, Andersons B (2011) Lignins as agents for bio-protection of wood, Holzforschung 65:497

dos Santos PSB, Garcia A, de Cademartori PHG, Gatto DA, Labidi J (2012) Study of the use of organosolv lignin as bio-preservative of wood, Proceedings Annual Meeting International Research Group on Wood Protection, IRG/WP 12-30603

Gordobil O, Herrera R, Llano-Ponte R, Labidi J (2017) Esterified organosolv lignin as hydrophobic agent for use on wood products, Progress in Organic Coatings 103:143

Herrera R, Poohphajai F, Sandak A, Gordobil O (2023) Simultaneous improvement of surface wettability and UV resistance of wood with lignin-based treatments, Polymers, 15:3409

Sanson CSL, Helm CV, Magalhães WLE, de Muniz GIB, Missio AL, de Cademartori PHG (2022) Enhancing water repellency and decay resistance of wood by using water-soluble fractions separated from pyrolytic lignin of fast-pyrolysis bio-oil, Industrial Crops & Products 177:114540

# Potential of Chemically Pretreated and Thermomechanically Densified Wood of Different Tree Species in the Development of High - Added Value Biomaterials

**Krista Dimante**[1], **Laura Andze**[2]

[1]Latvian State Institute of Wood Chemistry, Latvia, krista.dimante@kki.lv, [2]Latvian State Institute of Wood Chemistry, Latvia, laura.andze@kki.lv

## Background

Wood modification via chemical pretreatment and thermomechanical densification is a promising approach for developing high-value-added biomaterials, as it significantly improves the wood's physical and mechanical properties. While the effectiveness of NaOH pretreatment has been demonstrated in previous studies, the influence of anatomical structure, chemical composition, and initial density - varying across tree species - on densification outcomes remains insufficiently explored. This study compares birch, aspen, beech, and hawthorn wood by analyzing the density, modulus of elasticity (MOE), and modulus of rupture (MOR) of the resulting material. The findings will improve understanding of the suitability of various wood species for producing sustainable, mechanically enhanced biomaterials.

**Keywords:** chemical pretreatment, wood densification, high-added value biomaterials.

## Experimental

A 1 M NaOH solution was used for the chemical pretreatment of the wood samples. The samples were placed under vacuum for 15 minutes to remove air from their structure, after which the NaOH solution was added under vacuum. After releasing the vacuum, the samples were left in the solution for one hour to allow impregnation. Subsequently, the samples were placed in autoclaves, covered with the 1 M NaOH solution, and treated in a glycerol bath at 145 °C for 10, 20, or 30 minutes. After treatment, the samples were rinsed with water until they reached neutral pH. The samples were then placed in a mold and densified at 100 °C and 25 MPa for 24 hours, followed by a cooling period under pressure for 6-8 hours. Density, the modulus of elasticity (MOE) and the modulus of rupture (MOR) were determined for the obtained samples.

## Results and Discussion

Density measurements demonstrated that, despite differences in initial density – from 450 $kg \cdot m^{-3}$ for aspen, 560 $kg \cdot m^{-3}$ for birch, and 680 $kg \cdot m^{-3}$ for beech to 770 $kg \cdot m^{-3}$ for hawthorn – all wood samples reached a density of approximately 1200-1250 $kg \cdot m^{-3}$ after densification. This value approaches the theoretical maximum density of wood, corresponding to a wood cell-wall density of approximately 1500 $kg \cdot m^{-3}$.
Chemical pretreatment followed by densification significantly improved the mechanical properties of all wood species. Aspen exhibited the greatest relative increase in the modulus of elasticity, increasing from 1450 MPa before densification to 29 400 MPa after densification, representing an approximately twenty-fold increase. However, among the

densified wood species, birch samples had the highest MOE, exceeding 30 000 MPa, whereas beech samples had the lowest, at approximately 18 000 MPa (Figure 1).

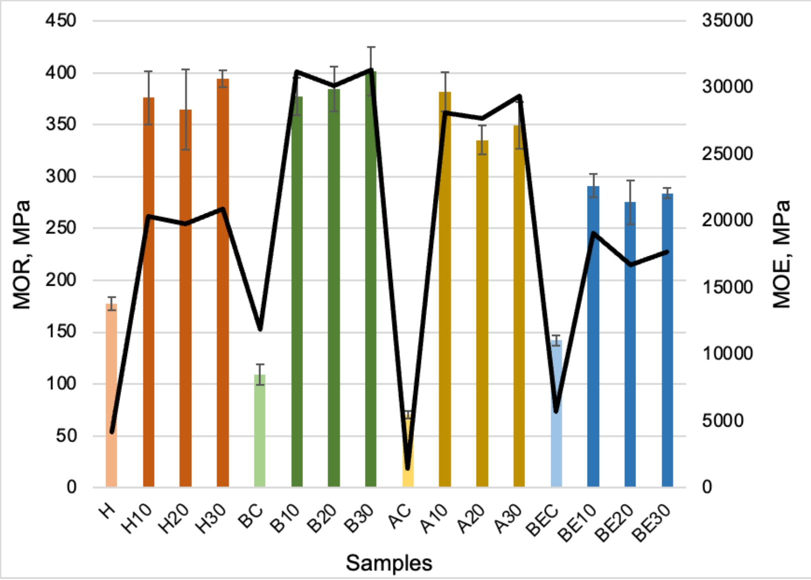


Figure 1. MOE (Young's modulus) of hawthorn (H, orange), birch (B, green), aspen (A, yellow), beech (BE, blue), and at different times (10, 20, 30 min), NaOH treated densified wood. MOR (strenght) - black line

Modulus of rupture (MOR) results indicate that the lowest values were obtained for BE samples. For example, BE10 reached 290 MPa, whereas the MOR for H10, B10 and A10 samples was approximately 380 MPa. This highlights distinct differences between wood species following densification.
Other authors, as Song et al. reported a more than tenfold increase in strength. But Alqrinawi et al. - an increase in MOE of up to 810 %, and Shi et al. - a 169 % increase in density. Andze et al. also describe similar densification efficiency.

## Conclusions

Chemical pretreatment and densification significantly improve the mechanical properties of wood, increasing the modulus of elasticity, bending strength, and density. Results vary among wood species, with a more pronounced densification effect observed in more porous, softer wood. Overall, this method holds promise for the development of high – value - added wood materials.

**References**

Alqrinawi H, Ahmed B, Wu Q, Lin H, Kameshwar S, Shayan M (2024) Effect of partial delignification and densification on chemical, morphological, and mechanical properties of wood: Structural property evolution. Industrial Crops and Products 213: 118430.

Andze L, Nefjodovs V, Andzs M, Skute M, Zoldners J, Kapickis M, Dubnika A, Locs J, Vetra J (2024) Chemically Pretreated Densification of Juniper Wood for Potential Use in Osteosynthesis Bone Implants. Journal of Functional Biomaterials 15(10): 287.

Shi J, Peng J, Huang Q, Cai L, Shi SQ (2020) Fabrication of densified wood via synergy of chemical pretreatment, hot-pressing and post mechanical fixation. Journal of Wood Science 66: 5.

Song, J.; Chen, C.; Zhu, S.; Zhu, M.; Dai, J.; Ray, U.; Li, Y.; Kuang, Y.; Li, Y.; Quispe, N.; et al. Processing Bulk Natural Wood into a High-Performance Structural Material. *Nature* 2018, *554*, 224–228.

# Investigation of Resin Pocket Exudation from Norway Spruce Sawnwood

**Matīss Ķevers[1,2], Edgars Kuka[1], Dace Cīrule[1], Ingeborga Andresone[1], Errj Sansonetti[1], Bruno Andersons[1]**

[1]Latvian State Institute of Wood Chemistry, Latvia, matisskevers@gmail.com, edgars.kuka@kki.lv, dace.cirule@kki.lv, ingeborga.andersone@kki.lv, errj.sansonetti@kki.lv, bruno.andersons@kki.lv
[2] University of Latvia, Latvia

### Background

Softwood products are very popular due to abundance of material and ecological impact, but defects can lower their quality and thus value (Jones et al. 2022). It is speculated that due to changes of weather patterns and or droughts the amount of resin pockets, at least in Norway spruce (*Picea abies* (L.) Karst.) have increased (Seifert et al. 2010), therefore lowering the quality of the material. In this study, we have taken closer look into the resin pockets found in Norway spruce and investigated their physical characteristics and evaluated condition at which the resin can exude form them. In addition, non-invasive possibilities of hidden resin pocket detection were investigated.

**Keywords:** Resin pockets, Norway spruce, Exudation, Wood defects

### Experimental

In the study, 24 sections measuring 100 mm × 100 mm × 500 mm were prepared from five beams of Norway spruce (*Picea abies* (L.) Karst.), which had the highest possibility of having hidden resin pockets based on various factors, mainly, high abundance of visible resin pockets. The sections were scanned by X-ray computed tomography (CT) at the CEITEC institute at Brno, Czech Republic. The obtained volume data was analysed using myVGL programme. From the CT data, the following characteristics of the resin pockets were obtained: dimensions (length, width, thickness) and location (annual ring, earlywood, latewood). The dimensions were measured by assuming that high density regions correspond to the resin pocket area (Oja et al. 1999). As all identified resin pockets (63 in total) had spherical cavities, their dimensions were measured and considered in the calculation of the total resin volume. For the exudation tests, the locations of the hidden resin pockets were marked on the corresponding sections, after which the wood covering the resin pocket was gradually removed using an electric planer. When the covering wood layer was about 5 mm, the planing of each subsequent 2 mm increment was followed by the surface heating with an infrared (IR) light up to 80-90 °C, maintaining it for 30 min and then cooling down. The process was controlled by thermal camera. The planning increment was reduced to 0.2 mm when the resin pocket covering wood layer was approximately 1 mm. The planing and heating steps were performed until seeping of resins was detected.

### Results and Discussion

The length (Figure 1a) and width (Figure 1b) of the resin pockets varied in cm range between and within beams, but the distribution in thickness (Figure 1c) was relatively small approximately within 1-2 mm range (Gjerdrum et el. 2007). At some extent, the width of the earlywood restricts the thickness of the resin pocket, as crossing of the latewood was not observed. No such restrictions are in the other directions (Somerville 1980). All resin pockets were type 1, according to Somerville (1980), and they were distributed in the earlywood mainly closer to the beginning of the growth ring. Furthermore, if one resin pocket was found in a specific growth ring there was high probability that there would be more.

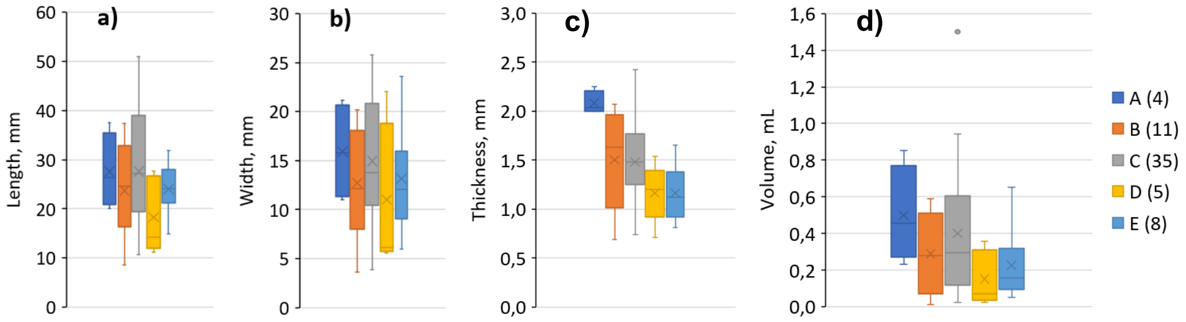


Figure 1. Dimensions (a) length, b) width, c) thickness, d) volume) of hidden resin pockets in the analysed beams (A, B, C, D, E) with the number of hidden resin pockets in each beam indicated in brackets; the minimum and maximum values are shown with dashes; the first and third quartile limits with rectangles; the line inside the rectangle is the median; the cross is the mean value

Not all of the volume of resin pocket was filled with resin (Figure 2) as there were spherical cavities occupying on average 12 % of the volume. These have not been reported for green wood and could be formed during drying of the wood. Considering them the average resin volume in a resin pocket was around 0.3 mL.

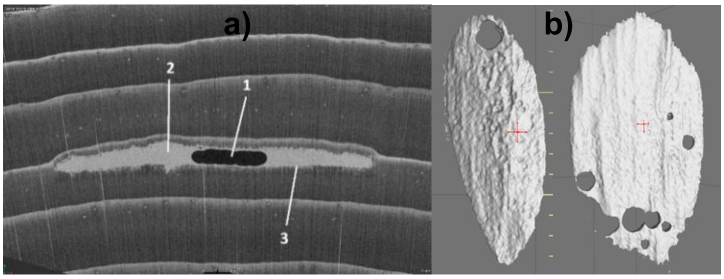


Figure 2. Computed tomography images of a) cross-section of a beam with a hidden resin pocket located at the end of earlywood formation: 1-enclosed cavity, 2-resin, 3-hard resin outer layer; b) resin in a hidden resin pocket

Exudation tests showed that resin pockets have to be opened for the resin to exude, which occurs when the temperature reaches 50 °C. If the cavities contain vapour, it may facilitate the exudation process due to vapour expansion when heating. The bordering lining of the resin pocket is made out of hard, crumbly resin (Figure 3) with similar or a slightly higher density than the resin in the pocket. The bordering lining could be responsible for no exudation of the resin before opening the resin pocket. The thickness of the hard resin layer was around 300 μm and it does not dissolve in acetone.

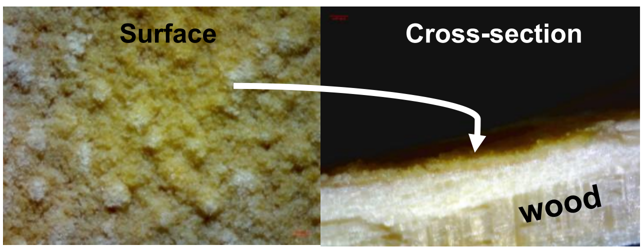


Figure 3. Resin pocket bordering lining

The hidden resin pockets were detected by CT, but this method is costly with limited accessibility for most manufacturers. During testing of the exudation process, it was observed that, if the resin pocket is located near the surface (still intact and invisible), it can be seen when heated and observed with thermal camera (Figure 4). With further dedicated research, the use of thermal imaging might be valid detection method for low-cost identification of hidden resin pockets.

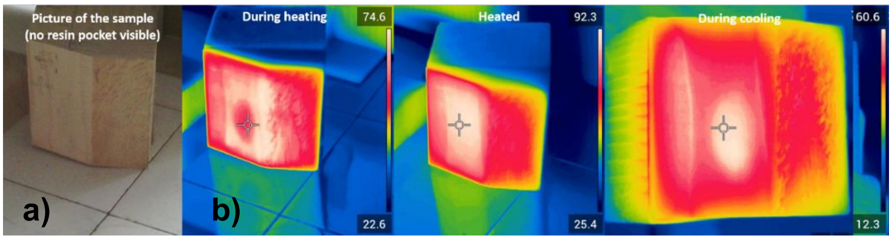


Figure 4. Wood sample with a hidden resin pocket: a) picture of wood sample, b) thermal camera images during heating, when heated to max temperature, and during cooling

## Conclusions

The resin pockets were of various size with limited variability in thickness. They were not completely filled with resin, but contained on average 12 % cavities. The average resin amount was around 0.3 mL. For a hidden resin pocket to exude, it has to be cut open and has to reach temperature of at least 50 °C for rapid exudation. Thermal imaging could be a viable method for close to the surface resin pocket identification.

## Acknowledgment

This project has received funding from Procurement Contract No. EKJ 02/01 “Study of features and modelling of conditions for preventing the risk of resin exudation” within the framework of project 2.2.1.3.i.0/1/24/A/CFLA/001 “Use of AI technologies for resin identification, classification and post-processing methods in the wooden furniture production process” and from the European Union’s Horizon Europe research and innovation programme under grant agreement No 101131765 (EXCITE2) for Transnational Access conducted at CEITEC Brno University of Technology.

## References

Gjerdrum P., Bernabei M. (2007) Three-dimensional model for size and location

Jones T.G., Yang J.I., McConchie D.L., Downes G.M. (2022) Predicting resin pockets and blemishes in radiata pine lumber from log properties. New Zealand Journal of Forestry Science 52.

of resin pockets in stems of Norway spruce Holz als Roh- und Werkstoff 65: 201–208.

Oja J., Temnerud E. (1999) The appearance of resin pockets in CT-images of Norway spruce (Picea abies (L.) Karst.) Holz als Roh- und Werkstoff 57: 400–406.

Seifert T., Brebeck J., Seifert S., Biber P. (2010) Resin pocket occurrence in Norway spruce depending on tree and climate variables. Forest Ecology and Management 260 (3): 302–312.

Somerville A. (1980) Resin pockets and related defect if Pinus Radiata grown in new Zealand. New Zealand Journal of Forestry Science. 10 (2): 439-444.

# Changes in Pine (*Pinus sylvestris* L.) Wood Induced by Aging

**Monta Druviņa[1,2], Lotārs Olivers Vasiļjevs[1,2], Edgars Kuka[1], Gundars Kalniņš[3], Dace Cīrule[1]**

[1]Latvian State Institute of Wood Chemistry, Dzerbenes street 27, LV-1006, Riga, Latvia
[2]University of Latvia, Jelgavas street 1, LV-1004, Riga, Latvia
[3]Cēsis Museum, Pils Square 9, LV-4101, Cēsis, Latvia
*monta.druvina@kki.lv

## Background

Wood is a natural and biodegradable material that has been used for human needs for many centuries. Over time, wood experiences both chemical and physical transformations (Kranitz et al. 2015, Matsuo et al. 2011, Fengel 1991). Understanding its long-term aging behaviour is important for evaluating degradation processes and developing effective conservation approaches (Nillson and Rowell 2012). This study investigates aging-related changes in pine (*Pinus sylvestris* L.) wood using samples obtained from the 15$^{th}$ century castle. The results provide valuable insights into the long-term aging of pine wood and contributes to its preservation, assessment and sustainable use in both historical and modern wooden structures.

**Keywords:** aged wood, pine wood, elemental composition, extractives, colour

## Experimental

As a research material, 8 pine (*Pinus sylvestris* L.) logs from the outer walls of the western tower of the Cēsis castle forecourt were used in the study. As a control, heartwood and sapwood of recent pine wood was used. Colour (CIELAB colour model) measurements from sample discs were taken using spectrophotometer. For chemical analyses, approximately 0.5 - 1.5 cm thick discs were cut and the elemental composition (C, O, H and N) of dry samples was analysed using an elemental analyser. To assess the potential influence of microorganisms, the samples were examined using scanning electron microscope (SEM). To analyze water-soluble extractives (WE), samples were dried, weighed into conical flasks and mixed with water in a 1:20 ratio (w/w), then stirred for 6 hours using a magnetic stirrer at room temperature. The extracts were filtered through a glass filter and the pH of the extracts was measured using a pH meter. The remaining material on the filter was rinsed with deionized water, which was combined with the extract, and diluted to volume of 200 mL. Content of carbohydrates in the extract were determined using Albalasmeh et al. (2013) method. Measurements were performed using UV-Vis spectrophotometer at a wavelength of 315 nm. Phenolic content was analysed using a method reported by Margraf et al. (2015). Absorption was measured using spectrophotometer at 725 nm.

## Results and Discussion

Analysis of the colour parameters (Fig.1) showed that recent pine heartwood and sapwood had high lightness values ($L^*$ = 74 – 83) compared to the aged samples ($L^*$ = 43 - 54), indicating darkening, which agrees with observations of others (e.g. Matsuo et al. 2011). In contrast, the chromatic components ($a^*$ and $b^*$) changed only slightly, suggesting that aging mainly affects the achromatic (lightness) component of wood colour. Accordingly, the total colour difference ($\Delta E^*ab$ = 20 - 40) between recent and aged wood was primarily determined by the decrease in the achromatic component, while the input of the chromatic components was minor. Similar discolouration trend was also reported by Xin et al. (2022) in their study of recent and aged larch and nanmu timber. These changes are likely related to oxidation (Matsuo et al. 2011, Kranitz et al. 2015).

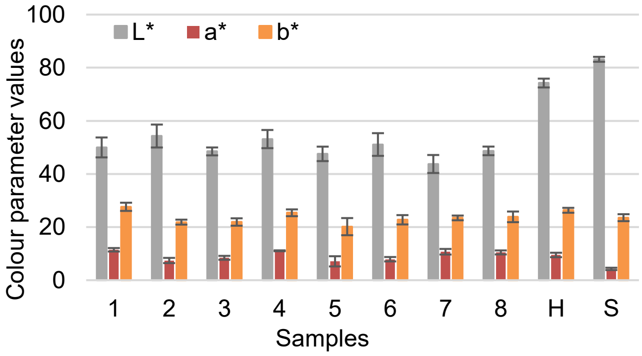


Figure 1. Colour parameter values: 1-8 aged samples, H-heartwood, S-sapwood

Comparing with recent pine, the carbon (C) mass fraction in aged wood samples decreased by approximately 6.8 – 13.7 %, while the oxygen (O) mass fraction increased by 9.7 – 19.3 %. Together with higher O/C ratio, these changes indicate prolonged oxidation and degradation of the wood structure, similar also observed by Mi et al. (2023) in their study of wood samples from Buddhist temple in China. The nitrogen (N) content increased from approximately 0.08 – 0.10 % in recent pine to 0.15 - 0.85 % in aged samples. Although signs of biological activity were not observed for all samples during SEM examination, increased N concentration implies activity of biological agents, which can contribute to wood degradation.

Table 1. Water-soluble extractives (WE)

| Sample | WE content, % | pH | Water-soluble carbohydrate content, % | Water-soluble phenolic content, % |
|---|---|---|---|---|
| **1** | 14.2 (0.2) | 9.6 (0.4) | 2.01 (0.08) | 0.038 (0.001) |
| **2** | 9.4 (0.2) | 7.3 (0.1) | 1.21 (0.07) | 0.037 (0.002) |
| **3** | 18.3 (0.3) | 8.5 (0.1) | 0.98 (0.06) | 0.009 (0.001) |
| **4** | 22.0 (0.6) | 9.3 (0.1) | 1.20 (0.06) | 0.000 (0.000) |
| **5** | 10.6 (0.2) | 8.5 (0.2) | 1.00 (0.04) | 0.029 (0.002) |
| **6** | 9.3 (1.2) | 8.1 (0.2) | 1.15 (0.12) | 0.037 (0.008) |
| **7** | 7.9 (0.6) | 7.4 (0.0) | 1.75 (0.12) | 0.033 (0.002) |
| **8** | 4.3 (0.4) | 8.1 (0.0) | 0.77 (0.09) | 0.018 (0.001) |
| **Heartwood** | 1.8 (0.4) | 4.3 (0.1) | 0.94 (0.13) | 0.020 (0.004) |
| **Sapwood** | 2.0 (0.4) | 4.2 (0.0) | 0.57 (0.03) | 0.010 (0.001) |

* Standart deviations are reported in parentheses.

Recent pine wood had a relatively low content of WE (<2 %) and an acidic pH (4.0 - 4.3), whereas aged pine samples showed significantly higher levels of WE, reaching up to 22 %, accompanied by a shift in pH towards neutral or alkaline conditions (7 - 10) (Table 1). A similar increase in pH was also observed by Hernandez (2013) in the study of recent and aged pine wood samples. These changes indicate the degradation of wood components and the accumulation of water-soluble products, as well as the activity of microorganisms during aging (Blanchette et al. 1989). Water extracts of recent pine contained lower concentrations of carbohydrates and phenolic compounds than aged pine samples, indicating a degradation of hemicellulose, cellulose and lignin (Aniza et al. 2026). Analyzing the total content of WE and the relative proportions of carbohydrates and phenolic compounds, it was seen that, while aged wood had higher total extractives content, the relative proportions of carbohydrates and phenols were lower than in recent wood, which suggests that aging promotes the accumulation of other water-soluble degradation products.

## Conclusions

The present study showed that, in terms of discolouration, natural aging mainly affects wood lightness. Aged wood is characterized by a decrease in carbon and the increase in oxygen and nitrogen content, indicating prolonged exposure to oxidation and biological activity. Increase in water-soluble extractives, pH and changes in concentrations of degradation products, suggests changes in lignin, cellulose and hemicellulose.

## References

Albalasmeh, A. A., Berhe, A. A., Ghezzehei, T. A (2013) A new method for rapid determination of carbohydrate and total carbon concentrations using UV spectrophotometry. Carbohydrate Polymers, 97 (2): 253–261.

Aniza, R., Petrissans, A., Petrissans, M (2026) Polymers and chemical composition of hardwood and softwood (bark, sapwood, and heartwood) for biofuel production: a comprehensive review. Polymers, 18 (11), 1340.

Blanchette, R. A., Nilsson, T., Daniel, G., Abad, A (1989) Biological degradation of wood. Archaeological Wood: 141–174.

Fengel, D (1991) Aging and fossilization of wood and its components. Wood Science and Technology, 25 (3): 153 – 177.

Hernandez, V (2013) Radiata pine pH and buffering capacity: effect of age and location in the stem. Ciencia y tecnología, 15 (1).

Kránitz, K., Sonderegger, W., Bues, C.-T., Niemz, P (2015) Effects of aging on wood: a literature review. Wood Science and Technology, 50 (1): 7–22.

Margraf, T., Karnopp, A. R., Rosso, N. D., Granato, D (2015) Comparison between folin ciocalteu and prussian blue assays to estimate the total phenolic content of juices and teas ussing 96-well microplates. Journal of Food Science, 80 (11): 2397–2403.

Matsuo, M., Yokoyama, M., Umemura, K., Sugiyama, J., Kawai, S., Gril, J., Kubodera, S., Mitsutani, T., Ozaki, H., Sakamoto, M., Imamura, M (2011) Aging of wood: analysis of colour changes during natural aging and heat treatment. Holzforschung, 65 (3).

Mi, X., Li, Y., Qin, X., Li, J (2023) Effects of natural weathering on aged wood from historic wooden building: diagnosis of the oxidative degradation. Heritage science, 11 (1).

Nillson, T., Rowell, R (2012) Historical wood – structure and properties. Journal of Cultural Heritag, 13(3): 5-9.

Xin, Z., Fu, R., Zong, Y., Ke, D., Zhang, H., Yu, Y., Zhang, W (2022) Effects of natural ageing on macroscopic physical and mechanical properties, chemical components and microscopic cell wall structure of ancient timber members. Construction and Building Materials 2022, 359: 1-11.

# Long-Term Re-use of Timber in Structures and The Effects Thereof

**Niklas Elsgaard[1], Emil Engelund Thybring[2], Ana Teresa Lima[1]**

[1]Danmarks Tekniske Universitet, Denmark, nikels@dtu.dk, [2] Københavns Universitet, Denmark, eet@ign.ku.dk [3] Danmarks Tekniske Universitet, Denmark, atmli@dtu.dk

## Background

Timber construction can retain biogenic carbon throughout a building's service life (Churkina et al., 2020). Reusing structural timber extends this storage while reducing demand for newly harvested wood (Köhne & Churkina, 2026). Reliable assessment of reused members is therefore important for circular timber use. However, most mechanical characterization covers periods that are short relative to structural service lives, and long-term predictions remain sensitive to test method and extrapolation model (Hoffmeyer & Sørensen, 2007; Naghdinasab et al., 2025; Svensson, 2009). Timber recovered from existing structures can provide evidence at realistic load durations, but material representing a member's original unloaded condition is rarely available. This study examines a within-beam method in which spatially separated regions of one member serve as internal references, reducing the variability introduced by unrelated control specimens (Svensson, 2009; Toumpanaki et al., 2021). In a simply supported beam, bending stress varies across both depth and length. The upper and lower zones experience compression and tension, respectively, while the neutral axis carries comparatively little longitudinal normal stress. Under a central point load, the bending moment increases linearly from zero at the supports to a maximum at midspan. Local wood structure can nevertheless disturb this idealized response (Forsberg et al., n.d.). The resulting spatial gradient provides a basis for testing whether sustained-load history can be detected within a single beam.

**Keywords:** timber reuse, duration of load, sustained bending, tensile testing

## Experimental

Eight C18 Scots pine beams measuring 38 × 73 × 2400 mm were subjected to three-point bending over a 2000 mm span for six months at 23 °C and 60% relative humidity. Five beams carried a freely suspended 46.5 kg mass, approximately 0.456 kN. Three beams were initially loaded with 173 kg, approximately 1.70 kN, and subsequently restrained at a fixed deflection. Supporting the mass after restraint allowed the reaction force to decrease through stress relaxation while maintaining the imposed geometry. For a central load (P) and span (L), the maximum moment is (PL/4); moments at the sampling positions follow the triangular distribution. Midspan deformation was recorded using a laser rangefinder with a stated accuracy of ±0.5 mm. Measurements were taken hourly during the first 24 hours, daily for the remainder of the first week, and weekly thereafter. Following unloading, the beams recovered for one month under the same climate. Beam C8 from the fixed-deflection group was selected for destructive sampling. It had been displaced to −77 mm at midspan, corresponding to an initial maximum moment of approximately 0.85 kNm. The moment subsequently decreased as the restraint force relaxed. C8 was divided into ten longitudinal subsections of approximately 210 mm. Each subsection supplied five specimens from each original compression, neutral, and tension zone, producing 150 specimens. The specimens had nominal 10 × 10 mm gripping regions and a central 4 × 4 mm waist. Waist dimensions, fracture locations, knots, grain deviations, and visible defects were documented and linked to a scan of the original beam. After one week of acclimatization, specimens were tested using an MTS servo-hydraulic frame with a calibrated 10 kN load cell. Jawhead movement was imposed at 1 mm/min until failure, while force, time, and movement were recorded at 68.27 Hz. Tests were video recorded for subsequent optical displacement analysis. For waist failures, nominal tensile strength was calculated as maximum force divided by measured waist area. Non-waist failures were classified separately.

**Results and Discussion**

The raw force–movement curves displayed substantial specimen variability and overlap among the compression, neutral, and tension zones. Several curves contained abrupt force reductions accompanied by audible fibre fracture, followed by renewed load increase. These events and the distinction between waist and non-waist failures require consistent classification. The unprocessed results therefore do not establish a systematic transverse-zone effect. Mapping the results to their original beam coordinates nevertheless revealed potentially informative spatial structure (Fig. 1). Specimens nearer midspan appeared to reach higher nominal stresses than specimens nearer the supports, qualitatively following the original bending-moment gradient. This tendency has not yet been quantified or separated from anatomical variability. Several locally inconsistent values coincided with small knots and grain deviation, indicating that defects may obscure a weaker load-history signal.

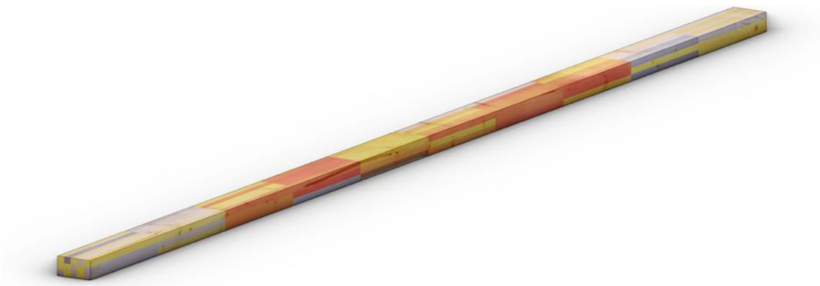

Figure 1. Preliminary tensile stress mapped onto the original scan of beam C8. Blue indicates lower and red higher values; colour contrast was uniformly amplified

**Conclusions**

This case study evaluates the use of a timber beam as its own spatial reference after sustained bending. Although the preliminary data do not resolve a compression-, neutral-, or tension-zone effect, the apparent longitudinal tendency and correspondence between local deviations and visible defects demonstrate the value of preserving specimen origin. The contribution is a traceable framework for separating possible load-history effects from natural wood heterogeneity. Fracture classification and defect-aware, section-matched analysis will determine whether the spatial signal can be quantified. The method provides a foundation for application to historic timber members for which original baseline properties are unavailable.

**References**

Churkina, G., Organschi, A., Reyer, C. P. O., Ruff, A., Vinke, K., Liu, Z., Reck, B. K., Graedel, T. E., & Schellnhuber, H. J. (2020). Buildings as a global carbon sink. In *Nature Sustainability* (Vol. 3, Number 4, pp. 269–276). Nature Research. https://doi.org/10.1038/s41893-019-0462-4

Elsgaard, N., & Lima, A. T. (2026). *Timber Metropolis: Cities as Carbon Retaining Ecosystems*.

Forsberg, F., Sjö Dahl, M., Mooser, R., Hack, E., & Wyss, P. (n.d.). *Full Three-Dimensional Strain Measurements on Wood Exposed to Three-Point Bending: Analysis by Use of Digital Volume Correlation Applied to Synchrotron Radiation Micro-Computed Tomography Image Data*.

Hoffmeyer, P., & Sørensen, J. D. (2007). Duration of load revisited. *Wood Science and Technology*, *41*(8), 687–711. https://doi.org/10.1007/s00226-007-0154-5

Köhne, L., & Churkina, G. (2026). Cascading use of timber-based construction materials and its contribution to the urban carbon sink. *Frontiers in Built Environment*, *12*. https://doi.org/10.3389/fbuil.2026.1839696

Naghdinasab, M., Töpler, J., & Grönquist, P. (2025). COMPARATIVE STUDY OF CREEP MODELS FOR WOOD AND TIMBER EXTRAPLOATED OVER 100 YEARS IN CONSTANT CLIMATE. *Proceedings from the 14th World Conference on Timber Engineering: Advancing Timber for the Future Built Environment, WCTE 2025*, 4466–4474. https://doi.org/10.52202/080513-0550

Svensson, S. (2009). Duration of load effects of solid wood: A review of methods and models. *Wood Material Science and Engineering*, *4*(3–4), 115–124. https://doi.org/10.1080/17480270903326157

Toumpanaki, E., Shah, D. U., & Eichhorn, S. J. (2021). Beyond What Meets the Eye: Imaging and Imagining Wood Mechanical–Structural Properties. In *Advanced Materials* (Vol. 33, Number 28). John Wiley and Sons Inc. https://doi.org/10.1002/adma.202001613

# Wood-Mimicking Materials from Lignocellulosic Residues Using Biobased Crosslinkers

**Rudolfs Gravitis[1], Oskars Platnieks[1], Sergejs Beluns[1], Sergejs Gaidukovs[1]**

[1]Riga Technical University, Faculty of Natural Sciences and Technology, Institute of Chemistry and Chemical Technology, Riga, Latvia, rudolfs.gravitis@rtu.lv

## Background

Wood is a hierarchical natural material composed of cellulose, hemicellulose and lignin, which can be extracted from wood and agricultural residues and reassembled into new materials with tailored properties. Wood-derived nanoparticles and nanofibers enable lightweight porous structures such as foams and aerogels with high surface area, low density and tunable functionality. Their performance depends strongly on the biomass source, as different feedstocks vary in fiber morphology, composition and processability. Hemp is a particularly promising resource because it provides strong fibers that can be converted into nanofibrillated cellulose through relatively simple mechanical processing, while also offering useful side fractions for full biomass utilization.

Foams and aerogels are attractive due to their high surface area, low weight and 3D porous structure. Cellulose-based foams have been studied for adsorption and thermal insulation, but they often lose stability in water. Many stabilization methods rely on non-renewable chemicals, costly reagents or additional processing steps that may generate waste (Ferreira et al. 2021; Dudeja et al. 2023).

Hemp can be mechanically processed into nanofibrillated cellulose, and its residual fractions can be used in circular material systems. Citric acid enables simple thermal crosslinking via ester formation, while xylan densifies networks, lignin acts as a natural binder, and pectin forms additional nanofibrillar structures. Glycerol can participate in polyester formation and act as a plasticizer (Zhang et al. 2018; Miranda-Valdez et al. 2023; Groult et al. 2022). In this work, wood-mimicking foams were prepared from hemp waste, lignin, xylan and pectin, with glycerol and citric acid used to tune the structure. The goal was to study how composition affects morphology, mechanical performance, absorption, surface properties and thermal conductivity while avoiding harsh chemical treatments.

**Keywords:** wood mimic, biopolymers, circular economy, cellulose, reassembly.

## Experimental

Dried Santhica 27 hemp stalks were ground in several steps and used to prepare a 1.5 wt% aqueous suspension. The suspension was processed in a microfluidizer at 30,000 psi for five pass-through cycles to obtain hemp nanofibrillated cellulose. Kraft lignin was prepared as an aqueous alkaline solution and beechwood xylan was dissolved in deionized water at 80-85 °C. For wood-mimic (WM) foams, the components were combined to obtain 45% hemp, 35% xylan and 20% lignin by dry weight.

Citric acid was added to the hemp or WM suspension in amounts from 0.5 to 5 g per 100 g of suspension. Tert-butanol was added before the suspensions were cast into cylindrical molds, frozen at -80 °C and freeze-dried under 0.03 mbar vacuum for 72 h. The dried foams were thermally crosslinked at 140 °C for 6 h using a small amount of dicumyl peroxide as

catalyst. Additional compositions contained pectin (0.25-1 g), glycerol (0.5-2 g), or both, while 1 g of citric acid was kept constant in these series.
Foam density and porosity were calculated from sample mass, dimensions and component densities. Chemical interactions were analyzed by ATR-FTIR spectroscopy and morphology by field-emission scanning electron microscopy. Compression testing was performed at 25 °C and 5 mm/min. Surface hydrophobicity was evaluated by static water contact angle measurements. Absorption capacity was measured after 5 min immersion in water, rapeseed oil or kerosene, with selected samples tested for repeated cycles.

## Results and Discussion

FTIR analysis confirmed the formation of a crosslinked network. In hemp foams, the broad -OH band decreased while the carbonyl C=O band at 1733 cm-1 increased after crosslinking, indicating ester bond formation. In WM foams the same effect was less pronounced because of the higher amount of hydroxyl-containing lignin and xylan. Compositions containing both pectin and glycerol showed the highest carbonyl peak intensity among the selected spectra.
The foam morphology changed strongly with composition. Hemp and WM foams contained both sheet-like and fibrillar structures, while increasing citric acid concentration reduced the amount of nanostructured elements and promoted larger fiber structures. Pectin formed a nanofibrillar network with diameters below 100 nm and filled larger pores between cellulose structures. Glycerol coated and thickened structural elements, producing a microfiber-sized network with diameters mainly above 1 µm. Combining pectin and glycerol formed a denser and more agglomerated structure. Bulk densities ranged from about 13 to 153 mg/cm3, while most compositions maintained porosities of approximately 97-99%.
These structural changes were reflected in compression performance. Increasing citric acid concentration increased foam rigidity, specific compressive modulus and specific strength. A tenfold increase in citric acid content from 0.5 to 5 g produced an approximately sixfold increase in the specific modulus of hemp foams and a threefold increase for WM foams. Pectin had an even stronger reinforcing effect for pectin-containing hemp foams showed four- to sevenfold higher specific modulus and seven- to elevenfold higher specific strength. Hybrid pectin-glycerol foams were the most rigid compositions, although they also showed high shrinkage and density.
Absorption and surface properties were also highly tunable. H-CA0.5 showed the highest absorption capacity, reaching about 50 g/g for water, 51 g/g for rapeseed oil and 46 g/g for kerosene. Most foams absorbed between 20 and 50 g/g of the tested liquids. Increasing citric acid content generally reduced total absorption but improved selectivity toward organic liquids in hemp foams. Pectin promoted rapid absorption of all tested liquids, whereas glycerol increased hydrophobicity and stabilized water contact angles between 140° and 150° for glycerol-modified hemp foams. Several compositions completed ten water absorption cycles with capacities close to their initial values. Kerosene cycling was limited to five cycles, while rapeseed oil could not be repeatedly cycled.

## Conclusions

Sustainable lignocellulose foams were prepared by reassembling hemp nanofibrillated cellulose with lignin, xylan, pectin and glycerol and using citric acid for thermal crosslinking. The materials combined very high porosity with tunable mechanical and surface properties. Higher citric acid and pectin contents increased specific compressive modulus and strength, glycerol increased surface hydrophobicity, and pectin promoted rapid liquid uptake. The highest absorption values were approximately 50 g/g for water and similar for rapeseed oil and kerosene. The results demonstrate the potential of hemp-waste-based wood-mimicking foams for thermal insulation, filtration and environmental cleanup applications.

**Acknowledgments**

This work was supported by the Latvian Council of Science in the famework of FLPP “Next-Generation Nature-Inspired Recyclable Bioplastic Materials from Lignocellulosic Residues to Replace Fossil Wood Plastic Composites (ReBioCell)” (lzp-2025/1-0432) and Riga Technical university project “for strengthening scientific personnel capacity” (ZM -2026/24).

**References**

Beluns S, Platnieks O, Jurinovs M, Buss R, Gaidukovs S, Orlova L, Starkova O, Thakur VK (2024) Sustainable foams from hemp, lignin, xylan, pectin, and glycerol: tunable via reversible citric acid crosslinking for absorption and insulation applications. Giant 19: 100295.

Dudeja I, Mankoo RK, Singh A, Kaur J (2023) Citric acid: An ecofriendly cross-linker for the production of functional biopolymeric materials. Sustain. Chem. Pharm. 36: 101307.

Ferreira ES, Rezende CA, Cranston ED (2021) Fundamentals of cellulose lightweight materials: bio-based assemblies with tailored properties. Green Chem. 23(10): 3542-3568.

Groult S, Buwalda S, Budtova T (2022) Tuning bio-aerogel properties for controlling drug delivery. Part 2: Cellulose-pectin composite aerogels. Biomat. Adv. 135: 212732.

Miranda-Valdez IY, Coffeng S, Zhou Y, Viitanen L, Hu X, Jannuzzi L, Puisto A, Kostiainen MA, Mäkinen T, Koivisto J, Alava MJ (2023) Foam-formed biocomposites based on cellulose products and lignin. Cellulose 30(4): 2253-2266.

Zhang K, Cheng X, Cheng F, Lin Y, Zhou M, Zhu P (2018) Poly(citrate glyceride): a hyperbranched polyester for starch plasticization. Polym. Int. 67(4): 399-404.

# The Wood Biorefinery Product as a Functional Additive for Wood-Plastic Composite

**Anrijs Verovkins, Galia Shulga, Janis Rizikovs, Brigita Neiberte, Daniela Godina, Laima Vevere, Rudolfs Berzins, Talrits Betkers**

Latvian State Institute of Wood Chemistry, Riga, Latvia, anrijs.verovkins@kki.lv, galija.shulga@kki.lv, janis.rizikovs@kki.lv, bricic46@inbox.lv, daniela.godina@kki.lv, laima.vevere@kki.lv, rudolfs.berzins@kki.lv, betalrit@gmail.com

## Background

Extrusion is one of the widespread industrial methods for processing wood-plastic composites (WPCs). To improve WPC extrusion, special functional additives – lubricants – are used in their formulations (Dai et al. 2019). Lubricants reduce the melt viscosity of WPCs and significantly improve their rheological properties. Fatty acids and their esters, fatty acids, amides, and paraffin waxes are the most well-known commercial lubricants. Unfortunately, they are not biodegradable. Pulp and woodworking plants generate a large amount of outer birch bark containing suberin, which is a valuable feedstock for obtaining various value-added products. Depolymerisation of suberin is the most widely exploited biorefinery mode for obtaining suberinic acids (SAs) (Rizhikovs et al 2015), representing a complex of fatty acids covalently bonded with aromatic structures. The main objective of the study was to examine whether SAs could be used as a lubricant in WPC containing pine wood and recycled polypropylene.

**Keywords:** suberinic acids, lubricant**,** wood-plastic composite

## Experimental

*Materials.* Pine wood sawdust was sourced from a Latvian private industry. Before use, the pine particles were fractionated, and the fraction smaller than 0.25 cm was subjected to treatment with a 2% NaOH solution at 90 °C for 90 min. Recycled polypropylene (rPP) with a density of 0.9 t/m³ and a melt flow index of 5.2 g/10 min (230 °C, 2.16 kg) was used as a polymer matrix. Suberinic acids (SAs) were extracted from outer birch bark (Latvijas Finieris, Latvia) under different conditions, differing in the medium – water at various pH values and ethanol. The characterisation of the SAs by GPC, GC–MS, FTIR, DTA, and DSC demonstrated substantial variations in chemical composition, molecular weight, and molecular weight distribution. The pine particles were treated with the water SA suspensions at a defined concentration to achieve a 4.0% SAs optimal content in the composite samples, as established earlier (Shulga et al. 2023).

*Methods.* The composite samples containing 70% rPP and 30% pine sawdust particles were processed in a twin-screw extruder (HAAKE MiniLab) at a rotation speed of 130 rpm, a circulation time of 5 min, and a temperature of 175 °C. The injection moulding was carried out at 120 °C. The extruder rotor minimal torque (MT), injection pressure, and apparent viscosity of the rPP/PLA melt were measured using the HAAKE MiniLab, which is designed for compounding polymer blends and composite materials and for testing their rheological properties.

**Results and Discussion**

Three samples of SAs were extracted under different conditions. The acids extracted at pH 2 contained a broader mixture of esters, diols, and carboxylic acids and exhibited a weight-average molecular weight of 63.1 kDa and the highest polydispersity index. In contrast, the SAs extracted at pH 5 were enriched in hydrophobic triterpenes and higher-molecular-weight oligomers, resulting in the highest molecular weight of 79.6 kDa, but a narrower molecular weight distribution. The acids extracted in ethanol exhibited the lowest molecular weight of 3.12 kDa and the lowest polydispersity index. The SAs extracted at pH 5 contained the largest amount of betulin (~86%), which likely accounted for their weaker lubricating efficiency and reduced effect on torque reduction. The ethanol-extracted SAs were rich in methyl and ethyl esters of long-chain fatty acids. These compounds were more fluid and thermally stable at processing temperatures, leading to improved lubrication and reduced melt viscosity. The incorporation of 4.0 wt% SAs into the composite samples resulted in improved extrusion conditions, as evidenced by reductions in the minimum torque (MT) values of 18.2–27.3%, respectively, demonstrating their lubricating function in the composites. The SAs extracted in ethanol produced a greater reduction in the torque than those obtained in an aqueous medium, whereas the composite containing the acids extracted at pH 5 exhibited the lowest torque reduction (Figure 1).

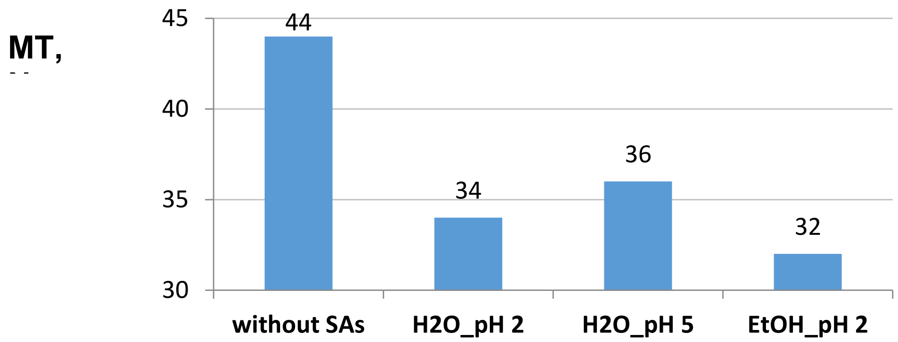


Figure 1. Minimal torque for WPC samples containing different SAs

The relatively small differences in the minimal torque of the samples containing the SAs with different chemical compositions, molecular weights, and molecular polydispersity may be attributed to the specifics of the adsorption of the compounds within the SAs onto the surface of the pine sawdust characterising the enhanced content of the hydrophobic extractives.

**Conclusions**

The incorporation of 4.0 wt% SAs into the composite samples resulted in improved extrusion conditions, as evidenced by a reduction in the minimum torque and apparent viscosity relative to these indices for the sample filled with only the alkaline-treated pine sawdust, confirming the lubricating function of these acids. The impact of the extraction conditions of SAs on their ability to improve extrusion processing of the WPC samples filled with pine sawdust was not significant.

**References**

Dai L, Wang X, Zhang J, Wang F, Ou R, Song Y (2019) Effects of lubricants on the rheological and mechanical properties of wood flour/polypropylene composites. J. Appl. Polym. Sci. 136: 47667.

Rizhikovs J, Zandersons J, Dobele G, Paze A (2015) Isolation of triterpene-rich extracts from outer birch bark by hot water and alkaline pre-treatment for the appropriate choice of solvents. Ind. Crops Prod*. 76:* 209–214.

Shulga G, Rizhikovs J, Neiberte B, Verovkins A, Vitolina S, Betkers T, Makars R (2023) Processing and Properties of Wood-Plastic Composite Containing Alkali-Treated Birch Wood Shavings and Bioadditive Obtained by Biorefinery of Birch Bark. Forests *14*: 1906.

# Microalgal Protein as a Base for Indoor Decorative Plywood Production Adhesives

**Aurelie Gouneaud[1], Heikko Kallakas[2], Jacob Skov Pedersen[3], Thue Trofod[3], Anand Ramesh Sanadi[1]**

[1]University of Copenhagen Department of Geosciences and Natural Resource Management 1958 Frederiksberg, Denmark: anrs@ign.ku.dk, augo@ign.ku.dk,
[2]Laboratory of Wood Technology, Tallinn University of Technology, Tallinn, Estonia: heikko.kallakas@taltech.ee
[3]Danish Technological Institute, Høje Taarstrup, Denmark: jsp@teknologisk.dk, TTR@teknologisk.dk

## Background

The plywood industry relies on large quantities of adhesives that are primarily fossil-based and often contain carcinogenic compounds such as formaldehyde. However, the depletion of fossil resources, the need to reduce the use of carcinogenic chemicals, and the increasing demand to allocate agricultural crops for food production have created a need for alternative adhesive sources. One such alternative is soy flour protein (SF), which has been successfully developed and commercialized in the United States as a wood adhesive (Solenis, 2021; Frihart & Satori, 2013). Nevertheless, the cultivation of soybeans competes directly with food production for agricultural land. Microalgae (MA), which are fast-growing and require relatively little space, are already utilized in several industries but have not yet been widely explored as adhesive materials. The objective of this study was to evaluate the potential of protein-rich microalgal biomass as a plywood adhesive. This potential was assessed using plywood adhesive formulations and tested according to ASTM D7998-19, the Standard Test Method for the Cohesive Strength Development of Wood Adhesives (Wescott et al., 2007; Frihart & Lorenz, 2020).

**Keywords:** Adhesive, protein, shear strength

## Experimental

### Material

The formulations contained a ratio of 20 wt% MA- dry matter. After addition of deionized water, polyamidoamine epichlorohydrin (PAE), a cross-linker was added from 1,3 to 15 wt% of the total mass. The mixtures were neutralized with an 1.5M NaOH solution to obtain a pH of about 7 and to ensure 20% MA DM in the mixture. An ABES (Automated Bonding Evaluation System, Corvallis, OR97333, USA) was used to make and test the samples. 5 ply birch plywood were made at Tallinn University of Technology and tested according to the appropriate standards.

### Shear strength and tensile test

After at least seven days in a climate chamber at 20°C and 65% RH, half of the batch of samples was tested directly with a 4s pull and the other soaked for 4h in deionized water before test. The test was conducted with the ABES following ASTM D-799819. All the results were expressed in MPa. Plywood bonding quality was tested according to the EN 314, class 1 and ASTM D906. In EN 314, plywood samples were soaked for 24h in deionized water before testing.

## Results and Discussion

MA adhesive was compared to SF adhesive, and the shear strength is not significantly different between SF-based and MA-based adhesives suggesting that MA has the potential to be an adhesive.
The amount of PAE in the MA mixtures has an influence on both dry and 4h water-soaked samples with PAE of 7,5. wt% resulting in the best results although there are not significant differences at higher concentrations.

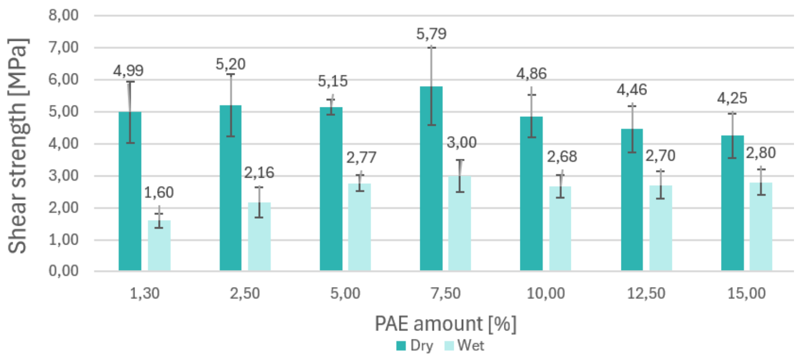


Figure 1. Shear strength depending on the content of PAE in the micro-algae protein-based adhesive mixture. The dimension of all the adhesive joints was measured individually to convert the force in N to a constraint in MPa. Error bars are 95% confident on five samples

Plywood panels containing 12.5% PAE were produced using hot pressing, showed the better overall performance compared to 15% PAE in limited testing. Its mean EN 314 bond-line shear strength was 1.31 ± 0.23 MPa. According to EN 314-2, This panel passed the bonding-quality requirement in the EU because its mean shear strength exceeded 1.0 MPa, above which no minimum wood-failure percentage is required. The ASTM D906 shear-strength results achieved the highest mean value of 2.62 ± 0.39 MPa. However, these panels cannot formally be classified as passing or failing ASTM D906 because the standard provides a comparative test procedure rather than acceptance thresholds.

## Conclusions

Microalgal protein showed better mechanical properties with addition of PAE. Initial tests indicate the plywood with MA crosslinked with PAE adhesive may pass both ASTM and EN standards. Further testing should be conducted to improve mechanical properties, optimize PAE % and confirm that MA adhesive can be used for plywood to pass North American and EN standards.


## Acknowledgement

The authors would like to thank Aase og Ejnar Danielsens Fond and Johan Heinrich Hoffmann og hustrus Mindefond for partial funding of this research, without which this publication would not have happened, Loretta Kalju and Kevin Kuusemäe for helping to make the samples and testing them and Marta Otolani and Mari Carmen Reyes Munoz from Solenis for supplying the PAE.


**To whom correspondence should be addressed Email- anrs@ign.ku.dk**

**References**

Barzegar, Mahsa, Linda F. Lorenz, Rabi Behrooz, and Charles R. Frihart. 2022. “Improved Wood-Bond Strengths Using Soy and Canola Flours with pMDI and PAE.” *Polymers* 14 (7): 1272. https://doi.org/10.3390/polym14071272.

Frihart, Charles R., Rishawn Brandon, Rebecca E. Ibach, Christopher G. Hunt, and Wolfgang Gindl-Altmutter. 2021. “Comparative Adhesive Bonding of Wood Chemically Modified with Either Acetic Anhydride or Butylene Oxide.” *Forests* 12 (5): 546. https://doi.org/10.3390/f12050546.

Frihart, Charles R., and Linda Lorenz. 2020. “Standard Test Method ASTM D 7998-19 for the Cohesive Strength Development of Wood Adhesives.” *Journal of Visualized Experiments*, no. 159 (May): 61184. https://doi.org/10.3791/61184.

Frihart, Charles R., and Holly Satori. 2013. “Soy Flour Dispersibility and Performance as Wood Adhesive.” *Journal of Adhesion Science and Technology* 27 (18–19): 2043–52. https://doi.org/10.1080/01694243.2012.696948.

Lambuth, Alan L. 2018. “Protein Adhesives for Wood.” In *Wood Adhesives*, 1st ed., edited by A. Pizzi. CRC Press. https://doi.org/10.1201/9780203733721-1.

Li, Kaichang, Svetlana Peshkova, and Xinglian Geng. 2004. “Investigation of Soy Protein-Kymene® Adhesive Systems for Wood Composites.” *Journal of the American Oil Chemists’ Society* 81 (5): 487–91. https://doi.org/10.1007/s11746-004-0928-1.

Roy, Joseph Jegan, Longhua Sun, and Lianghui Ji. 2014. “Microalgal Proteins: A New Source of Raw Material for Production of Plywood Adhesive.” *Journal of Applied Phycology* 26 (3): 1415–22. https://doi.org/10.1007/s10811-013-0169-2.

“Soyad™ Adhesive Technology | Solenis.” 2021. March 2. https://www.solenis.com/en/the-solenis-way/innovation-solenis/our-product-innovations/soyad-adhesive-technology/.

Wescott, James M., Michael J. Birkeland, Amy E. Traska, Charles R. Frihart PhD, and Brice N. Dally. 2007. “New Method for Rapid Testing of Bond Strength for Wood Adhesives.” *Proceedings : 30th Annual Meeting of the Adhesion Society, Inc. : February 18-21, 2007, Tampa Bay, FL. [S.l. : S.n.], C2007: Pages 219-221.* https://research.fs.usda.gov/treesearch/27682.

Yue, Hangbo, Lingwei Mai, Chao Xu, Chufen Yang, Peter S. Shuttleworth, and Yingde Cui. 2023. “Recent Advancement in Bio-Based Adhesives Derived from Plant Proteins for Plywood Application: A Review.” *Sustainable Chemistry and Pharmacy* 33 (June): 101143. https://doi.org/10.1016/j.scp.2023.101143.

# The Survey of Lithuania's Population on the Construction of Wooden Houses

**Benas Šilinskas[1], Marius Aleinikovas[1], Lina Beniušienė[1]**

[1]Lithunaian Research Centre for Agriculture and Forestry, Forest resource, economics and policy department.
Benas.silinskas@lammc.lt; Marius.aleinikovas@lammc.lt; lina.beniusiene@lammc.lt

**Abstract**

The New European Bauhaus (NEB) is a creative and policy initiative launched by the European Commission in 2021. It supports the objectives of the European Green Deal by promoting solutions that are not only environmentally sustainable but also aesthetically appealing and socially inclusive. Wooden buildings align with the aims of the NEB by contributing to the transformation of neighbourhoods, cities, and rural areas into sustainable and attractive places. Multi-story wooden buildings closely support NEB objectives because they: Reduce embodied carbon compared with concrete and steel structures; Store carbon within the building structure; Utilize renewable materials sourced from sustainably managed forests; Create visually appealing and human-cantered environments and support local forestry and construction economies.

This study aims to determine how residents perceive wooden buildings and assess the demand for such buildings in Lithuania. A total of 1,019 individuals aged 18 to 75 from across the country participated in the survey. A combined methodology was applied, consisting of CATI (Computer-Assisted Telephone Interviewing) and CAWI (Computer-Assisted Web Interviewing). The data were processed using SPSS/PC statistical software.

The results showed that 17% of respondents believed that the construction of wooden buildings in Lithuania should definitely be encouraged, while 48% thought it should rather be encouraged. In contrast, 28% believed it should rather not be encouraged, and 7% stated that it definitely should not be encouraged. A majority of respondents (72%) believed that the maximum permitted height of wooden buildings in Lithuania should be three stories. Another 7% supported a limit of five stories, 5% favoured nine-story buildings, and 16% supported the construction of even taller buildings, including skyscrapers, if technological developments make this feasible. More than half of the respondents (53%) believed that multi-story wooden buildings should be primarily residential in purpose, consisting mainly of apartments. An additional 25% stated that such buildings should be exclusively residential. Meanwhile, 14% favored predominantly commercial use, such as offices and other commercial premises, while 8% believed that these buildings should be used exclusively for commercial purposes. Forty percent of respondents indicated that they would like to live in a modern multi-story wooden building, whereas 60% would not. Similarly, 54% stated that they would like to work in such a building, while 46% would not.

In conclusion, the survey indicates generally positive public attitudes toward wooden construction in Lithuania. Most respondents support encouraging the development of wooden buildings and favour limiting their height to three stories. Multi-story wooden buildings are primarily perceived as suitable for residential use.

# Longitudinal Eigenfrequency Responses to Thermal Treatment Intensity in Beech and Spruce

**Carlo Kupfernagel[1*], Marlene Cramer[2,3], Kordula Jacobs[1]**

[1]Institut für Holztechnologie Dresden gGmbH, Zellescher Weg 24, 01217 Dresden, Germany *Carlo.kupfernagel@ihd-dresden.de

[2]Edinburgh Napier University, 37 Bankhead Crossway South, EH11 4EP, Edinburgh
[3]Forest Research NRS, Bush Estate, EH25 9SY, Roslin

## Background

Thermal modification improves the dimensional stability and biological durability of wood and alters mechanical performance, depending on treatment intensity. Because temperature, duration, and treatment atmosphere interact, process-induced mass loss (ML) is frequently used as an indicator of treatment intensity (Hill, 2006; Esteves and Pereira, 2009). However, ML determination is complicated outside the laboratory. Therefore, rapid non-destructive methods for the assessment of treatment intensity in thermally modified wood are required. Acoustic methods are established in wood testing, but studies on thermally modified wood have mainly focused on strength prediction using the dynamic modulus of elasticity ($MOE_{dyn}$), which is derived from the acoustic response together with density (Niemz and Mannes, 2012; Holeček et al., 2017). Longitudinal eigenfrequency (Ef) alone does not require density determination and could be a relevant parameter for the rapid non-destructive assessment of treatment intensity. The present study therefore evaluates how treatment-induced changes in longitudinal eigenfrequency relate to ML in beech and spruce exposed to identical thermal schedules. The paired before-and-after design reduces the influence of initial specimen variability and enables direct comparison of hardwood and softwood responses.

**Keywords:** thermal modification, non-destructive testing, longitudinal eigenfrequency, mass loss, beech, spruce

## Experimental

A total of 50 beech (Fagus sylvatica L.) and 50 spruce (Picea abies (L.) Karst.) specimens (300 × 20 × 20 mm; n = 10 per species and temperature) were thermally modified at 160, 175, 190, 205, or 220 °C for 3 h in a 0.75 m³ kiln operated at atmospheric pressure under constant steam supply. Before and after treatment, specimens were oven-dried at 103 °C, cooled in a desiccator, and their mass and dimensions recorded. ML was calculated from the change in oven-dry mass. For the acoustic measurement, specimens were placed on an elastic support to approximate free–free boundary conditions and excited by 5–10 short axial impacts. The signal was recorded at the opposite end with a microphone and processed in R using a fast Fourier transform (FFT), grouped into 20 Hz intervals, and normalised. The first longitudinal resonance was identified as the dominant peak at approximately 8–9 kHz. Treatment-induced change was expressed as the difference between the thermally modified and native eigenfrequencies, and linear regressions between this change and ML were evaluated separately for each species.

## Results and Discussion

The longitudinal resonance peak could be identified consistently in both species. The selected spectra in Figure 1 illustrate the contrast between mild and severe treatment. At 160 °C, the native and thermally modified spectra nearly overlapped, whereas at 220 °C the treated peak shifted visibly to a lower frequency. The spectral contrast coincided with the increase in treatment-induced ML.

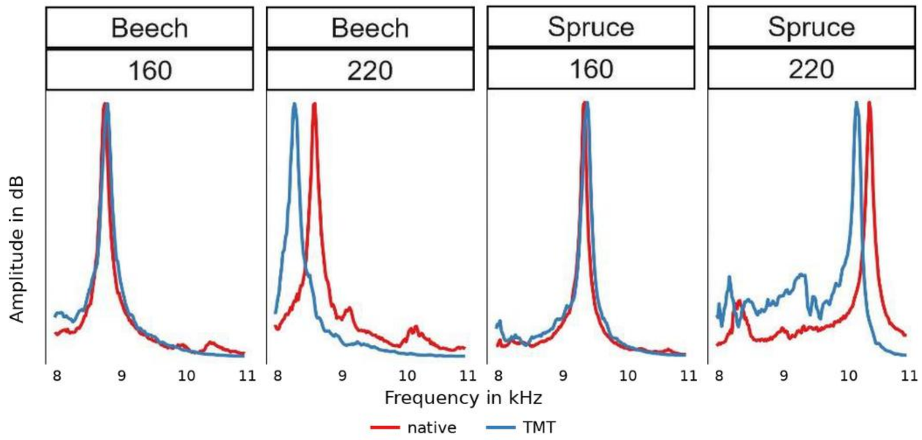


Figure 1. Selected longitudinal eigenfrequency spectra of native and thermally modified (TMT) beech and spruce specimens at 160 and 220 °C. At 160 °C, native and treated spectra nearly overlap; at 220 °C, the longitudinal resonance peak shifts visibly after treatment

In beech, ML increased from 0.7 ± 0.1 % at 160 °C to 17.0 ± 1.8 % at 220 °C. In spruce, it increased from 0.8 ± 0.1 % to 9.9 ± 0.8 %. The relationship between the change in eigeneigenfrequency and ML differed between the two species (Figure 2).
In spruce, the change in Ef became progressively more negative with increasing ML and the linear relationship was comparatively strong ($R^2 = 0.76$). Beech showed the same overall tendency, but with substantially greater scatter and a weaker relationship ($R^2 = 0.36$). At low and intermediate treatment intensities, many specimens exhibited near-zero or slightly positive changes.

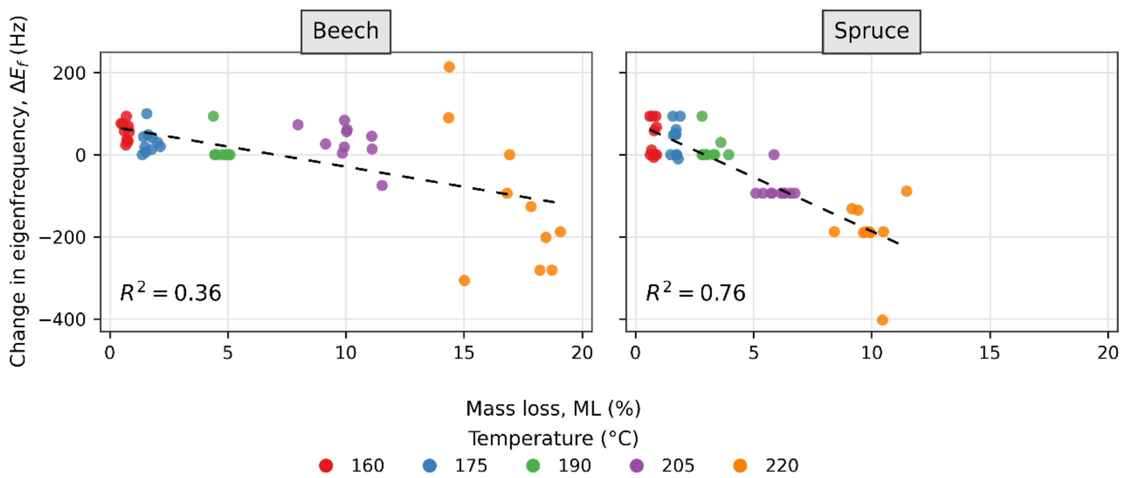


Figure 2. Relationship between treatment-induced mass loss (ML) and change in longitudinal eigenfrequency (ΔEf) for beech and spruce. Points represent individual specimens and colours indicate treatment temperature; dashed lines show species-specific linear regressions. The relationship was stronger in spruce ($R^2 = 0.76$) than in beech ($R^2 = 0.36$)

The near-zero response at mild to intermediate treatment intensities may reflect competing mechanisms: a temporary increase or preservation of stiffness under mild conditions and thermal degradation at greater treatment intensities (Hill et al., 2021). Variability increased at high ML, particularly in beech. Intrinsic material variability and the small group size (n = 10) make the regression sensitive to individual observations. Treatment-induced microscopic damage may also contribute. Vessel collapse and radial cracking have been

reported for heat-treated beech (Sedighi Gilani et al., 2013), although the present specimens were not examined microscopically and this mechanism remains a hypothesis.
For rapid screening, longitudinal eigenfrequency is potentially useful because it is obtained directly from the resonance signal and avoids the density input required to calculate $MOE_{dyn}$. The substantially clearer relationship between ΔEf and ML in spruce nevertheless shows that this direct parameter cannot be assumed to respond uniformly across species. The present results therefore support eigenfrequency as a potentially useful screening response for spruce while indicating that additional material descriptors or larger calibration datasets are required for beech.

## Conclusions

Longitudinal eigenfrequency measured by impulse excitation can detect treatment-induced changes in thermally modified wood, but its performance differed between beech and spruce. Under the present oven-dry laboratory conditions, mild treatments produced little change in eigenfrequency, whereas treatment at 220 °C caused pronounced peak shifts and the largest negative frequency changes. The relationship with ML was promising for spruce ($R^2$ = 0.76) but weak and variable for beech ($R^2$ = 0.36). Eigenfrequency is therefore attractive as a rapid parameter that does not require density determination, but several questions remain. Validation should include larger sample sets, industrial dimensions, variable moisture conditions, and direct assessment of treatment-related defects.

## References

Esteves BM and Pereira HM (2009) Heat treatment of wood. BioResources 4(1): 370–404.

Hill CAS (2006) Wood Modification: Chemical, Thermal and Other Processes. John Wiley & Sons Ltd.

Hill CAS, Altgen M and Rautkari L (2021) Thermal modification of wood—a review: Chemical changes and hygroscopicity. Journal of Materials Science 56(11): 6581–6614.

Holeček T, Gašparík M, Lagaňa R, et al. (2017) Measuring the modulus of elasticity of thermally treated spruce wood using the ultrasound and resonance methods. BioResources 12(1): 819–838.

Niemz P and Mannes D (2012) Non-destructive testing of wood and wood-based materials. Journal of Cultural Heritage 13(3): 26–34.

Sedighi Gilani M, Fife JL, Boone MN, et al. (2013) Dynamics of microcrack propagation in hardwood during heat treatment investigated by synchrotron-based X-ray tomographic microscopy. Wood Science and Technology 47(5): 889–896.

# Engaging Youth in Circular Wood Use: Insights from “Wood for All 2026” Competition

**Eli Keržič[1], Bojan Gospodarič[1], Drago Vidic[1], Miha Humar[1], Gorazd Fajdiga[1]**

[1]University of Ljubljana, Biotechnical faculty, Department of wood science and technology, eli.kerzic@bf.uni-lj.si, bojani.gospodaric@bf.uni-lj.si, drago.vidic@bf.uni-lj.si, miha.humar@bf.uni-lj.si, gorazd.fajdiga@bf.uni-lj.si

## Background

Climate change, extreme weather events, and pest outbreaks are increasingly affecting forest ecosystems. As a result, the quality and market value of wood resources are declining, highlighting the need for their efficient and sustainable use. Various approaches to the valorisation and utilisation of low-quality wood have already been developed (Kržišnik et al. 2018, Hýsek et al. 2021, Garcia et al. 2026). However, educational initiatives that combine sustainable wood use with awareness of climate-related challenges among younger generations remain relatively uncommon.
The Wood for All 2026 competition, organised in collaboration with the WoodInnovate project, invited primary and secondary school students to create products from low-quality wood affected by climate change and pests. Through hands-on activities, participants explored wood valorisation, circular economy principles, and opportunities to extend the life cycle of underutilised wood resources. At the same time, they increased their awareness of the challenges that climate change poses to the forest-based sector.

**Keywords:** Innovative and Sustainable Wood Utilisation, Low-Quality Wood, Youth Awareness

## Experimental

The Wood for All 2026 competition was organised by the Department of Wood Science and Technology at the University of Ljubljana, in collaboration with the WoodInnovate project. The competition aimed to promote sustainable wood use and creativity among young people. Participants were encouraged to use low-quality wood affected by bark beetle infestations and blue-stain fungi. Primary school students designed and produced wooden birds, while secondary school students produced folding chairs. Participants were required to submit both photographs of the finished product and a documented manufacturing process, which formed an integral part of the evaluation procedure (Figure 1).

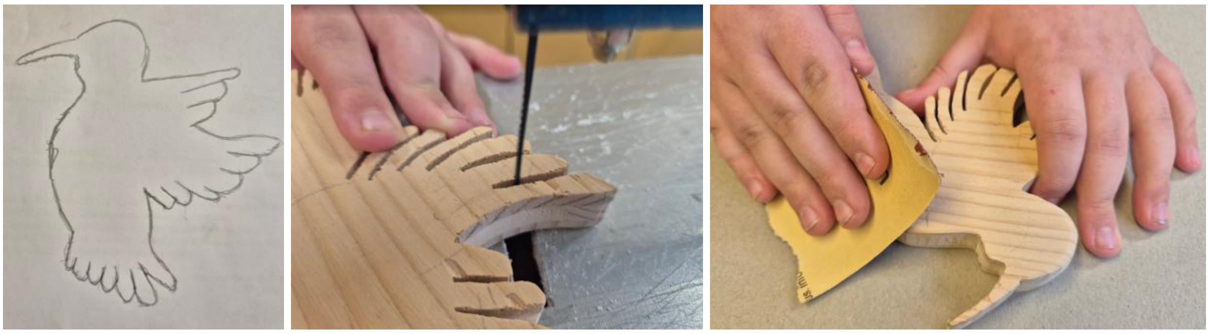

Figure 1. Participants were required to submit a photograph of the final product together with a documented manufacturing process, which formed part of the evaluation procedure. (*Photo: Rok and Jan Škraban*)

## Results and Discussion

A total of 12 primary schools and 3 secondary schools from across Slovenia participated in the competition. In all, 25 wooden birds and 5 folding chairs were submitted. These products were manufactured either from locally sourced material or from wood supplied through the WoodInnovate project. The products showed that wood affected by climate-related disturbances can still be transformed into attractive, functional objects (Figure 2). Participants demonstrated a high level of originality, craftsmanship and design quality. Beyond the technical outcomes, the competition served as an effective platform for raising awareness among younger generations of sustainable wood utilisation, circular economy principles and the impacts of climate change on forest resources.

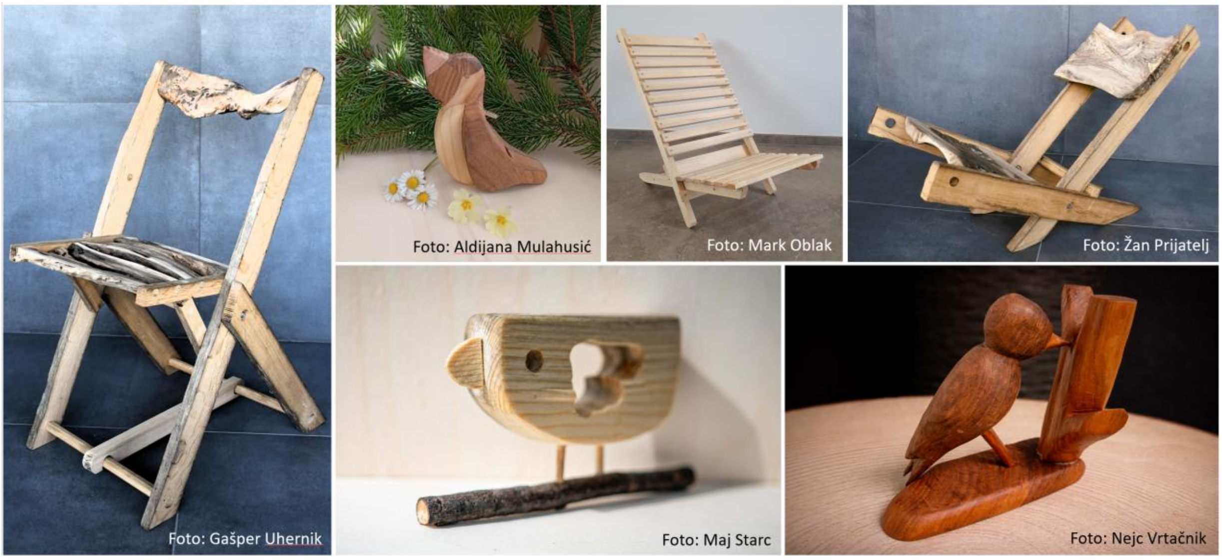


Figure 2. Award-winning products submitted to the *Wood for All 2026* competition, demonstrating creative and value-added utilisation of low-quality wood. (*Photo: Gašper Uhernik, Aldijana Mulahusić, Maj Starc, Mark Oblak, Žan Prijatelj, Nejc Vrtačnik*)

## Conclusions

The *Wood for All 2026* competition demonstrated the value of combining practical wood education with sustainability challenges. Young participants explored creative uses for lower-quality wood and became more aware of climate-related challenges affecting forest resources. The competition highlighted the potential to extend the life of wood through higher-value applications and to support a more circular forest-wood value chain.

## References


Garcia R, Duchesne I, Giasson LD, Cloutier, A (2026) Processing and End-Uses of Wood Affected by Forest Fires, Eastern Spruce Budworm and Mountain Pine Beetle Outbreaks. Current Forestry Reports 12: 12.

Hýsek Š, Löwe R, Turčáni M (2021) What Happens to Wood after a Tree Is Attacked by a Bark Beetle? Forests 12: 1163.

Kržišnik D, Lesar B, Thaler N, Humar M (2018) Performance of bark beetle damaged Norway spruce wood against water and fungal decay. BioResources, 13(2): 3473–3486.


www.ita-slo.eu/en/woodinnovate

woodinnova

The WoodInnovate 2.0 project is co-financed by the European Union in the framework of the Interreg VI-A Italy-Slovenia Programme.

# Characterization of Wood Materials and Dowels Properties for Wood-Only Outdoor Products

**Errj Sansonetti[1], Edgars Kuka[1], Dace Cirule[1], Ingeborga Andersone[1], Matiss Kevers[1], Bruno Andersons[1]**

[1]Laboratory of Wood Degradation and Protection, Latvian State Institute of Wood Chemistry, Riga, Latvia, errj.sansonetti@kki.lv, edgars.kuka@kki.lv, dace.cirule@kki.lv, ingeborga.andersone@kki.lv, matisskevers@gmail.com, bruno.andersons@kki.lv

## Background

The use of metal fasteners is the standard practice for outdoor wood furniture. The connections are reliable, however there are several drawbacks that are not aligned with the modern circular economy and sustainability principles due to high environmental impacts of steel production and reuse challenges of these products at the end of life. Wooden dowels offer a renewable and material-compatible alternative to metal fasteners and synthetic adhesives, while enabling disassembly, recycling and reuse of timber components without introducing additional non-wood materials into the material stream (Salzberger et al., 2024). Their mechanical compatibility with timber, biodegradability and potential for adhesive-free connections make them particularly promising for sustainable and circular engineered wood products (De Santis et al., 2025). The objective of the study was to explore the possibility to develop wood-only exterior products by using wood connections based on swelling force from denser wood dowels. To achieve this, dimensional changes at different environmental conditions and hardness of the connecting materials (unmodified and thermally modified spruce) and the connectors (beech wood) were studied.

**Keywords:** wood dimensions, wooden dowel, mechanical properties, circular economy

## Experimental

Spruce (*Picea abies*) wood and thermally modified (TM) spruce wood were considered as the softwood material to be connected and beech (*Fagus sylvatica*) wood as the potential hardwood connector e.g. dowel. Ten boards for each of these wood species were used to prepare samples for physical and mechanical tests. **Brinell hardness (HB)** was carried out according to the EN 1534:2020 standard in all three directions for spruce and TM spruce, but for the beech only in tangential and radial directions as these are the only directions that are relevant for connectors in wood-wood connections (Figure 1).

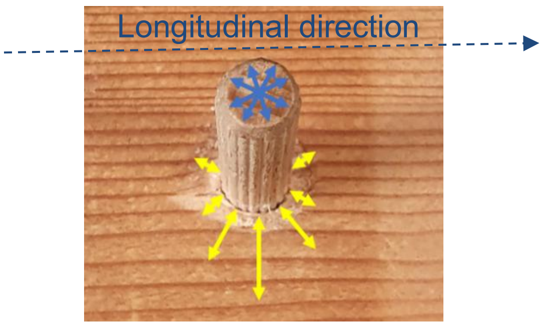


Figure 1. Wood-wood connections with the corresponding swelling/shrinking directions

**Maximum dimensional changes** for all wood materials were studied by subjecting 20 replicate samples of each wood type measuring 20 mm × 20 mm × 20 mm to three consecutive drying (103 °C)/wetting (vacuum impregnation with water) cycles.

## Results and Discussion

HB test results are presented in Figure 2. While minimal anisotropy between radial and tangential directions was observed for all wood types, similar as reported by Antons et al., 2018, the beech wood exhibited higher hardness than spruce and TM spruce in both these directions. However, HB values of spruce and TM spruce in longitudinal direction were higher than those of beech wood in radial and tangential directions. These results suggest that beech as a connector will deform spruce and TM spruce wood in the presence of sufficient swelling force in all but the longitudinal direction. On the contrary, the relatively high HB values in the longitudinal direction of spruce and TM spruce imply that the beech wood connector may itself be deformed in the direction aligned with the longitudinal direction of the spruce or TM spruce. The characterization of wood hardness provides insight into the characteristics of the wood and wood connections, helping to anticipate potential interactions between the wood pieces with different responses depending on their orientation.

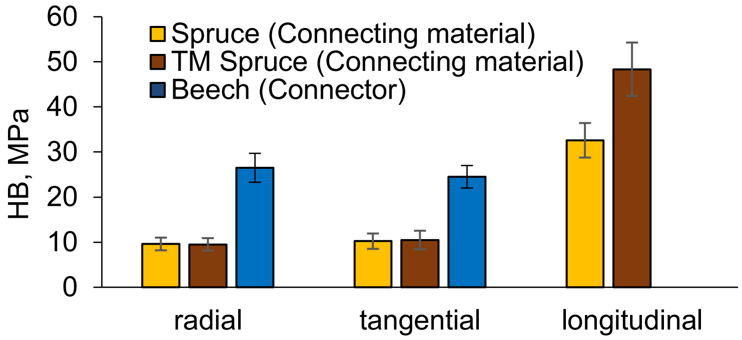


Figure 2. Comparison of Brinell hardness (HB) values according to wood surface orientation for connecting material (spruce and thermally modified (TM) spruce) and connector (beech)

The mechanical properties obtained from the HB tests are complemented by the swelling and shrinkage results presented in Figure 3. Together, these results help identify potential interaction mechanisms, find optimal connecting conditions, and model possible performance outcomes in assembled wood products. The anisotropic dimensional response of wood, characterized by the greatest changes in the tangential direction and minor changes in the longitudinal direction, can affect the geometry of the wood-wood connections during wood moisture fluctuations. Furthermore, repeated moisture cycling slightly increased the amplitude of dimensional change for all wood types with higher increase in tangential direction and for the spruce wood. As observed by Eckelman (1998), anisotropic dimensional changes can cause the drill holes to deform into an elliptical shape, potentially altering the geometry and contact conditions of the wood–wood dowel joints. For TM spruce wood, the dimensional changes were significantly smaller than for spruce wood suggesting that wood-wood joints for TM wood could be more stable with less significant anisotropic deformations. In contrast, beech wood exhibited the largest dimensional fluctuations. This is beneficial for the connectors as larger and controlled swelling force can be ensured by adjusting the initial moisture content of beech wood (connector) prior to jointing. The differences in both mechanical and physical properties should be understood and careful consideration should be given to the selection of wood species, joint geometry, and connection design to minimize the potential adverse effects of moisture-induced dimensional changes on the performance and quality of the final product, which in outdoor condition can be very relevant.

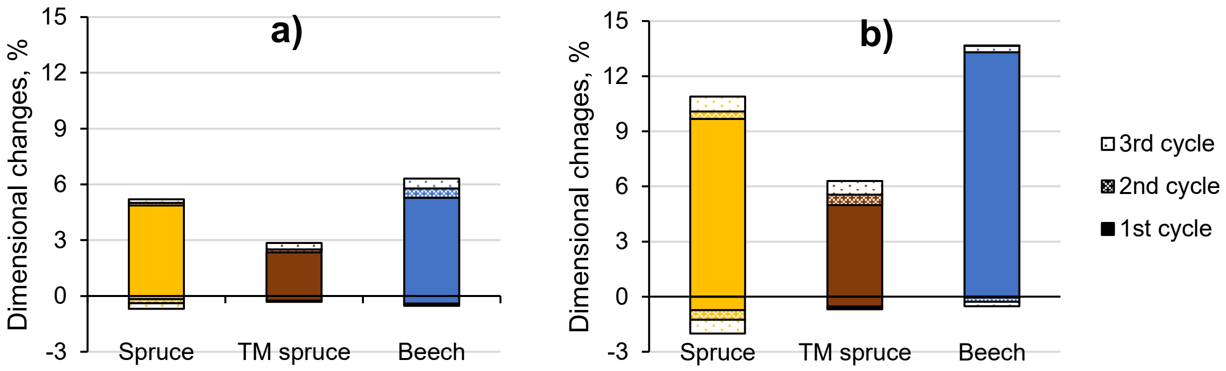


Figure 3. Effect of three wetting-drying cycles on the maximum dimensional fluctuations (indicated by the double arrows) from oven dry (dotted lines) to fibre saturation (solid lines) in: a) radial direction, b) tangential direction

## Conclusions

Wood species, dowel dimensions, initial wood moisture content should be carefully selected to ensure adequate swelling force, mechanical integrity under cyclic moisture variations, such as those experienced in outdoor conditions. The difference in dimensional changes, leading to elliptical deformation of the spruce and beech wood due to anisotropy, may progressively reduce the contact between the connector and the surrounding wood, potentially compromising joint performance and, ultimately, its structural function. Smaller impact is expected for TM spruce wood. Differences in hardness depending on wood species and fibre orientation may introduce additional deformations. It could promote localized damage or failure in the surrounding wood both for connecting material and connector itself, potentially reducing the load-bearing capacity and overall efficiency of the joint.

## Acknowledgment

This research was funded by the European Regional Development Fund under project No. 1.1.1.3/1/24/A/011 “Advancing sustainable wood-only surface assemblies for uses in exterior products (WOODy)”

## References

Antons A, Cirule D, Verovkins A, Kuka E (2018) Effect of thermal treatment on physical and mechanical properties of birch and pine wood. Research for Rural Development. 1:78–85.

De Santis Y, Aloisio A, Fragiacomo M (2025) Stiffness prediction of wooden dowel connections with beam-on-foundation models. Journal of Structural Engineering 151(12): 04025220.

Eckelman CA (1998) The shrinking and swelling of wood and its effect on furniture. *FNR-163*. Purdue University, Department of Forestry and Natural Resources, West Lafayette, IN, USA, 26 pp.

Salzberger M, Klein T, Hemmerling M, Konstantinou T (2024) Shape-changing wood joints in crafts and industry and their potential for building construction and wood culture. International Journal of Wood Culture 4(1): 58–95.

# Wood Surface Quality Analysis: A Comparative Study of 2D Profilometry and 3D Scanning Methods

**Gintaras Keturakis, Darius Albrektas and Žygimantas Kujalavičius**

Kauno kolegija Higher Education Institution, Pramonės pr.20, LT-50468 Kaunas, Lithuania, gintaras.keturakis@kaunokolegija.lt; darius.albrektas@kaunokolegija.lt; zygimantas.kujalavicius@kaunokolegija.lt

## Background

The surface roughness of wood is one of the most important quality indicators in the production of furniture, construction elements, and decorative components. The micro-geometry of the surface determines not only aesthetic properties but also coating adhesion, glue penetration, moisture absorption, and performance characteristics (Yu et al., 2023). Roughness is particularly important when evaluating the efficiency of sanding, milling, CNC machining, and other mechanical processes (Adamčík et al., 2025; Henke, Lis, & Krystofiak, 2022). In recent years, a clear trend has emerged in the wood industry toward shifting from traditional two-dimensional (2D) profilometric measurements to advanced three-dimensional (3D) optical methods, which allow more accurate assessment of surface topography and anatomical structure (Magoss, Rozs, & Tatai, 2022; Wang et al., 2022).
*2D profilometry*. Traditionally, needle-type profilometers are used in the wood industry to measure the linear surface profile and calculate parameters such as $R_a$, $R_z$ and $R_t$ (Kminiak & Kúdela, 2022). These devices are characterized by simplicity, fast measurement, and wide industrial applicability. However, their drawbacks are evident: the stylus falls into wood pores and anatomical structures, distorting the results; the measurement depends on direction (along or across the grain); it is impossible to evaluate areal parameters such as $S_a$ or $S_q$; contact-related defects (microcracks, fiber tear-out) often remain undetected (Kang et al., 2023). For these reasons, 2D methods are suitable only for quick production-level assessment, but not for detailed quality analysis.
*3D scanning methods*. 3D optical profilometers (laser microscopes, light interferometers, structured-light scanners) enable acquisition of surface topography in three-dimensional space (Iglesias et al., 2023a). Such devices generate parameters $S_a$, $S_q$, $S_z$, $S_{sk}$, $S_{ku}$ and Abbott–Firestone curves, which more accurately reflect the functional behavior of the surface (Iglesias et al., 2023b). Advantages of 3D methods include non-contact measurement that does not damage the surface; full topography instead of a single linear profile; the ability to distinguish anatomical roughness from machining marks; precise detection of microdefects, grain tear-out, and depressions; measurement independent of direction (Korkmaz, Budakçı, & Kılınç, 2024). Due to these features, 3D methods are becoming the industrial standard for evaluating high-quality wood machining.

**Keywords:** wood, surface roughness, contact profilometry, three-dimensional topography.

## Experimental

The testing samples with radial-section surface were made from wood of pine, birch and oak grown in Lithuania (Table 1). The samples were prepared for testing, with a length of 300 mm, a width 10 mm, and a thickness 25 mm. The average temperature in the testing room was 20 ± 2° C, while relative air humidity was 60 ± 5 %.

Table 1. Physical characteristics of wood

| Wood species | Moisture content $\omega$, % | Number of annual rings per 1 cm | Density, kg/m$^3$ |
|---|---|---|---|
| Pine (*Pinus sylvestris*) | 9.76…10.3 | 4.40…6.21 | 451…523 |
| Birch (*Betula pendula*) | 9.52…10.1 | 4.64…6.04 | 582…613 |
| Oak (*Quercus robur*) | 9.85…10.4 | 5.07…5.25 | 678…696 |

The tests were performed in the wood cutting stand that was created through modernization of vertical spindle moulder. The specimens were milled at oppositely directed vectors of the cutting speed ($v_c$) and feed ($v_f$). The milling cutters (HS 18–0–1) were fixed to the cutterhead. Two cutters were fixed; however, one cutter was in operation. Second cutter was used to balance the system. The conditions of milling test are presented in Table 2.

Table 2. Milling test conditions

| | | | |
|---|---|---|---|
| Cutting speed $v_c$, m/s | 40 | Cutting circle diameter $D$, mm | 123 |
| Feed speed $v_f$, m/min | 3 | Cutting angle $\delta$, degree | 60 |
| Feeding per cutter $f$, mm | 0.5 | Number of cutting edges $z$, unit. | 1 |
| Depth of milling $h$, mm | 2 | Edge rounding radius $r$, µm | 10; 20; 30 |

The parameters of surface roughness $R_a$, $R_z$ and $R_{max}$ were measured by electronic contact stylus-tip profilometer PCE-RT 1200 (PCE Instruments) and 3D optical measurement system MikroCAD Lite (GF Messtechnik GmbH). The surface roughness was measured after milling. Five surface sectors (2.5×2.5 mm) were chosen in one sample, which roughness was measured along (II) and across (⊥) wood grain. To examine one milling cutter, five samples were used. Therefore, total number of measurements for each operating regime was 25. All the measurement results were processed by Gaussian digital filter.

## Results and Discussion

The study showed that the 3D measurement method provides a more precise and comprehensive evaluation of milled wood surface quality than 2D profilometry, as it captures both linear and areal parameters. Surface roughness and topography are strongly affected by wood species, grain orientation, machining method, processing parameters, and anatomical defects. A consistent difference between contact stylus profilometry and 3D optical scanning was observed when assessing radial section surfaces.

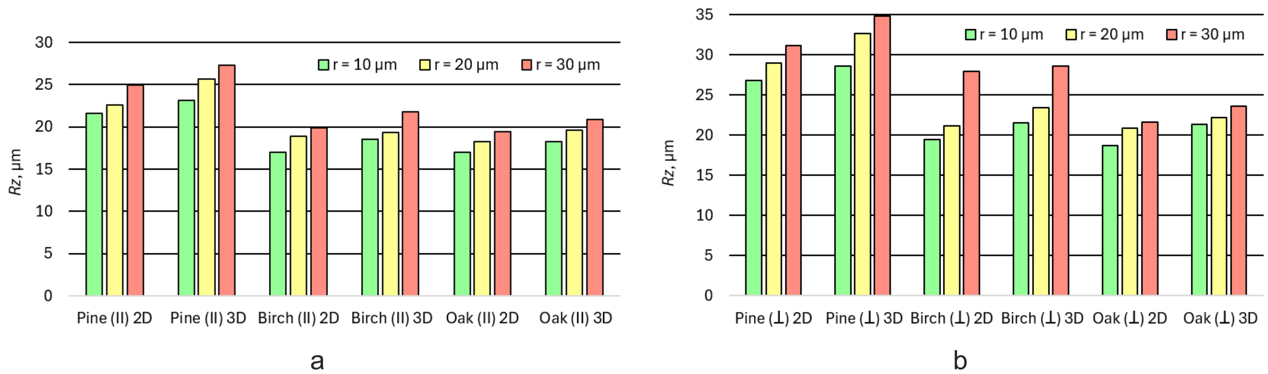


Figure 1. Surface roughness $R_z$ measured by 2D and 3D methods:
a – along the grain; b - across the grain

Roughness $R_z$ measurements along the grain differed by 8.11%, while across the grain the difference reached 9.33%, demonstrating the importance of measurement direction. Wood species also influenced discrepancies between methods: pine showed a 10.2% difference, birch 7.35%, and oak 8.59%. These results confirm that wood density and anatomical structure significantly affect measurement accuracy and the reliability of surface roughness evaluation, highlighting the advantages of 3D assessment for complex or irregular wood surfaces.

## Conclusions

The 3D measurement method provides a more accurate and comprehensive evaluation of milled wood surfaces than the 2D method because it captures both linear and areal parameters. Surface roughness and topography are strongly affected by wood species, grain orientation, machining method, processing parameters, and anatomical defects, which directly influence measurement accuracy. Clear differences were observed between contact stylus profilometry and 3D optical scanning: $R_z$ values differed by 8.11% along the grain and 9.33% across it, confirming the importance of measurement direction. Wood species also affected discrepancies, with average differences of 10.2% for pine, 7.35% for birch, and 8.59% for oak, highlighting the role of density and anatomical structure. Overall, the 3D method is more suitable for irregular or complex wood surfaces, as it more accurately reflects real topography and reduces the influence of structural defects.

## References

Adamčík, L., Giudice, V.L., Todaro, L. et al. Surface roughness of thermally modified and unmodified selected wood species after sanding. *Eur. J. Wood Prod. 83, 105* (2025).

Henke, M., Lis, B., & Krystofiak, T. (2022). Evaluation of surface roughness parameters of HDF for finishing under industrial conditions. *Materials, 15*(18), 6359.

Iglesias, F., Aguilera, A., Padilla, A., Madaf, M., & Diez, E. (2023a). Optical evaluation of surface roughness in wood parts and composites. *Journal of Wood Science, 69*, 35.

Iglesias, F., Aguilera, A., Padilla, A., Vizan, A., & Diez, E. (2023b). Application of computer vision techniques to estimate surface roughness of sanded wood. *Measurement, 219*, 112779.

Kang, C.-W., Hashitsume, K., Jang, E.-S., & Kolya, H. (2023). Relationship between wood anatomical features and surface roughness characteristics. Wood Research*, 68*(3), 455–464.

Kminiak, R., & Kúdela, J. (2022). Comparison of 2D and 3D surface roughness parameters of machined wood-based panels. *Coatings, 12*(4), 494.

Korkmaz, M., Budakçı, M., & Kılınç, İ. (2024). Assessment of surface roughness in milling of wood with different material temperatures and cutting parameters. *BioResources, 19*(4), 9343–9357.

Magoss, E., Rozs, R., & Tatai, S. (2022). Evaluation of wood surface roughness by confocal microscopy. *Wood Research, 67*(6), 919–928.

Wang, Z., Chao, J., Long, J., & Zhou, J. (2022). Measurement and analysis of three-dimensional surface roughness of wood after mechanical processing. *Measurement, 204*, 112136.

Yu, Q., Pan, X., Yang, Z., Zhang, L., & Cao, J. (2023). Effects of surface roughness of six wood species for furniture production on the wettability and bonding quality of coating. *Forests, 14*(5), 996.

# Material-Driven Microbial Taxa on Indoor Hospital Surfaces

**Ilse Ekman[1], Oksana Suokas[2], Marko Suokas[2], Pekka Kilpeläinen[1]**

[1]University of Oulu, Kajaani, Finland, ilse.ekman@oulu.fi, pekka.t.kilpelainen@oulu.fi
[2] University of Oulu, Oulu, Finland, oksana.suokas@outlook.fi, marko.suokas@oulu.fi

## Background

Wood is a sustainable building material that has been associated with positive well-being outcomes in healthcare buildings.[1,2] In healthcare environment, however, material choices must also support good hygiene and infection prevention and thus wood has largely remained limited to decorative elements in entrance halls and public spaces. Previous studies have shown that building materials differ in their ability to support microbial communities, and wood is of particular interest because its properties may affect microbial persistence differently from conventional hospital materials.[3] Despite increasing interest in indoor microbiomes, little is known about how wood surfaces shape microbial community composition in real healthcare setting. This study compared bacterial communities on wood and other common indoor hospital surface materials to evaluate the influence of material choice on the hospital microbiome.

**Keywords:** microbiome, wood material, hospital

## Experimental

### Samples

Environmental surface samples were collected from Kainuu Central Hospital (Kajaani, Finland) to compare microbial communities on wood and other common hospital surface materials (ceramic, composite, gypsum, laminate, metal, and vinyl). A total of 13 surfaces were sampled from various hospital environments, including waiting room of paediatric ward, lobby, nurse station, rehabilitation space, patient room, and clean space. Surfaces (10 cm × 10 cm) were swabbed three times using premoistened cotton swabs, and DNA was extracted using a commercial kit. Viable bacterial abundance was assessed from all sampled surfaces using tryptic soy agar (TSA) contact plates following standard microbiological procedures.

### DNA Sequencing

Amplicon sequencing of the 16S rRNA gene V3-V4 region was performed at the DNA Sequencing and Genomics Laboratory (BIDGEN), University of Helsinki. A single library was prepared from all the samples and the library was sequenced using both the Element Biosciences AVITI and Illumina MiSeq platforms. Data from the two sequencing platforms were treated as technical replicates. The sequencing data were analysed and visualized in R Statistical Software.

## Results and Discussion

We wanted to investigate whether wood differs in microbial taxonomic distribution or in core taxa compared to other building materials. At the phylum level, the three most abundant taxa in all building materials were Actinobacteriota, Firmicutes, and Proteobacteria, with a combined relative abundance of 0.88. The five most prevalent genera included human skin-associated taxa; *Corynebacterium*, *Staphylococcus*, *Streptococcus*, *Cutibacterium* and *Micrococcus*. There was no distinct similarity among the wood samples at the phylum or genus level. Statistically significant differences (Kruskal-Wallis and Dunn’s tests) between the wood and non-wood materials were found for several taxa. Based on the relative abundance data, in phylum level the materials were found to differ in Actinobacteriota and SAR324 clade (Marine group B). Also 107 genera with a total relative abundance of 0.09 and 251 species with a total relative abundance of 0.08 were found.
Next, we wanted to investigate whether the surface or the space in which wood was used is impacting the taxonomic distribution compared to other building materials. The samples taken from walls are distinct from other samples both based on Shannon diversity index which measures species richness and evenness, and viable bacteria recovered from the surfaces. This means that the surface orientation influences on microbial community composition. Additionally, wood used on walls differ from other wood surfaces and non-wood samples captured by Pricipal Coordinated Analysis. The samples taken from painted gypsum wall showed higher abundances of *Streptococcus*, *Rothia*, and *Haemophilus*, while wood wall samples were characterized by *Bacillus* and *Finegoldia*.
Altogether, we were able to produce close to 3 million sequence reads which corresponded to almost 6000 taxa from the hospital surfaces. The microbiomes of built environments are impacted by variable factors like air exchange, cleaning practises, plant and animal diversity.[4] The biggest factor influencing the microbiomes is occupancy of the building recognised by human skin bacteria as also seen in our study. The results of the present study suggests that wood as an indoor material in hospitals could be more broadly used especially in walls in which both the recovered viable bacteria count and observed taxa count was low. The major limitation of our study is insufficient data due to low sample number to confirm the differences at common level between wood and other materials. More data is also needed to evaluate the impact of wood treatments on microbiomes.

## Conclusions

In conclusion, our findings reveal that wood surfaces harbour distinct bacterial communities compared to non-wood materials. This suggests that the materials used are not merely passive surfaces; they actively contribute to shaping the microbial ecology of indoor environments. These results may open a new perspective on hospital design. If materials influence microbial communities, material selection could become an additional tool in creating healthier and more sustainable healthcare environments.

**References**

Gilbert J. A. & Hartmann E. M.(2024) The indoors microbiome and human health. Nature Reviews Microbiology, Volume 22, 742-755

Kettunen E., Ahlblad J., Kurkilahti M. et al. (2026) From antimicrobial activity to microbial ecology: Untreated and treated wood surfaces shape bacterial survival and community diversity in indoor environments. Journal of Hazardous Materials Advances, 22, 101090

Nyrud, A. Q., Bringslimark, T., & Bysheim, K. (2014). Benefits from wood interior in a hospital room: a preference study. Architectural Science Review, 57(2), 125–131.

Ulrich R. S., Bogren L., Gardiner S.K et al. (2018) Psychiatric ward design can reduce aggressive behavior, Journal of Environmental Psychology, Volume 57, 53-66.

# Quantifying the Cascade: Irreversibility, Option Value, and the Limits of Scoring in RVI-based Cascade Governance

**Stephan Ott**[1], **Jan Lüdtke**[1]

[1]Thünen Institute of Wood Research, Hamburg, Germany
stephan.ott@thuenen.de and jan.luedtke@thuenen.de

## Background

EU policy now treats the cascading use of wood as binding: RED III Article 3(3) establishes "material-before-fuel" as a principle, and the Waste Framework Directive reinforces it. But neither law says how to measure it. There is no shared way to quantify how much value a piece of wood in a product still holds at a given point in its life, or to check whether a supply chain actually complies with the cascade principle. This gap has real consequences: producers, recyclers and regulators must choose end-of-life routes without a common yardstick, and the resulting vacuum is being filled by unsubstantiated environmental claims — a 2020 EU screening found more than half of examined green claims vague, misleading or unfounded, and 40% entirely unsubstantiated. The proposed Green Claims Directive will require science-based, life-cycle substantiation of such claims, which presupposes exactly the measurement infrastructure that cascade policy currently lacks. We present the Resource Value Indicator (RVI) to close this gap: a continuous, auditable score between 0 and 1 per kilogram of dry wood matter, built around a RED III compliance penalty. It is not a tool for optimising a single company's decisions, but a framework for observing and evaluating how cascade policy actually plays out across national and EU value chains. Because cascade decisions affect what is available to future generations, the instrument is designed to remain trustworthy even if society's priorities shift over time.

**Keywords**: resource value indicator; cascading woody biomass; RED III; green-claims substantiation; non-compensatory MCDA

## (Experimental) Methodology & Model Architecture

The RVI scores four measurable properties of a wood-based material at each stage of its life: material quality, economic value, environmental value (including cascade compliance), and energy content. These are combined using a transparent, rule-based calculation and Multi Criteria Decision Analysis (MCDA) over a one-kilogram reference unit, aligned with the EN 15804 standard used in construction-product declarations. A key design decision is to separate two very different kinds of judgement. Most of the RVI's criteria are scored — good performance on one can offset weaker performance on another, the way a strong exam grade can offset a weaker one. But one criterion is treated differently: irreversibility. Some decisions close doors that can never be reopened — burning wood is the clearest example: once burned, it cannot be reused, recycled, or reconsidered. Because this is a decision that cannot be undone, it is not scored and traded off against other benefits — it is screened before scoring even begins, as an admissibility test. This distinction is what we mean when we describe the RVI as an instrument "that can refuse": no amount of favourable scoring elsewhere can buy back an option that has already been foreclosed.
Crucially, we don't have to guess how much future generations will value wood or carbon to make this argument. Whether a step is reversible or not is a factual, structural property of the decision — it does not depend on prices, weights, or assumptions about the future. This supports prioritising reuse over burning a second, independent foundation: reuse keeps options open; combustion does not, regardless of how tomorrow's preferences turn out.

## Results and Discussion

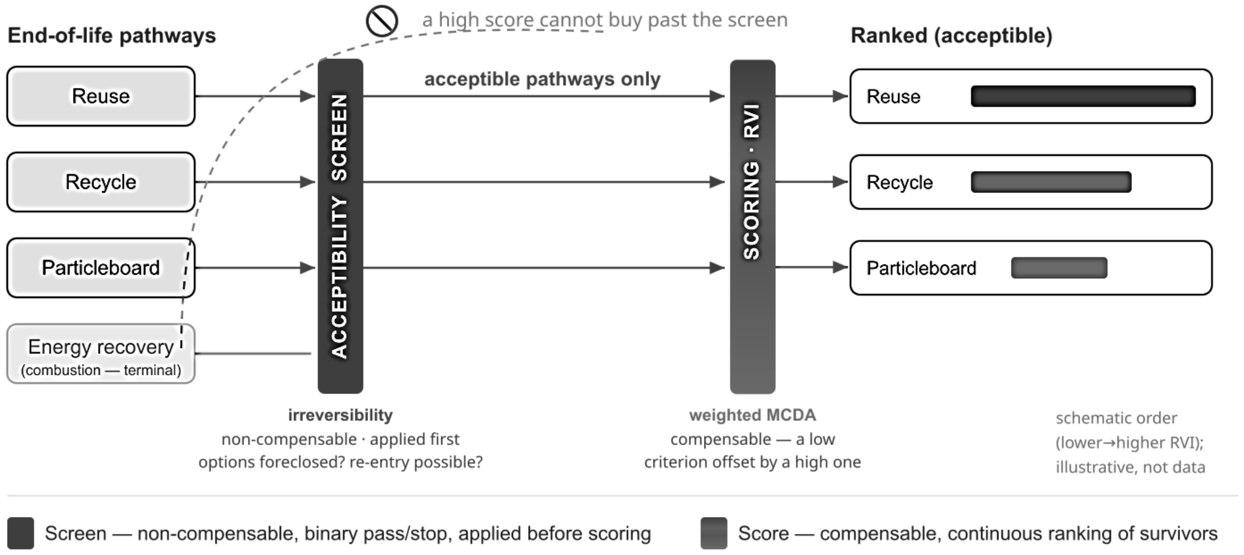


Figure 1. Acceptability screen versus scored dimension. A scored dimension can be compensated away by strong performance elsewhere; a safeguard, applied first, cannot. Irreversibility is computed as options foreclosed and re-entry possible — independent of weights, discount rate and assumed future preferences

We identify three situations that no current life-cycle model captures well. First, if carbon-removal technologies mature, the climate benefit of using wood instead of other materials could shrink over time — a shift in the background against which wood is compared, not in wood itself. Second, natural events — insect infestation, fire, storm damage — can destroy stored wood value abruptly, while most models assume smooth, predictable retention times. Third, we spot a genuine methodological conflict in current carbon accounting: the EU's own EN 15804+A2 standard uses a simple rule (carbon uptake counted as −1, release counted as +1) that keeps every calculation balanced and lets cascades be added up consistently across a whole supply chain. France's RE2020 regulation instead credits wood for delaying carbon release, which reflects how climate damage from an early ton of $CO_2$ differs from a later one — but this approach cannot be consistently combined across a multi-stage cascade, because there is no single shared timeline across different products and companies. These are not two versions of the same idea; they answer different questions, and an indicator that borrows from both without acknowledging this inherits an unresolved inconsistency.

We are equally clear about the limits of our own argument. Keeping options open has a cost, and where that cost is too high, keeping the option is not automatically the right choice. Our acceptability screen creates an indirect bar for irreversible decisions — it does not forbid them outright. And irreversibility is not black-and-white: even leaving a forest unharvested is, in its own way, irreversible. The argument for treating combustion specially works because the asymmetry is unusually clear-cut in that case, not because irreversibility always favours one option.

## Conclusion and outlook

The RVI offers policymakers, regulators and industry something the cascade principle alone does not: a transparent, checkable, common basis for comparing end-of-life choices, so that green claims can be confirmed or rejected on stated evidence rather than asserted on trust. By keeping irreversibility outside the scoring system — as a structural fact rather than a preference to be weighed — the RVI is designed to remain sound even as valuation frameworks and technologies change over coming decades. The current version applies to a fixed, one-directional model of how wood moves through the economy. The next stage of development will make this probabilistic: instead of assuming wood follows one predictable path, the model will estimate the range of paths real material actually takes. This is the step needed to use the RVI as a genuine monitoring tool for cascade policy at national and EU scale.

**References**

Arrow KJ, Fisher AC (1974) Environmental preservation, uncertainty, and irreversibility. Quarterly Journal of Economics 88: 312–319.

CEN (2019) EN 15804:2012+A2:2019 — Sustainability of construction works: Environmental product declarations, core rules for the product category of construction products. European Committee for Standardization, Brussels.

European Commission (2023) Proposal for a Directive on substantiation and communication of explicit environmental claims (Green Claims Directive). COM(2023) 166 final, Brussels.

Leskinen P, Cardellini G, González-García S, Hurmekoski E, Sathre R, Seppälä J, Smyth C, Stern T, Verkerk PJ (2018) Substitution Effects of Wood-Based Products in Climate Change Mitigation. From Science to Policy 7, European Forest Institute, Joensuu.

Henry C (1974) Investment decisions under uncertainty: the irreversibility effect. American Economic Review 64: 1006–1012.

Knight FH (1921) Risk, Uncertainty and Profit. Houghton Mifflin, Boston.

Lempert RJ, Popper SW, Bankes SC (2003) Shaping the Next One Hundred Years: New Methods for Quantitative, Long-Term Policy Analysis. RAND Corporation, Santa Monica.

Ministère de la Transition écologique (2021) Arrêté du 4 août 2021 relatif aux exigences de performance énergétique et environnementale des constructions de bâtiments (RE2020). Journal officiel de la République française, France.

Sirkin T, ten Houten M (1994) The cascade chain: a theory and tool for achieving resource sustainability with applications for product design. Resources, Conservation and Recycling 10: 213–276.

Weitzman ML (2009) On modeling and interpreting the economics of catastrophic climate change. Review of Economics and Statistics 91: 1–19.

# Valorisation of Bark Residues by Producing Stable Tannin Extracts

**<u>Lena Schnarr</u>[1], Reza Hosseinpourpia[1]**

[1]Department of Forestry and Wood Technology, Faculty of Technology, Linnaeus University, Lückligs Plats 1, Växjö 35195, Sweden, lena.schnarr@lnu.se, reza.hosseinpourpia@lnu.se

## Subtitle

Understanding the Biological Stability of Tannin Extracts: Identifying and Quantifying Microbial Contamination

## Background

For effective utilisation of forest biomass, tannins can be extracted from residual bark and used for a variety of applications (Hoque, Ayman et al. 2025). Life cycle assessments of the tannin extract production suggest optimising the energy consumption to improve the sustainability of the process (Ding, Bianchi et al. 2017, Niiranen, Forssell et al. 2026). Hence, as an alternative to energy-intensive drying to obtain a powder, the tannin extracts could be used in their liquid form. Presence of water in liquid tannin extracts, however, make them susceptible to abiotic and biotic degradation. To obtain insights into the biological stability of liquid tannin extracts, microorganisms capable of proliferating in them were identified. Moreover, a high-throughput method for quantifying microorganisms in complex matrices such as tannin extracts was developed. These insights contribute to the development of high-quality, durable bio-based products, hence promoting a shift towards a circular, bio-based economy.

**Keywords:** biomass, liquid tannin extract, biological stability, Geometric Viability Assay

## Experimental

Identification of the microorganism was performed by isolating pure cultures from softwood tannin extract (kindly provided by industrial partner) using the streak technique and 4.8% Malt Extract Agar (MEA) or 4.0% Tryptic Soy Agar (TSA). DNA from the pure cultures was extracted with the DNeasy PowerLyzer Microbial Kit (Qiagen), amplified by PCR (primer yeast: ITS1F, ITS4, primer bacteria: 27F, 1492R) and sent to Eurofins for Sanger Sequencing.
A Geometric Viability Assay (GVA) according to C.T. Meyer *et al.* (Meyer, Lynch et al. 2023) was performed with slight modifications: 2.4% MEA and 4%TSA were used as media, the distance of the colonies from the pipette tips was measured with ImageJ, and cell concentration was calculated in Excel. Under the same conditions, samples (100 µL) were spread on agar plates, and colonies were counted after 24 and 48 h.

## Results and Discussion

The DNA sequencing of the strains isolated from the tannin extract led to the identification of the two yeasts species *Nakazawaea holstii* and *Hanseniaspora valbyensis*. Insights into the bacterial community were less precise revealing the presence of a Bacillus species and a strain similar to *Lysinibacillus macrolides.* While Bacillus species (B. licheniformis and B.

cereus) and *Lysinibacillus macrolides* were previously described to use tannins as carbon source (Mohapatra 2006, Suhaimi, Zailani et al. 2024), *N. holstii* and *H. valvyensis* were isolated from a tannin extract for the first time.
To quantify these microorganisms in the tannin extract, the high-throughput Geometric Viability Assay was adapted for this purpose and validated against the common Colony Forming Unit Assay (CFUA). The cell concentrations of four samples (2-fold dilution series) determined with the two methods show a good correlation (Figure 1). However, the GVA resulted in higher cell concentrations than the CFUA by a factor of 1.6 to 3.1. Only in one of the *N.holstii* samples the cell concentration determined with both methods is similar. The tendency of the GVA to yield higher cell concentrations than the CFUA could be due to the better distribution of colony forming units in the 3D space in the pipette tip compared to the 2D plane of the agar plate. Despite differences in the actual number of CFU, both methods show a linear decrease in cell concentration as dilution progresses. Hence, the GVA is a suitable method to compare the effect of different treatments of tannin extract on contained microorganisms.

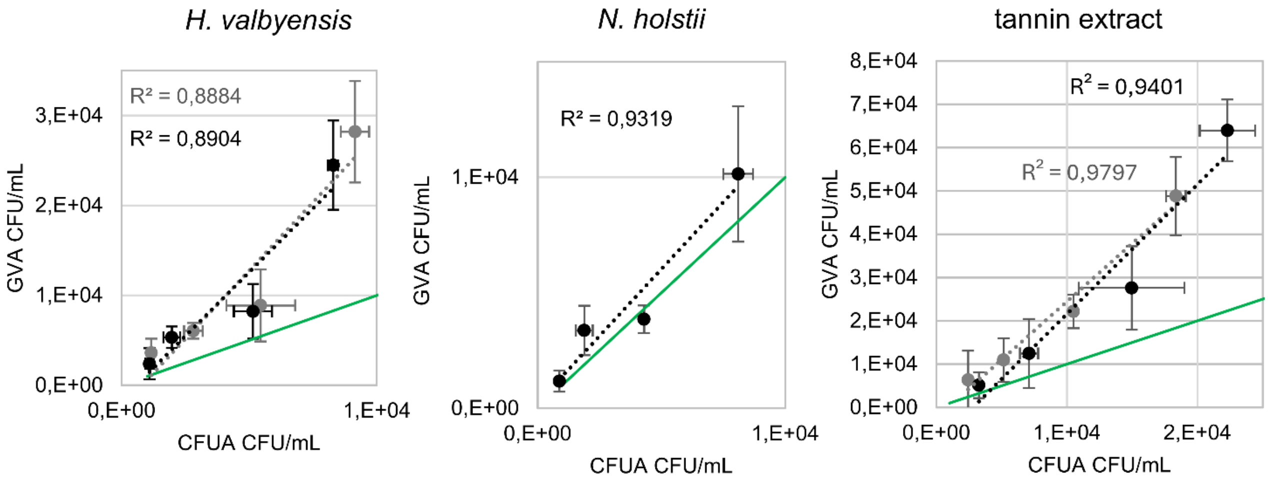


Figure 1. Correlation of the cell concentration determined with the Colony Forming Unit Assay on agar plates (CFUA, n=2) and the Geometric Viability Assay (GVA, n=3). Cell concentrations of pure yeast cultures *H. valbyensis* and *N. holstii* and of the tannin extract were determined. Grey dots: 24 h, black dots: 48h; dashed lines: linear fit with $R^2$, green line: 1:1 ratio

## Conclusions

This study takes two important steps toward understanding the biological stability of aqueous tannin extracts. Firstly, it provided insight into the microbial community able to proliferate in tannin extracts. Secondly, a high-throughput method to quantify these microorganisms was adapted to the challenging matrix tannin extract represent. This method enables further research to find more sustainable treatments and storage conditions that ensure a stable product.

**References**

Ding, T., S. Bianchi, C. Ganne-Chédeville, P. Kilpeläinen, A. Haapala and T. Räty (2017). Life cycle assessment of tannin extraction from spruce bark. iForest - Biogeosciences and Forestry 10(5): 807–814.

Hoque, M. B., U. Ayman, M. S. Sheikh, M. A. Hannan, P. Haque, B. Baria, M. M. Rahman, M. A. Jalil and D. Das (2025). An in-depth review on tannin sources, extraction methods, and industrial applications. Discover Food 5(1).

Meyer, C. T., G. K. Lynch, D. F. Stamo, E. J. Miller, A. Chatterjee and J. M. Kralj (2023). A high-throughput and low-waste viability assay for microbes. Nat Microbiol 8(12): 2304–2314.

Mohapatra, P. D., Keshab C. Mondal, and Bikas R. Pati. (2006). Production of tannase through submerged fermentation of tannin-containing plant extracts by Bacillus licheniformis KBR6. Polish Journal of Microbiology 55(4): 297–401.

Niiranen, I., S. Forssell, P. Oinas and R. Dickson (2026). Techno-economic and life cycle assessment of tannin production from spruce bark for leather industry applications. Green Chemistry 28(14): 6284–6294.

Suhaimi, M. S., F. A. Zailani, N. F. S. Mohd Zaki, F. Aris, M. T. Mat Jalil and N. A. Zakaria (2024). Isolation and Identification of Tannin-Degrading Bacteria From Goat Feces, Ruminal Fluid, and Rumen Gut. Malaysian Applied Biology 53(3): 23–37.

# Monitoring Structural Changes in Modified Beech Wood Using Multiscale Computed Tomography

**Lucie Zárybnická[1*], Petra Mácová[1], Jozef Ráhel'[2], Laurenz Schröer[3], Chandra Winardhi[3], Veerle Cnudde[3,4]**

[1]Institute of Theoretical and Applied Mechanics of the Czech Academy of Sciences, Czech Republic
[2]Department of Wood Science and Technology, Mendel University, Brno, Czech Republic
[3]Department of Geology, Ghent University, Ghent, Belgium
[4]Department of Earth Sciences, Utrecht University, Utrecht, the Netherlands

## Abstract

Monitoring structural changes in modified Beech wood (Fagus sylvatica L.) using high-resolution X-ray micro-computed tomography (micro-CT) and nano-CT offers non-destructive 3D visualization of internal anatomy and density analysis, which is crucial for validating sustainable wood protection technologies. While micro-CT tracks modifier distribution and cell network integrity, nano-CT provides a detailed view of submicron changes within the cell wall. The combination of both methods enables multiscale analysis for precise material lifespan prediction. The obtained results of the analysis of modified beech wood samples show that advanced CT imaging serves as a tool for environmentally friendly modification processes.

## Acknowledgments

This research was supported by the Czech Science Foundation (GAČR), project [24-10430S], and by the Czech Academy of Sciences, Institute of Theoretical and Applied Mechanics – RVO 68378297. This research has received funding from the European Union's Horizon 2020 research and innovation programme under grant agreement No 101005611 & Horizon Europe grant agreement No 101131765 (EXCITE) for Transnational Access conducted at the Centre for X-ray Tomography (UGCT) of Ghent University (BOF.COR.2022.008).

# Can Biochemicals Beat the Wood Burn? A Cone Calorimetry Investigation

**Konrad Wilkens Flecknoe-Brown[1], Reza Hosseinpourpia[2], Sheikh Ali Ahmed[2], Emil Engelund Thybring[3], Nils Johansson[1], Maria Fredriksson[4]**

[1]Division of Fire Safety Engineering, Lund University, Lund, Sweden, konrad.wilkens@brand.lth.se, nils.johansson@brand.lth.se,
[2]Department of Forestry and Wood Technology, Linnaeus University, Växjö, Sweden, reza.hosseinpourpia@lnu.se, sheikh.ahmed@lnu.se
[3]Bioresource Chemistry and Technology, University of Copenhagen, Frederiksberg, Denmark eet@ign.ku.dk
[4]Division of Buildings Materials, Lund University, Lund, Sweden, maria.fredriksson@byggtek.lth.se

## Abstract

Wood is combustible and depending on where in a building wood is used there are requirements regarding the use of fire retardants. However, several fire retardants have negative impact on human health or the environment and problems with leaching can cause decreased fire performance over time. In a previous study, we studied three bio biobased chemicals for use as fire retardant in small scale using micro combustion calorimetry (MCC) with samples of a few mg. In this study, we scaled up and performed cone calorimetry experiments for the two biobased chemicals (phytic acid and lignosulphonates) that performed best in the small-scale study.

## Acknowledgements

Funding from Åforsk is gratefully acknowledged.

# Integrated Evaluation of Biomass Productivity, Lignocellulosic Quality, and Carbon Sequestration Potential in Hybrid *Populus* Clones under Hemi-Boreal Conditions

**Marius Aleinikovas, Yanal Alkuddsi, Benas Silinskas, Mindaugas Skema, Lina Beniusiene[1]**

[1] Institute of Forestry, Lithuanian Research Centre for Agriculture and Forestry, Kaunas district, Lithuania, marius.aleinikovas@lammc.lt, yanal.alkuddsi@lammc.lt, benas.silinskas@lammc.lt, mindaugas.skema@lammc.lt, lina.beniusiene@lammc.lt

## Abstract

### Introduction & Methodology

Efficient woody biomass utilization for bioenergy and biorefineries requires an integrated understanding of yield, chemical composition, energetic value, and carbon potential. This study evaluated 19 hybrid *Populus* clones (hybrid poplars [HT] and aspens [HD]) from eight European provenances under Lithuanian hemi-boreal conditions. Clones were assessed for aboveground biomass (AGB), stem–branch partitioning, theoretical energy yield, carbon/$CO_2$ sequestration, lignocellulosic composition (cellulose, hemicellulose, lignin), mineral profiles, and multi-criteria suitability.

### Key Results

- **Yield & Energy:** Mean AGB reached 214.60 t ha$^{-1}$ (71.77–456.91 t ha$^{-1}$), yielding an average 3982.92 GJ ha$^{-1}$ and sequestering 393.79 t $CO_2$ ha$^{-1}$. Swedish clones produced the highest average biomass (369.92 t ha$^{-1}$).
- **Quality & Partitioning:** Samples averaged 50.76 % cellulose, 15.93 % hemicellulose, 17.20 % lignin, and 2.30 % ash. Stems contained significantly higher cellulose (56.69 % vs. 44.84 %) and hemicellulose, making them ideal for biochemical conversion, whereas branches concentrated ash and minerals (Ca, K, Mg).
- **Correlations & Taxa:** Strong correlations occurred between ash and Ca ($r$ = 0.981) and cellulose with NDF ($r$ = 0.933). HT clones led in biomass, while HD clones offered lower lignin levels.

### Conclusion & Ranking

Integrated ranking identified **SvSF Po 11** as the premier clone (biofuel score: 87.02), followed by Nyd3261-Degrosso, SvSF Po 12, D19, and Sv SF Po 7. Multi-trait screening provides an optimal decision framework for hemi-boreal bioenergy deployment.

**Keywords:** *Populus*; hybrid poplar; biomass quality; cellulose; carbon sequestration; clone ranking; biorefinery.

# Integrating Wood Density and Dendrometric Traits for Biomass and Carbon Prediction in Hybrid Populus Clones

**Mindaugas Škėma[1], Yanal Alkuddsi[1], Marius Aleinikovas[1], Benas Šilinskas[1], Lina Beniušienė[1]**

[1]Lithunaian Research Centre for Agriculture and Forestry, Forest resource, economics and policy department. Mindaugas.Skema@lammc.lt; Yanal.Alkuddsi@lammc.lt; Benas.Silinskas@lammc.lt; Marius.Aleinikovas@lammc.lt; Lina.Beniusiene@lammc.lt

**Abstract**

Hybrid Populus plantations are increasingly important as renewable wood resources for the emerging bioeconomy because they combine rapid growth, high biomass productivity and substantial carbon sequestration potential. However, reliable assessment of their productivity requires more than conventional tree-size measurements, as genetically diverse clones may differ markedly in wood density and biomass allocation. This study evaluated the relationships between dendrometric traits, wood density, above-ground biomass, bioenergy yield and carbon sequestration in 19 hybrid Populus clones grown under hemi-boreal conditions in Lithuania. The plant material represented hybrid poplars and hybrid aspens originating from eight European countries and was assessed within a long-term clonal trial established in 2012.

Diameter at breast height (DBH), tree height and stem volume were determined using standard dendrometric procedures. Representative trees were destructively sampled to quantify oven-dry stem and branch biomass, while apparent wood density was calculated from stem dry mass and corresponding stem volume. Total above-ground biomass was extrapolated to a stand density of 1,923 trees $ha^{-1}$. Biomass-derived energy yield was estimated using a lower heating value of 18.564 GJ $t^{-1}$, carbon stock was calculated assuming a carbon fraction of 0.50, and $CO_2$-equivalent sequestration was derived using the standard molecular conversion factor. Pearson correlation analysis and linear regression were used to quantify the relationships between structural and material traits and biomass productivity.

Substantial clonal variability was observed. Mean above-ground biomass reached 214.6 t $ha^{-1}$ and ranged from 71.8 to 456.9 t $ha^{-1}$, while mean energy yield was 3,982.9 GJ $ha^{-1}$. Mean carbon stock reached 107.3 t C $ha^{-1}$, corresponding to 393.8 t $CO_2$ $ha^{-1}$. DBH showed the strongest correlation with total biomass ($r = 0.768$, $p < 0.001$), followed by stem volume ($r = 0.724$, $p < 0.001$) and wood density ($r = 0.647$, $p = 0.0028$), whereas tree height showed only a weak and statistically non-significant relationship. Among single-predictor models, DBH explained 58.9% of biomass variation. In contrast, a multiple regression model integrating stem volume and wood density explained 94.8% of total biomass variation ($R^2 = 0.948$), demonstrating the strong complementary value of combining structural and material properties. The highest biomass productivity and energy potential were recorded for the clones SvSF Po11, SvSF Po12 and Nyd3261-Degrosso.

Branch biomass represented an important component of total productivity. On average, branches accounted for 23.83% of total dry biomass, with clone-specific values ranging from 10.59% to 32.56%. Excluding branches reduced estimated biomass, energy yield, carbon stock and $CO_2$-equivalent sequestration by 24.63%, showing that stem-only approaches may systematically underestimate the actual resource and climate-mitigation potential of hybrid poplar plantations. The results demonstrate that biomass formation in hybrid Populus cannot be explained by tree size alone. Integrating dendrometric traits with wood density and whole-tree biomass allocation provides a more accurate and biologically meaningful

basis for biomass prediction, clone selection and resource assessment. This approach can support sustainable wood-resource planning, bioenergy-oriented plantation management and more reliable carbon accounting under Northern European conditions.

**Keywords:** Hybrid Populus; wood density; dendrometric traits; biomass prediction; bioenergy; carbon sequestration; sustainable forestry.

# Effect of Process-Modulating Coatings on Plasma and Microwave Treatment of Beech Wood

**Petra Mácová**[1], **Lucie Zárybnická**[2], **Jozef Ráhel**[3]

[1,2]Institute of Theoretical and Applied Mechanics of the Czech Academy of Sciences, Prague, Czech Republic, macova@itam.cas.cz, zarybnicka@itam.cas.cz
[3]Department of Wood Science and Technology, Mendel University, Brno, Czech Republic, jozef.rahel@mendelu.cz

## Abstract

To mitigate internal strength loss during conventional wood thermal processing, this study investigates surface-localized thermal modification of beech wood (Fagus sylvatica L.). The effect of process-modulating coatings on the response of wood to arc-discharge plasma and microwave-assisted treatment was evaluated. The coatings were designed to influence heat distribution and stabilize the wood surface during thermal exposure. Chemical changes after exposure to the thermal treatments, together with surface performance, were analysed using Fourier Transform Infrared Spectroscopy (FTIR) and hardness measurements. The findings provide insight into optimalisation of surface hardness and efficiency of localized thermal wood modification.

## Acknowledgments

This research was supported by the Czech Science Foundation (GAČR), project [24-10430S] and by the Czech Academy of Sciences, Institute of Theoretical and Applied Mechanics – RVO 68378297.

# Chemical and Microstructural Changes in Thermally Treated Spruce Wood

**Radek Ševčík**[1], **Petra Mácová**[1], **Aneta Vyvadilová**[1], **Lucie Zárybnická**[1]

[1]Institute of Theoretical and Applied Mechanics of the Czech Academy of Sciences, Centre Telč, Prosecká 809/76, Prague 19000, Czechia, sevcik@itam.cas.cz, macova@itam.cas.cz, vyvadilova@itam.cas.cz, zarybnicka@itam.cas.cz

## Background

Wood remains a key building material due to its unique properties, such as sustainability and excellent thermal insulation (Chen et al., 2026). However, its degradation due to moisture, environmental factors, and biological organisms may cause serious breakdown of the wood structure (Cao et al., 2026). To maximise wood durability, surface protection is often used. For example, thermal treatment offers an effective modification method (Esteves et al., 2008). This method has been used since ancient times to improve some properties of wood (Sandberg et al., 2013). Nowadays, the interest in wood heat treatment is rising because of, e.g., a lack of high-quality timber and regulatory restrictions (Esteves et al., 2008). Even though numerous works on thermal treatment have been published, a comprehensive study of the gradual changes in chemical and microstructural properties induced by increasing temperature is missing. Thus, this research focuses on evaluating the physicochemical changes in Norway spruce (*Picea abies* L.) induced by thermal loads (150-500°C). A combination of analytical techniques, including UV spectroscopy, X-ray powder diffraction (XRPD), and scanning electron microscopy (SEM), was employed.

**Keywords:** spruce, thermal treatment, crystallinity.

## Experimental

Samples were produced from the Norway spruce (*Picea abies* L.). The wood dust samples were obtained by 5-minute grinding in a Mini-Mill Pulverisette 23 (30 osc/s; Fritsch, Germany) of 200 μm thin layers cut with a microtome (Leica RM2125 RTS, Germany). Dust samples (0.5 g) were thermally loaded in the range from 150 to 500 °C for 5 min.
The concentration of non-structural carbohydrates (NSC) was determined following the procedure described elsewhere (Teslová et al., 2010). The spectra were measured using a UV/VIS spectrophotometer Cary 60 Agilent. XRPD patterns were collected using a Bruker D8 Advance with the following set-up: Cu $K_\alpha$ radiation ($\lambda$ = 1.5418 Å) at 40 kV and 40 mA in the angular range 5–40°. Microstructural characterisation was performed using a SEM (Quanta 450 FEG, FEI), at an acceleration voltage of 20 kV. Before the observation, samples were gold-coated (10 nm).

## Results and Discussion

The determined NSC content is depicted in Figure 1 (on the left). Their maximum concentration was found to be in the sample loaded at 275°C. The gradual decrease in NSC concentration was then measured. A steep decrease was detected for the sample loaded at 375°C, as a consequence of lignin decomposition and transformation to char (Esteves et al., 2008). The measured XRPD patterns are visualised in Figure 1 (on the right). The typical reflections of cellulose assigned to the 1$\bar{1}$0, 110, and 200 crystallographic planes (Poletto et al., 2012) were identified in samples loaded up to 350°C. Higher thermal loads resulted in a significant decrease in the peak intensity of the 200 plane, suggesting a steep decline in crystallinity. Subsequently, only a broad peak, characteristic of the presence of biochar (Behazin et al., 2015), was recorded.

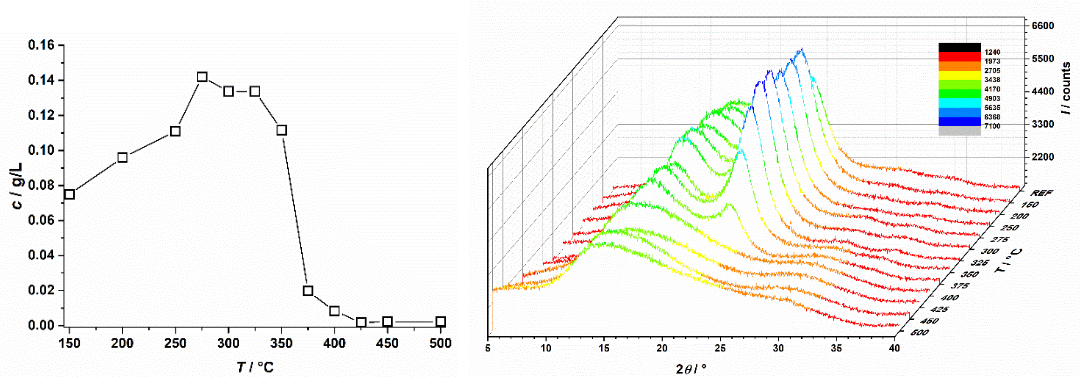


Figure 1. Determined content of non-structural carbohydrates (on the left) and collected XRPD patterns (on the right) of the spruce dust samples

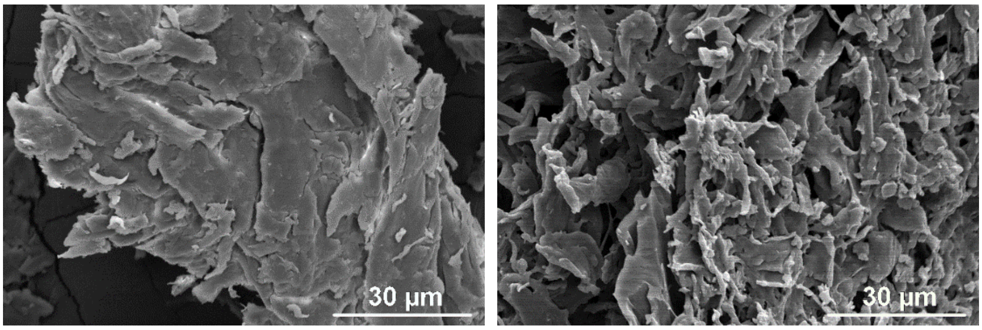


Figure 2. Collection of SEM images of the reference sample (on the left) and the sample after thermal loading at 500°C (on the right)

In Figure 2, examples of spruce dust morphology are shown. The high impact of the thermal treatment on the wood dust microstructure is clearly visible. The reference sample (105°C) was composed of well-preserved dense particles of irregular shapes due to the grinding procedure. In contrast, the sample heated at 500°C was observed to have grains with a highly porous structure full of defects. In recent work (Dúbravská et al., 2008), significant thinning of cell walls in tracheids, deterioration of bordered pits and localised structural collapses were identified in solid blocks at around 255°C.

## Conclusions

The results showed significant changes in non-structural saccharide content, cellulose crystallinity, and microstructure with regard to temperature loads. These findings can contribute to the design of procedures for long-term wood protection against moisture and UV radiation. To gain a more complex insight, the study will be supported by results from other tests like thermogravimetry, infrared spectroscopy, and colorimetry.

## Acknowledgements

This research has been supported by the Czech Science Foundation (GAČR), project No. 24-10430S, and by the Czech Academy of Sciences, Institute of Theoretical and Applied Mechanics – RVO 68378297.

**References**

Behazin, E.; Ogunsona, E.; Rodriguez-Uribe, A.; Mohanty, A.K.; Misra, M.; Anyia, A.O. (2015) Mechanical, Chemical, and Physical Properties of Wood and Perennial Grass Biochars for Possible Composite Application. BioResources, 11, 1334–1348.

Cao, Y.; Fang, J.; Chen, S.; Zhu, L.; Xie, X.; Xing, H.; Liu, M.; Ding, Y.; Qiao, Y. (2026) Preservation of Wood-Based Products against Biotic and Chemical Degradation: Past, Present and Future. Wood Mater. Sci. Eng. 21, 871–892.

Chen, L.; Tamagnone, G.; Wan-Wendner, L. (2026) Review of Wood Species and Material Characteristics of Mass Timber for Structural Applications. Low-Carbon Mater. Green Constr. 4, 8, 1–42.

Dúbravská, K.; Mamoňová, M.; Kučerová, V. (2026) Microstructural Features of the Transition from Thermal Degradation to Initial Char Formation in Spruce Wood. Fire, 9, 333,1–24.

Esteves, B.M.; Pereira, H.M. Wood Modification by Heat Treatment: A Review. (2008) BioResources, 4, 370–404.

Poletto, M.; Zattera, A.J.; Forte, M.M.C.; Santana, R.M.C. (2012) Thermal Decomposition of Wood: Influence of Wood Components and Cellulose Crystallite Size. Bioresour. Technol., 109, 148–153.

Sandberg, D.; Haller, P.; Navi, P. (2013) Thermo-Hydro and Thermo-Hydro-Mechanical Wood Processing: An Opportunity for Future Environmentally Friendly Wood Products. Wood Mater. Sci. Eng., 8, 64–88.

Teslová, P.; Kalina, J.; Urban, O. (2010) Simultaneous Determination of Non-Structural Saccharides and Starch in Leaves of Higher Plants Using Anthrone Reagent. Chem. Listy, 867–870.

# A Pilot Study on the Influence of Previous Service Orientation on the Reuse of Structural Timber

**Serkan Karatosun**[1], **Lisbeth Ottosen**[2]

[1] Technical University of Denmark, Denmark, serkar@dtu.dk,
[2] Technical University of Denmark, Denmark, limo@dtu.dk

## Background

Reusing structural timber elements can extend their service life and reduce the demand for virgin timber. However, timber recovered from existing structures has already been exposed to sustained loading during its previous service life, resulting in time-dependent deformation and changes that may not be uniform across the cross-section. When a timber beam is reused, the previously tensioned and compressed sides may either retain their loading orientation or be reversed. It remains unclear whether this previous loading orientation influences deformation during a subsequent service phase and, consequently, whether orientation should be considered when documenting structural timber for reuse.
This pilot study investigates the response of timber beams subjected to repeated sustained loading, with the previous loading orientation either retained or reversed during the second loading phase. Mid-span deflection is used to evaluate the load–deformation response, while indirect ultrasonic pulse velocity (UPV) is investigated as a complementary non-destructive method for monitoring changes during sustained loading and recovery. Previous laboratory investigations have reported that the applied load has a negligible influence on UPV in clear wood specimens under short-term loading (Shaji et al., 2000). However, the UPV response of strength-graded structural timber under sustained loading remains less understood.

**Keywords:** reclaimed timber, reuse, NDT, ultrasonic pulse velocity (UPV)**.**

## Experimental

Two C18 strength-graded timber beams (C1 and C2), with a span of 2.0 m, were subjected to two phases of sustained three-point bending under controlled environmental conditions. Both specimens were loaded in the same orientation during Phase 1 for approximately 31 days, then unloaded and allowed to recover. Before Phase 2, C1 was flipped 180° about its longitudinal axis, reversing the previously tensioned and compressed sides, while C2 retained its previous orientation. The same loading configuration and load magnitude were applied for approximately 112 days.
Mid-span deflection was regularly monitored using a laser distance meter referenced to a fixed point above the beam. Indirect UPV measurements were conducted on the upper surface, corresponding to the compression side during loading, using a Pundit 200 with 54 kHz round transducers. Measurements were taken before and after loading, before and after unloading, and following recovery.
Two indirect UPV approaches were used. In the fixed-distance approach, the transducers were positioned 600 mm apart and centred around the beam midpoint. In the variable-distance approach, the transmitter remained fixed while the receiver was moved to different distances, enabling evaluation of the relationship between transmission time and propagation distance rather than determining UPV from a single transducer distance. The

minimum stable transmission time was recorded for both approaches. Only results from the fixed-distance approach are presented in this work.

## Results and Discussion

During Phase 1, C1 and C2 showed comparable deformation responses (Table 1). This comparable initial response provides a reference for evaluating the effect of changing the loading orientation in Phase 2. In Phase 2, both specimens again exhibited the same normalised immediate deflection (0.95%). However, their responses diverged during sustained loading, with additional normalised deflections of 0.30% for the flipped C1 and 0.10% for C2, which retained its previous orientation. These results indicate that previous loading orientation may influence the time-dependent deformation of structural timber during subsequent reuse.

Indirect UPV showed relatively small changes during sustained loading and recovery, ranging in magnitude from 0.31% to 1.82%, with no consistent trend between specimens or loading phases. Therefore, the measurements do not indicate a systematic UPV response associated with sustained loading, unloading, or the observed differences in deformation. This is consistent with Shaji et al. (2000), who reported that applied load had a negligible influence on UPV in clear wood specimens.

Table 1. Normalised mid-span deflection and relative changes in fixed-distance indirect UPV during the two loading phases

| Phase | Specimen | $\delta_{\mathrm{im}}/L$ | $\delta_{\mathrm{SL}}/L$ | $\delta_{\mathrm{tot}}/L$ | $\delta_{\mathrm{res}}/L$ | $\Delta\mathrm{UPV}_{\mathrm{SL}}$ | $\Delta\mathrm{UPV}_{\mathrm{R}}$ |
|---|---|---|---|---|---|---|---|
| 1 | C1 | 1.10 | 0.25 | 1.35 | 0.35 | −0.90 | −1.72 |
| 1 | C2 | 1.05 | 0.35 | 1.40 | 0.35 | 1.65 | −1.31 |
| 2 | C1-Flipped | 0.95 | 0.30 | 1.25 | 0.25 | −1.82 | 1.03 |
| 2 | C2-Retained | 0.95 | 0.10 | 1.05 | 0.05 | 1.03 | 0.31 |

All values are expressed in %. Deflections were normalised by the beam span, $L = 2.0\ m$. $\delta_{im}$: immediate deflection; $\delta_{SL}$: additional deflection during sustained loading; $\delta_{tot}$: total deflection; $\delta_{res}$: residual deflection after recovery; SL: sustained loading; R: recovery.

## Conclusions

This pilot study indicates that previous loading orientation may influence the time-dependent deformation of structural timber during a subsequent service phase. While the immediate response to reloading was comparable, a difference developed during sustained loading after one specimen was flipped. The findings suggest that previous loading orientation may therefore be relevant when assessing structural timber for reuse. Indirect UPV showed limited changes, with no consistent response between specimens or loading phases. Further testing with additional specimens is needed to confirm these findings.

## References

Shaji, T., Somayaji, S. and Mathews, M.S., 2000. Ultrasonic pulse velocity technique for inspection and evaluation of timber. Journal of Materials in Civil Engineering, 12(2), pp.180-185.

# Image Segmentation of CT and Microscopy Images for the Identification of Earlywood and Latewood in Fagus S. to Determine the Accuracy of CT Scans

**Felix Stegmann[1], Anja Kampe[1], Lennart Blümel[1], Luis Miranda[1]**

[1]Department Forest - Wood - Environment, Eberswalde University for Sustainable Development, Schicklerstraße 5, 16225 Eberswalde, Germany, felix.stegmann@hnee.de, anja.kampe@hnee.de, blümel.lennard@hnee.de luis.miranda@hnee.de

## Background

The establishment of the computer tomography (CT) facility within an infrastructure project at the Eberswalde University for Sustainable Development has opened new possibilities for research in forestry, wood science and environmental studies. As part of this initiative, 298 cubic samples from 12 wood species (softwood, hardwood) were prepared, dried, and analysed in accordance with DIN 52182 standards for usage as dataset to investigate. This dataset is necessary to investigate the reliability of x-ray computer tomography scans to determine wood properties. The properties are needed for further research into the mechanical and physical characteristics of wood, with the intention to create processes that show greater appreciation for nature due to the climatic circumstances and higher need of living than dying trees.
This paper searches for a ground truth to identify earlywood (EW) and latewood (LW) from (*Fagus sylvatica L.)* samples with microscopic images to compare it with the measured results of the CT scan. The comparison is essential in order to draw conclusions about the potential accuracy of the CT scans. The identification of EW and LW is part of the process that could enable more efficient use of wood resources towards an optimized wood usage across diverse fields such as construction, furniture design, mobility solutions, and device manufacturing.

**Keywords:** computer tomography, microscopy, Fagus Sylvatica, image segmentation, earlywood and latewood

## Material and Methods

25 (20*20*20 mm) beech (*Fagus sylvatica L.)* samples were used for Microscopy and a CT scan. The samples were stored in a climate chamber at 65% humidity and 20 C°. For the microscopic imaging the cross section was sanded with 120 and 400-grit sandpaper.

### Microscope

The samples were examined with the Microscope Leica DVM6 A to prepare TIFF images with the Software LAS X for the segmentation of EW and LW with following settings for a wide field, low magnification imaging (resolution 1600*1200 (2MP), magnification 0.223x, FOV43.75, autofocus).

### CT

Furthermore, the samples were measured with the CT Pegaso Evolution to create DICOM images for the segmentation. The following settings were used for the scan. Voltage

140kVp, current 50mA, exposure time 10ms, HEAVY collimator filter Cu 2mm, Voxel size 0.25mm and standard FOV settings 265mm, 230mm.

**Program**

For the image segmentation of the CT and microscopic images a python program was created with the support of Claude Haiku 4.5 (GPT, LLM Model) for the image segmentation based on grey values. Both programs need more research in the field of image segmentation and the usage of simple and adaptive threshold algorithms which are provided by the Python library OpenCV.

Table 1: Microscopic segmentation statistics for EW and LW

| Sample | Image Size | Total Pixels | EW Pixels | LW Pixels | EW % | LW % |
|---|---|---|---|---|---|---|
| BU1 | 1113 × 1123 | 1,249,899 | 1,060,368 | 248,767 | 84.84% | 19.90% |
| BU2 | 1144 × 1145 | 1,309,880 | 1,079,322 | 293,571 | 82.40% | 22.41% |
| BU3 | 1091 × 1119 | 1,220,829 | 1,037,788 | 263,837 | 85.01% | 21.61% |
| BU4 | 1080 × 1157 | 1,249,560 | 1,065,227 | 245,145 | 85.25% | 19.62% |
| BU5 | 1090 × 1126 | 1,227,340 | 1,040,297 | 261,536 | 84.76% | 21.31% |

## Results and Discussion

First estimations of EW and LW shares of beech with the created program for image segmentation of microscopic images are promising but further investigations and verification are necessary. As well as an optimization of the programs for a more precise segmentation of sample/object table recognition and EW and LW boundaries. The Initial investigations showed that it is possible to distinguish between EW and LW in Beech using microscopic and CT measurements.

The questions to be addressed by the experimental design, how accurately can the respective proportions be determined using the selected methods? Are the values sufficiently accurate to create digital models or simulations for beech? Which scale is the most suitable for future processes in wood processing (micro-, macro-, nanoscale)?

## Conclusions

This abstract should be understood as experimental exploration of image segmentation for beech with CT and microscopy. It raises further questions about sample preparation, image segmentation and programming, with the aim of providing a basis for discussion and knowledge exchange with other researchers and institutions.

**References**

Charline Freyburger, Fleur Longuetaud*, Frédéric Mothe, Thiéry Constant, Jean-Michel Leban (2009), Measuring wood density by means of X-ray computer tomography, INRA, UMR1092 LERFoB, 54280 Champenoux, France, AgroParisTech, UMR1092 LERFoB, 54000 Nancy, France

Daniela Diaconu, Jan Hackenberg, Dominik Florian Stangler, Hans-Peter Kahle, Heinrich Spiecker, Simulation study to determine necessary sample sizes for image analysis-based quantitative wood anatomy of vessels of beech (Fagus sylvatica), Dendrochronologia, Volume 45, 2017, Pages 35-38, ISSN 1125-7865

Georg von Arx, Marco Carrer, ROXAS – A new tool to build centuries-long tracheid-lumen chronologies in conifers, Dendrochronologia, Volume 32, Issue 3, 2014, Pages 290-293,

Peters RL, Klesse S, Van den Bulcke J, Jourdain LMY, von Arx G, Anadon-Rosell A, Krejza J, Kahmen A, Fonti M, Prendin AL, Babst F and De Mil T (2025) Quantitative vessel mapping on increment cores: a critical comparison of image acquisition methods.

# Peel Behavior for MAH Modified PLA Filament Printed on Wood

**Anja Kampe[1], Lennart Blümel[1], Tobias Cremer[1]**

[1]Eberswalde University for Sustainable Development, Germany,
anja.kampe@hnee.de; lennart.bluemel@hnee.de;
tobias.cremer@hnee.de

## Background

Additive manufacturing is becoming increasingly important as a resource-efficient and geometrically flexible manufacturing process, particularly when combined with bio-based materials. Direct 3D printing on wood surfaces opens up new possibilities for hybrid components, for example, in furniture, design, and prototyping, but at the same time presents various challenges at the interface between the polymer and the wood.
Our study investigates the adhesion properties of polylactid acid (PLA) structures between PLA and wood, that were 3D-printed directly on wood. More specifically, we were focusing on improving interfacial bonding through maleic anhydride (MAH) modification. The hypothesis was that a higher proportion of MAH in filaments leads to a greater surface soundness.

**Keywords:** additive manufacturing, wood surfaces, Surface Soundness Test

## Experimental

### Wood

The specimens were taken from beech (*Fagus sylvatica* L.) and pine (*Pinus sylvestris* L.). The surfaces were sanded with P150 grit sandpaper. All specimens were conditioned by 20°C and 65% relative humidity before printed directly using the various filaments.
The dimensions of the specimens used for the printing process were 210 mm x 235 mm x 1,5 mm (length x width x thickness). After printing the specimens were reinforced with plywood and cut into 50 mm x 50 mm parts for peel testing.

### Filaments

For this study filaments made of polylactid acid (PLA) were used. Unmodified PLA served as a reference, the other PLA filaments were compounded with 3, 7, and 10 wt% maleic anhydride (MAH). For each filament and each type of wood 30 test specimens were produced.

### Printing

For printing directly on the wood surfaces a Prusa MK4 printer was used. Steel mushroom-shaped pads (Figure 1) made from various filaments in accordance with DIN EN 311 were printed onto the wooden surfaces.

Figure 1. PLA based steel mushroom-shaped pad

**Surface Soundness Test**
The surface soundness test and the calculation of the surface soundness (SS) were conducted in accordance with the DIN EN 311.

**Results and Discussion**

The results show that the surface soundness of the test specimens made from unmodified PLA is significantly higher than that of the modified PLA (see Table 1). In addition, it became apparent during the test specimens preparation that some of printed steel mushroom-shaped pads already detached from the wood before the peel testing.

Table 1. Average surface soundness (SS) [N/mm²]

| Material | PLA unmodified | PLA 3% MAH | PLA 7% MAH | PLA 10% MAH |
|---|---|---|---|---|
| Beech | 0,838 | 0,381 | 0,270 | 0,285 |
| Pine | 0,816 | 0,696 | 0,192 | 0,267 |

**Conclusions**

The results show that compounding PLA with MAH did not result in any improvement in interfacial adhesion, and that surface soundness tended to decrease as the additive content increased.
The following studies will focus on the chemical incorporation of the MAH and the adjustment of the printing parameters (for example bed temperature of the printer, construction of the steel- mushroom shaped pads, etc.).

## References

DIN EN 311:2002. Abhebefestigkeit der Oberfläche- Prüfverfahren. Wood-based panels — Surface soundness — Test method — German version EN 311:2002.

# Mechanical and Vibroacoustic Performance of Birch, Hybrid Aspen and Hybrid CLT Panels

**Martins Irbe[1], Andrejs Pupurs[2], Edgars Kuka[3], Dace Cirule[4]**

[1,2] Riga Technical University, Latvia, martins.irbe@rtu.lv, andrejs.pupurs@rtu.lv
[3,4] Latvian State Institute of Wood Chemistry, edgars.kuka@kki.lv, dace.cirule@kki.lv

## Background

Cross-laminated timber (CLT) structures increasingly require alternative material solutions with shorter wood rotation cycles, improved availability, and lower production costs while maintaining structural performance and acoustic properties. However, the CLT industry remains conservative, relying primarily on softwood species due to their proven mechanical properties and durability. Recent studies have demonstrated the potential of hardwood species, particularly fast-growing hardwoods, for use in less critically loaded layers of hybrid CLT panels, thereby reducing the overall timber rotation cycle. Mixed-species CLT Das et al., (2023), combining hardwood and softwood, has emerged as a promising research direction, where stronger softwood is used in the outer load-bearing layers and fast-growing hardwood in the inner layers. Although Satir et al. (2024) have investigated combinations such as southern pine–yellow poplar and maple–poplar, research remains limited to a few species. This study focuses on birch and fast-growing hybrid aspen, two hardwood species available in the Baltic region, evaluated both as homogeneous CLT panels and as mixed-species CLT hybrids. The static and dynamic bending stiffness properties, bending strength, and vibroacoustic performance of the developed CLT panels are investigated and compared to assess the potential of fast-growing hardwood species for sustainable engineered timber construction.

**Keywords:** hybrid CLT, fast-growing wood, MOE, MOR, Transmission Loss

## Experimental method

Three groups of three-layer CLT panels (0/90/0) with a layer thickness of 20 mm were manufactured: A – hybrid aspen CLT panel; B – birch CLT panel; and BAB – modified CLT panel with birch face layers and a hybrid aspen cross layer. The static modulus of elasticity (MOE) was determined by four-point bending with minor modifications to the EN 408 standard. Two methods were used to calculate MOE depending on the displacement measurement technique: 1) from the displacement of the upper loading support, and 2) using Digital Image Correlation (DIC) by measuring beam deflection on the panel surface. The dynamic MOE was determined using a modified ASTM E1876 procedure with laser vibrometry and ultrasonic excitation. The modulus of rupture (MOR) was determined by three-point bending in accordance with DIN 52186, which was selected due to the limited panel length. The sound transmission loss (TL) was measured in an impedance tube following the procedures specified in ISO 10534-2.

## Results and Discussion

The highest modulus of elasticity (MOE) in Fig. 1a is observed for the birch (B) CLT panel, with slightly lower values for the modified (BAB) panel, where the difference ranges from −0.22% (DIN 52186) to −2.25% (DIC according to EN 408). In contrast, the MOE of pure hybrid aspen (A) CLT is on average 17% lower than that of B CLT across all testing methods (±1.5%). Comparing MOE between the methods in Fig. 1a, the largest difference is observed for results based on testing-machine displacement (DIN 52186). However, the MOE determined from machine displacement shows a more consistent trend with the dynamic MOE, which is on average 13% higher. The average difference between DIC and dynamic MOE is 5%, although the trend is not consistent. The MOE of CLT panels follows the characteristic relationship for wood, with stiffness increasing with density. More stable MOR values (Fig. 1b) are observed for B panels, exceeding 80 MPa, whereas A and BAB panels show considerable scatter from 60 to 80 MPa. For the CLT panels in Fig. 1c, the damping coefficient η shows no correlation with stiffness or density, and the values indicate no clear trend among the wood types used. In contrast, as shown by the averaged transmission loss (TL) values for each panel series in Fig. 1d, TL increases from 100 to 350 Hz and follows a similar trend regardless of the wood species used in the panel.

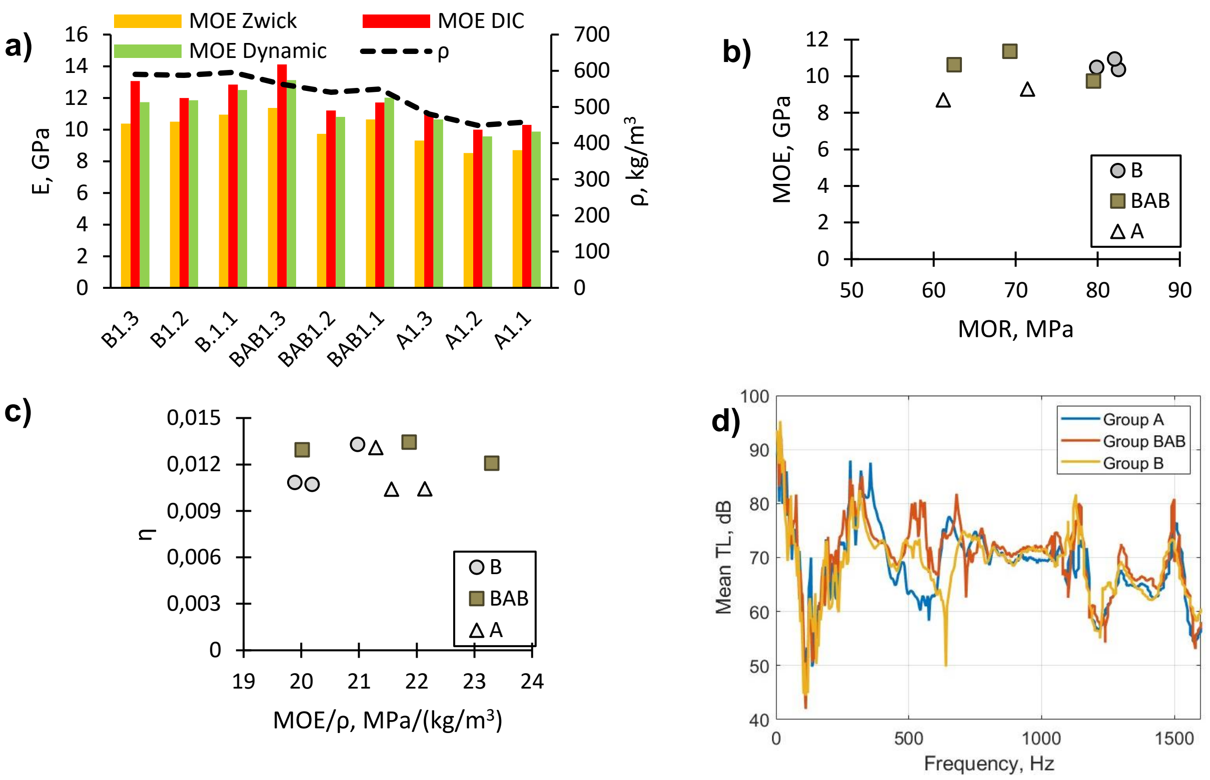


Figure 1. Experimental results of CLT panel types: a) MOE – Zwick and DIC with 4-p static test, and Dynamic with free-free vibration modal analysis; b) Stiffness and Strength; c) Loss factor and specific modulus of elasticity; d) Average Transmission Loss

## Conclusions

The experimental results indicate that the use of fast-growing hybrid aspen in CLT panels affects the overall mechanical properties by increasing result variability while maintaining relatively high performance. Vibroacoustic measurements do not clearly demonstrate an advantage of either wood species.

**Acknowledgment**

This research is funded byVPP-IZM-Sports-2023/1-0001 Innovations, Methodologies and recommendations for the development and management of the sports sector in Latvia.

**References**

Das, S., Gašparík, M., Sethy, A. K., Kytka, T., Kamboj, G., & Rezaei, F. (2023). Bonding performance of mixed species cross laminated timber from poplar (Populus nigra L.) and maple (Acer platanoides L.) glued with melamine and PUR adhesive. *Journal of Building Engineering*, *68*, 106159. https://doi.org/10.1016/J.JOBE.2023.106159

Satir, E., Adhikari, S., & Hindman, D. P. (2024). Evaluation of bending and shear properties of mixed softwood & hardwood cross-laminated timbers. *Journal of Building Engineering*, *96*, 110646. https://doi.org/10.1016/J.JOBE.2024.110646

# SESSION 3:
# NEW APPROACHES IN WOOD RESEARCH

# Deep Learning-Based Knot Segmentation in Wet-State X-Ray CT Images of Norway Spruce

**Shuai Zou[1], Linus Olofsson[1], Johannes A. J. Huber[1,2], Magnus Fredriksson[1]**

[1]Luleå University of Technology, Skellefteå, Sweden, shuai.zou@ltu.se, linus.olofsson@ltu.se, johannes.huber@ltu.se, magnus.1.fredriksson@ltu.se,
[2]Wood K Plus – Kompetenzzentrum Holz GmbH, St. Veit an der Glan, Austria

## Background

Knots affect timber quality, mechanical performance, sawing decisions, and product value. X-ray computed tomography (CT) enables non-destructive visualisation of internal wood features, but knot segmentation in wet-state CT remains challenging in sapwood because free water reduces contrast. Recent studies have shown the applicability of deep learning for this task (Stefano et al. 2019; Hossain et al. 2026), yet systematic comparisons of network architectures under a unified protocol remain limited. This work evaluates deep learning models for slice-wise binary segmentation of knots in wet-state CT images of Norway spruce. Here, knot segmentation refers to identifying the complete knot region in each CT slice. The resulting masks are intended to support downstream live/dead knot analysis, quantitative knot measurement, and CT-based timber assessment.

**Keywords:** Computed Tomography, Non-destructive Testing, Knot Segmentation, Deep Learning.

## Experimental

Norway spruce (Picea abies (L.) Karst.) knot whorl discs from ten trees were scanned in both wet and dry states using an X-ray CT system. The reconstructed CT volumes had an isotropic spatial resolution of 0.5 mm. Wet-state CT images were used as model input because they represented the intended application condition, while dry-state scans provided higher knot–sapwood contrast and were used to support expert annotation.
Knot regions were annotated on dry-state CT images and then transferred to a wet-state voxel grid by rigid image registration. This provided paired wet-state CT slices and binary ground-truth masks for knot versus non-knot segmentation. Axial 2D slices were extracted from the wet-state volumes, resized to 256 × 256 pixels, and split at the tree level into training, validation, and test sets to avoid data leakage.
Five 2D segmentation networks were trained and evaluated under the same preprocessing and optimisation protocol: U-Net (Ronneberger et al. 2015), Attention U-Net (Oktay et al. 2018), SegResNet (Myronenko 2019), Swin-UNet (Cao et al. 2022), and U-Net++ (Zhou et al. 2018). The networks were trained on knot mask targets from wet-state CT slices using a Dice-based loss with lightweight boundary-focused regularisation. Performance was assessed by comparing predicted and ground-truth masks using overlap-based segmentation metrics, i.e. Dice and Intersection over Union (IoU).

## Results and Discussion

Table 1 shows the segmentation results on wet-state CT slices. U-Net++ achieved the best performance, with a Dice coefficient of 0.7312 and an IoU of 0.6328, while also using the fewest parameters. Attention U-Net and SegResNet showed similar performance, both outperforming the standard U-Net baseline. Swin-UNet achieved intermediate results despite having the largest model size, suggesting that convolutional architectures may be more suitable for this task under the available data conditions. Qualitative inspection showed that most models captured the main knot bodies, while remaining errors occurred mainly near thin branches, knot boundaries, and low-contrast regions.

Table 1. Knot segmentation performance on wet-state CT slices

| Model | Dice coefficient | Intersection-over-Union | Parameters (M) |
|---|---|---|---|
| U-Net | 0.6661 | 0.5580 | 6.495 |
| SegResNet | 0.7105 | 0.6047 | 6.299 |
| Swin-UNet | 0.6886 | 0.5856 | 25.157 |
| Attention U-Net | 0.7114 | 0.6136 | 7.946 |
| U-Net++ | 0.7312 | 0.6328 | 2.410 |

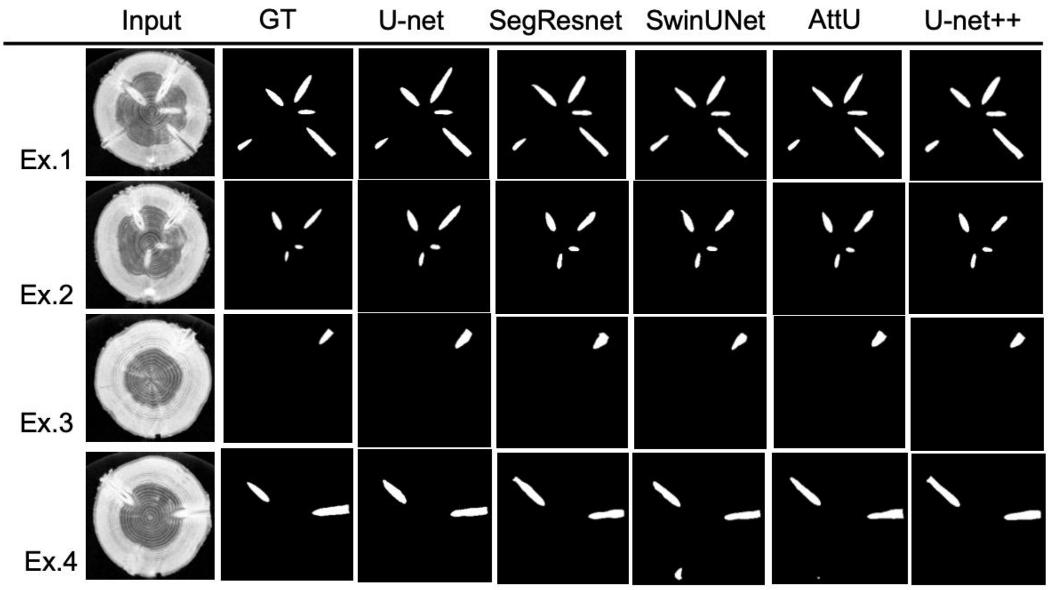


Figure 1. Qualitative comparison of knot segmentation results on wet-state X-ray CT slices. Columns show the input CT image, ground truth (GT), and predictions from U-Net, SegResNet, Swin-UNet, Attention U-Net and U-Net++

## Conclusions

This study presents a controlled benchmark for knot segmentation in wet-state X-ray CT slices of Norway spruce, enabling a comparison of modern 2D segmentation networks under a unified protocol. U-Net++ achieved the highest Dice and IoU while using the fewest parameters, suggesting that nested multi-scale feature fusion is effective for capturing elongated knot structures under low-contrast wet-state CT conditions.

**References**

Cao H, Wang Y, Chen J, Jiang D, Zhang X, Tian Q, Wang M (2022) Swin-Unet: Unet-like pure transformer for medical image segmentation. In: Computer Vision – ECCV 2022 Workshops, Lecture Notes in Computer Science 13803: 205-218.

Giovannini S, Boschetto D, Vicario E, Cossi M, Busatto A, Ghidoni S, Ursella E (2019) Improving knot segmentation using deep learning techniques. In: Proceedings 21st International Nondestructive Testing and Evaluation of Wood Symposium, pp 40-47. US Department of Agriculture.

Hossain MJ, Vestøl GI, Broman O, Reichert T, Tomic O, Olofsson L (2026) KnotSegNet3D: high precision knot segmentation in Norway spruce CT logs via mixed training and fine-tuned transfer learning. Wood Science and Technology 60: 54.

Myronenko A (2019) 3D MRI brain tumor segmentation using autoencoder regularization. In: Crimi A, Bakas S, Kuijf H, Keyvan F, Reyes M, van Walsum T (eds) Brainlesion: Glioma, Multiple Sclerosis, Stroke and Traumatic Brain Injuries. Springer, Cham: 311-320.

Oktay O, Schlemper J, Folgoc LL, Lee M, Heinrich M, Misawa K, Mori K, McDonagh S, Hammerla NY, Kainz B, Glocker B, Rueckert D (2018) Attention U-Net: Learning where to look for the pancreas. arXiv preprint arXiv:1804.03999.

Ronneberger O, Fischer P, Brox T (2015) U-Net: Convolutional networks for biomedical image segmentation. In: Medical Image Computing and Computer-Assisted Intervention – MICCAI 2015, Lecture Notes in Computer Science 9351: 234-241.

Zhou Z, Siddiquee MMR, Tajbakhsh N, Liang J (2018) UNet++: A nested U-Net architecture for medical image segmentation. In: Deep Learning in Medical Image Analysis and Multimodal Learning for Clinical Decision Support, Lecture Notes in Computer Science 11045: 3-11.

# CT-Sinogram Visualizer: Interactive Visualization of CT Acquisition Geometry and Sinogram Data in Wood Research

**Oualid Burström[1], Julius Häger[2], Ozan Öktem[3]**

[1]Luleå University of Technology, Sweden, oualid.burstrom@ltu.se,
[2]KTH Royal Institute of Technology / InfraVis, Sweden, juliusha@kth.se,
[3]KTH Royal Institute of Technology, Sweden, ozan@kth.se

## Background

Computed tomography (CT) is increasingly used in wood research to study internal structures such as knots, density variation, cracks and growth-related features. In many workflows, the reconstructed volume is the first object of analysis, while the acquisition geometry and measured projection data are difficult to inspect directly. This limits the possibility to relate reconstruction quality to source position, detector geometry, projection sampling and scan trajectory.

Sinogram data are the measured X-ray projection data before reconstruction. They contain important information about the acquisition process, but are commonly stored as large numerical arrays that are not easily accessible to wood researchers or CT scan operators. A visual tool that links acquisition geometry and sinogram data can therefore support quality assessment, methodological transparency and clearer communication of CT-based methods.

This work presents the CT-sinogram visualizer, a Python-based 3D Slicer plugin developed through collaboration between KTH, InfraVis and Luleå University of Technology. The objective is to visualize acquisition geometry and measured sinogram data before reconstruction, thereby helping users investigate how acquisition geometry may affect reconstruction quality and interpretation of wood structures. Although the present application is wood CT, the same visualization principle is relevant for other CT-based fields where raw projection data and acquisition geometry must be inspected before reconstruction.

**Keywords:** computed tomography, sinogram, 3D Slicer, wood science, acquisition geometry, visualization.

## Experimental

The solution follows a client-server design. 3D Slicer provides the graphical user interface, while a Docker/FastAPI backend handles loading, preprocessing and sub-selection of large projection datasets. This separation keeps the interactive visualization responsive while avoiding the need to load complete sinogram datasets into the 3D Slicer client.

The plugin visualizes source positions, detector geometry, projection rays and scan trajectory in the 3D viewport. It also displays selected sinogram data and links these measurements to the corresponding acquisition geometry. The current implementation is flexible at the software-workflow level, but it is not a universal scanner interface. It requires geometry metadata describing source positions, detector configuration and sinogram indexing in a format that the backend can parse, new scanner types therefore require a geometry/data-loader adapter.

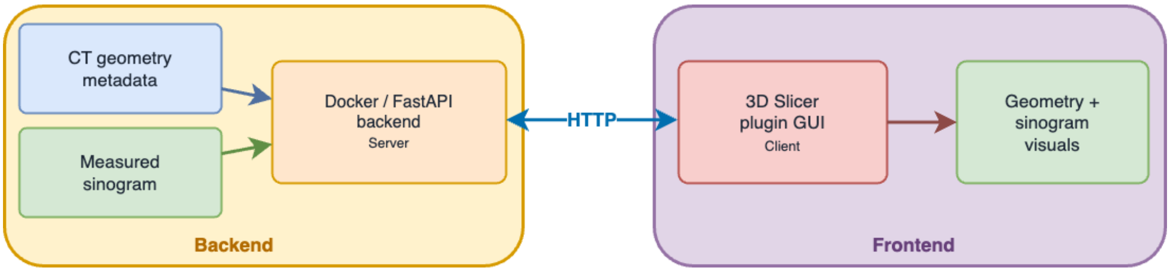


Figure 1. Workflow of the CT-sinogram visualizer. CT scan metadata and measured sinogram data are handled by a Docker/FastAPI backend and presented interactively in a 3D Slicer plugin

## Results and Discussion

The main result is a visualization workflow that exposes acquisition information before reconstruction. The tool makes it possible to inspect whether the defined scan geometry is consistent with the expected setup and whether selected sinogram regions contain artefacts, incomplete data or other irregularities that may influence reconstruction.
Figure 2 illustrates the prototype interface. The user can inspect the physical acquisition geometry, including source positions, detector rows and projection rays, together with the corresponding sinogram view. This connection is important because errors or limitations in the acquisition setup may later appear as reconstruction artefacts or be confused with material-related features.

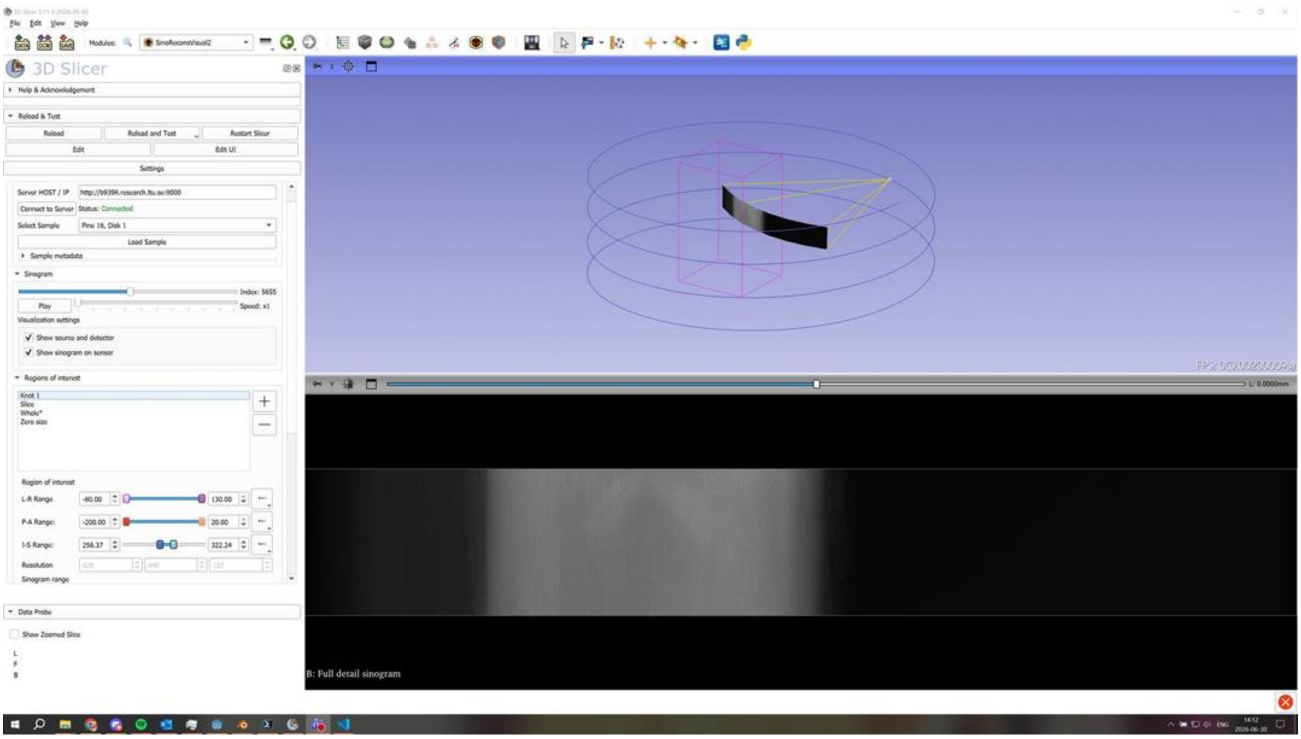


Figure 2. Prototype CT-sinogram visualizer in 3D Slicer, showing the acquisition geometry in the 3D viewport and the corresponding measured sinogram data below. The interface links selected projection geometry to the raw measurement data before reconstruction

The current prototype should be understood as a methodological visualization tool rather than a complete reconstruction framework. Its immediate contribution is to make otherwise hidden acquisition information visible and easier to document. The workflow can be used for teaching, user testing, publication figures and quality-oriented inspection of CT measurement data in wood science and related CT applications.
Planned extensions will make the geometry support more explicit. These include support for additional detector configurations, such as flat, curved and multi-row detectors, different

projection geometries such as cone-beam, fan-beam and parallel-beam setups, visualization of region-of-interest overlap with the cone beam, voxel heatmaps of acquisition coverage, and tools for defining reconstruction workloads through regions of interest or sinogram sub-ranges.

## Conclusions

A Python-based 3D Slicer plugin was developed for interactive visualization of CT acquisition geometry and measured sinogram data before reconstruction. By combining a containerized backend with a user-facing Slicer interface, the workflow supports inspection of large projection datasets while retaining an accessible visual environment.
The tool improves methodological transparency in CT-based wood research by helping researchers and CT scan operators relate acquisition geometry to measured projection data and potential reconstruction quality. The approach is also applicable beyond wood, provided that the CT system can export sufficient projection and geometry metadata. Future work will focus on broader user testing, scanner-specific geometry adapters and integration with reconstruction-workload definition.

## Acknowledgements

This work was developed with support from InfraVis user support project T-2511-2307. The final acknowledgement wording should follow the formal InfraVis text provided for resulting publications.

## References

Burström O, Julius H and Öktem O (2026) CT_GUI_Docker: CT-sinogram visualizer software repository. https://github.com/ouaburst/CT_GUI_Docker.

Fedorov A, Beichel R, Kalpathy-Cramer J, Finet J, Fillion-Robin J-C, Pujol S, Bauer C, Jennings D, Fennessy F, Sonka M, Buatti J, Aylward S, Miller JV, Pieper S and Kikinis R (2012) 3D Slicer as an image computing platform for the Quantitative Imaging Network. Magnetic Resonance Imaging 30: 1323-1341.

Kak AC and Slaney M (1988) Principles of Computerized Tomographic Imaging. IEEE Press, New York.

Slicer Community (2026) 3D Slicer documentation and software platform. https://www.slicer.org/.

# Hyperspectral Detection of Cellulose-Based Coatings on Wood for End-of-Life Sorting Application

**Luka Kopač**[1], **Miha Humar**[1]

[1]University of Ljubljana, Slovenia, luka.kopac@bf.uni-lj.si, miha.humar@bf.uni-lj.si

## Background

The increasing emphasis on circular economy principles has stimulated interest in the recovery and reuse of reclaimed timber from end-of-life buildings and products (Rebhi et al., 2026). Effective use of reclaimed wood requires reliable characterisation and sorting, particularly when wood species information is needed for grading, reuse decisions, or compliance with existing standards (Bergsagel & Heisel, 2023). Hyperspectral imaging (HSI) has shown considerable potential as a rapid, non-destructive tool for wood species identification (Chen et al., 2024) and waste material assessment (Hao et al., 2025; Schild, 2015). However, reclaimed wood often contains surface treatments such as paints, varnishes, and coatings that alter the spectral response of wood and may reduce the reliability of HSI-based classification. This study investigates the effect of a transparent cellulose-based coating on the near-infrared spectral response of 25 wood species and evaluates its implications for future HSI-assisted sorting of reclaimed wood.

**Keywords:** hyperspectral imaging, near-infrared, coatings, end-of-life sorting**.**

## Experimental

The analysis was based on 25 European wood species. For each species, a single sample was available, with one coated side and one uncoated side. Both surfaces (size: 125 mm × 55 mm) of all samples were acquired using a HSI system (ClydeHSI, Clydebank, UK) in the short-wave infrared spectrum (1000–2500 nm). For each species, ten median spectra were extracted from regions of interest on the coated side, and likewise on the uncoated side. A single matrix was thus constructed, consisting of 500 observations and 288 spectral bands. To obtain a “pure” coating spectrum, the coating was applied on glass, with aluminium foil placed underneath as background, and acquired using HSI. A median spectrum over a larger area was calculated to reduce noise and the effect of outliers. Exploratory data analysis was first carried out to evaluate the condition of data and identify the main trends. The next step was to examine whether the spectral response resulting from differences in surface treatment across species is comparable. In the final part of the research, a machine learning model was constructed to transform spectra of coated surfaces into spectra of reference wood.

## Results and Discussion

Investigation of mean plotted spectra revealed coating-dependent absorption changes in three broader wavelength regions. The first three components of principal component analysis (PCA) explained 93% of the variance, indicating several smaller effects rather than one dominant effect. The biplot showed that the observed absorption peaks were the main drivers of separation between reference and coated wood clusters. Certain individual species, such as larch, appeared spectrally distinct from other species and formed their own clusters.

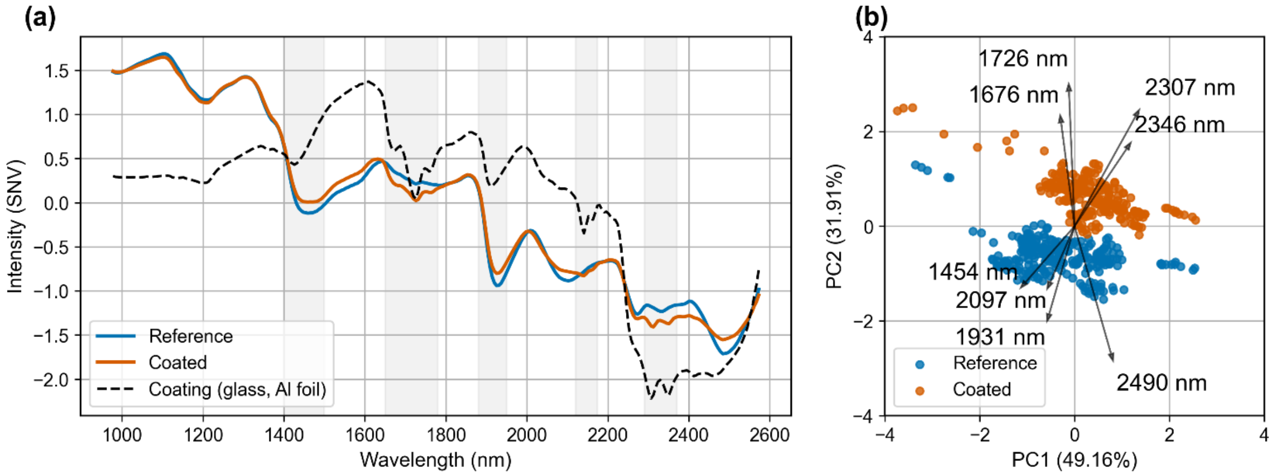


Figure 4. (a) Mean coated vs reference spectrum along with "pure" coating spectrum. Grey shaded regions indicate coating-associated spectral changes. (b) PCA biplot. Loading vectors highlight spectral regions contributing to sample separation

Coated samples were projected into a reference space of linear discriminant analysis. The difference of means between reference and coated samples of each species showed a relatively consistent shift in direction, though less so in magnitude. To quantify this shift, difference spectra of means were calculated. Wavelength-dependent changes were analysed using cosine similarity of difference spectra, which revealed certain species with distinct coating effects. Including pear, larch, plumwood, olivewood and plane, these formed a separate group in hierarchical clustering.

Two different transformation techniques were tested, and their correction performance evaluated using root mean square error (RMSE). The mean difference spectrum was first used for the correction transformation and achieved RMSE of 0.064. A multi-output partial least squares (PLS) regression was then trained with a 5-fold cross-validation, and the optimal number of components (5) was selected. The mean RMSE was 0.041, representing a 36% improvement over the mean difference model. Species with the highest RMSE were aspen, plumwood and robinia. Visual inspection of corrected spectra confirmed that the transformation was highly successful for most species.

## Conclusions

The coating introduced identifiable spectral features and a consistent directional shift in multivariate spectral space across investigated species. The indication of a similar spectral response of most species to coating enabled the successful construction of a model that, independently of species, transforms the spectrum of a coated surface to that of reference wood. In future research, wood species classification model should be applied to the corrected spectra and its performance evaluated in comparison with uncorrected spectra. Other surface treatments and their effects should also be explored for general-purpose impurity or defect classification in end-of-life sorting applications.

**References**

Bergsagel, D., & Heisel, F. (2023). Structural design using reclaimed wood – A case study and proposed design procedure. *Journal of Cleaner Production*, *420*. https://doi.org/10.1016/j.jclepro.2023.138316

Chen, Z., Xue, X., Wu, H., Gao, H., Wang, G., Ni, G., & Cao, T. (2024). Visible/near-infrared hyperspectral imaging combined with machine learning for identification of ten Dalbergia species. *Frontiers in Plant Science*, *15*. https://doi.org/10.3389/fpls.2024.1413215

Hao, W., Chen, L., Cheng, G., & Tian, Y. (2025). Machine Learning Techniques Based on Hyperspectral Imaging for Waste Classification: A Review. *2025 IEEE 8th International Conference on Mechatronics and Computer Technology Engineering, MCTE 2025*, 155–160. https://doi.org/10.1109/MCTE67374.2025.11213672

Rebhi, A., Coureau, J. L., Garnesson, T., Galimard, P., De Haeck, M., & Lanvin, J. D. (2026). Reclaimed structural timber: Adapting visual grading to the specificities of materials from deconstruction. *Construction and Building Materials*, *528*. https://doi.org/10.1016/j.conbuildmat.2026.146554

Schild, A. H. (2015). *Sensor-based sorting of waste wood composites and the use of composite particles in cement-bonded wood composites*.

# AI for Wood Identification in Wood-Based Panels

**Jördis Sieburg-Rockel[1], Sven Koch[2]**

[1]Thünen Institute of Wood Research, Germany, joerdis.sieburg-rockel@thuenen.de, [2]Faculty of Computer Science and Digital Society, Hamburg University of Applied Sciences, Germany, sven.koch@haw-hamburg.de

## Background

With an annual global production volume of more than 122 million m³ in 2024 (FAO, 2026), particleboard is one of the most important wood-based products which also uses recycled wood. To ensure compliance with EU Deforestation Regulation (European Commission, 2023) and identify illegal or misdeclared timber, knowledge of the wood species contained in a product is essential. The wood composition is currently identified using wood anatomy (Schmitz et al., 2020). The method is time-consuming and requires a high level of expertise. To streamline this process, a simple classifier was trained using transfer learning (Kornblith et al., 2019). State-of-the-art convolutional neural networks (CNNs) are used as the base model. The presented research provides machine learning using images from particleboard cross-sections to distinguish softwood and hardwood, serving as an initial approach to estimate relative proportions and verify the declaration of wood contained within a panel.

**Keywords:** Particleboard, wood anatomy, machine learning, convolutional neural networks

## Experimental

Single-layer particleboards were produced using a laboratory hot press (Siempelkamp GmbH & Co. KG, Krefeld, Germany). The panels were composed of three softwood genera (*Picea*, *Pinus*, *Pseudotsuga*) and three hardwood genera cultivated worldwide (*Acacia*, *Populus*, *Eucalyptus*) in varying proportions. These genera were regularly identified anatomically in commercial particleboard (Sieburg-Rockel and Koch 2020). Pure hardwood and softwood panels, mixed panels and panels composed of a single genus were produced. For the analysis, images of polished cross-sectional surfaces were acquired using high-resolution 3-D reflected-light microscopy (Keyence VHX-5000). These overview images were divided into 1,500 to 2,000 non-overlapping image tiles per image, each measuring 223×223 µm (224×224 px), resulting in a training dataset consisting of a total of 30,559 image tiles, comprising 16,533 image tiles of pure hardwood and 14,026 of pure softwood. The dataset was split into an 80% training and a 20% validation set. To further increase variance and mitigate overfitting, the training set was augmented using class-preserving transformations, including horizontal and vertical flips and rotations, which maintain anatomical features. The image tiles from the mixed panels and the single-genus panels served as the test dataset. This enables an analysis of the results obtained from three different CNN architectures: EfficientNetV2-S, ConvNeXt-Tiny and MobileNetV2.

## Results and Discussion

The models scan each overview image using a sliding window approach, label each tile as hardwood or softwood, and then compute the total counts and their ratio. For the test dataset, consisting of images of pure hardwood and softwood panels, all three networks achieved good per-class accuracy (Figure 1): EfficientNetV2-S (0.985 HW and 0.963 SW), ConvNeXt-Tiny (0.986 HW and 0.98 SW) and MobileNetV2 (0.947 HW and 0.976 SW).

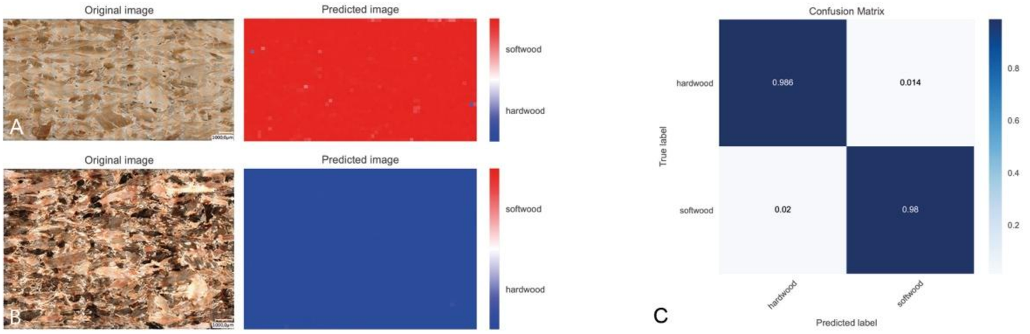


Figure 1. Examples of cross-sectional images of a pure softwood (A) and a pure hardwood (B) panel with the classification results using ConvNeXt-Tiny. Classified tiles are highlighted in red (softwood) and blue (hardwood). The overall model performance is summarized in confusion matrix (C)

Although the compositions of the mixed panels are known, it cannot be assumed that the expected ratio is represented in every image. Therefore, these values should not be taken as absolute truth. In some cases, however, the network's predictions closely match the actual values (Table 1). Any deviations may also be related to the genera included. Morphological similarities between *Populus* and softwoods, such as single-row wood rays could lead to confusion. The single-genus samples also confirm this (not shown here).

Table 1. Results for the test dataset consisting of mixed hardwood (HW) and softwood (SW) panels with the actual mixture and the network's predictions

| **Sample** | **Expected value SW/HW [%]** | **EfficientNetV2-S SW/HW [%]** | **ConvNeXt-Tiny SW/HW [%]** | **MobileNetV2 SW/HW [%]** |
|---|---|---|---|---|
| 1 | 50 / 50 | 49,52 / 50,48 | 47,93 / 52,08 | 55,28 / 44,73 |
| 2 | 40 / 60 | 11,32 / 88,68 | 11,09 / 88,91 | 17,74 / 82,26 |
| 4 | 40 / 60 | 33,22 / 66,78 | 29,92 / 70,08 | 40,56 / 59,44 |
| 5 | 80 / 20 | 60,65 / 39,35 | 62,63 / 37,37 | 64,65 / 35,35 |
| 6 | 60 / 40 | 53,57 / 46,43 | 54,18 / 45,82 | 62,34 / 37,66 |
| 7 | 80 / 20 | 83,01 / 16,99 | 84,93 / 15,07 | 93,15 / 6,85 |
| 8 | 60 / 40 | 72,36 / 27,64 | 74,84 / 25,17 | 78,49 / 21,76 |
| 12 | 80 / 20 | 83,38 / 16,62 | 85,39 / 14,61 | 87,19 / 12,81 |
| 13 | 20 / 80 | 10,51 / 89,49 | 9,95 / 90,05 | 18,76 / 81,24 |

## Conclusions

In general, this first approach already yields good results for classifying hardwood and softwood in the images of the panel cross-sections. The existing uncertainties could be mitigated by introducing confidence thresholds for image tiles with lower certainty, thereby providing even more reliable results. Overall, this work provides important conceptual evidence for the feasibility of machine learning-based analysis of wood-based materials.

**References**

EuropeanUnion (2023). Regulation (EU) 2023/1115 of the European Parliament and of the Council of 31 May 2023 on the making available on the Union market and the export from the Union of certain commodities and products associated with deforestation and forest degradation and repealing Regulation (EU), Available at: http://data.europa.eu/eli/reg/2023/1115/oj.

FAO (2026). FAOSTAT, https://www.fao.org/faostat/en/#data/FO (Accessed 09 Jun 2026).

Kornblith, S., Shlens, J., & Le, Q. V. (2019). Do Better ImageNet Models Transfer Better?. In Proceedings of the IEEE/CVF Conference on Computer Vision and Pattern Recognition (pp. 2661-2671).

Schmitz N, Beeckman H, Blanc-Jolivet C, Boeschoten L, Braga JWB, Cabezas JA, Chaix G, Crameri S, Deklerck V & Degen B, et al (2020). Overview of current practices in data analysis for wood identi0cation. a guide for the different timber tracking methods. Technical report.

Sieburg-Rockel, J. and Koch, G. (2020). Identification of wood species used in particleboard production. IAWA journal, 41(4), 751-760.

# Understanding Liquid Transport Through Biomimetic Softwood Tracheid Networks

**Frauke Sonne[1], Staffan Lundström[1], Sofia Larsson[1], Jasmina Casals-Terre[1,2], Josep Farr-Llados[2]**

[1]Luleå University of Technology, Sweden
[2] Polytechnic University of Catalonia, Spain

## Background

Water transport through the xylem is central to tree hydraulics, drought resilience, and many wood processing applications. However, direct visualization of liquid transport at the cellular scale remains difficult because of the opacity and fragility of the wood structure (Cermak et al., 1992; Brodersen, 2013; Lundström et al., 2025). Biomimetic microfluidic models provide an alternative approach by reducing the system to its essential anatomical features while allowing direct optical measurements.
Therefore, this work suggests an experimental model cell, in which different anatomical features can be isolated, thereby addressing the question how different parts of the xylem influence liquid transport between neighbouring cells.

## Experiments

Based on the literature (Saren et al., 2001; Gryc and Horáček, 2005; Trtik et al., 2007; Irbe et al., 2015) and previous work from our group (Lundström et al. 2025), pits and tracheids were abstracted as the most relevant features influencing bulk flow. As part of the experimental-cell design, the pits were deliberately simplified to accommodate fabrication constraints, allowing the study to focus on xylem connectivity and the relative dimensions of the pits and conduits.
A silicon-based polymer two-dimensional model was printed using lithography, resulting in a microchannel device with tracheids of 300 μm diameter and randomised pits between 30 and 60 μm in diameter (Fig. 1). The pits were positioned, such that they were never located directly opposite each other on the tracheid walls. Due to larger pits at the ends of the tracheids, a higher pit density was represented in the longitudinal direction.

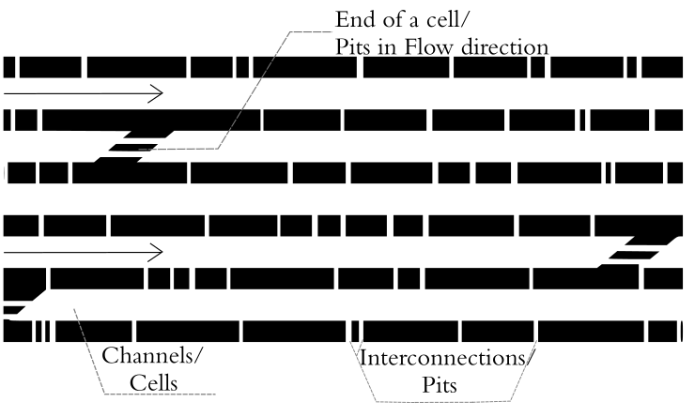


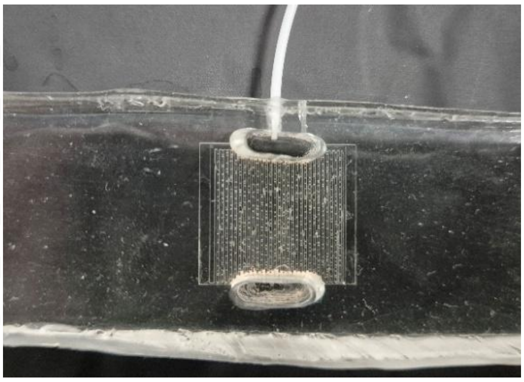

Figure 1. Left: Schematic of wood model. Right: Printed multichannel network

The microchannel models are investigated using optical measurements, including Micro-Particle Image Velocimetry (µPIV). Using a microscope and particle-seeded fluid, the flow can be traced through the channels, allowing direct visualization and quantification of liquid transport. In the first experimental series, the flow is driven by capillary action under ambient pressure.

## Conclusions

Initial measurements reveal heterogeneous filling dynamics and liquid exchange between adjacent tracheids (Fig. 2), even in the presence of clogging or embolism. Local flow behaviour through the pit connections indicates that tracheid connectivity has a strong influence on liquid redistribution within the network.

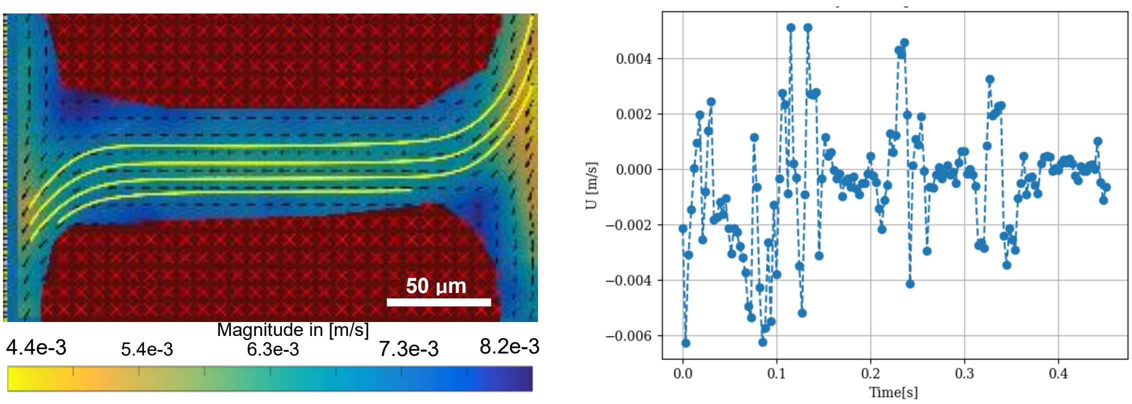


Figure 2. Left: Mean velocity magnitude over the complete measurement time within one model pit, including streamlines. Right: Velocity over time, measured in one point in the middle of the pit

The presented platform provides a basis for systematically investigating the influence of pit connectivity, tracheid arrangement, and anatomical variability on xylem transport. Future work will compare different network topologies and relate the observations to water transport and embolism propagation in natural softwood, using X-ray microtomography for comparison.

**References**

Brodersen, Craig R. “Visualizing Wood Anatomy in Three Dimensions with High-Resolution X-Ray Micro-Tomography (µCT ) – a Review –.” *IAWA Journal* 34, no. 4 (2013): 408–24.

Cermak, J., E. Cienciala, J. Kucera, and J.-E. Hallgren. “Radial Velocity Profiles of Water Flow in Trunks of Norway Spruce and Oak and the Response of Spruce to Severing.” *Tree Physiology* 10, no. 4 (1992): 367–80.

Gryc, V., and P. Horáček. “Effect of the Position in a Stem on the Length of Tracheids in Spruce (Picea Abies [L.] Karst.) with the Occurrence of Reaction Wood.” *Journal of Forest Science* 51, no. 5 (2005): 203–12.

Irbe, Ilze, Inese Sable, Guna Noldt, et al. “Wood and Tracheid Properties of Norway Spruce (Picea Abies [L] Karst.) Clones Grown on Former Agricultural Land in Latvia.” *BALTIC FORESTRY* 21, no. 1 (2015).

Lundström, T.S., Hellström, J.G.I., Ljung, AL. *et al.* Capillary-Driven Flow Through Biological Porous Media: X-ray Microtomography and Computational Fluid Dynamics. *Transp. Porous Med* 152, 101 (2025)

Sarén, Matti-P, Ritva Serimaa, Seppo Andersson, Timo Paakkari, Pekka Saranpää, and Erkki Pesonen. “Structural Variation of Tracheids in Norway Spruce (Picea Abies [L.] Karst.).” *Journal of Structural Biology* 136, no. 2 (2001): 101–9

Trtik, P, J Dual, D Keunecke, et al. “3D Imaging of Microstructure of Spruce Wood.” *Journal of Structural Biology* 159, no. 1 (2007): 46–55.

# Fighting Timber Fraud: Establishing Elemental Fingerprints for the Georeferencing of Wood

**Dennis M. J. Möck[1], Havva Ceylan[2], Volker Heidemann[3], Jörn Appelt[4]**

[1,3,4] Institute of Wood Research, Johann Heinrich von Thünen Institute, Federal Research Institute for Rural Areas, Forestry and Fisheries, Haidkrugsweg 1, 22885 Barsbüttel, Germany, dennis.moeck@thuenen,de, volker.heidemann@thuenen.de, joern.appelt@thuenen.de
[2] Technischen Hochschule Lübeck, Mönkhofer Weg 239 23562 Lübeck, Germany, Havva.ceylan@stud.th-luebeck.de

## Background

The EU Deforestation Regulation (EUDR) requires proof of the origin of wood and wood products to combat illegal logging (European Union, 2023). However, reliable origin identification remains challenging. Besides genetic and stable isotope approaches (Lowe and Cross 2011, Boeschoten et al. 2025), the elemental fingerprint has emerged as a promising method for geographical traceability of wood (Boeschoten et al. 2022). While this approach has already been successfully applied to products such as honey, olive oil and wine (Gonzálvez et al. 2009, Mara et al. 2022, Nasr et al. 2022), only limited reference data are currently available for wood.
The "GeoRef4Wood" project aims to establish an elemental fingerprint database for wood origin identification through collaboration with partners in Peru and Brazil. The results will support the development of reliable tools for tracing wood provenance and contribute to reducing illegal timber trade.

**Keywords:** Elemental fingerprinting, Illegal timber trade, EUDR, ICP-OES, XRF

## Experimental

The elemental fingerprint of 13 spruce wood samples collected across Germany was determined using inductively coupled plasma optical emission spectrometry (ICP-OES) and X-ray fluorescence spectroscopy (XRF). For ICP-OES analysis, the wood samples were digested using microwave-assisted digestion with nitric acid ($HNO_3$). This method requires daily calibration of the instrument for each element, resulting in increased analytical effort and the need for well-equipped laboratory facilities.
In contrast, XRF measurements were performed directly on solid wood samples (14 mm diameter cores) as well as on digested samples. XRF requires only an initial calibration and offers the potential for rapid, on-site determination of elemental fingerprints using handheld devices. However, ICP-OES provides higher sensitivity and lower detection limits, enabling a more precise characterization of elemental patterns.

## Results and Discussion

Figure 1. shows the elemental fingerprint of a spruce wood sample determined by ICP-OES for the elements Li, Na, Mg, Al, Ca, Cr, Mn, Fe, Co, Ni, Cu, Zn, Ga, Rb, Sr, Ag, Cd, In, Ba, Ir, Hg, Ti, Pb, Bi. The colors represent the elemental concentrations within the sample, with red indicating high concentrations (>1000 ppm) and purple representing very low concentrations (<0.04 ppm).

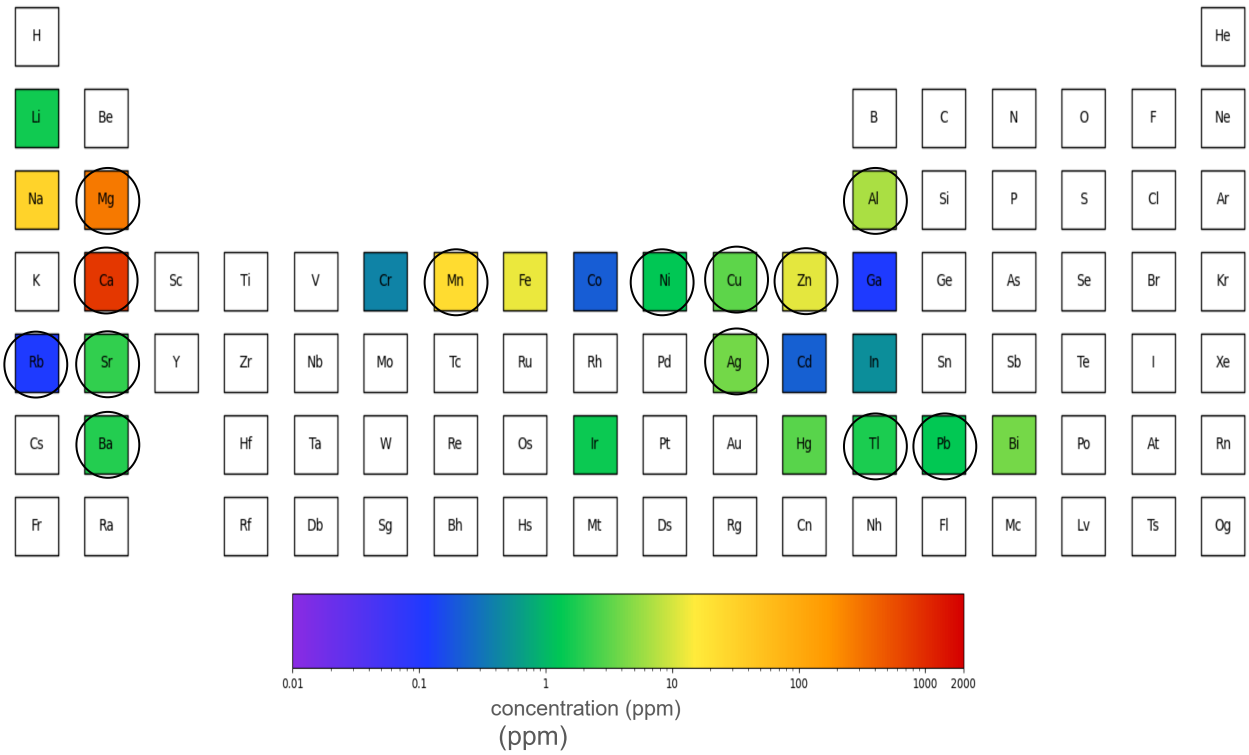


Figure 1. Example of an elemental fingerprint (Li, Na, Mg, Al, Ca, Cr, Mn, Fe, Co, Ni, Cu, Zn, Ga, Rb, Sr, Ag, Cd, In, Ba, Ir, Hg, Ti, Pb, Bi) of a German spruce wood sample determined by ICP-OES and displayed within the periodic table. The color scale indicates the concentration of each element in the sample, while elements exhibiting high variability across the samples are highlighted by circles

The elemental composition varies with geographical origin. Among the 13 German spruce wood samples analyzed, Mg, Al, Ca, Mn, Ni, Cu, Zn, Rb, Sr, Ag, Ba, Ti, and Pb exhibited the greatest variation in concentration (circled in Figure 1). Ca and Mn are essential macronutrients that generally occur at relatively high concentrations in plants (Grusak et al., 2016). Gonzálvez et al. (2009) demonstrated that the Mn concentration can be used as a marker for the geographical origin of red wine. Mn, Cu, Zn, and Ni are essential micronutrients that typically occur at relatively low concentrations in wood (Grusak et al., 2016). Boeschoten et al. (2022) showed that, among micronutrients, Mn, Zn, and Mo are particularly relevant for timber tracing. Among the remaining elements (Al, Rb, Sr, Ag, Ba, Ti, and Pb), Sr was identified as a particularly important element for provenance determination (Boeschoten et al. 2022).

## Conclusions

The elemental composition of wood is influenced by the soil conditions, resulting in unique elemental fingerprints that have the potential to support the georeferencing of wood origin. Future work will focus on the statistical analysis of these fingerprints to identify characteristic elemental patterns linked to geographical provenance. Subsequently, machine learning approaches could be applied to automatically classify wood samples based on their elemental fingerprints, enabling rapid and reliable provenance determination.

**References**

Boeschoten, LE., Sass-Klaassen, U., Vlam, M. Comans, RNJ. Koopmans, GF., Meyer-Sand, BRV., Tassiamba, SN., Tchamba, MT., Zanguim, HT., Zemtsa, PT. , Zuidema, PA. (2022) Clay and soil organic matter drive wood multi-elemental composition of a tropical tree species: Implications for timber tracing. Science of the Total Environment 849: 157877.

Boeschoten, L.E., Rocha Venancio Meyer-Sand, B., Boom, A. et al. (2025) Combined genetic and chemical methods boost the precision of tracing illegal timber in Central Africa. Commun. Earth Environ. 6:789

European Union (2023) European Regulation (EU) 2023/1115 of the European Parliament and of the Council of 31 May 2023 on the making available on the Union market and the export from the Union of certain commodities and products associated with deforestation and forest degradation and repealing Regulation (EU) No 995/2010, Official Journal of the European Union.

Gonzálvez, A., Llorens, A., Cervera, ML., Armenta, S., de la Guardia, M. (2009) Elemental fingerprint of wines from the protected designation of origin Valencia. Food Chemistry 112: 26-34.

Grusak, M.A., Broadley, M.R. and White, P.J. (2016). Plant Macro- and Micronutrient Minerals. In eLS, John Wiley & Sons, Ltd (Ed.)

Lowe, A. J., & Cross, H. B. (2011). The Application of DNA methods to Timber Tracking and Origin Verification. IAWA Journal, 32: 251-262.

Mara, A., Deidda, S., Caredda, M., Ciulu, M., Deroma, M., Farinini, E., Floris, I., Langasco, I., Leardi, R., Pilo, MI., Spano, N., Sanna, G. (2022) Multi-Elemental Analysis as a Tool to Ascertain the Safety and the Origin of Beehive Products: Development, Validation, and Application of an ICP-MS Method on Four Unifloral Honeys Produced in Sardinia, Italy. Molecules 27.

Nasr, EG., Epova, EN., de Diego, A., Souissi, R., Hammami, M., Abderrazak, H., Donard, OFX. (2022) Trace Elements Analysis of Tunisian and European Extra Virgin Olive Oils by ICP-MS and Chemometrics for Geographical Discrimination. Foods 11.

# Influence of Indentation Location in Wood Cell Wall: Numerical Analysis

**Václav Sebera[1], Dimitrios Tsalagkas[1], Irena Sochova[1]**

[1] Department of Wood Science and Technology, Faculty of Forestry and Wood Technology, Mendel University in Brno, Czech Republic, vaclav.sebera@mendelu.cz, dimitrios.tsalagkas@mendelu.cz, irena.sochova@mendelu.cz

## Background

The cell wall of wood behavior is often studied using indentation-based techniques such as nanoindentation (NI) and atomic force microscopy (AFM). However, due to laminate composition of cell wall and wood porous structure, their responses are strongly affected by the location of the indent. The proposed study examines the effect of the location on nanoindentation outputs using finite element analysis as a complementary tool to experimental investigation.
This work is part of the project focusing on a change of sessille oak wood cell wall properties due to global climate change that was proved to have an impact on wood anatomy and growth (Pandey 2021). The properties of wood are often studied by using high-speed indentation techniques (NI and atomic force microscopy – AFM) that provide fast and high quantity of outputs such as hardness and reduced modulus. However, these are strongly variable and depending on location of indent and size of the indent (Golovin et al 2021 and Golovin et al 2023). Therefore, the goal of the work is to map such variability using 3D numerical model of indentation into cell wall. The model is built by finite elements since they present effective tool for such a task (Mishnaevsky and Quing 2008). The model includes cell wall layers and orthotropic elastoplastic material behavior and provides an important insight into such phenomenon on this level of observation. The paper fills up the gap in knowledge by including of elasto-plastic response on wood material level of cell walls.

**Keywords:** Nanoindentation, finite element analysis, oak, cell wall, elasto-plastic material

## Numerical model

The numerical model consists of a 3D model of four oak wood cells with five different layers (S3, S2, S1, primary wall - PW and middle lamella - ML), each layer defined by its own chemical composition that was as follows: Cellulose: 45% (S3), 50% (S2), 35% (S1), 15% (PW) and 3% (ML); hemicelluloses: 35% (S3), 27% (S2), 30% (S1), 33% (PW) and 35% (ML); lignin: 20% (S3), 23% (S2), 35% (S1), 52% (PW) and 62% (ML). By combination of basic elastic properties of these chemical constituents, this resulted in five different material models utilizing bilinear orthotropic elasto-plasticity based on Hill's theory. The generated material models were then checked if they meet conditions of Hill's plasticity and in case of need, they were adjusted using optimization approaches (Zlámal et al. 2024).
The FE model includes contact between the wood cell wall and indentor and at anticipated location of the indent, the FE mesh was refined to capture deformation gradient and initial contact (Fig. 1a and 1b). The mesh of wood is composed of SOLID186 finite element, the contact is created uing TARGE170 and CONTA174 elements with friction defined by friction coefficient 0.33. The simulation of the indent covers loading and unloading phases as being used in experimental NI, so the output is the whole curve that provides data to comput hardness and reduced modulus.

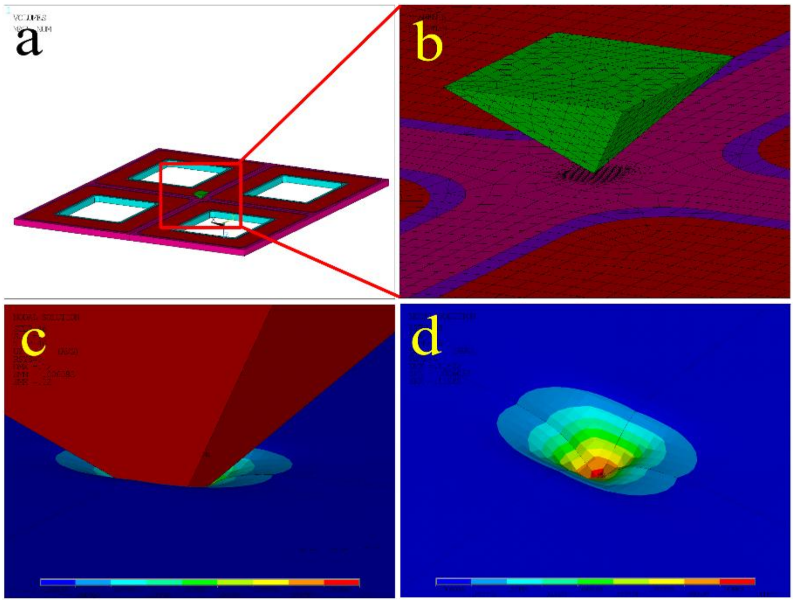


Figure 1. a) geometry of four wood cells with low height, b) detail of nanoindentation tip and FE mesh, c) detail of indentation with tip, and d) indentation hole without tip

### Results and Discussion

The FE model of nanoindentation process is still under development, but already provides indentation curves and mechanical properties that are within the variability of wood properties on such scale. The contact between indentor and wood cell material was established well and, therefore, high plastic deformation of cell wall was well modeled (Fig. 1c and 1d). The simplified orthotropic elasto-plastic material of cell wall layers provide reasonable predictions, although knowledge of more accurate cell wall plasticity would bring higher accuracy into the model.

### Conclusions

The FE model shows well that a location of NI indent within wood cell wall strongly influences obtained mechanical properties of wood, and, therefore, the instrumented measurement should care for high-quality targeting. In future, the FE models of NI process should focus also on delamination/fracture analysis since such effects occur during measurement by NI.
The work was supported by Czech Science Foundation (GAČR), Grant No. 25-18144S, “Change of wood properties on nano-to-meso scale from perspective of climate change’.

**References**

Golovin YI, Gusev AA, Golovin DY, Matveev SM, Tyrin AI, Samodurov AA, Korenkov VV, Vasyukova IA, Yunack MA (2023) Multiscale wood micromechanics and size effects study via nanoindentation. Journal of Bioresources and Bioproducts 8: 246-264.

Golovin YI, Gusev AA, Golovin DY, Matveev SM, Vasyukova IA (2022) Multiscale Mechanical Performance of Wood: From Nano- to Macro-Scale across Structure Hierarchy and Size Effects. Nanomaterials 12(7):1139.

Mishnaevsky L, Qing H (2008) Micromechanical modelling of mechanical behaviour and strength of wood: State-of-the-art review. Computational Materials Science 44: 363-370.

Pandey S (2021) Climatic influence on tree wood anatomy: A review. Journal of Wood Science 67, 24.

Zlámal J, Mařík R, Vojáčková B, Cristini V, Brabec M, Praus L, Tippner J (2024) Elasto-plastic material model of green beech wood. J. Wood Sci 70, 29.

# SESSION 4:
# COMPOSITE MATERIALS

# From Underutilized Willow to Cascading Use: Characterization of Foam-Formed Acoustic Panels from PHWE-Treated Residues

**Elina Kettunen[1], Jani Lehmonen[2], Jussi Hautala[2], Veikko Möttönen[3], Marta Cortina-Escribano[3], Rok Prislan[4], Petri Kilpeläinen[3], Dmitry Tarasov[5], Kerttu Suominen[5], Juha Vinha[6], Chunlin Xu[5], Tuula Jyske[1]**
[1]University of Helsinki, Finland, elina.h.kettunen@helsinki.fi, tuula.jyske@helsinki.fi,[2]Fiberwood Ltd, Finland,[3]Natural Resources Institute Finland, Finland,[4]InnoRenew CoE, Slovenia,[5]Åbo Akademi University, Finland,[6]Tampere University, Finland

## Background

Forests face pressure from climate change, increasing biomass demand, and competing sustainability goals, underscoring the need for more efficient use of lignocellulosic biomass and alternative raw material sources. Willow (*Salix* spp.) is a fast-growing but underutilized species that has mainly been considered for energy applications, despite its potential for higher-value uses (Baker et al., 2022; Dou et al., 2018). Integrated cascade-use pathways for willow remain insufficiently explored. To address this gap, we used pressurized hot water extraction (PHWE) and foam forming (Pöhler et al., 2016) to produce bio-based acoustic panels and characterize their properties. PHWE is used to recover valuable compounds using hot pressurized water, while the remaining lignocellulosic residue is blended with spruce fibers for panel production. A two-stage PHWE treatment enables recovery of both polyphenols and hemicelluloses before panel manufacture (Kilpeläinen et al., 2014).

**Keywords:** willow, biorefinery, acoustics.

## Experimental

### Panel production

Panels in the target size of 300 x 300 x 30 mm were produced using a laboratory-scale foam forming setup with crushed PHWE-treated willow and spruce fibers at ratios of 100:0, 90:10, 50:50, 10:90, and 0:100. Water, sodium dodecyl sulfate (SDS), and PVOH (3–4wt% in process water) were mechanically mixed. The mixed foam was drained in a mold under a 20 kPa vacuum while wet-pressed to the target thickness, followed by oven drying at 105°C.

### Measurements

Normal incidence sound absorption coefficients (SAC) were measured in a 100 mm diameter Brüel & Kjær impedance tube according to ISO 10534-2. Airflow resistance was assessed according to ISO 9053-1:2018. Thermal conductivity (λ) was measured according to ISO 8301:1991. Strength properties were determined using a three-point bending test following EN 310. Mold sensitivity class (MSC) was determined from a nine-month mold growth trial (constant conditions 22°C, 94.8% RH) analyzed according to the Finnish mold growth model (Viitanen et al., 2010), using both untreated and PHWE-treated willow.

## Results and Discussion

The properties of foam-formed panels depended on the willow content (Table 1). Spruce fibers enabled the formation of a porous fibrous network, whereas coarse willow particles reduced bonding, as evidenced by the 100% willow panel, which was too fragile to handle. Increasing willow content increased panel density and decreased both MOR and airflow

resistivity, indicating weaker bonding. Thermal conductivity also increased with willow content, resulting in poorer insulation performance.
Panels containing up to 50% willow showed SAC values similar to the spruce reference. In contrast, panels with 90% willow content had lower SAC. However, the 90% willow panel was also thinner than the others, which may have contributed to the reduced absorption performance (Figure 1).
Spruce, PHWE-treated willow, and untreated willow had similar mold sensitivity. All were classified as MSC1 (very sensitive), typical for biobased fibrous panels. Thus, any effect of lower hemicellulose content after PHWE on mold growth was not sufficient to alter the MSC.

Table 1. Produced 300 x 300 mm panels and measured average properties (mean ± SD, n = 4–6)

| **Panel type** | **Dry density [kg/m³]** | **Thickness [mm]** | **Thermal conductivity [W/(m·K)]*** | **MOR [MPa]** | **Airflow resistivity [Pa·s/m²]** |
|---|---|---|---|---|---|
| Spruce 100% | 84 ± 1 | 32 ± 1 | 0.036 | 0.11 ± 0.01 | 16 000 ± 1 900 |
| Willow 10% | 85 ± 1 | 33 ± 1 | 0.036 | 0.13 ± 0.01 | 14 000 ± 200 |
| Willow 50% | 96 ± 4 | 33 ± 2 | 0.039 | 0.06 ± 0.002 | 9 000 ± 200 |
| Willow 90% | 117 ± 3 | 29 ± 1 | 0.043 | 0.02 ± 0.001 | 4 000 ± 900 |
| Willow 100% | - | - | - | - | - |

*Thermal conductivity was measured at a mean temperature of 10°C. Standard deviations were ≤ 0.0002 W/(m·K).

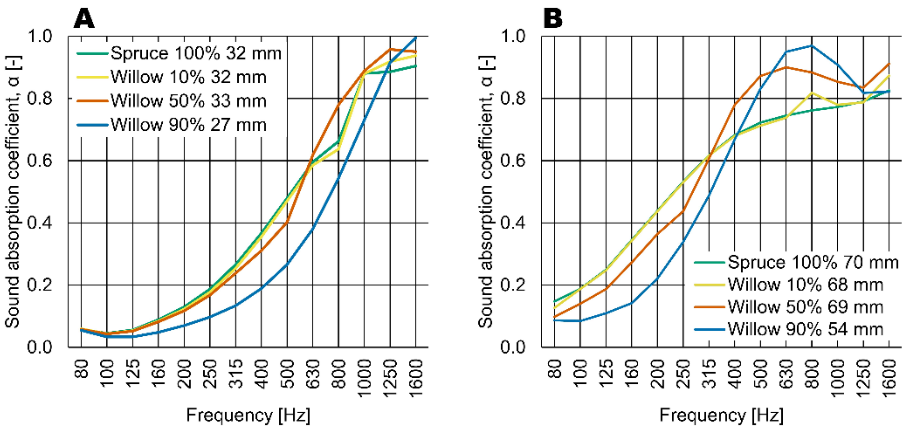


Figure 1. Mean SAC as a function of 1/3-octave-band frequency for four panel types. (A) Mean values of four replicates. (B) SAC measured for two stacked specimens to simulate a thicker panel. SAC increased with frequency and improved at lower frequencies with increasing panel thickness

## Conclusions

This study demonstrates that up to 50% of PHWE-treated willow can substitute spruce fibers in foam-formed panels without compromising acoustic performance. This cascading use enables more complete utilization of willow biomass in a multi-product biorefinery. The approach broadens the wood resource base, enables resource-efficient processing with low chemical input, and valorizes wood-based side streams in long-life building applications.

**References**

Baker P, Charlton A, Johnston C, Leahy JJ, Lindegaard K, Pisano I, Prendergast J, Preskett D, Skinner C (2022) A review of Willow (Salix spp.) as an integrated biorefinery feedstock. Industrial Crops and Products 189: 115823. https://doi.org/10.1016/j.indcrop.2022.115823

Dou J, Xu W, Koivisto JJ, Mobley JK, Padmakshan D, Kögler M, Xu C, Willför S, Ralph J, Vuorinen T (2018) Characteristics of Hot Water Extracts from the Bark of Cultivated Willow (Salix sp.). ACS Sustainable Chemistry & Engineering 6(4): 5566-5573. https://doi.org/10.1021/acssuschemeng.8b00498

EN (1993) Wood-based panels. Determination of modulus of elasticity in bending and of bending strength. EN 310. Brussels, European Committee for Standardization.

ISO (1991) Thermal insulation — Determination of steady-state thermal resistance and related properties — Heat flow meter apparatus. ISO 8301:1991. Geneva, International Organization for Standardization.

ISO (2018) Acoustics — Materials for acoustical applications — Determination of airflow resistance — Part 1. Static airflow method. ISO 9053:1991. Geneva, International Organization for Standardization.

ISO (2023) Acoustics — Determination of acoustic properties in impedance tubes — Part 2: Two-microphone technique for normal sound absorption coefficient and normal surface impedance. ISO 10534-2:2023. Geneva, International Organization for Standardization.

Kilpeläinen P, Hautala SS, Byman OO, Tanner LJ, Korpinen RI, Lillandt M.K. J., Pranovich, A. V., Kitunen, V. H., Willför, S. M., & Ilvesniemi, H. S. (2014). Pressurized hot water flow-through extraction system scale up from the laboratory to the pilot scale. Green chemistry 16(6): 3186–3194. https://doi.org/10.1039/c4gc00274a

Pöhler T, Jetsu P, Isomoisio H (2016) Benchmarking new wood fibre–based sound absorbing material made with a foam-forming technique. Building Acoustics 23(3-4): 131-143. https://doi.org/10.1177/1351010x16661564

Viitanen H, Vinha J, Salminen K, Ojanen T, Peuhkuri R, Paajanen L, Lähdesmäki K (2010) Moisture and Bio-deterioration Risk of Building Materials and Structures. Journal of building physics 33(3): 201-224. https://doi.org/10.1177/1744259109343511

# Influence of Local Thickness on Transillumination-Based Lathe Check Characterization in Silver Birch Veneer

**Ignatius Kristia Adikurnia[1], Anti Rohumaa[1], Jaan Kers[1]**

[1]Laboratory of Wood Technology, Department of Materials and Environmental Technology, Tallinn University of Technology, TalTech, ignatius.adikurnia@taltech.ee, anti.rohumaa@taltech.ee, jaan.kers@taltech.ee

## Background

Lathe checks are defects that arise during veneer production through the peeling process. Peeling thickness (Pałubicki *et al.*, 2010), roller compression type and ratio (McKenzie and Karpovich, 1975), and log preconditioning regime (Rohumaa *et al.*, 2018) are known to have an impact on the development of lathe check. Visually, at the cross-section edge of the veneer lathe checks appear as cyclical cracks that run parallel to the wood grain, originating at the loose side of the veneer and extending inward toward the tight side. While on the tangential side, specifically on loose side of the veneer, lathe check propagation is visible as long continuous crack parallel to the grain (Figure 1B). Lathe check depth (Rohumaa *et al.*, 2013) and lathe check interval (DeVallance, Funck and Reeb, 2007) are critical parameters that significantly influence the bonding performance and mechanical performance of plywood. Nonetheless, the impracticality of observing lathe checks still limits its supervision. This study presents further development in measuring lathe check depth and interval using transillumination properties. We investigated the sources of lathe check variability within and between veneers peeled from silver birch *(Betula pendula)* logs under consistent processing parameters.

**Keywords:** veneer, lathe check, non-destructive method, transillumination

## Experimental

The proposed method uses a simple, cost-effective setup. It features wide green light projection, light hoods, a DSLR camera, and an image analysis pipeline (Figure 1A). The pipeline was written in python, able to produce measurements of lathe check interval from transillumination image ($LCI_{trans}$) and then compared to manual lathe check interval measurement from cross sectional area ($LCI_{cross}$) illustrated in Figure 1C. In total, 20,665 individual lathe checks were measured across 152 subsamples of 3mm thick veneer produced from 2 silver birch logs with identical peeling parameters.

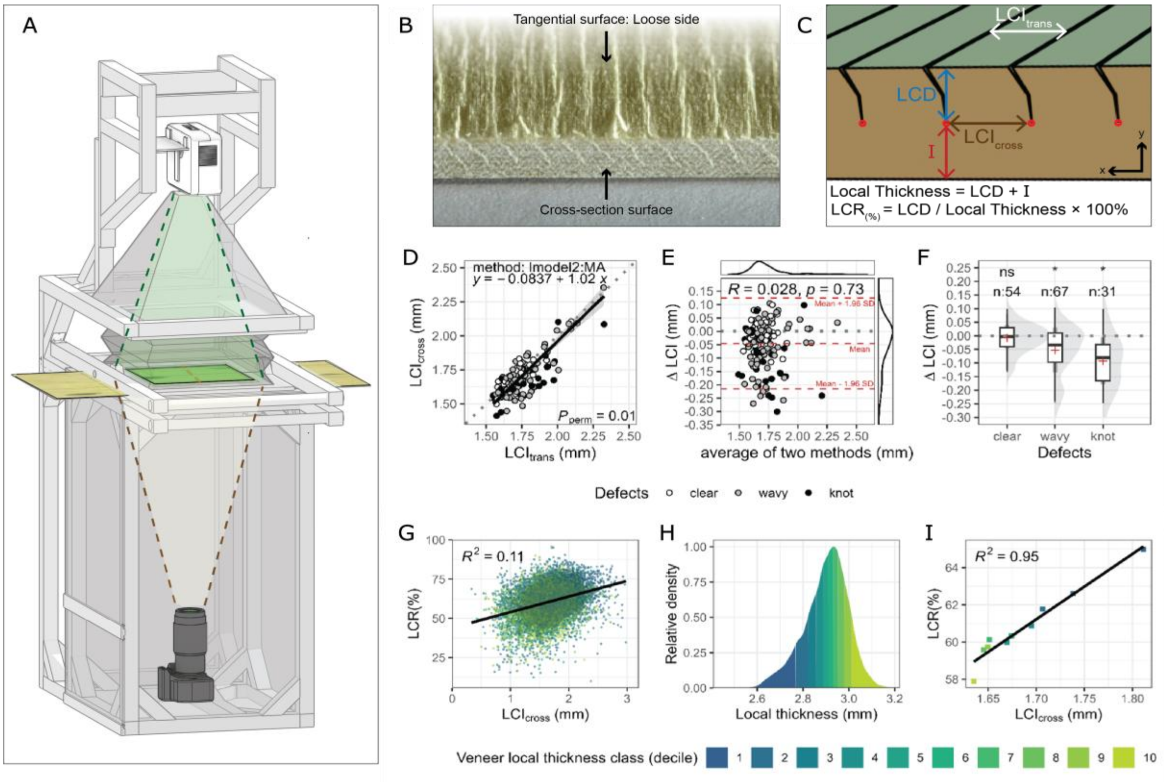

Figure 1. Transillumination setup (A), lathe check propagation (B), lathe check interval measurement validation (C), MA regression plot (D), Bland-Altman plot (E), and boxplots of delta LCI (F) between methods, relationship between lathe check depth ratio and lathe check interval (G), local thickness distribution of studied veneer (H), and relationship between lathe check depth ratio and lathe check interval when grouped by local thickness class (I)

A high level of agreement was found between transillumination and cross-section methods. Major axis regression (MA) revealed a slope statistically equal to 1 and an intercept equal to 0 (Pperm = 0.01). This is shown in Fig 1D. No structural bias was observed across LCI magnitude (Fig 1E), with upper, mean, and lower limits-of-agreement of 0.22mm, -0.05mm, and -0.12mm consecutively. However, disagreement between the methods was influenced by the presence of wavy grain and knots (Fig 1F). This is because transillumination captures larger lathe check variability from a wider observation area. The $R^2$ of ordinary-least-squares regression (OLS) between individual lathe check depth ratio (LCR) and LCI was 0.11 (P<0.001) (Fig 1G). Studied veneers exhibited a range of local thickness variations (Fig 1H). When considering local thickness groupings, the $R^2$ increased to 0.95 (P<0.01) (Fig 1I). This demonstrates that the relationship between LCR and LCI is dependent on local thickness.

## Conclusions

Non-destructive transillumination methods provide results comparable to destructive cross-section methods. Transillumination offers the benefit of observing larger areas and capturing more representative lathe check characteristics across the entire veneer. Lathe check interval measurements are straightforward, while lathe check depth ratio prediction requires additional local thickness measurements.

**References**

DeVallance, D.B., Funck, J.W. and Reeb, J.E. (2007) “Douglas-fir plywood gluebond quality as influenced by veneer roughness, lathe checks, and annual ring characteristics.,” *Forest Products Journal*, 57(1/2), pp. 21–28.

McKenzie, W.M. and Karpovich, H. (1975) “Measured strains in slow linear veneer cutting: Effects of nosebar form and gap,” *Wood Science and Technology*, 9(3), pp. 213–231. Available at: https://doi.org/10.1007/BF00364639.

Pałubicki, B. *et al.* (2010) “A method of lathe checks measurement; SMOF device and its Software,” *European Journal of Wood and Wood Products*, 68(2), pp. 151–159. Available at: https://doi.org/10.1007/s00107-009-0360-y.

Rohumaa, A. *et al.* (2013) “The influence of lathe check depth and orientation on the bond quality of phenol-formaldehyde - Bonded birch plywood,” *Holzforschung*, 67(7), pp. 779–786. Available at: https://doi.org/10.1515/hf-2012-0161.

Rohumaa, A. *et al.* (2018) “Lathe check development and properties: effect of log soaking temperature, compression rate, cutting radius and cutting speed during peeling process of European beech (Fagus sylvatica L.) veneer,” *European Journal of Wood and Wood Products*, 76(6), pp. 1653–1661. Available at: https://doi.org/10.1007/s00107-018-1341-9.

# Evaluating Estonian Hardwood Substrates for Mycelium Composites: A Comparative Study of Fungal Strain–Substrate Interactions

**Sandra Rose Biby**[1*], **Jie Li**[1], **Percy Festus Alao**[1], **Jaan Kers**[1]

[1]Laboratory of Wood Technology, Department of Materials and Environmental Technology, School of Engineering, Tallinn University of Technology, Ehitajate tee 5, 19086 Tallinn, Estonia
[*]Corresponding Author's E-mail: sandra.biby@taltech.ee

## Background

Mycelium based composites (MBCs) are promising bio-based alternatives to conventional insulation products due to their low environmental impact, biodegradability and tuneable properties. Previous studies have demonstrated that fungal strain and lignocellulosic substrate selection can significantly influence mycelial growth and the resulting properties of MBCs (Felle et al., 2025). However, the suitability of locally available Estonian hardwood species and their interactions with different fungal strains for MBC production remain insufficiently understood.

Understanding these interactions is important because the availability, chemical composition and structural characteristics of local wood resources can influence fungal colonization and consequently, the performance of the resulting composites. Evaluating Estonian hardwoods can support the utilization of locally available lignocellulosic resources in biobased construction materials while providing substrate specific information relevant to the development of MBCs for insulation applications. Identifying suitable combinations of Estonian hardwood species and fungal strain may therefore contribute to more locally adapted and resource efficient MBC production.

Hence, the current work investigates the feasibility and performance of Estonian hardwood substrates for MBC production, focusing on substrate-strain interactions. Three fungal strains *Pleurotus ostreatus, Ganoderma lucidum and Trametes versicolor* were cultivated on birch, aspen, grey alder and black alder substrates. Preliminary observations showed distinct colonization patterns among substrate-strain combinations, indicating their potential to influence composite density, structural integrity and mechanical performance. The results contribute to identifying promising combinations for optimizing the production process and developing fire retardant MBCs for future insulation applications.

**Keywords:** mycelium based composites, hardwood, insulation

## Experimental

Aspen, birch, grey alder and black alder were used as substrates. The substrates were chopped into fine pieces of size 1-2 mm. They were soaked in distilled water to ensure moisture content above 60% and autoclaved at 121°C for 20 min (Fritz et al., 2025). Spawn was prepared using barley grain and three strains grown on potato dextrose agar (PDA) media. The substrates were then combined with a fixed quantity of fungal inoculum (15 wt%). The substrate spawn mixture was uniformly packed into sterile moulds of the desired dimensions for incubation (Aquino et al., 2022).

## Results and Discussion

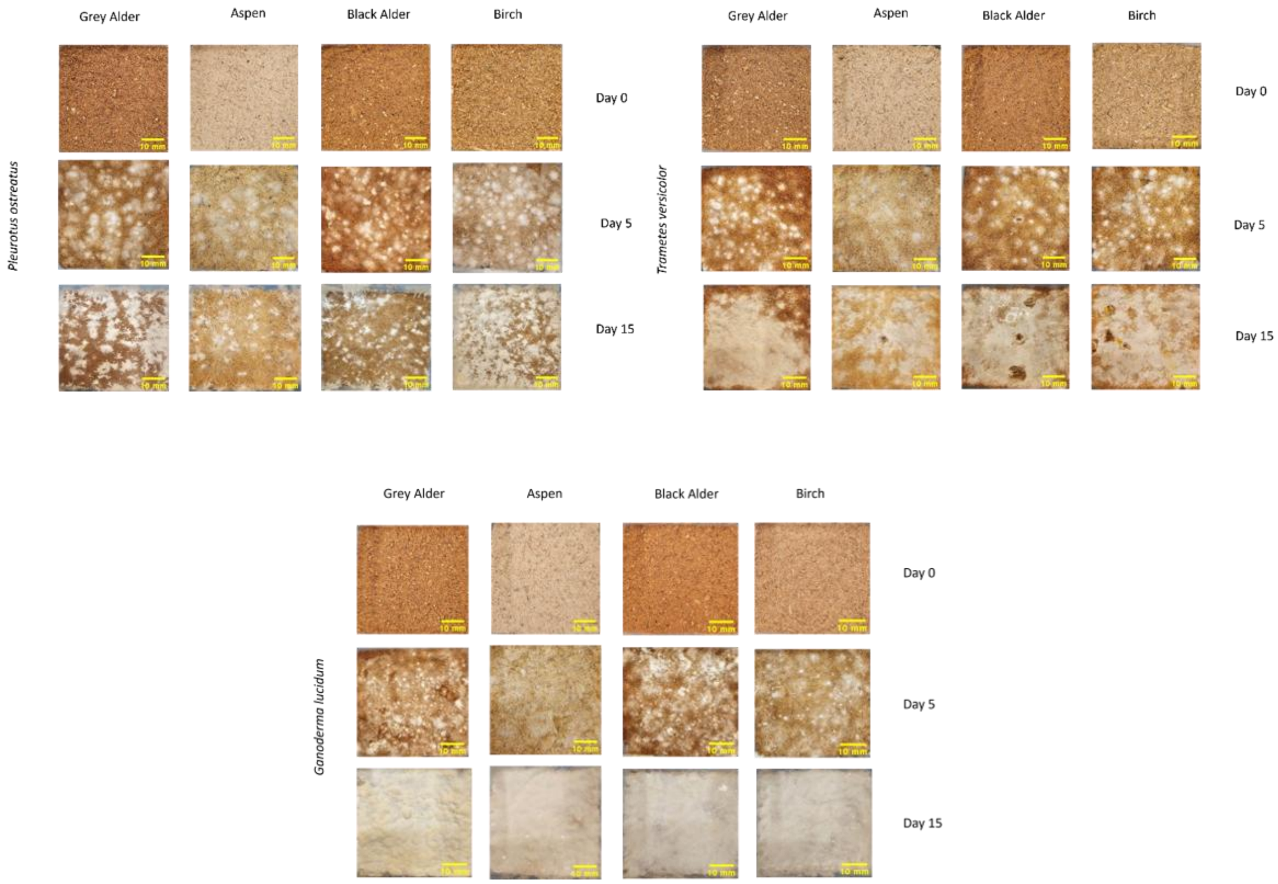


Figure 5. Image of samples after 15 days of growth at scale bars of 10mm

### Colonization pattern of mycelia

Visual observations (Figure 1) of mycelial growth demonstrated substrate and species dependent colonization patterns throughout the incubation period. Mycelial growth increased progressively from Day 0 to Day 15 for all fungal species. *Trametes versicolor* and *Ganoderma lucidum* exhibited relatively rapid and extensive colonization across all wood substrates, whereas *Pleurotus ostreatus* developed a more heterogeneous growth pattern characterized by discrete colonies during the early incubation period. This delayed and spatially heterogenous colonization maybe associated with species specific adaptation to the physicochemical characteristics of the wood substrates. Grey alder and black alder generally supported faster mycelial establishment than aspen, while birch demonstrated moderate initial colonization followed by substantial surface coverage by Day 15.

## Conclusions

Overall, *Ganoderma lucidum* exhibited the most extensive and uniform surface colonization by Day 15 across all wood substrates. *Trametes versicolor* demonstrated moderate colonization with substrate-dependent variation, whereas *Pleurotus ostreatus* showed comparatively slower and patchier surface colonization despite progressive mycelial expansion throughout the incubation period. These findings highlight species-specific differences in colonization patterns and indicate that both fungal species and substrate type influence mycelial development.

**References**

Aquino, M., Rugolo, M., Robledo, G., & Kuhar, F. (2022). Evaluation of mycelium composite materials produced by five Patagonian fungal species. *Maderas. Ciencia y Tecnología*, *24*. https://doi.org/10.4067/S0718-221X2022000100435

Felle, T. K., Estenfelder, J., Wenig, C., Berendt, F., Eder, M., Cheng, T., & Benz, J. P. (2025). Tree bark as a substrate for mycelium-bound composites with two Ganoderma species. *Discover Materials*, *6*(1), 30. https://doi.org/10.1007/s43939-025-00507-0

Fritz, C., Olivera, J. F., Garrido-Manque, V., & Garay, R. (2025). Development and Evaluation of Mycelium-Based Composites from Agroforestry Residues: A Sustainable Approach to the Design of Innovative Building Materials. *Buildings*, *15*(11), 1764. https://doi.org/10.3390/buildings15111764

# Mycocomposites for Reducing the Weight of Concrete Structures

**<u>Paul Langlois</u>[1], Marie-Laure Antoine[1,2], Christelle Perrin[1], Julien Lallemand[1], Ximena Walerstein[3], Jean-Michel Mechling[4], Nicolas Brosse[1], Arnaud Besserer[1]**

[1]Université de Lorraine, LERMAB, Epinal 88000, France, [2]ENSTIB 27 RUE Phillipe Seguin, Epinal 88000, France, [3]Modulatio, Auxerre 89000, France, [4]IJL, Nancy 54000, France

## Background

Cement, the main component of concrete, accounts for 52% of greenhouse gas emissions associated with the construction sector (Feraille et al., 2022). Reducing concrete use by limiting it to mechanically stressed areas of slabs could help decrease $CO_2$ emissions. In this approach, the remaining volume is filled with a lightweight, non-structural material, here a mycocomposite acting as permanent bio-inspired formwork. Mycocomposites are low-cost bio-based materials consisting of a biological substrate bound by a growing mycelial network, enabling applications across various sectors (Alaneme et al., 2023). However, their industrial-scale production for the building industry remains largely underexplored, particularly within the framework of wood cascading and circular bioeconomy strategies. In this context, recycled wood (BR1/BR2 class) represents a promising substrate due to its availability and low cost, facilitating industrialisation. Nevertheless, this feedstock often contains more than 50% particleboards and fibreboards bonded with urea-formaldehyde (UF) resin, whose formaldehyde content may inhibit fungal growth (Dennis et al., 1974). This study presents the first step toward the reproducible large-scale production of mycocomposites using recycled wood as a growth substrate.

**Keywords:** Mycocomposite, recycled wood, steam explosion

## Experimental

### Decontamination of recycled wood:

Recycled wood (particleboard) was pretreated using a steam explosion process under various conditions to evaluate the impact of pretreatment on adhesive removal according to the Troilo et al., 2023 method.

### Fungal colonization in mycocomposites

*Trametes versicolor* was used for the production of mycocomposites. Two substrates are used: beech wood (control) and recycled wood pretreated by steam explosion at 12 bars. Surface colonization is analyzed using image analysis with the Fiji software. A triplicate experiment is conducted for each substrate.

## Results and Discussion

The monitoring of UF resin in the growing substrate was performed by florescence microscopy and infrared spectrometry (NIRS) coupled to PCA based clustering. Despite use of recycled wood as substrate reduced by 20% the fungal colonization when compared control (Figure 2) no significant change in mycelial properties were observed. Optimal growth parameters were implemented to produce concrete slab cores prototypes with satisfying properties.

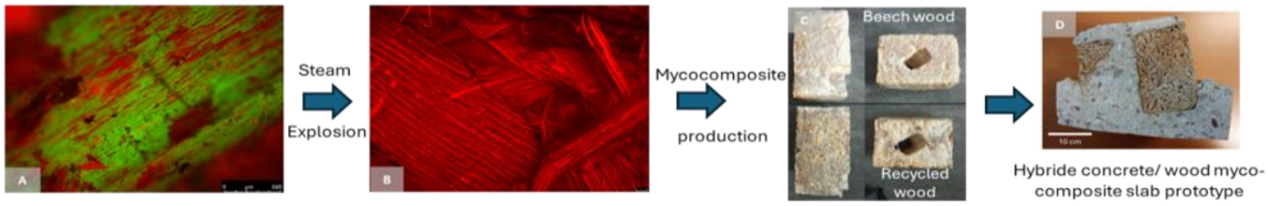


Figure 1. Workflow for hybride concrete/ wood myco-composite slab prototype production. A: Untreated particles; B: Particles treated by steam explosion at 12 bars; C: Mycocoposites with different substrate; D: Hybrid lightweight slab prototype

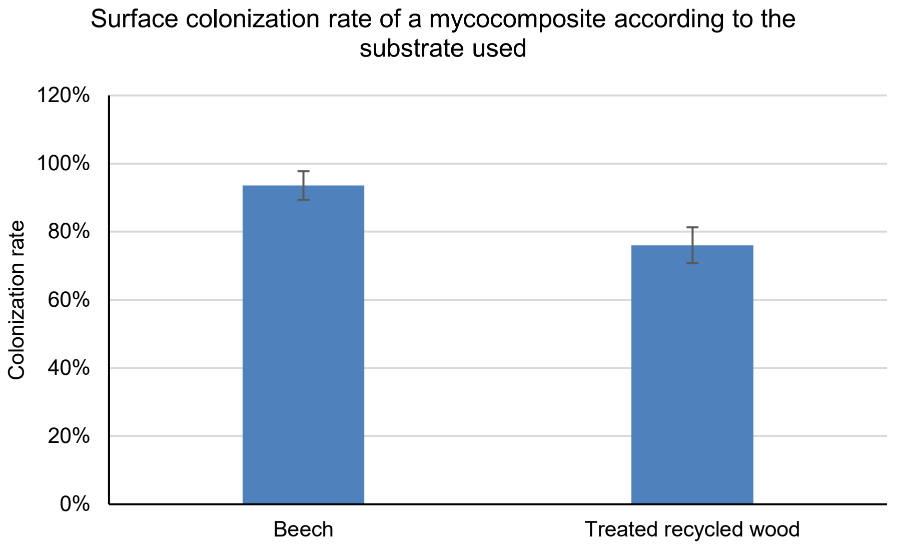


Figure 2. Surface colonization of a mycocomposite as a function of the substrate used

## Conclusions

Recycled wood treated by steam explosion can be used to produce mycocomposites for use in structure application in sustainable buildings. Methodological implementations allowed routine monitoring of feedstock quality, process efficiency and fast assessment of fungal colonization and compliency with targeted applications. More than 50% reduction of $CO_2$ emission and 60% of primary resources use can be achieved in building using this strategy.

## References

Alaneme K.K., Anaele J.U., Oke T.M., Kareem S.A., Adediran M., Ajibuwa O.A., Anabaranze Y.O. (2023) Mycelium based composites: A review of their bio-fabrication procedures, material properties and potential for green building and construction applications, Alexandria Engineering Journal 83: 234-250

Dennis C. and Gaunt H. (1974) Effect of Formaldehyde on Fungi from Broiler Houses, J. appl. Bact. 37, 595-601.

Feraille A., Desbois T., Saadé M. (2022) L'ACV dans le domaine de la construction: le cas du matériau béton. AJCE, vol. 40(2)

Troilo S., Besserer A., Rose C., Saker S., Soufflet L., and Brosse N. (2023) Urea-Formaldehyde Resin Removal in Medium-Density Fiberboards by Steam Explosion: Developing Nondestructive Analytical Tools, ACS Sustainable Chem. Eng. 11 3603-3610

# Density-Driven Thermal Conductivity and Thermal Degradation Behavior of Mycelium Composite as Insulation Material from Estonian Hardwood Species

**Eldwin Maidiono**[1], **Jie Li**[2], **Heikko Kallakas**[3], **Percy F Alao**[4], **Dmitri Goljandin**[5], **Oliver Järvik**[6], **Arnaud Besserer**[7], **Jaan Kers**[8]

[1,2,3,4,5,6,8]Tallinn University of Technology, Ehitajate tee 5, 19086 Tallinn, Estonia, eldwin.maidiono@taltech.ee, jie.li@taltech.ee, heikko.kallakas@taltech.ee, percy.alao@taltech.ee, dmitri.goljandin@taltech.ee, oliver.jarvik@taltech.ee, jaan.kers@taltech.ee, [7]University of Lorraine, INRAE, F-54000 Nancy, France, arnaud.besserer@univ-lorraine.fr

## Background

Low thermal conductivity and less environmental impacts criteria are essential towards sustainable and efficient thermal insulation material. In this regard, preliminary study on mycelium composite (MC) was conducted from under-utilized, low-quality Estonian hardwoods. However, the direct correlation between the density and thermal conductivity of MC utilizing locally resourced Estonian hardwoods is less explored.  Therefore, this study determined this correlation, as well as thermal degradation behavior of MC while employing uncommon, less-studied hardwood species as raw materials, which have different inherent bulk density. Integration of abundant forest materials, either as primary or waste stream, are relevant towards circular economy implementation on wood-based insulation products in Baltic regions.

**Keywords:** Mycelium composites, insulation material, thermal properties, hardwoods.

## Experimental

### Hardwood substrate and mycelium pellet preparation

Aspen (*Populus tremula* L.), birch (*Betula pendula* Roth), and grey alder (*Alnus incana*) low-quality lumbers were grinded and sieved to 1.4-5.6 mm particle size, supplemented with malt-extract powder (3% dry weight) and 60% moisture content. *Trametes versicolor* pellet was cultivated based on previous study (Aguilar *et al.*, 2024)

### Mycelium composite fabrication and testing

Mycelium pellets were inoculated onto each hardwood substrate with 1:7 v/v inoculation ratio inside 0.36 L cylindrical polypropylene (PP) box, then incubated for 28 days under 28$^{o}$C and 60% relative humidity. Resulting mycelium-substrates mixture was mixed with fresh hardwood substrates (1:2 v/v ratio) in 0.6L PP box with inner 160 mm length, 125 mm width, and 30 mm thickness. The mixture was incubated for 30 days under previous conditions and resulting MC was de-moulded and dried under 70$^{o}$C for 18 hours. The MC density and thermal conductivity were determined based on EN-ISO 29768 and ASTM D5334, respectively under constant mass after being conditioned under 23±5$^{o}$C and 50±10% relative humidity. Thermogravimetric analysis (TGA) was performed using 10 mg sample at 30 mL/min nitrogen gas flowrate and 10 °C/min heating rate from 30˚C to 600˚C.

**Results and Discussion**


Figure 1. Mycelium Composites (MC) in this study

The correlation between density and thermal conductivity was presented in Fig. 2. Different commercial insulations were compared, including rock wool, extruded polystyrene (EPS), sheep wool (Elsacker *et al.*, 2019), glass wool (Jeon *et al.*, 2017), and kenaf (Kašpar *et al.*, 2026). Proportional correlation was obtained between density and thermal conductivity in overall insulation material categories. Current MC study on aspen-MC, birch-MC, and grey alder (Fig. 1) showed thermal conductivity of 0.048±0.001, 0.058±0.001, and 0.052±0.0004 W/m. K with density of 146±3, 186±7, and 179±2 kg/m$^3$, respectively. In comparison, thermal conductivity obtained in current study was higher than previous study with citrus peel and paper waste (Fernández *et al.*, 2025) or hemp and wheat straw (Elsacker *et al.*, 2019), due to lower density and lower moisture content of measured specimens. Accordingly, thermal conductivity of MC-Flax fibers (Elsacker *et al.*, 2019) and MC-ash wood (Szymczak-Graczyk *et al.*, 2026) were similar to current MC-Birch and MC-Grey Alder, due to similar substrate's bulk density and high cellulose content.

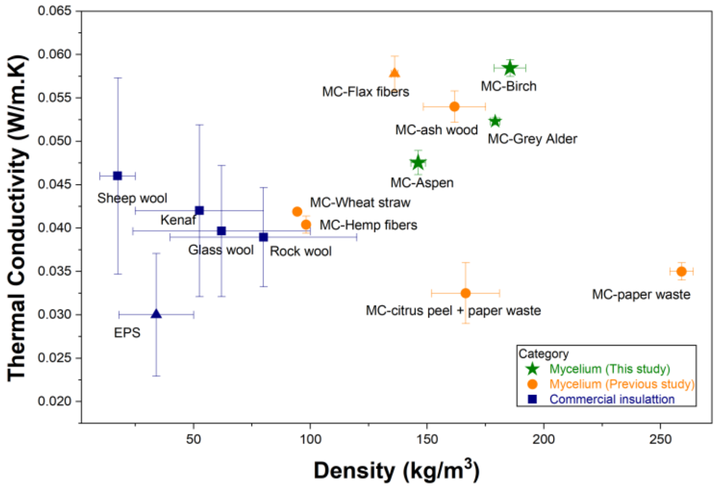


Figure 2. Correlation between density and thermal conductivity

Furthermore, the degradation rate of derivative thermogravimetric (DTG) and remaining mass (%TG) of current MC study was presented in Fig. 3. In grey alder-MC, hemicellulose degradation occurred earlier at 296˚C, compared to aspen-MC and birch-MC (316˚C), which lowered thermal stability at this temperature. Subsequently, remaining mass (%TG) at respective hemicellulose degradation temperature was higher on grey alder-MC (77.2%) than aspen-MC (65.4%) and birch-MC (66.3%) due to relatively well-preserved cellulose structure and better thermal stability beyond 300˚C. This observation matched the higher cellulose degradation temperature ($T_{peak}$) on grey-alder-MC at 359˚C than aspen-MC (350˚C) and birch-MC (356˚C), especially since cellulose's matrix was notably degraded on birch-MC compared to the others as result of mycelium growth.

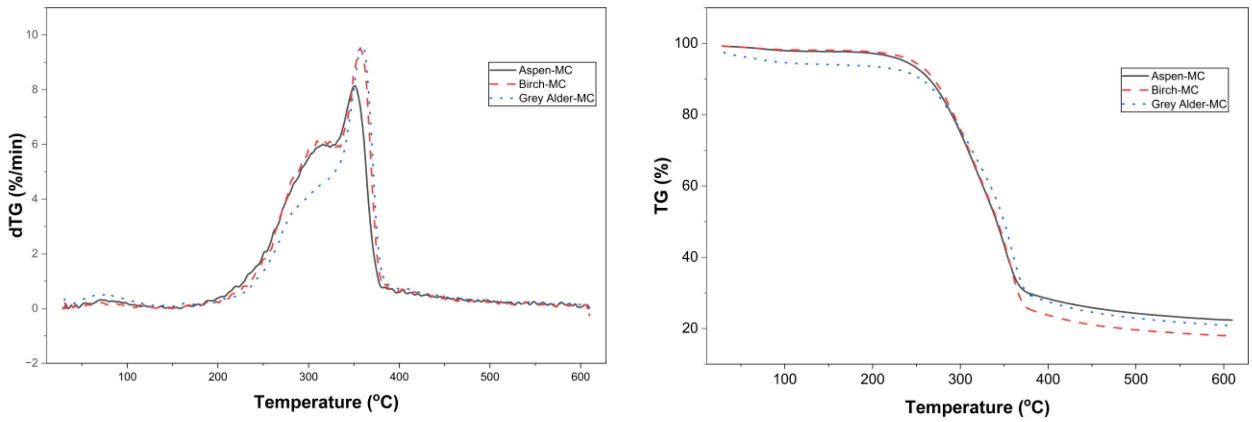


(a) (b)

Figure 3. Derivative thermogravimetric (dTG) (a) and remaining mass (%TG) (b)

## Conclusions

The correlation between MC's density and thermal conductivity was proportional on MC-based insulation materials. MC's Thermal conductivity was also influenced by inherent raw materials density, porosity, specimen's moisture content, and mycelium colonization rate, which are also related to the composite's density.

## References

Aguilar, K. *et al.* (2024) "Steam Explosion: A Booster for Fungal Growth in a Myco-composite," *ACS Sustainable Chemistry & Engineering*, 12(31), pp. 11650–11659. Available at: https://doi.org/10.1021/acssuschemeng.4c03099.

Elsacker, E. *et al.* (2019) "Mechanical, physical and chemical characterisation of mycelium-based composites with different types of lignocellulosic substrates," *PLOS ONE*, 14(7), p. e0213954. Available at: https://doi.org/10.1371/journal.pone.0213954.

Fernández, N. *et al.* (2025) "A Novel Biocomposite Made of Citrus Peel Waste and Mushroom Mycelium: Mechanical, Thermal, and Bio-Repellency Studies," *Recycling*, 10(6), p. 216. Available at: https://doi.org/10.3390/recycling10060216.

Jeon, C.-K. *et al.* (2017) "A Study on Insulation Characteristics of Glass Wool and Mineral Wool Coated with a Polysiloxane Agent," *Advances in Materials Science and Engineering*, 2017, pp. 1–6. Available at: https://doi.org/10.1155/2017/3938965.

Kašpar, J. *et al.* (2026) "Multifunctional performance assessment of insulation panels from recycled textiles and Kenaf/Hemp Fibers: thermal, acoustic, and fire behavior," *Cleaner Materials*, 19, p. 100373. Available at: https://doi.org/10.1016/j.clema.2026.100373.

Szymczak-Graczyk, A. *et al.* (2026) "Mycelium-bound ash sawdust biocomposite as a sustainable thermal insulation material for construction applications," *Advances in Science and Technology Research Journal*, 20(9), pp. 461–475. Available at: https://doi.org/10.12913/22998624/224404.

# Surface Characterisation of Fresh, Reclaimed, and Hybrid Pine Wood Adhesion Interfaces

**Nametso Linda Moumakwa[1], Katarina Culina[1], Kristian Korhonen[2], Mark Hughes[1]**

[1]Department of Bioproducts and Biosystems, School of Chemical Engineering, Aalto University, Espoo, Finland, [2]Department of Chemistry and Materials Science, Aalto University, Finland
nametso.moumakwa@aalto.fi,katarina.culina@aalto.fi, kristian.korhonen@aalto.fi, mark.hughes@aalto.fi

## Background

The recovery and reuse of wood from building demolition is a cornerstone of the circular economy, reducing demand for fresh timber, greenhouse gas emissions and construction waste (Nasiri & Hughes, 2026). Reclaimed Scots pine (Pinus sylvestris L.) offers significant potential, however its long service history of 60 years in a residential building in Espoo (built 1956, demolished 2022), changes its surface and mechanical behaviour (Moumakwa & Hughes, 2025). Prolonged loading and environmental exposure induce leaching of extractives, lignin cross-linking, hemicellulose degradation, increased porosity, microcracks, surface contamination and dimensional variation (Gérardin et al., 2007). These aging effects change surface topography, wettability and surface free energy, making adhesion less predictable than in graded fresh wood, where standards such as EN 302-1 and EN 14081-1 allow systematic optimisation of adhesive, pressure and preparation (Adamčík et al., 2025). While planing (cutting) usually produces continuous, directional tool marks and sanding (abrasion, P120) generates fragmented, fibrillated debris (Gurau, 2022), it remains unclear whether both methods affect reclaimed wood as they do fresh wood, and how topography couples to bond strength.
Therefore, this study addresses the gap by linking areal surface characterisation to mechanical properties.

**Keywords:** reclaimed wood, Scots pine, surface roughness, wettability, surface free energy, adhesion strength, hybrid joints, circular economy.

## Materials and Methods

Reclaimed pine was sampled from roof elements of a single building with uniform exposure history; fresh pine was sourced from a sawmill in Eastern Finland (Uimaharju) and stored sheltered (not climate-controlled). All panels were cut to dimensions of 150 × 20 × 10 mm, two 5 mm lamellae, paired as FF, RR and FR hybrid joints. Samples were planed with the Proxxon DH 40 planer and sanded with a belt-sander then hand-finished parallel to grain with P120 aluminium oxide (MIRKA).

### Characterisation & Mechanical Testing

Surface characterisation

(i) Areal topography by Sensofar S Neox CSI (20×, piezo z-scan ≤150 µm, 3×3 stitch = 2087×1744 µm, 0.6835 µm pixel; SensoVIEW, plane-levelled; $S_a$, $S_q$, $S_z$ per ISO 25178; n = 3 per condition).

(ii) Wettability by Theta Flex sessile drop and SFE by Owens–Wendt–Rabel–Kaelble (OWRK/Fowkes) separating polar ($\gamma_p$) and dispersive ($\gamma_d$) components.

(iii) SEM with a Phenom Pure G5 at specifications of Au/Pd 80:20, 30s.

## Results and Discussion

### Surface topography & areal roughness

Planed surfaces were continuous and directional cutting marks, sanded were fragmented/fibrillated. Sanding had opposite effects (Fig. 1; Table 1): fresh wood $S_a$ 3.02 of 5.13 µm (+70 %), $S_q$ 2.86 of 6.08 µm, and $S_z$ at 111.3 to 135.5 µm. Reclaimed wood recorded a $S_a$ from 3.21 down to 2.15 µm, a reduction of 33 %, $S_q$ 5.60 to 4.24 µm, and $S_z$ 136.0 to 105.1 µm. Height histograms broadest for sanded fresh, narrowest for reclaimed sanded; centre-line profiles showed irregular sharp peaks after sanding fresh but suppressed extremes after sanding reclaimed. Planed reclaimed retained directionality but with disturbed, locally elevated layers and exposed degraded outer layers after 60 yr aging and not simple roughening.

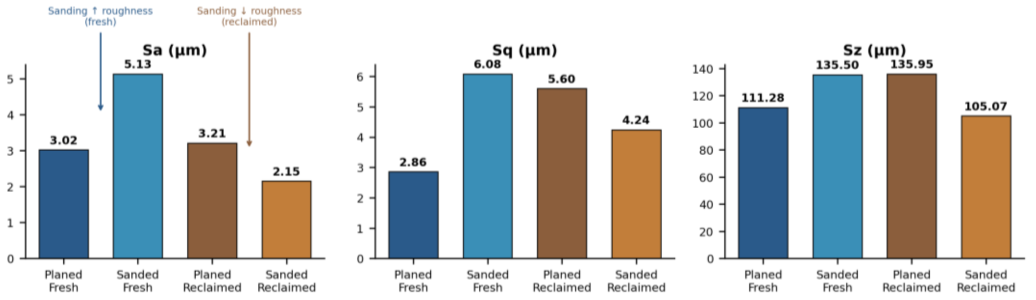


Figure 1. Areal roughness (Sa, Sq, Sz, µm) for Planed/Sanded × Fresh/Reclaimed (n=3; points=measurements, black=mean±95%CI). Sanding increases roughness in fresh, decreases it in reclaimed; interaction significant for Sq, Sz

Table 1. Mean areal roughness (ISO 25178) and change after P120 sanding. ANOVA: $S_a$ $p=0.082$, $S_q$ $p=0.043$*, $S_z$ at $p=0.010$

| Surface | Sa (µm) | Sq (µm) | Sz (µm) | Change vs. planed |
|---|---|---|---|---|
| Planed Fresh | 3.02 | 2.86 | 111.3 | — |
| Sanded Fresh | 5.13 | 6.08 | 135.5 | +70/+113/+22% |
| Planed Reclaimed | 3.21 | 5.60 | 136.0 | — |
| Sanded Reclaimed | 2.15 | 4.24 | 105.1 | −33/−24/−23% |

### Wettability & surface free energy (SFE, OWRK)

Sanded was less wettable than planed and reclaimed less than fresh, despite opposite roughness trends (Fig. 2). Starting with Water CA (mean), in comparison planed Fresh recorded 95.6° and Planed Reclaimed 96.6° while was Sanded Fresh 104.5° and Sanded Reclaimed 122.8°. On the other hand, glycerol contact angles were higher in the same trend with values of 107.5°, 109.7°, 122.4° and 137.4°. Table 2 shows the polar $\gamma_p$ which dropped from 29.4-31.9 to 14.6-15.8 mN/m; and the dispersive $\gamma_d$ low at 0.6-4.6 mN/m. The results show that CA/$\gamma$p increased after sanding irrespective of $S_a$ direction because of Cassie-Baxter partial wetting on fibrillated, air-trapping surfaces and redistribution of extractive-rich weak boundary layers on sanded reclaimed.

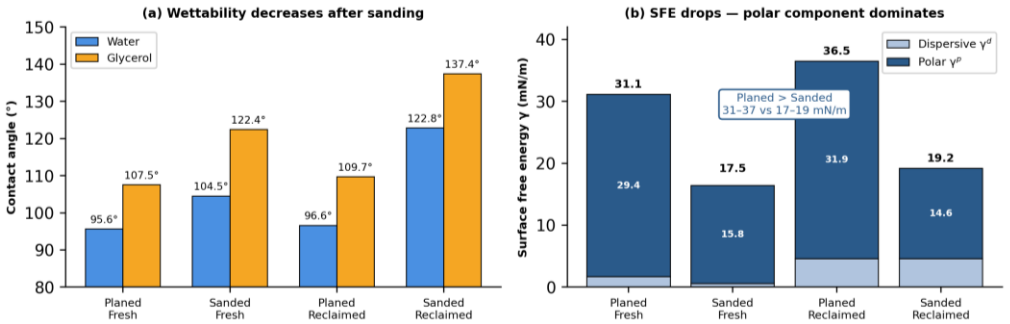


Figure 2. Contact angles (°) for water (left) and glycerol (right) + OWRK SFE (mN/m, polar vs. dispersive). Planed > sanded, Fresh > Reclaimed in wettability; n=3, SD bars

Table 2. OWRK surface free energy (mN/m) and mean contact angles. Polar component dominates loss after sanding

| Group | γtot | γd | γp | Water CA | Glycerol CA |
|---|---|---|---|---|---|
| Planed Fresh | 31.1±4.0 | 1.7±0.95 | 29.4±3.4 | 95.6° | 107.5° |
| Planed Reclaimed | 36.5±7.1 | 4.6±5.3 | 31.9±4.0 | 96.6° | 109.7° |
| Sanded Fresh | 17.5±4.2 | 0.6±0.4 | 15.8±2.9 | 104.5° | 122.4° |
| Sanded Reclaimed | 19.2±4.8 | 4.6±1.2 | 14.6±2.9 | 122.8° | 137.4° |

*Full data: Moumakwa et al. (2026) DOI 10.1080/17480272.2026.2699415.*

### Conclusions

The results show that aging changes machining response as sanding increased $S_a$/$S_q$/$S_z$ in fresh wood but lowered the parameters in reclaimed showing that preparation is not transferable. Furthermore, planed fresh had lowest CA/highest $\gamma_p$ (29–32 mN/m) but lower $\sigma_{max}$ displaying that adhesion strength needs both interlocking and energetics. In overall, the results display the potential to reuse reclaimed wood from demolished buildings, as surface treatments did improve the adhesion strength of wood and using reclaimed wood in hybrid element configurations mitigates the weaknesses displayed by reclaimed wood, therefore allowing reclaimed wood to reach mechanical performance comparable to fresh wood and rendering it a viable material for reuse in structural applications.

### Acknowledgements

We would like to thank VTT (profilometry), and the project funder, Aalto University DUET Project & Finnish Ministry of Agriculture and Forestry.

### References

Adamčík, L., Giudice, V. L., Todaro, L., Dudiak, M., & Kminiak, R. (2025). Surface roughness of thermally modified and unmodified selected wood species after sanding. *European Journal of Wood and Wood Products*, *83*(3). https://doi.org/10.1007/s00107-025-02260-w

Gérardin, P., Petrič, M., Petrissans, M., Lambert, J., & Ehrhrardt, J. J. (2007). Evolution of wood surface free energy after heat treatment. *Polymer Degradation and Stability*, *92*(4), pp. 653–657. https://doi.org/https://doi.org/10.1016/j.polymdegradstab.2007.01.016

Gurau, L. (2022). Testing the Processing-Induced Roughness of Sanded Wood Surfaces Separated from Wood Anatomical Structure. *Forests*, *13*(2), pp. 331. https://doi.org/10.3390/f13020331

Moumakwa, N. L., & Hughes, M. (2025). Assessing changes in the mechanical properties of wood recovered from demolished buildings. *Construction and Building Materials*, *504*, pp. 144612. https://doi.org/https://doi.org/10.1016/j.conbuildmat.2025.144612

Nasiri, B., & Hughes, M. (2026). Lifetime effects on wood waste generation and the cascading potential of waste wood from Finnish houses. *Resources, Conservation and Recycling*, *228*, pp. 108804. https://doi.org/https://doi.org/10.1016/j.resconrec.2026.108804

Qin, Z., Chen, H., Gao, Q., Zhang, S., & Li, J. (2015). Wettability of sanded and aged fast-growing poplar wood surfaces: I. Surface free energy. *BioResources*, *10*(1), pp.1008–1023.

# Ageing Induced Changes in Fracture Performance of Bonded Beech Wood

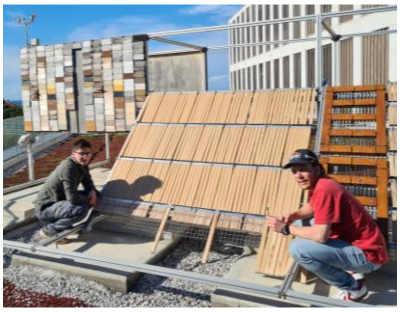

**Martin Capuder [1], Václav Sebera[2], Boris Azinović[1], Jaka Gašper Pečnik[1]**

[1]Slovenian National Building and Civil Engineering Institute, Slovenia, martin.capuder@zag.si[1], boris.azinovic@zag.si[1], jaka.pecnik@zag.si,
[2]Mendel University in Brno, Czechia, vaclav.sebera@mendelu.cz

## Background

European beech (*Fagus sylvatica* L.) is one of the most economically and ecologically important hardwood species in Central Europe. However, climate change is expected to significantly affect its growth and distribution in the future (Martinez del Castillo et al., 2022) which could lead to increased demand on its utilization. Beech has great mechanical properties, which can be beneficially used in engineered timber products and when properly protected such products have already demonstrated significant advantages in outdoor applications (Burgherr and Stadler, 2021). Nevertheless, the performance of bonded beech-based composites under fluctuating environmental conditions remains challenging because of the poor dimensional stability causing internal stresses within the adhesive bondline. In recent years, increasing attention has been devoted to the fracture behaviour of bonded beech wood, particularly under Mode II loading conditions (Capuder et al., 2026). In that study, authors demonstrated importance of surface preparation for enhanced fracture resistance of bonded beech. Limited information is available regarding long-term durability of bonded beech-based composites for more demanding service life conditions. The objective of this study was to evaluate the impact of natural ageing on bonded beech composites manufactured with different surface preparation on Mode II - shear fracture energy ($G_{II}$), with respect to the degree of delamination.

**Keywords:** European beech, Mode II, bondline testing, natural ageing

## Experimental

1C PUR bonded European beech 3 ENF specimens were prepared according to Capuder et. al. (2026). To study the effect of sample preparation with respect to natural ageing, bonded surfaces were prepared by a) planing (R), b) planing + sanding (S) and c) combining two anatomical orientations (RT). Orientation of lamellas in group R and S was R/R, while in group RT, one lamella had radial and one tangential orientation. Within each of three groups, 40 DCB specimens were edge sealed with thick protective coating, to limit wood end grain wetting. DCB specimens were exposed to natural aging located in Izola (Slovenia) between February and August 2024. Half of the specimens were exposed for 3 months (3M) while another half were exposed for 6 months (6M). To validate the level of delamination within bonded specimens, prior to the Mode II testing, delaminated areas, and area around the crack tip were brushed with the white low viscosity paint, allowing penetration of white pigment into the delaminated area. After the test, all specimens were manually cleaved into two halves for image analysis in order to quantify the delaminated areas. Mode II strain energy release rate ($G_{II}$) based on 3ENF and equivalent crack length was conducted as in Capuder et al. (2026) as well as the comparison with the unaged groups.

## Results and Discussion

Due to the natural ageing, samples underwent different levels of delamination which influenced behaviour during 3-ENF test. One of the main findings of the study was that unlike the unaged specimens, with increasing delaminated area, samples did not exhibit a distinct sudden failure event associated with a rapid increase in beam shear slip, which was used to identify crack initiation (Figure 1a). Instead, damage evolution appeared more gradual, making the identification of significant crack initiation and subsequent data analysis considerably more challenging. The synchronization between local slip measurements and the applied force for the R group is shown in Figure 1b. By combining information from force-displacement and force-slip responses, it was generally possible to identify the point corresponding to the Mode II energy release rate at $F_{max}$, $G_{IIc}$. The recorded $F_{max}$ values associated with the slip in the 3M and 6M aged specimens were lower than those of the unaged group, while the difference between the two ageing periods is less obvious. Specimens exhibiting higher levels of delamination particularly the R and RT groups, showed a pronounced nonlinear force-displacement response (Figure 1a) lacking a distinct critical event associated with $G_{II,c}$. This behaviour can be explained by the reduced DCB response of partially delaminated specimens. Unlike fully bonded beams, where the lamellae act as a single member and efficiently transfer interlaminar shear stresses, delamination reduces shear transfer and allows greater relative slip between lamellae, decreasing the effective bending stiffness. Consequently, crack propagation becomes more gradual and stable, while ageing-induced delamination shortens the effective bondline area and reduces the energy required for crack propagation.

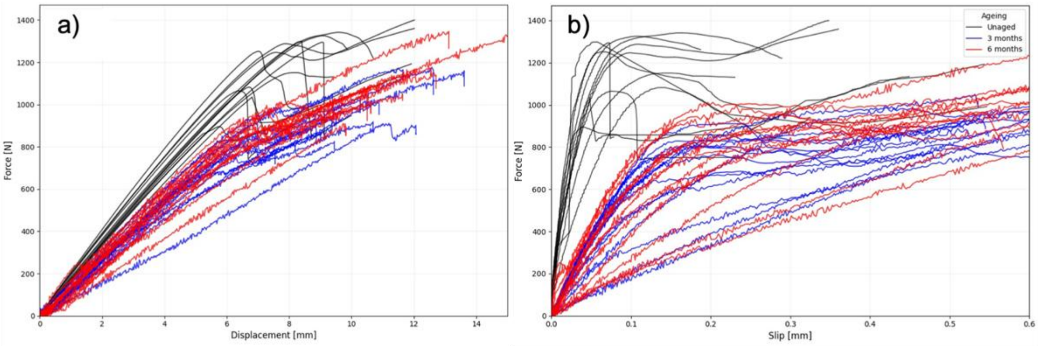


Figure 1. Force-displacement diagrams for unaged (black) aged 3M (blue) and aged 6M (red) (a) and force-slip diagrams (b) for R group

## Conclusions

Natural ageing reduced the Mode II fracture performance of bonded beech composites. Increased delamination was associated with nonlinear load-displacement behaviour, indicating reduced interlaminar shear transfer and loss of composite stiffness. Further numerical simulations will be applied to quantify the influence of delamination extent on stress redistribution, crack propagation, and the residual fracture toughness of aged, bonded composites.

### References

Burgherr A. and Stadler C. (2022) A new pedestrian bridge made of regional beech wood in Adliswil. In Proc. 4th ICTB, 2022. Doi: https://doi.org/10.24451/p33k-vn37.

Capuder, M., Azinović, B., Merhar, M. et al (2026) Effect of moisture content, surface preparation and lamellae orientation on Mode II strain energy release rate of polyurethane-bonded beech wood. Eur. J. Wood Prod. 84, 90. https://doi.org/10.1007/s00107-026-02447-9.

Martinez del Castillo, E., Zang, C.S., Buras, A. et al. (2022) Climate-change-driven growth decline of European beech forests. Commun Biol 5, 163. https://doi.org/10.1038/s42003-022-03107-3.

# Partial Replacement of Melamine-Urea-Formaldehyde (MUF) Resin with Modified Lignin for MDF Manufacturing and Characterization

**Gorakh Hiraman Ghuge**[1], **Siva Ponnupandian**[2], **Sean Warren**[2]
**Ramesh Babu Padamati**[1]*

[1] School of Chemistry, CRANN Research Centre, Trinity College Dublin, Dublin, Ireland.
[2] MEDITE SMARTPLY, Redmondstown, Clonmel, Co. Tipperary, Ireland
*Corresponding author: BABUP@tcd.ie

## Background

Medium-density fiberboard (MDF) is one of the most widely used engineered wood products, typically manufactured by bonding wood fibers with synthetic adhesives such as melamine-urea-formaldehyde (MUF) resin (Lee TC et al. 2020). Although MUF resin provides excellent bonding performance and moisture resistance, its dependence on fossil-based chemicals and the release of formaldehyde during production and use have raised increasing environmental and health concerns (Lee TC et al. 2020). Therefore, the development of sustainable adhesive systems with reduced synthetic resin content has become an important research focus in the wood composite industry. Lignin, the second most abundant natural polymer after cellulose, is an attractive renewable resource due to its aromatic structure, abundance, and potential reactivity after modification (Luis AZT et al., 2020). Previous studies have investigated lignin-based additives and substitutes in various wood adhesive systems (Johannes K et al., 2021); however, the application of amine-modified lignin (AML) as a partial replacement for MUF resin in MDF manufacturing, and its influence on bonding performance, physical properties, and emission characteristics, remain largely unreported in the literature. This study aims to address this knowledge gap by incorporating AML into MUF resin systems for MDF production and evaluating the resulting panels in terms of bonding performance, physical properties, and formaldehyde emissions (FA). The findings are expected to highlight the potential of lignin as a sustainable partial replacement for conventional synthetic resins in MDF manufacturing.

**Keywords:** amine modified lignin (AML), melamine-urea-formaldehyde (MUF), medium-density fiberboard (MDF), formaldehyde emission.

## Experimental

**(a) Preparation of Amine-Modified Lignin (AML):** The AML was prepared in two sequential steps. First, DES-lignin was synthesized from lignin using a deep eutectic solvent (DES) system to increase the hydroxyl groups of lignin (Step 1) (Wang S. et al., 2020). The resulting DES-lignin was subsequently subjected to amine modification using DMC and 1,4-butanediamine to introduce amine functional groups onto the lignin structure, yielding amine-modified lignin (AML) (Step 2). The resulting AML was dispersed in water, and the resulting dispersion was used as a lignin-based resin component for blending with commercial MUF resin (Jaša S. et al., 2021).

**(b) Formulation Preparation:** Four formulations containing 10, 20, 30, and 40% AML were prepared by blending AML dispersion with commercial MUF resin using standard procedure, as shown in Table 1.

Table 1. AML and MUF Composition in the Resin Formulations

| | | | | |
|---|---|---|---|---|
| AML % | 10 | 20 | 30 | 40 |
| MUF % | 90 | 80 | 70 | 60 |

**(c) Fabrication Process of MDF:** MDF panels were fabricated by mixing wood fibers with resin as per industry protocol, forming the fiber mat, and hot-pressing it under controlled temperature and pressure, followed by cooling and cutting.

**(d) Characterization:** The fabricated boards will be characterized for formaldehyde emission, internal bond strength (IB), density profile, and moisture content.

**Results and Discussion**

Initially, we successfully synthesized amine modified lignin and their modification were analyzed by FTIR, and $^{13}C$ NMR.

**FTIR:** The appearance and enhancement of absorption near 3300-3400 $cm^{-1}$ in the modified samples are associated with N-H stretching vibrations of primary amine ($NH_2$) groups (Jaša S. et al. (2021). This confirms the successful amination reaction on the lignin backbone (Figure 1a).

**$^{13}$C NMR:** $^{13}C$ NMR: The appearance of signals at 51.5 and 157.1 ppm, assigned to the α-$CH_2$ group attached to $NH_2$ and the urethane carbonyl (C=O), respectively, supports the successful incorporation of amine functionalities into the lignin backbone (Figure 1b).

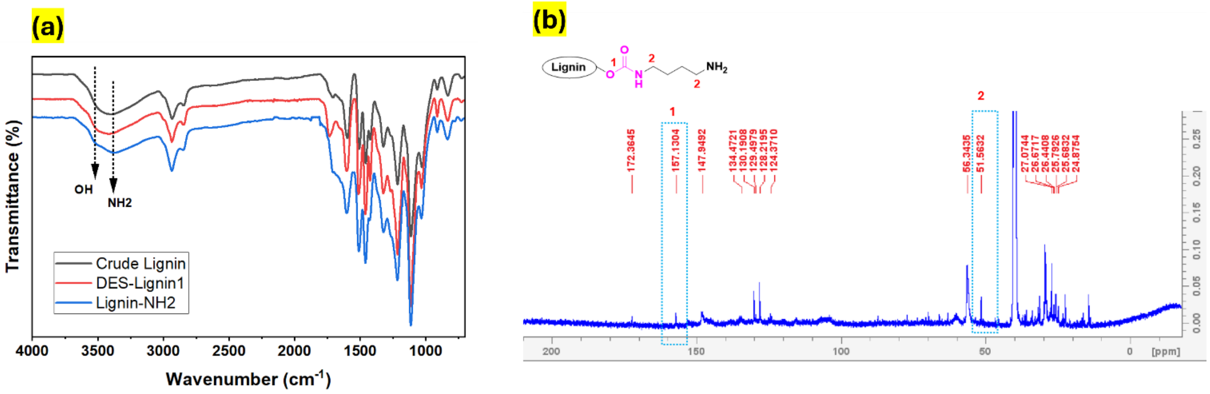


Figure 1. (a) FTIR spectra of crude lignin, DES-lignin, and aminated lignin; (b) $^{13}C$ NMR spectrum of aminated lignin

After synthesizing amine-modified lignin, an AML dispersion in water was prepared and mixed with MUF resin at different proportions (Table 1). The formulations were characterized for solid content and viscosity, and their curing behavior was analyzed by DSC. The total solid content was maintained at 63%, with a viscosity of approximately 124 cP. DSC showed that curing was completed during the first heating cycle, with no curing peak observed in the second cycle. The main curing peaks appeared between 105 and 125 °C, while water evaporation and curing peaks partially overlapped in the 60-130 °C range (Jianlin L et al., 2015).

The formulations were used to fabricate MDF boards, following the fabrication process schematically illustrated in Figure 2. Pressing parameters, including resin sprayability, moisture content, and pressing conditions, were optimized at the laboratory scale. Subsequently, four MDF boards were fabricated at the industry partner's facility in Ireland. Characterization of the fabricated boards, including FA emission, IB, density profile, and moisture content, is currently in progress.

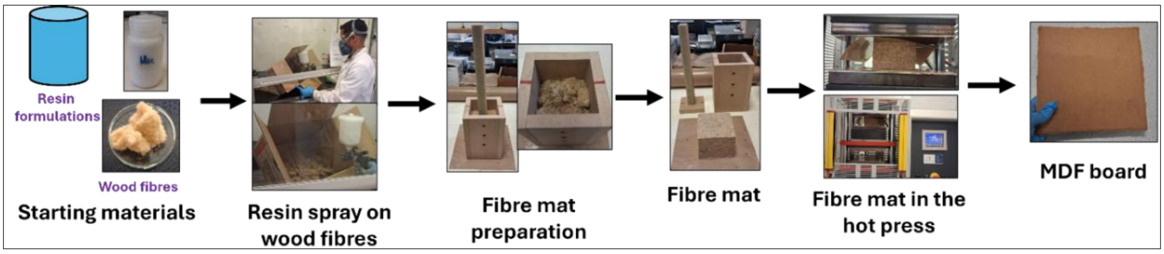


Figure 2. Steps involved in the MDF fabrication process at the laboratory scale

## Conclusions

AML was successfully synthesized and incorporated into MUF resin for MDF fabrication. Board characterization is ongoing, and the findings are expected to demonstrate lignin's potential as a sustainable partial replacement for conventional synthetic resins.

## References

Jaša S. et al. (2021) Organosolv Lignin for Non-Isocyanate Based Polyurethanes (NIPU) as Wood Adhesive. JRM, vol.9, no.5

Jianlin L et al. (2015) Effect of Melamine Allocation Proportion on Chemical Structures and Properties of Melamine-Urea Formaldehyde Resins. Bio Resources 10(2), 3265-3276.

Johannes K et al. (2021) Lignin and Lignin-Derived Compounds for Wood Applications-A Review: Molecules, 26, 2533.

Lee TC et al. (2020) An overview on development of environmental friendly medium density fibreboard. Materials Today: Proceedings 29, 52–57.

Luis AZT et al. (2020) Lignin as a potential source of high-added value compounds: A review. Journal of Cleaner Production 263: 121499.

Wang S et al. (2020) Unraveling the Structural Transformation of Wood Lignin During Deep Eutectic Solvent Treatment: Front. Energy Res. 8:48.

# Improving the Moisture Resistance of Steam-Exploded Binderless Particleboards

**Andris Berzins[1], Ramunas Tupciauskas[2], Martins Andzs[3], Gunars Pavlovichs[4]**

[1,2,3,4]Latvian State Institute of Wood Chemistry, Latvia,
andris.berzins@kki.lv, ramunas.tupciauskas@kki.lv,
martins.andzs@kki.lv, pavlovichs@inbox.lv

## Background

Binderless particleboards offer a sustainable alternative to conventional wood-based panels by exploiting the self-bonding capacity of lignocellulosic biomass. Steam explosion (SE) promotes fibre defibrillation and chemical modification of hemicelluloses and lignin, which can enhance bonding during subsequent hot pressing (Luo and Yang, 2011; Boon *et al.*, 2019; Audibert *et al.*, 2025). However, moisture resistance remains a major challenge and is strongly affected by raw material, particle morphology and pressing conditions (Widyorini, Yudha and Prayitno, 2011; Boon *et al.*, 2019; Audibert *et al.*, 2025).
Our previous study developed high-density bio-based particleboards from grey alder, softwood and wheat straw for façade applications (Tupciauskas *et al.*, 2025). SE grey alder boards showed the best overall performance, but further improvement of moisture resistance was required. The present study therefore investigates pressing moisture content, hydrolysate retention and particle refinement/homogenisation, with suberinic acids (SA) included as a bio-based binder comparison (Tupciauskas *et al.*, 2026).

**Keywords:** steam explosion, binderless particleboard, moisture resistance, particle size, self-bonding.

## Experimental

Steam-exploded grey alder (GA), softwood (SW) and wheat straw (WS) were used to produce high-density binderless particleboards. Pressing moisture contents of 2, 5 and 9% and hydrolysate retention were investigated. Particle preparation progressed from wire-brush defibration to 2 mm milling, milling only the coarse fraction (>2 mm), and wet defibration combined with removal of the water-soluble fraction. Selected materials were also bonded with 15 wt.% birch-bark-derived SA.
Binderless boards were hot-pressed at 160 °C for 10 min to 10 mm thickness; SA-bonded boards at 180 °C. Bending strength was determined according to EN 310 and 24 h thickness swelling according to EN 317. Moisture resistance was evaluated using the modified EN 1087-1 boil procedure specified in EN 622-5, Annex A, followed by residual internal bond testing according to EN 319.

## Results and Discussion

Pressing moisture content affected both bending performance and bond retention after boiling (Table 1). Increasing moisture content from 2 to approximately 5% generally improved residual bonding, while 9% provided no consistent additional benefit and reduced bending strength. Moisture may promote plasticisation and mobility of lignocellulosic components during hot pressing, including moisture-dependent lignin softening reported for binderless bonding (Börcsök and Pásztory, 2021). Börcsök and Pásztory specifically describe moist lignin softening at elevated temperature and discuss its relevance to binderless-board manufacture.

Table 1. Selected board variants illustrating the effects of raw material and particle preparation on mechanical properties and moisture resistance

| Material / processing | MC % | Density kg/m$^3$ | MOR MPa | TS 24 h % | IB after boil MPa |
|---|---|---|---|---|---|
| SW, SE, milled, hydrolysate retained | 5 | 1247 | 18.8 | 5.82 | 0.015 |
| WS, SE, milled, hydrolysate removed | 9 | 1277 | 28.2 | 2.46 | 0.034 |
| GA, SE, milled | 5 | 1247 | 49.0 | 5.73 | 0.109 |
| GA, SE, milled, high-density | 5 | 1351 | 47.7 | 2.25 | 0.169 |
| **GA, SE, wet-defibrated** | **5** | **1381** | **77.4** | **0.78** | **0.366** |
| GA, SE, wet-defibrated + 15% SA | 5 | 1277 | 32.8 | 1.71 | 0.204 |

Hydrolysate retention was beneficial under some conditions, particularly at low pressing moisture, but strong residual bonding was also obtained after removal of the water-soluble fraction. Steam treatment can generate simple sugars and other degradation products that may contribute to self-bonding, while lignin-related mechanisms may also be involved (Hubbe *et al.*, 2018; Boon *et al.*, 2019). The present results therefore suggest that water-soluble SE products are not essential for moisture-resistant bonding and that water-insoluble lignocellulosic components may also contribute. The individual bonding mechanisms, however, could not be identified in the present study.

Particle homogenisation produced the strongest overall improvement. Wet-defibrated GA reached 77.4 MPa MOR, 0.78% thickness swelling after 24 h and 0.366 MPa residual IB after boiling. The improvement may result from reduced coarse-particle content, increased contact between material elements and a more fibrous morphology. This interpretation is consistent with (Audibert *et al.*, 2025), who found chemical composition and particle size to affect internal bonding and thickness swelling, while flexural properties were mainly related to fibre aspect ratio. Because washing and wet defibration occurred simultaneously, their individual contributions could not be separated.

SA-bonded boards showed good moisture resistance but no clear overall advantage over the best binderless formulation. Under the investigated conditions, optimisation of particle preparation and pressing moisture therefore provided the strongest overall improvement.

## Conclusions

Pressing moisture content and particle preparation strongly influenced the moisture resistance of SE binderless boards. The best overall performance was obtained after wet defibration, combining high bending strength, low 24 h thickness swelling and substantial residual bond strength after boiling. The results indicate that particle homogenisation is a promising route for further development of moisture-resistant fully bio-based panels.

## Acknowledgements

This research was funded by the LATVIAN SCIENCE COUNCIL, Project “Investigation of innovative biomass-based panels for application in external building façade,” grant number lzp-2023/1-0348.

**References**

Audibert, E. et al. (2025) ‘Binderless particleboards from steam exploded woody biomass: chemical and morphological properties relate to their mechanical and physical behavior’, Industrial Crops and Products, 229(January). Available at: https://doi.org/10.1016/j.indcrop.2025.120983.

Boon, J.G. et al. (2019) ‘Physical and mechanical properties of binderless particleboard made from steam-pretreated oil palm trunk particles’, Journal of Composites Science, 3(2), pp. 1–45. Available at: https://doi.org/10.3390/jcs3020046.

Börcsök, Z. and Pásztory, Z. (2021) ‘The role of lignin in wood working processes using elevated temperatures: an abbreviated literature survey’, European Journal of Wood and Wood Products, 79(3), pp. 511–526. Available at: https://doi.org/10.1007/s00107-020-01637-3.

Hubbe, M.A. et al. (2018) ‘Critical links governing performance of self-binding and natural binders for hot-pressed reconstituted lignocellulosic board without added formaldehyde: A review’, BioResources, 13(1), pp. 2049–2115. Available at: https://doi.org/10.15376/biores.13.1.Hubbe.

Luo, P. and Yang, C. (2011) ‘Binderless particleboard from steam exploded wheat straw’, Advanced Materials Research, 179–180, pp. 807–811. Available at: https://doi.org/10.4028/www.scientific.net/AMR.179-180.807.

Tupciauskas, R. et al. (2025) ‘Physical–Mechanical Properties of Innovative Biobased Particleboards for Application in External Building Façades’, Forests, 16(8), pp. 1–14. Available at: https://doi.org/10.3390/f16081359.

Tupciauskas, R. et al. (2026) ‘Development of Suberinic Acids-Bonded Medium-Density Particleboard’, Polymers, 18(4), pp. 1–14. Available at: https://doi.org/10.3390/polym18040487.

Widyorini, R., Yudha, A.P. and Prayitno, T.A. (2011) ‘Some of the properties of binderless particleboard manufactured from bamboo’, Wood Research Journal, 2(2), pp. 1–5.

# Non-Isocyanate Polyurethane Adhesives from Forest-Based Feedstocks for Wood Bonding

**John Tosin Aladejana[1], Reza Hosseinpourpia[1,2,3]**

[1]Department of Forestry and Wood Technology, Linnaeus University, Lückligs Plats 1, 35195 Växjö, Sweden, johntosin.aladejana@lnu.se, reza.hosseinpourpia@lnu.se
[2]College of Forest Resources and Environmental Science, Michigan Technological University, Houghton, Michigan 49931, United States
[3]Linnaeus University Centre for Competitive Timber Structures, Linnaeus University, Universitetsplatsen 1, 351 95 Växjö, Sweden

## Background

Non-isocyanate polyurethane (NIPU) adhesives are of great interest as alternatives to traditional polyurethane adhesives, due to the elimination of toxic isocyanates (Zhang et al., 2025). However, the use of these adhesives in industry is limited by the relatively high curing temperature (180 °C) required during hot-pressing of the wood substrate, which increases energy consumption and reduces efficiency in plywood production (Chen et al., 2021; Wang et al., 2024). Several chemical modifications have been attempted to overcome this limitation, but no substantial progress has been reported. Therefore, an effective strategy that simultaneously reduces curing temperature and improves bonding performance remains necessary, especially in plywood production. In the present study, a stepwise modification strategy was developed, and the chemical structure and plywood bonding performance of the resulting NIPU adhesives were investigated to evaluate the effectiveness of the proposed strategy.

**Keywords:** Lignin, Tannin, NIPU curing, Plywood, Bio-adhesives

## Experimental

Lignin and tannin (LT) were used as the primary materials for synthesizing the LT-NIPU adhesive. The formulated LT-NIPU adhesives were further crosslinked with microcrystalline cellulose (MCC), and each adhesive type was designated by the MCC content (MLT-NIPU 5%, MLT-NIPU 15%, and MLT-NIPU 30%). FTIR was used to study the chemical characteristics of formulated adhesives. Three-ply birch plywood specimens were bonded at 130 °C under controlled hot-pressing conditions for 10 min, and their dry shear strengths were determined according to EN 314-1. For comparison, control plywood panels were prepared using phenol-formaldehyde (PF) adhesives at the same hot-pressing conditions.

## Results and Discussion

### Characterisation of NIPU adhesives

FTIR spectra confirmed the formation of urethane structures and the incorporation of microcrystalline cellulose (MCC) into the LT-NIPU adhesive (Figure 1a). The spectra show a broad –OH stretching band at 3369 $cm^{-1}$, which is less pronounced for MLT-NIPU, indicating reactions between β-hydroxyl groups and MCC. The peak at 2936 $cm^{-1}$ corresponding to the C-H stretching mode indicates the presence of methylene groups from modified tannin and lignin, and its intensity changes upon incorporation of MCC (Ding et al., 2016). In MLT-NIPU, the bands at 1606 and 1690 $cm^{-1}$ (aromatic C=C, C=O, and C=N vibrations) overlapped, indicating structural interactions (Krapp et al., 2006; Mazumder et al., 2025). The C–N band at 1355 $cm^{-1}$, confirming the formation of urethane, shifted to

1413 cm $^{-1}$ after the incorporation of MCC, indicating changes in the polyhydroxyurethane structures. The C–O band at 1059 cm$^{-1}$ is assigned to cellulose and urethane-type bonds, and its decreased intensity indicates the involvement of cellulose via hydroxyl linkages. The persistent band at 845 cm$^{-1}$ shows that aromatic structures of lignin are retained (Wang et al., 2026).

The crosslinking effects of MCC and the stepwise strategy on the bonding performance of plywood are shown in Figure 1b. The shear strength of the PF-based plywood is 1.65 MPa, while the shear strength of the LT-NIPU-based plywood is slightly lower (1.58 MPa). This slight decrease shows that LT-NIPU had a competitive bonding strength compared with the PF adhesive. A similar shear strength of about 1.62 MPa was obtained with a 5% MCC inclusion, indicating that the initial addition of MCC has very little effect on the adhesive strength. However, the shear strength increases with increasing MCC content, reaching about 1.74 (15%) and 1.89 (30%) MPa, respectively. The improvement suggests that the large number of hydroxyl groups in MCC can interact with the LT-NIPU network, forming more hydrogen bonds and thereby enhancing the cohesive strength and interfacial bonding of the adhesive. In general, MCC at 30% exhibits the highest shear strength, exceeding that of PF and LT-NIPU adhesives.

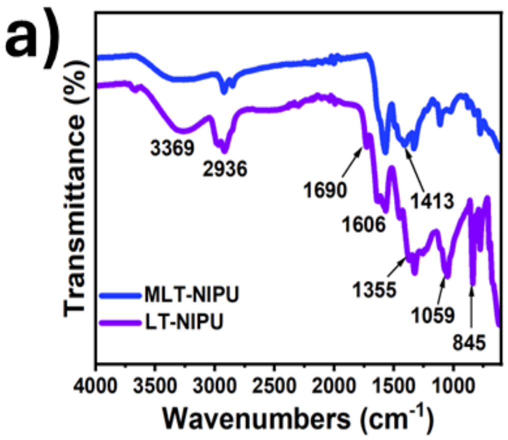


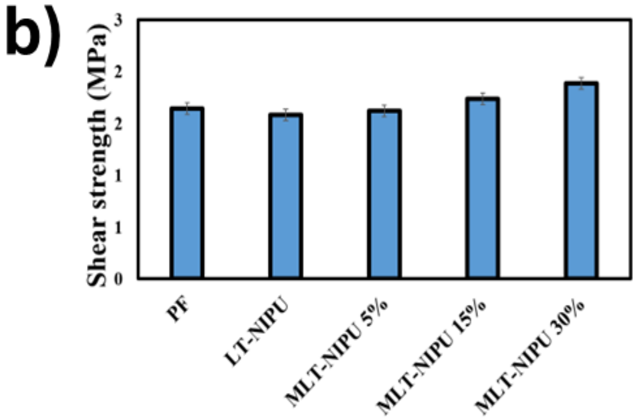


Figure 1. Characterisation of LT-NIPU and MLT-NIPU adhesives by FTIR spectra (1a), tensile shear strength of plywood bonded with NIPU adhesives compared with plywood bonded with phenol formaldehyde resin at the same hot-pressing conditions (1b)

## Conclusions

The stepwise modification strategy using various forest-based biopolymers successfully yielded NIPU adhesives with low hot-pressing temperature. The plywood panels bonded with NIPU adhesives showed comparable tensile shear strength under the same hot-pressing conditions to that of phenol formaldehyde adhesive. The findings offer insight into the design of forest polymer-based NIPU adhesives for wood bonding, achieving comparable pressing temperatures and product performance to formaldehyde-based adhesives.

**Reference**

Chen, X., Pizzi, A., Xi, X., Zhou, X., Fredon, E., and Gerardin, C. (2021). Soy Protein Isolate Non-Isocyanates Polyurethanes (NIPU) Wood Adhesives. *Journal of Renewable Materials* **9**, 1045--1057.

Ding, R., Wu, H., Thunga, M., Bowler, N., and Kessler, M. R. (2016). Processing and characterization of low-cost electrospun carbon fibers from organosolv lignin/polyacrylonitrile blends. *Carbon* **100**, 126-136.

Krapp, A., Bickelhaupt, F. M., and Frenking, G. (2006). Orbital Overlap and Chemical Bonding. *Chemistry – A European Journal* **12**, 9196-9216.

Mazumder, N., Zhuo, G.-Y., Jain, S., and Thomas, A. (2025). Fourier Transform Infrared (FTIR) Spectroscopy of Biomolecules. *In* "Recent Advances in Infrared Spectroscopy and Its Applications in Biotechnology" (N. Mazumder and G.-Y. Zhuo, eds.). IntechOpen, London.

Wang, S., Ren, X., Dai, J., Gan, T., Qi, J., Chen, L., Xie, J., and Pan, H. (2026). Comprehensive analysis of the molecular structure of lignin from microwave-assisted fractionation. *Industrial Crops and Products* **239**, 122529.

Wang, X., Wei, Z., Han, L., and Zhu, X. (2024). Preparation of natural adhesives with high-strength and low temperature fast-curing properties. *International Journal of Biological Macromolecules* **281**, 136507.

Zhang, P., Wang, Y., Wu, X., Cao, Y., Wang, J., Wang, Z., and Jin, C. (2025). Spider Silk-Inspired NIPU Adhesives with High Bonding Strength and Avoidance of Isocyanate Harm Derived from CO2 and Biomass. *ACS Sustainable Chemistry & Engineering* **13**, 15726-15737.

# SESSION 5: ENVIRONMENTAL PERFORMANCE

# pLCA Scenario Based Production Pathways of Mycelia-Wood Bio-Composite

**Maciej Biedacha[1], Lars Gunnar Furelid Tellnes[1], Anna-Lena Kjøniksen[1]**

[1]Department of Engineering, Østfold University of Applied Sciences, Norway
maciej.biedacha@hiof.no

Shortly about presenting author
https://www.hiof.no/hvo/english/people/aca/maciejbi/
https://norsus.no/en/ansatt/maciej-biedacha/

**Background**

Novel bio-based construction materials and phase-change materials (PCMs) have attracted increasing attention due to their potential to reduce operational energy demand and improve building sustainability, and the potential to enlarge anthropogenic carbon sinks (Livne et al., 2022, Hawkins et al., 2023). However, current studies mainly assess their environmental performance through conventional life cycle assessment (LCA) based on laboratory-scale data. This approach has important limitations and may overlook environmental impacts associated with full-scale production (Alaux et al., 2024, Sacchi et al., 2022). To address this gap, this study applies a prospective, ex-ante LCA framework to evaluate the environmental performance of a novel bio-based composite.

**Keywords:** Biobased-materials, prospective LCA, SIMPL.

**Experimental**

A Stepwise Approach for Scenario-Based Modelling in Prospective Life Cycle Assessment (SIMPL) (Langkau et al., 2023) was applied to develop and assess future scenarios representing industrial-scale production of the mycelia-wood bio-composite in 2031. The method was used to define prospective inventories and manufacturing technologies based on anticipated technological developments and process improvements. As part of the SIMPL framework, an expert panel was consulted to identify realistic assumptions regarding future production parameters.

Three scenarios were evaluated:

- Scenario 1 (Control): Baseline scenario based on current laboratory-scale production data.
- Scenario 2: Original production inventory with reduced material waste and improved process efficiency.
- Scenario 3: Enhanced scenario incorporating changes in heat generation technology, further improvements in production efficiency, and substantial reductions in manufacturing waste.

## Results and Discussion

The results of the scenarios are shown in Figure 1. The laboratory-scale scenario returned the highest environmental impacts among the assessed alternatives, despite demonstrating substantial biogenic carbon storage potential. The primary reason was the exceptionally high waste generation during the initial cultivation phase of mycelial growth. Waste rates associated with the bio-based growth medium, consisting primarily of agar and malt extract, ranged between 80 and 90%. These losses contributed to production-stage emissions. Electricity consumption also contributed considerably to the overall climate change impact. Scenarios 2 and 3 were developed to address the low efficiency and high waste rates characteristic of laboratory-scale production. Scenario 2 assumed a substantial reduction in organic substrate waste, resulting in a net-negative outcome for the Climate Change impact category. This was attributed to carbon sequestration within the composite and its constituent bio-based materials, which outweighed emissions generated during production. Scenario 3 incorporated additional improvements in process efficiency together with modifications to heat supply. Specifically, it was assumed that waste heat generated during wood fibre production could be recovered and utilised at several stages of mycelium composite manufacturing. These changes further reduced the environmental impacts of the system. However, because the carbon intensity of the Norwegian electricity mix is already relatively low, the additional climate benefits achieved through heat optimisation were moderate compared to the gains obtained through waste reduction.

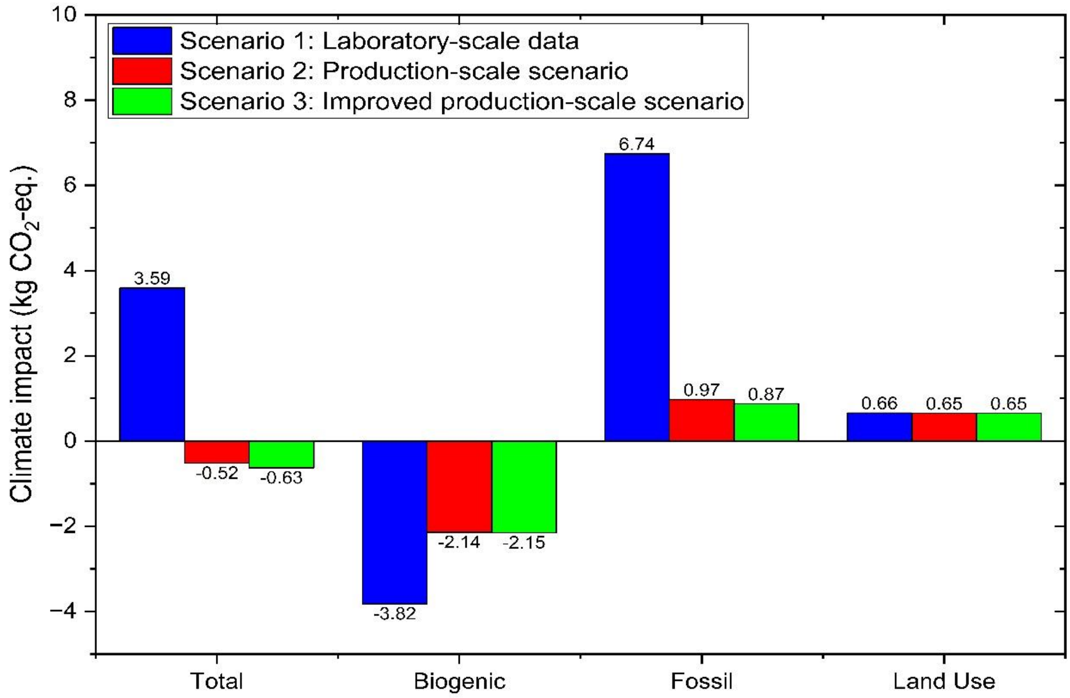


Figure 1. Results from prospective life cycle assessment (LCA) for potential production scenarios of wood fibre boards bonded with mycelium and phase change materials added. The results are presented cradle-to-gate (A1-A3) scope and climate change impact categories

## Conclusions

Overall, the results indicate that process efficiency and material yield represent the dominant environmental hotspots during technology development and that substantial environmental improvements can be achieved through successful scale-up and industrial integration.

**References**

Alaux, N., Vašatko, H., Maierhofer, D., Saade, M. R. M., Stavric, M. and Passer, A. (2024) Environmental potential of fungal insulation: A prospective life cycle assessment of mycelium-based composites. The International Journal of Life Cycle Assessment, 29, 255-272.

Hawkins, H.J., Cargill, R.I., van Nuland, M.E., Hagen, S.C., Field, K.J., Sheldrake, M., Soudzilovskaia, N.A. and Kiers E.T. (2023) Mycorrhizal mycelium as a global carbon pool. Current biology, 33, R560-R573.

Langkau, S., Steubing, B., Mutel, C., Ajie, M. P., Erdmann, L., Voglhuber-Slavinsky, A. and Janssen, M (2023) A stepwise approach for Scenario-based Inventory Modelling for Prospective LCA (SIMPL). The International Journal of Life Cycle Assessment, 28, 1169-1193.

Livne, A., Wosten, H. A., Pearlmutter, D. and Gal, E (2022) Fungal mycelium bio-composite acts as a CO2-sink building material with low embodied energy. ACS Sustainable Chemistry & Engineering, 10, 12099-12106.

Sacchi, R., Terlouw, T., Siala, K., Dirnaichner, A., Bauer, C., Cox, B., Mutel, C., Daioglou, V. and Lunderer, G. (2022) PRospective EnvironMental Impact asSEment (premise): A streamlined approach to producing databases for prospective life cycle assessment using integrated assessment models. Renewable and sustainable energy reviews, 160, 112311.

# Integrating Environmental Exposure and Timber Service Life Performance Modelling into Building Information Modelling Workflows

**Richard Acquah[1], Jakub Sandak[1]**

[1] InnoRenew CoE, UP IAM & UP FAMNIT, University of Primorska, Titov trg 4, 6000 Koper, Slovenia, richard.acquah@innorenew.eu

## Background

Timber façades degrade non-uniformly, driven by the local microclimate experienced by the material (Acquah et al., 2026). This is highly dependent on building geometry, orientation, and architectural detailing (Blocken & Carmeliet, 2004). While regional climate data and traditional dose-response models are well-established, they do not capture localized spatial variations across a single façade. Currently, there is a critical lack of integrated, design-stage tools that translate regional climate into spatially resolved "material climate" for both aesthetic and functional service life prediction. We propose a BIM-integrated framework that bridges this gap by using geometry-driven ray-tracing to map weathering dose and predict decay risk directly within Autodesk Revit.

**Keywords:** BIM, Service Life, Weathering, Timber, Material Climate

## Experimental

The framework is implemented as a C# plugin in Autodesk Revit, extracting geometry, orientation, and material properties directly from the BIM model. To resolve localized exposure, façade surfaces are discretized into computational cells, enabling cell-level analysis rather than whole-building averages.

For functional performance (decay risk), service life prediction relies on comparing material resistance against environmental exposure, based on established dose-response principles (Brischke & Rapp, 2008; Meyer-Veltrup et al., 2018; Acquah et al., 2025). Service life is expressed as the ratio of the material resistance dose to the annual exposure dose (time until the onset of decay). For above-ground elements, the exposure dose is calculated by applying five location-specific multipliers to a reference dose (wind-driven rain, local climate, sheltering, ground proximity, and design detailing); in-ground elements use a fixed dose with all multipliers set to unity.

For aesthetic performance, the framework employs a BIM-based geometry-driven material climate mapping approach (Acquah et al., 2026). It computes localized solar radiation via ray-casting, derives surface temperature from an energy balance, calculates local relative humidity from vapor pressure, and adjusts wind speed using a power-law profile. These five localized variables and their ten interactions form a cumulative weathering dose, weighted by optimized coefficients from a calibrated dose-response model (Sandak et al., 2026b). This dose explicitly maps to lab-measured CIE L* (lightness) through a universal weathering curve, predicting progressive greying. Both localized doses and exposure factors are embedded as BIM parameters and visualized as color-coded maps, providing direct inputs for service life estimation and weathering prediction.

## Results and Discussion

The framework was tested on a proof-of-concept building featuring a balcony, a recessed window, and an extended roof overhang to demonstrate its applicability. Results show significant spatial heterogeneity in exposure driven entirely by geometry (Fig. 1). The overhang and balcony cast a distinct shading zone, where annual solar radiation drops from ~1,233 kWh/m² on exposed regions to ~470 kWh/m² in protected zones, resulting in a surface temperature range of 19.3°C to 16.6°C.
Cumulative rainfall exhibits the most extreme geometry-driven contrast, varying from 287.5 l/m² on exposed surfaces to nearly dry (4.5 l/m²) beneath the balcony. Conversely, the sheltered recess acts as a "moisture trap," exhibiting the highest local relative humidity (up to 66%) due to lower surface temperatures and reduced drying potential. Wind speed ranges from 1.9 to 2.6 m/s, varying primarily with height. These maps provide the necessary cell-level inputs to resolve both functional (decay risk) and aesthetic (colour change) wood performance directly within the BIM environment.

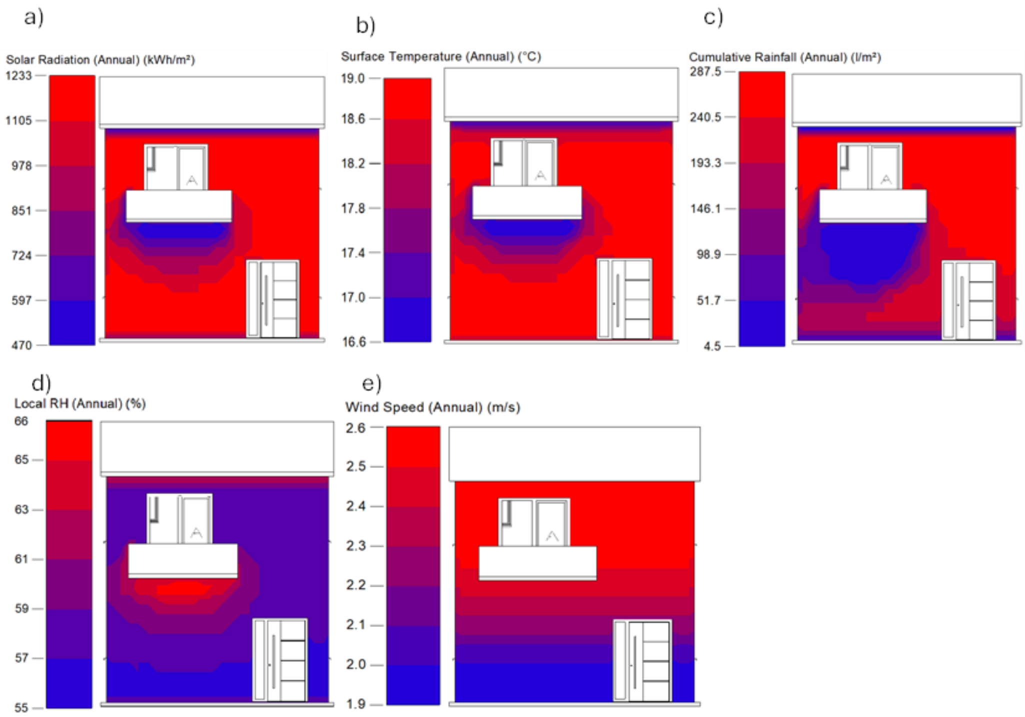


Figure 1. Spatially resolved annual material climate maps showing (a) solar radiation, (b) surface temperature, (c) cumulative rainfall, (d) local relative humidity, and (e) wind speed across the timber façade with balcony and roof overhang

## Conclusions

This study successfully demonstrates a BIM-integrated framework for mapping geometry-driven material climate on timber façades. Applied to a proof-of-concept building, the framework captured how roof overhangs and balconies create distinct shading zones and moisture traps, leading to significant spatial variations in solar radiation, rainfall, and local humidity. These cell-level maps provide the essential inputs required to resolve both aesthetic colour change and functional decay risk. By embedding these localized exposure maps directly within BIM, the framework enables proactive design evaluation and maintenance planning for timber structures.

**References**

Acquah R, Hazir E, Sandak J (2026) Geometry-Driven Material Climate Mapping for Weather Dose Assessment of Wood Facade Colour Change. Manuscript under review.

Acquah R, Niklewski J, Sandak A, Sandak J (2025) BIM-based framework for estimating service life duration of wood construction elements under environmental exposure. Building and Environment 287: 113890. https://doi.org/10.1016/j.buildenv.2025.113890

Acquah R, Niklewski J, Sandak J (2026) BIM-based wind-driven rain modelling using ISO 15927-3 and geometry-based exposure. Building and Environment 295: 114447. https://doi.org/10.1016/j.buildenv.2026.114447

Blocken B, Carmeliet J (2004) A review of wind-driven rain research in building science. Journal of Wind Engineering and Industrial Aerodynamics 92(13): 1079-1130. https://doi.org/10.1016/j.jweia.2004.06.003

Brischke C, Rapp AO (2008) Dose-response relationships between wood moisture content, wood temperature and fungal decay determined for 23 European field test sites. Wood Science and Technology 42(6): 507-518. https://doi.org/10.1007/s00226-008-0191-8

Meyer-Veltrup L, Brischke C, Niklewski J, Frühwald Hansson E (2018) Design and performance prediction of timber bridges based on a factorization approach. Wood Material Science & Engineering 13(3): 167-173. https://doi.org/10.1080/17480272.2018.1424729

Sandak J, Hazir E, Acquah R (2026) Towards a Dose-Response Model for Weather-Induced Colour Change in Wood - Part 2: Definition of the Weather Dose, Universal Curve of Weathering and Response Function. Manuscript under review.

# Enhancing Circularity in End-of-Life of Modular Cross-Laminated Timber Building: A Carbon Footprint Analysis

**Felix Quarcoo**[1], **Ambrose Dodoo**[2], **Jonn Are Myhren**[3], **Eva Binder**[4]

[1] Department of Building Technology, Linnaeus University, 351 95 Växjö, Sweden, felix.quarcoo@lnu.se
[2,4] Department of Building Technology, Linnaeus University, 351 95 Växjö, Sweden, ambrose.dodoo@lnu.se, eva.binder@lnu.se, [3] Building Technology, Dalarna University, 791 88 Falun, Sweden and Sustainable Energy Research Centre, Dalarna University, 791 88 Falun, Sweden, jam@du.se

## Background

Modular construction has garnered attention due to its potential to support climate change mitigation and circular economy (CE) objectives (Sajid et al. 2024). End-of-life (EoL) strategies such as deconstruction, reuse, recycling, and cascading use of materials extend material service life, reduce reliance on virgin resources, and minimize construction and demolition waste (Antunes et al. 2024). Life cycle assessment (LCA) has been used to analyse the environmental benefits of cross-laminated timber (CLT) multi-storey buildings (Younis and Dodoo 2022) and modular construction (Kamali, Hewage, and Sadiq 2019), but there is a paucity of comparative studies of EoL circularity solutions for modular CLT multi-storey structures. Limited material recovery and reuse in building design, construction, and management constrain the circularity of building components (Vilčeková et al. 2023). However, the environmental benefits of reusing and recycling modular building components across multiple life cycles remain uncertain (Yang et al. 2024). This study evaluates circularity strategies for modular CLT building components focusing on reuse, recycling and cascading use EoL scenarios.

**Keywords:** carbon footprint, circular economy, cross-laminated timber, end-of-life, modular multi-storey construction

## Method

This study applies a process-based life cycle approach to quantify the climate impact ($kgCO_2e$) of EoL scenarios for modular CLT multi-storey building. The system boundary of the system boundary of the analysis was defined to include the product stage (A1–A3) and Module D, encompassing the post-use material benefits and burdens. The functional unit study is 1m$^2$ of floor area over 50 years. Global warming potential (GWP-100-year) is assessed for the different scenarios including biogenic carbon and greenhouse gases emissions from fossil fuels and cement process reactions.

### Case Study Building

The case study is a modular CLT residential building in Stockholm County of Sweden. Table 1 lists its key characteristics It consists of 41 discrete CLT volumetric units, prefabricated with interior fixtures, plumbing, electrical and heating services for the residential units.

Table. 1 Key characteristics of the modular CLT building

| Type | Description |
|---|---|
| Building Use | Residential |
| Construction Type | Modular Volumetric Unit |
| Mass Timber | CLT (walls and floors) |
| Stories | 3-storey |
| Total Floor Area | 1440 $m^2$ |

**Life Cycle Inventory**

The building material inventory is based on design and specification data from the building's contractor. Material-related emissions for the product stage are modelled using the Ecoinvent 3.5 cut-off database, supplemented with Swedish market data where necessary to improve data reliability and representativeness (Mendoza Beltran, Cox et al. 2020). Module D accounts for potential benefits and burden from reuse, recycling, cascading, and energy recovery. A 90% recovery rate is assumed for all predominant materials in the building.

**Results and Discussion**

Table 2 presents the product-stage GWP of the building as a reference for evaluating the different EoL strategies and scenarios. The preliminary results indicate that EoL strategies such as reuse, recycling, cascading use, and energy recovery can influence the overall climate impact of the building. Cascading use of CLT combined with recycling of other materials provides the biggest potential climate benefits. Also, combining reuse of CLT with recycling of other building materials provides significant climate benefits. Still, further analysis is needed to refine the EoL calculations and assumptions to make robust quantitative comparison between the different scenarios.

Table 2. Product-stage GWP of the modular CLT building

| Descriptions | GWP (kg$CO_2$ eq/$m^2$) |
|---|---|
| Product Stage (A1-A3) | 237.34 |
| Scenario 1 (Baseline) | - 48.16 |
| Scenario 2 (Reuse CLT + Other materials) | - 132.01 |
| Scenario 3 (Recycling CLT + Other materials) | - 45.93 |
| Scenario 4 (Cascading CLT + Other materials) | - 141.40 |
| Scenario 5 (Reuse CLT + Other materials) | - 150.37 |
| Scenario 6 (Recycling CLT + Other materials) | - 51.92 |
| Scenario 7 (Cascading CLT + Other materials) | - 163.45 |

**Conclusions**

In this study, the GWP impact of different EoL options (energy recovery, reuse, recycling, and cascading) for a modular CLT multi-storey building is explored across different post-deconstruction scenarios. The preliminary results indicate that cascading use of CLT combined with recycling of other materials yields the greatest potential climate benefits, with additional gains from steel recycling. Integrating EoL considerations into production loops reduces resource consumption, waste, and emissions. Incorporating circular design principles at the early design stage, including design for adaptability and flexibility, can extend building's lifespan and further facilitate component reuse.

**References**

Antunes, A., et al. (2024). "Reducing the environmental impact of the end-of-life of buildings depending on interrelated demolition strategies, transport distances and disposal scenarios." JOURNAL OF BUILDING ENGINEERING 82: 108197.

Kamali, M., et al. (2019). "Conventional versus modular construction methods: A comparative cradle-to-gate LCA for residential buildings." Energy and buildings 204: 109479.

Mendoza Beltran, A., et al. (2020). "When the background matters: using scenarios from integrated assessment models in prospective life cycle assessment." JOURNAL OF INDUSTRIAL ECOLOGY 24(1): 64–79.

Sajid, Z. W., et al. (2024). "Climate change mitigation through modular construction." Smart Cities 7(1): 566–596.

Vilčeková, S., et al. (2023). "End-of-Life Stage Analysis of Building Materials in Relation to Circular Construction." Engineering Proceedings 57(1): 43.

Yang, Y., et al. (2024). "Towards a sustainable circular economy: Understanding the environmental credits and loads of reusing modular building components from a multi-use cycle perspective." Sustainable Production and Consumption 46: 543–558.

Younis, A. and A. Dodoo (2022). "Cross-laminated timber for building construction: A life-cycle-assessment overview." JOURNAL OF BUILDING ENGINEERING 52: 104482.

# Service Lives, Design Lives and Potential Lifespans: Data Sources and Strategies for Carbon Storage Calculations

**Morwenna Spear**[1]

[1] The BioComposites Centre, Bangor University, Bangor, United Kingdom, m.j.spear@bangor.ac.uk

## Background

Lifespan data is needed to increase accuracy in biogenic stored carbon calculations for wood products. Timber in the built environment, and wood in products all around us, can act as a store for biogenic carbon which was sequestered in wood during tree growth through photosynthesis in the forest (Hill 2019, Spear 2024). The calculations used to quantify this storage vary. In all cases it is recognised that the significance of carbon storage is sensitive to the time frame and supporting data is needed (Braun et al. 2016, Eberhardt et al. 2024, Spear and Hart 2025).
Lifespan for wood products is a complex topic. Service life is a result of multiple influences – from the inherent durability of the timber to the protection given by treatments , but also heavily influenced by in-use conditions. Such aspects are included in the ISO 15686 factor method. There is also a substantial societal and consumer psychological influence on whether wood products are removed or replaced 'early' or 'late' (Alfredsen et al. 2025).
Modelling the population residence times in the harvested wood products pool can be done in several ways. While the Tier 1 approach (using first order decay and half lives to amalgamate all types of material within the semifinished product categories 'sawnwood', 'wood based panels', and 'paper and paperboard') remains popular, Tier 2 and 3 options are becoming possible as more data emerges (IPCC 2014). Lifespans of individual products can be modelled (Spear 2023). Data often confirms that a sigmoidal function (such as normal distribution, gamma distribution or chi squared distribution) fits buildings or products (Spear and Hart 2025). However such models require input data to enable curve fitting.
Collating and reviewing lifespan and service life data from multiple studies and sources has shown that observational data from surveys or experiments are seldom well aligned with nominal service life, or design life, for buildings or components. The terms have different meanings. Attempts to combine reference values with factors for environmental conditions exist but no definitive set of factor values exist for reference service life calculations.

**Keywords:** biogenic carbon storage, HWP pool, lifespan, modelling, service life.

## Results and Discussion

If the average lifespan for a wood product can be estimated (based on survey data, analysis of wood waste or other investigations) a population distribution function can be assigned. In the example below normal distributions and standard error values define the curve form (Figure 1a). Adjustment to allow for skewness and kurtosis of populations could be done, or more complex curves to achieve better fit to the data. The corresponding residence profiles are indicated in Figure 1b. Quantity data and curve functions for a multitude of products allows a cumulative residence time function to be built up for the market (not shown).

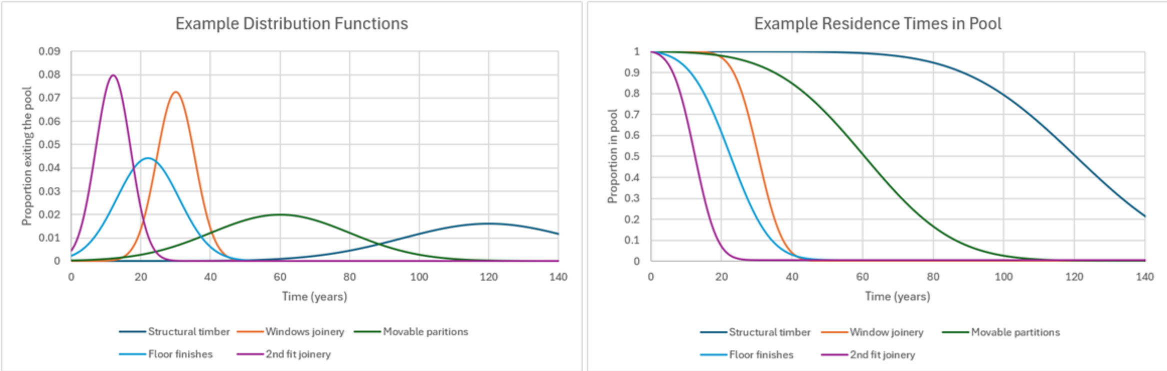


Figure 1. Example lifespan functions and residence time within the pool for a range of wood products

The question remains, where can researchers obtain this data? Additionally, if lifespan data or service life values are available, is this data suitable for building such models? Table 1 shows some of the groups who appear to consider or report lifespan or service life.

Table 1. Who keeps data and why

| Data holder | Purpose | Service life | Life-span | Replac. interval | Notes |
|---|---|---|---|---|---|
| Building surveyors | Estimating maintenance intervals | ✓ | | ✓ | Values tend to indicate an acceptable minimum |
| LCA professionals | Evaluating replacements in use phase | | | ✓ | High uncertainty (Warrier et al. 2024) |
| Wood preservation researchers | Assigning Use Class or expected service life | ✓ | ✓ | | Field tests most common for Use Class 3, 4, 5 (little data on other products) |
| Sales departments of product manufacturers | Indicating acceptable minimum lifespan to customers | ✓ | | | Complex mix of test data and customer behaviour estimates |
| Insurance bodies | Estimating risk of replacement and payout | | | ✓* | Underestimate true service life so only early failures incur financial payout |

Very few of the values in Table 1 offer a ‘mean’ average value. The majority are designed to meet a specific need or function in their own industry. Thus use of this data to give an ‘average’ within a model can lead to complications.

## Conclusions

Service life data for modelling carbon storage remains scarce. Awareness of the origins of bias in the data sources which do exist is needed, to avoid importing errors when using data from other disciplines. This will help prevent underestimating the storage effect.

**References**

Alfredsen G., Gustavsen G.W., Ross L., Niklewski J., van Niekerk P.B., and Brischke C. (2025) Aesthetic limit states and cultural variation in wooden cladding acceptance. In: Proceedings of the 21st Annual Meeting of the Northern European Network for Wood Science and Engineering (WSE), Växjö, Sweden, October 8-9, 2025.

Braun M., Winner G., Schwarzbauer P. and Stern T. (2016) Apparent Half-life Dynamics of Harvested Wood Products (HWPs) in Austria: Development and analysis of weighted time-series for 2002 to 2011. Forest Policy and Economics 63: 28-34.

Eberhardt L.C.M., Kuittenen M., Hakkinen T., Moinel C., Nibel S. and Birgisdottir H. (2024) Carbon handprint – a review of potential climate benefits of buildings. Building Research and Information 52(6): 708-723.

Hill C.A.S. (2019) The environmental consequences concerning the use of timber in the built environment. Frontiers in the Built Environment 5: 129.

International Standards Organisation (2011) ISO 15686-1:2011 Buildings and constructed assets – service life planning Part 1: General principles and framework.

IPCC (2014) 2013 revised supplementary methods and good practice guidance arising from the Kyoto protocol. Hiraishi T., Krug T., Tanabe K., Srivastava N., Baasansuren J., Fukuda M. and Troxler T.G. (eds). Published: IPCC, Switzerland.

Spear M.J. (2023) The benefits of circular economy approaches in the wood panels industry on the magnitude of harvested wood product carbon storage. In: Proceedings of the International Panel Products Symposium 2023, Llandudno, Wales, UK, October 3-4 2023: 23-40.

Spear M.J. (2024) How long is 'long enough'? Carbon storage and wood products. In: Ridley-Ellis D. and Cramer M. (eds) Proceedings of the 20th Annual Meeting of the Northern European Network for Wood Science and Engineering (WSE), Edinburgh, UK, October 23-24, 2024: 4pp.

Spear M.J. and Hart J. (2025) Modelling wood product service lives and residence times for biogenic carbon in harvested wood products: A review of half-lives, averages and population distributions. *Forests* 16: 1162

Warrier G.A., Palaniappan S. and Habert G. (2024) Classification of sources of uncertainty in building LCA. Energy and Buildings 305: 113892.

# Valuation of Carbon Storage in Public Procurement

**Lars Gunnar Furelid Tellnes[1], Maciej Biedacha[1], Anna-Lena Kjøniksen[1]**

[1]Østfold University of Applied Sciences, Norway, lars.g.tellnes@hiof.no, maciej.biedacha@hiof.no, anna.l.kjoniksen@hiof.no.

## Background

There are currently an increased used of life cycle assessment (LCA) in public procurement to select products with lower impact on climate and environment. Often this does not include biogenic carbon storage. Hence, the aim of this work is to suggest a method to include biogenic carbon storage with valuation of climate impacts in life cycle costing (LCC). Valuation is a method for evaluation of impacts in LCA that can be used for weighting of different impacts such has climate change, eutrophication and land use. However, valuation can also be combined with the market prices of the product to show the true cost of the product (Tellnes et al., 2026). This has been applied as a method in public procurement to select products that are both cost and climate effective. For instance, procurement of pavement in Norway has a guideline that recommends a carbon price of 7 NOK per kg $CO_2$-equivalent (DFØ, 2026). Then the sum of purchasing price and climate cost is used to select the best offer. However, this guide does not specify deprecation of future costs nor biogenic carbon. Hence, the objectives are:

1. Propose an approach to include evaluation of climate impacts that can be used for total greenhouse gas emissions and deprecation of future cost
2. To calculate an example of a commercial product with the proposed method

**Keywords:** life cycle assessment (LCA), green public procurement, valuation**.**

## Experimental

The LCC of the greenhouse gas emissions was estimated for an uncoated medium density fibreboard. The greenhouse gas emissions were based on an environmental product declaration (EPD) (Huntonit, 2025). The LCC was calculated with carbon prices from a Norwegian Green Public Procurement Guideline (NO GPP) (DFØ, 2026) and European emission trading scheme (EU ETS) (Trading Economics, 2026). First as a static estimate, then as dynamic with 4 % depreciation rate and 60-year service life.

## Results and Discussion

The results of the net present value (NPV) of greenhouse gas emissions and uptake of the fibreboard are shown in Figure 1.

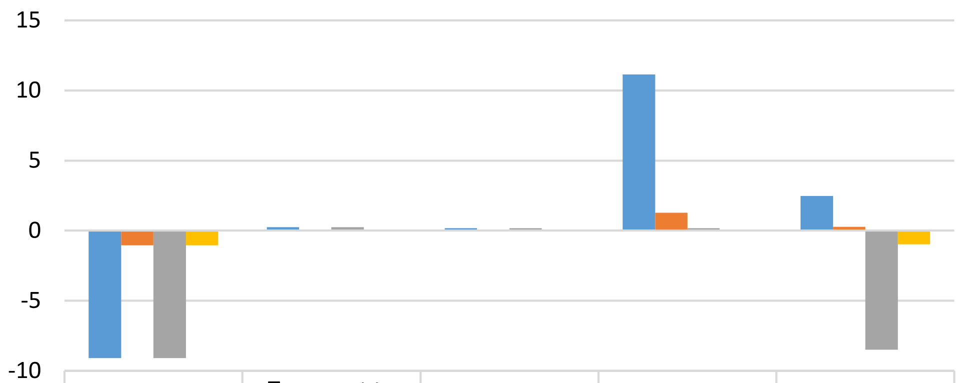


| | Cradle-to-gate | Transport to building site | Installation | End-of-life | Total |
|---|---|---|---|---|---|
| Static NPV NO GPP EUR | -9,1 | 0,25 | 0,18 | 11,14 | 2,47 |
| Static NPV EU ETS EUR | -1,04 | 0,03 | 0,02 | 1,27 | 0,28 |
| Dynamic NPV NO GPP EUR | -9,1 | 0,25 | 0,18 | 0,18 | -8,49 |
| Dynamic NPV EU ETS EUR | -1,04 | 0,03 | 0,02 | 0,02 | -0,97 |

Figure 1. Net present value of the valuation (NPV) of greenhouse gas emissions and uptake from a fibreboard over the life cycle. The results are shown as static first, then dynamic with 4 % depreciation and 60-year service life. Value of greenhouse gases are from Norwegian Green Public Procurement (NO GPP) and European Emission Trading Scheme (EU ETS)

The results show that the total life cycle NPV increases with higher carbon price under the static approach. However, under dynamic approach, the total NPV are reduced with higher carbon price. This is because the future prices in 60 years with 4 % depreciation is considerably lower than today. Hence, this makes a considerable higher negative cost initially from carbon uptake in fibreboards. While the net emissions are zero over the life cycle, the future emissions gas is much lower than the present. The results are quite dependent on the carbon price applied. The prices in NO GPP were 0.7 EUR per kg $CO_2$-eq and EU ETS 0.08 EUR per kg $CO_2$-eq. For this study these prices were selected as upper and lower estimates of carbon price. However, from an evaluation of green public procurement in Oslo Municipality a carbon price between 1 and 3 EUR per kg $CO_2$-eq. was recommended depending on the material (Oslo Municipality, 2025). Hence, future works should focus on finding the right carbon prices.

## Conclusions

The use of dynamic net present value of greenhouse gas emissions and uptake has great impact on the environmental evaluation of the fibreboard. If used in green public procurement, this can be a practical approach to include biogenic carbon in decision making.

**References**

DFØ. (2026). *Asfalt med lavt klimaavtrykk [In Norwegian]*. The Norwegian Agency for Public and Financial Management (DFØ). Retrieved 27.08.2026 from https://kriterieveiviseren.anskaffelser.no/valg/anlegg?language=nb#a19700bf-6fce-4331-8867-a7208c96eb80

Huntonit. (2025). *Environmental product declaration - Huntonit building boards without surface treatment*. https://huntonit.com/brochure-documents-and-declarations/epd-environmental-declaration/

Oslo Municipality. (2025). *CO2-vekting og CO2-tak i offentlige anskaffelser [In Norwegian]*. https://www.miljodirektoratet.no/ansvarsomrader/klima/for-myndigheter/kutte-utslipp-av-klimagasser/klimasats/2023/co2-vekting-og-co2-tak-i-offentlige-anskaffelser/#

Tellnes, L. G. F., Svanes, E., Pamies, R., & Kjøniksen, A.-L. (2026). Environmental sustainability of protein rich food from tunicates. Case study on Ciona aquaculture in Europe. *Future foods : a dedicated journal for sustainability in food science*, *14*, 101133. https://doi.org/10.1016/j.fufo.2026.101133

Trading Economics. (2026). *EU Carbon Permits*. Retrieved 27.08.2026 from https://tradingeconomics.com/commodity/carbon

# SESSION 6: RECOVERY AND CIRCULARITY

# Artificial Intelligence Applications for Sustainable Wood Waste Management in Developing Urban Environments: Challenges, Opportunities and Future Directions

**Abdullah Jan Frogh**[1]

[1]Veer Narmad South Gujarat University, Surat, India, abdullahfrogh.dmgphd22@vnsgu.ac.in

## Background

Wood waste from construction, demolition, furniture manufacturing, packaging, and household activities is increasing in developing urban environments. Improper disposal contributes to landfill accumulation, pollution, greenhouse gas emissions, and resource loss. Sustainable wood waste management is therefore important for circular bioeconomy and sustainable urban development (Akinade et al. 2015; Sharma et al. 2021).
Wood recycling, biomass utilization, and resource recovery can reduce environmental impacts (Kumar and Samadder 2017). Meanwhile, Artificial Intelligence (AI), Internet of Things (IoT), machine learning, and predictive analytics offer opportunities to improve waste management (Fang et al. 2023; Bibri et al. 2024; Chin et al. 2026). However, limited research has examined their specific application to wood waste collection, segregation, recycling, and resource optimization in developing cities.
This paper addresses this gap by examining the potential contribution of AI-driven technologies to improve wood waste recycling efficiency, reduce environmental impacts, and support circular economy objectives in developing urban environments.

**Keywords:** Artificial Intelligence, Wood Waste, Recycling, Circular Economy, Sustainability.

## Experimental

A mixed-method design combined secondary literature, government reports, and sustainability publications with primary questionnaires and interviews involving environmental researchers, waste management practitioners, recycling professionals, and academic experts. Descriptive and comparative analysis focused on smart monitoring, automated sorting, machine-learning classification, and predictive analytics for waste-generation forecasting.

### AI Applications in Wood Waste Management

AI technologies can improve wood waste management efficiency. IoT-enabled monitoring can track waste generation and optimize collection schedules, while machine learning can improve identification and sorting of wood fractions (Pardini et al. 2019). Automated sorting can support recycling, reuse, and biomass recovery, while predictive analytics can assist in planning collection and recycling infrastructure.
Key barriers include high implementation costs, limited digital infrastructure, insufficient technical expertise, and inadequate policy support. Informal recycling activities may further complicate technology integration in developing urban regions (Ferronato and Torretta 2019; Kaza et al. 2018).

## Results and Discussion

The analysis indicates that AI technologies have considerable potential to improve the sustainability and operational efficiency of wood waste management systems. Smart monitoring and automated sorting can improve waste identification and separation, enhance material recovery, reduce contamination, and support more efficient recycling. Machine-learning-based classification can distinguish recyclable, reusable, and energy-recoverable fractions, while predictive analytics can support waste-generation forecasting and infrastructure planning.
The findings further indicate that AI-supported decision-making can improve resource allocation, collection scheduling, and operational planning. However, successful adoption requires collaboration among government agencies, recycling industries, technology providers, and academic institutions. Investment in digital infrastructure, workforce training, supportive policies, and practical pilot projects will be essential for scalable and economically viable implementation.

## Conclusions

Artificial Intelligence represents a promising approach for advancing sustainable wood waste management in developing urban environments. AI-supported monitoring, sorting, classification, and predictive tools can improve collection, recycling efficiency, resource recovery, and operational decision-making while supporting circular bioeconomy objectives. Nevertheless, financial, technical, infrastructure, and policy barriers must be addressed through coordinated stakeholder action, digital infrastructure investment, workforce development, and practical pilot projects. Future research should prioritize cost-effectiveness assessments and quantitative evaluation of AI-driven technologies within urban wood waste recycling networks.

**References**

Akinade OO, Oyedele LO, Bilal M, Ajayi SO, Owolabi HA, Alaka HA, Bello SA (2015) Waste minimisation through deconstruction: A BIM based Deconstructability Assessment Score (BIM-DAS). Resources, Conservation and Recycling 105(A): 167-176.

Arthur MP, Shoba S, Pandey A (2024) A survey of smart dustbin systems using the IoT and deep learning. Artificial Intelligence Review 57: 56.

Bibri SE, Krogstie J, Kaboli A, Alahi A (2024) Smarter eco-cities and their leading-edge artificial intelligence of things solutions for environmental sustainability: A comprehensive systematic review. Environmental Science and Ecotechnology 19: 100330.

Chin T, Fan Y, Lin C-L, Lin Y-C, Liao K-T (2026) Artificial intelligence-related technologies for municipal solid waste management: A review and new insights from smart cities. Sustainable Cities and Society 147: 107530.

Fang B, Yu J, Chen Z, Osman AI, Farghali M, Ihara I, Hamza EH, Rooney DW, Yap PS (2023) Artificial intelligence for waste management in smart cities: A review. Environmental Chemistry Letters 21: 1959-1989.

Ferronato N, Torretta V (2019) Waste mismanagement in developing countries: A review of global issues. International Journal of Environmental Research and Public Health 16(6): 1060.

Hussain I, Elomri A, Kerbache L, Omri AE (2024) Smart city solutions: Comparative analysis of waste management models in IoT-enabled environments using multiagent simulation. Sustainable Cities and Society 103: 105247.

Kaza S, Yao L, Bhada-Tata P, Van Woerden F (2018) What a Waste 2.0: A Global Snapshot of Solid Waste Management to 2050. World Bank, Washington DC.

Kumar A, Samadder SR (2017) A review on technological options of waste-to-energy for effective management of municipal solid waste. Waste Management 69: 407-422.

Pardini K, Rodrigues JJPC, Kozlov SA, Kumar N, Furtado V (2019) IoT-based solid waste management solutions: A survey. Journal of Sensor and Actuator Networks 8(1): 5.

Sharma HB, Vanapalli KR, Samal B, Cheela VR, Dubey BK, Bhattacharya J (2021) Circular economy approach in solid waste management system to achieve UN-SDGs: Solutions for post-COVID recovery. Science of the Total Environment 800: 149605.

# Steam Explosion as an Integrated Process for Circular Recycling of Post-Consumer Particleboards

**Coline Giustiniani[1], Nicolas Brosse[1], Arnaud Besserer[1]**

[1]LERMaB, University of Lorraine, France,
coline.giustiniani@univ-lorraine.fr, nicolas.brosse@univ-lorraine.fr, arnaud.besserer@univ-lorraine.fr

## Background

Particleboards represented the predominant processed wood fraction in the investigated post-consumer wood waste stream. Their recycling potential is limited by the presence of contaminants, particularly adhesives and surface coatings. Current recycling strategies often lead to low-value applications. Steam explosion has previously shown promising results for UF-resin removal from MDF and the recovery of cleaner wood fibres (Troilo et al., 2023). However, decontamination does not necessarily eliminate contaminants from the overall process. Formaldehyde released from MDF can be transferred to an aqueous phase, generating a liquid effluent that requires further treatment (Zimmer and Bachmann, 2023). The fate of contaminants in the different streams generated during wood decontamination must therefore also be considered.
This study investigates an integrated thermochemical-biological process for post-consumer particleboards. Steam explosion is used to simultaneously fragment and decontaminate wood particles. The resulting aqueous effluent is subsequently treated by fungal bioremediation. The aim is to address both streams generated by the process and promote the circular recovery of post-consumer wood.
This work was conducted within the framework of the Horizon Europe Wood2Wood project.

**Keywords:** contaminated wood; steam explosion; formaldehyde; bioremediation.

## Experimental

### Material

Post-consumer wood was sorted into BR1 and BR2 categories according to the French waste wood classification framework (FCBA, 2022).

### Methods

Post-consumer particleboards were treated by steam explosion (SE) at 12 bars for 10 min. Urea-Formaldehyde resin (UF) distribution before and after treatment was assessed by fibre staining according to Grigsby et al. (2005). Formaldehyde ($CH_2O$) in the aqueous effluents was derivatized with 2,4-dinitrophenylhydrazine (2,4-DNPH) and quantified by HPTLC. The contaminated effluents were subsequently treated by optimized submerged fermentation with *Trichoderma sp*.

## Results and Discussion

SE generated two complementary streams (Figure 1): a fragmented solid fraction and an aqueous effluent.

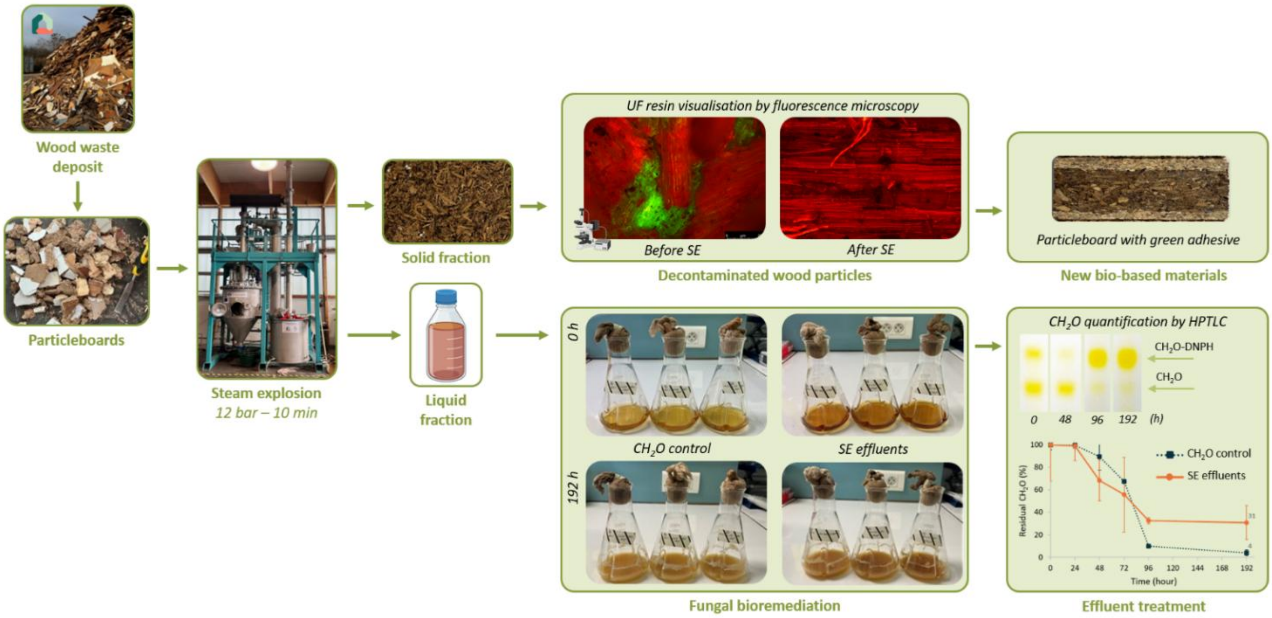


Figure 1. Schematic overview of the integrated process developed for the circular recycling of post-consumer particleboards

The melamine coating was completely removed during the process. Fibre staining showed no detectable UF-resin clusters at the particle surface under the investigated SE conditions, although residual resin could remain within some wood fibres. The recovered particles were subsequently reused for the production of new bio-based materials, including no-emission particleboards.

The aqueous effluent contained approximately 200-300 mg/L of formaldehyde, quantified by HPTLC after 2,4-DNPH derivatisation. Additional compounds were also detected under complementary HPTLC conditions. A *Trichoderma sp.* strain was able to grow in SE effluent and remove up to 95% of formaldehyde in the control solution and 70% in medium containing 50% SE effluent. The residual formaldehyde plateau observed specifically in SE effluent suggests occurrence of inhibitory compounds that may limit fungal detoxification (Figure 1). Further investigation is therefore required to optimize the biological treatment. The fungus growth was shown to be boosted by $CH_2O$ addition in the culture medium, suggesting the metabolization of $CH_2O$ by the fungus as a primary carbon source for its primary metabolism. Ecotoxicity investigations of the biologically treated effluents is under investigation but no toxicity was found on yeast (*Saccharomyces cerevisiae*).

Together, these results demonstrate that both streams generated during steam explosion can be further valorised rather than considered as secondary waste.

## Conclusions

Steam explosion efficiently generated two complementary valorisation streams from post-consumer particleboards. The solid fraction showed effective decontamination and potential for reuse in new bio-based materials. Fungal treatment markedly reduced formaldehyde concentrations in the aqueous effluent, demonstrating the potential of this integrated circular recycling approach. Future work will focus on process scale-up and further optimisation of effluent detoxification.

## References

FCBA, Groupe de travail Plan Déchets du CSF Bois (2022) Référentiel de classification des déchets bois [Waste wood classification framework] – Version 05/2022. 13 pages.

Grigsby WJ, Thumm A, Kamke FA (2005) Determination of resin distribution and coverage in MDF by fiber staining. Wood and Fiber Science 37: 258-269.

Troilo S, Besserer A, Rose C, Saker S, Soufflet L, Brosse N (2023) Urea-Formaldehyde Resin Removal in Medium-Density Fiberboards by Steam Explosion: Developing Nondestructive Analytical Tools. ACS Sustainable Chemistry & Engineering 11: 3603-3610.

Zimmer A, Bachmann SAL (2023) Challenges for recycling medium-density fiberboard (MDF). Results in Engineering 19: 101277.

*This work is part of Wood2Wood Horizon Europe project. Wood2Wood is funded by the European Union (Grant agreement ID: 101138789). Views and opinions expressed are, however, those of the author(s) only and do not necessarily reflect those of the European Union or HADEA. Neither the European Union nor the granting authority can be held responsible for them.*

# Ultrasonic Tomography as Assessment Tool for Reclaimed Timber

**Francisco Tienda Resendez[1], Alar Just[2]**

[1]Tallinn University of Technology, Estonia,
francisco.tienda@taltech.ee, [2]alar.just@taltech.ee

## Background

Circular construction increasingly relies on the structural reuse of timber to reduce embodied carbon and minimise demand for virgin raw materials. Confident reuse requires reliable regrading; however, internal defects such as cracks, voids, and decay remain invisible to visual inspection, leaving the assessment of load-bearing capacity uncertain and limiting the structural use of reclaimed timber. Non-destructive testing (NDT), particularly Ultrasonic Tomography (UT), has proven capable of detecting internal defects in wood using portable, low-cost equipment (Vössing & Niederleithinger, 2018; Niemz & Mannes, 2012; Zielińska & Rucka, 2023; Perlin et al., 2019). However, previous studies have mainly focused on laboratory specimens or historic timber, rather than addressing the challenge of low-quality ultrasonic signals typically encountered in reclaimed timber due to its heterogeneous nature. This study aims to address that gap. This extended abstract presents preliminary results from a robust UT workflow that combines multi-path data acquisition, ensemble arrival-time picking, and outlier rejection. The workflow was applied to reclaimed spruce boards with known surface defects as a step towards a deployable assessment tool.

**Keywords:** reclaimed timber, ultrasonic tomography, non-destructive testing.

## Experimental

### Material

The specimens consisted of Norway spruce (*Picea abies*) boards with a cross-section of 5 × 13 cm, reclaimed from a Norwegian barn that had been in service for over a century. The boards exhibited damage typical of long-service structural timber. Boards with visually confirmed surface cracks were selected to provide known reference defects for validation.

### Data Collection and Signal Processing

Measurements were acquired using a Proceq Pundit Lab+ device, equipped with 54 kHz exponential transducers. The specimens were inspected in the transverse direction using a direct-contact, through-transmission configuration.

Measurement nodes were spaced at 1 cm intervals along the vertical and horizontal sides of each cross-section, resulting in 6 vertical nodes and 14 horizontal nodes. By combining all possible transmission paths between opposite sides (top-to-bottom and left-to-right), a total of 232 ray paths were acquired (36 vertical and 196 horizontal).

Since the instrument's built-in time-of-arrival picker performs poorly on low-quality signals, and direct-contact measurements are sensitive to transducer pressure and sensor alignment, each ray path was measured five times. Median absolute deviation (MAD) outlier rejection was applied before averaging the measurements.

Travel times were then estimated using an ensemble of three arrival-time picking methods to obtain a robust consensus estimate: a) Akaike Information Criterion (AIC), b) Short-Term Average/Long-Term Average (STA/LTA), c) Hilbert envelope.
The resulting travel times were used to compute wave velocities.
Only travel-time information was considered in this study. Signal amplitude and other waveform characteristics were excluded because they are strongly affected by variations in contact pressure, significantly reducing their reliability.

**Tomographic Reconstruction**

A straight-ray system matrix was constructed for each cross-section, and the velocity field was reconstructed using the Simultaneous Iterative Reconstruction Technique (SIRT) (Perlin et al., 2019), minimising the residual between the observed and predicted travel times.
The overall ultrasonic tomography workflow, from data acquisition and signal processing to SIRT reconstruction, is summarised in Figure 1.

## Results and Discussion

The reconstructed velocity fields revealed internal variations consistent with the locations of visually identified surface cracks. Regions of reduced velocity, indicating open cracks or degraded material, were clearly distinguishable from intact wood and corresponded well with the observed defects, providing an initial validation of the proposed workflow on reclaimed timber.

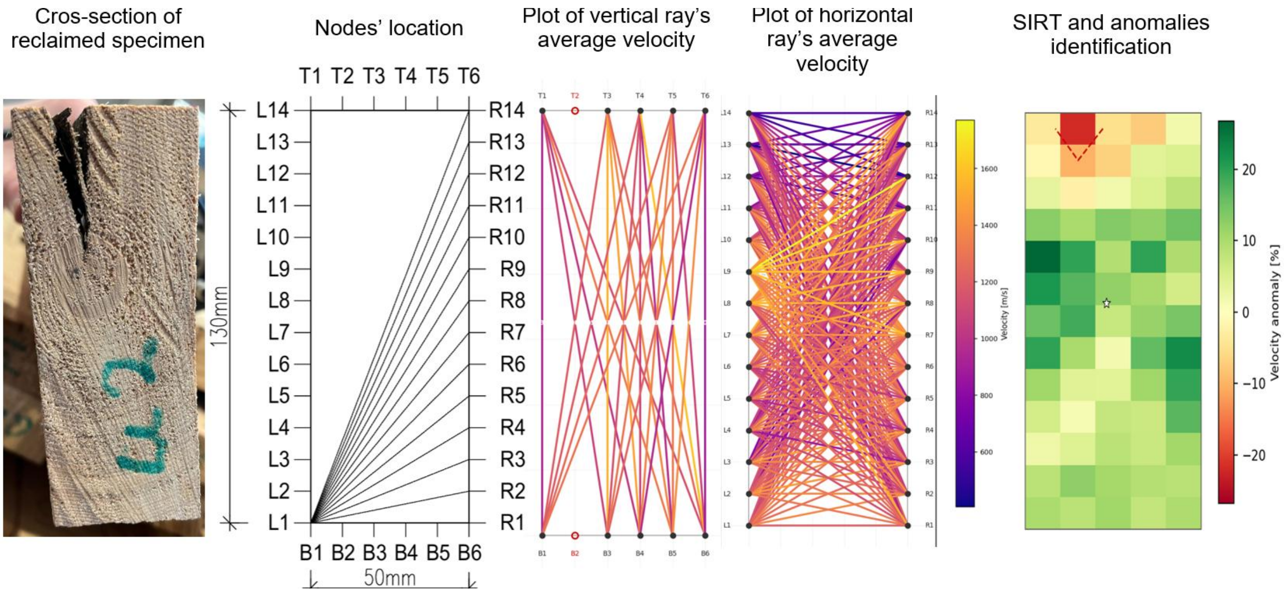


Figure 1. Workflow of the ultrasonic tomography reconstruction process using SIRT based on the time-of-arrival data acquired with a direct-contact, through-transmission inspection method

## Conclusions

This study shows that Ultrasonic Tomography is a potentially a viable NDT method for assessing reclaimed structural timber. On reclaimed spruce boards, it successfully detected and localized major cracks matching surface observations. Ongoing work targets: (i) higher resolution via higher-frequency and air-coupled transducers (Tiitta et al., 2020); (ii) correlating velocity with bending strength through destructive testing; and (iii) grading integration with standards such as EN 14081.

## References

Niemz, P., & Mannes, D. (2012). Non-destructive testing of wood and wood-based materials. Journal of Cultural Heritage, 13(3), S26–S34.

Perlin, L.P., Pinto, R.C.A., & Valle, Â. (2019). Ultrasonic tomography in wood with anisotropy consideration. Construction and Building Materials, 229, 116958. https://doi.org/10.1016/j.conbuildmat.2019.116958

Tiitta, M., Tiitta, V., Gaal, M., Heikkinen, J., Lappalainen, R., & Tomppo, L. (2020). Air-coupled ultrasound detection of natural defects in wood using ferroelectret and piezoelectric sensors. Wood Science and Technology, 54, 1051–1064. https://doi.org/10.1007/s00226-020-01189-y

Vössing, K.J., & Niederleithinger, E. (2018). Nondestructive assessment and imaging methods for internal inspection of timber. A review. Holzforschung, 72(6), 467–476.

Zielińska, M., & Rucka, M. (2023). Assessment of wooden beams from historical buildings using ultrasonic transmission tomography. International Journal of Architectural Heritage, 17(1), 249–261. https://doi.org/10.1080/15583058.2022.2086505

# Photogrammetry-Based Methodology for Enhancing Reclaimed Wood Salvageability with Load-Bearing Purposes

**Pablo de Castro-Cortizas[1], David Blanco Tortuero[2], Guillermo Íñiguez-González[3]**

[1,2,3]Timber Construction Research Group, Universidad Politécnica de Madrid, Spain, pablo.decastro.cortizas@gmail.com, 27dabla@gmail.com, guillermo.iniguez@upm.es

## Background

Besides an unequalled load-bearing material, wood as a resource also excels for its capability for lifetime extension through cascading and circularity strategies (Sirkin & Houten 1994, Jungmeier et al. 2001, Ramage et al. 2017, Wagner & Ott 2022).
However, when it gets to open R-paths (re-use, re-manufacture, etc.: Potting et al. 2018), reclaimed wood geometry uncertainties pose a challenge for the estimation of its physical and mechanical properties, thus harming its salvageability (Íñiguez-González et al. 2025).
Some previous works addressed this issue of cross-section heterogeneity through different approaches. To say a few: Osuna-Sequera et al. (2020) used forest-caliper for measuring thickness *b* and depth *h* on several sections along the length of the specimen, then merged into a single nominal cross-section; Nocetti et al. (2021) approximated the real irregular cross-section by octagonal and elliptical shapes; Cabaleiro et al. (2016) and Yen & Svilans (2025) applied laser scanning technology on irregular-shaped timber beams.
However, considering its affordability, flexibility and portability, image-based modelling techniques like Structure-from-Motion photogrammetry (Westoby et al. 2012) are not yet fully leveraged for assessment of reclaimed wood (Borghese et al. 2023).
In this research, a photogrammetry-based procedure was developed for accurate geometry reconstruction of reclaimed timber, streamlining image-acquisition, 3D-modelling and computing routines.

**Keywords:** cascading, upcycling, resources circulation, circular economy, nondestructive testing, reclaimed timber, structural reuse, structure-from-motion photogrammetry (SfM).

## Experimental: materials and methods

In the context of project TiReX, one specimen of European oak coming from demolition of over-100-year-old Spanish rural building was subjected to the workflow conceptualized in Figure 1. In essence: (1) 2D-images acquisition with rig-mounted cameras transversely shooting from different angles at adequate image-overlapping; (2) photogrammetric aligning of 2D-images for generation of 3D point cloud, later scaling to real size and filtering of outliers (Metashape); (and 3) automated computing (Grasshopper) of cross-section-related values on the 3D polygonal mesh (geometric twin), providing a longitudinal profile displaying the variation of geometric properties engaged in mechanical assessment (significantly: depth, thick, moment of inertia, as per formulae in mechanical testing standard EN 408).
Special attention was given to scrutinize the relative gain that higher computational effort delivered in terms of accuracy, in order to get the methodology adequately fit for mechanical assessment purposes.

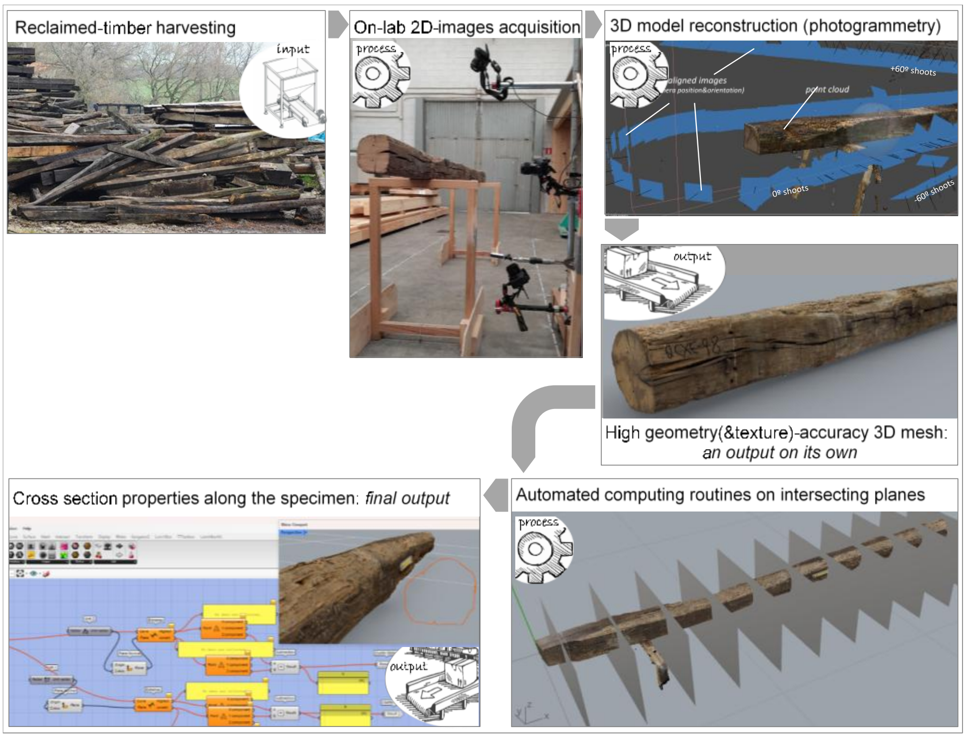


Figure 1. Research-workflow general conceptualization

## Results and Discussion

Five different-density meshes were generated, in order to assess accuracy/burden balance: a primary high-polygons mesh, weighing 6’4 GB, compound by 63’7 M faces (i.e. mesh triangular facets), which rates approx. 800 faces/cm$^2$; and four other lighter meshes at reductions rates of 1/10, 1/20, 1/40 and 1/80. The 1/10 reduction mesh provided computational manageability and yet outstanding accuracy: approx. 80 faces/cm$^2$, section curve discretized in segments 0’35mm long (Figure 2).

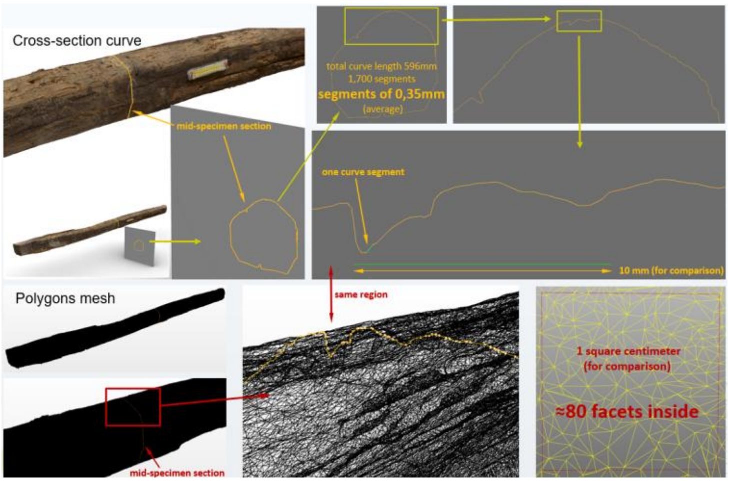


Figure 2. Obtained accuracy at 1/10 reduction rates

## Conclusions

The resulting methodology exhibits millimetric realism (while enabling computational-cost tuning) and suggests transferability to demolition sites and waste facilities, tackling the highly irregular geometry of reclaimed timber, providing reliability on its properties and boosting its re-circulation.

**Acknowledgement**

The TiReX project (ForestValue2 Joint Call 2023) has received funding from European Union's Horizon Europe under grant agreement No. 101094340 and funding in Spain from MICIU-Spain [PCI2024-153432].

**References**

Borghese V, Santini S, Sguerri L (2023) Sustainable assessment: a contribution to improve the reliability of NDT on old chestnut purlins. In: Proceedings from the 13th World Conference on Timber Engineering, Oslo, 957-966.

Cabaleiro M, Riveiro B, Arias P, Caamaño J C (2016) Algorithm for the analysis of the geometric properties of cross-sections of timber beams with lack of material from LIDAR data. Materials and Structures, 49, 4265–4278.

Íñiguez-González G, F Llana D, Ruy M, de Castro-Cortizas P, Arriaga F, Ostapska K (2025) Specific Features and Outcomes of Nondestructive Assessment for Extending the Structural Service Life of Reclaimed Timber. In: Proceedings of the 24th International Nondestructive Testing and Evaluation of Wood Symposium, Vicksburg.

Jungmeier G, Merl A, Mcdarby F, Gallis C, Hohenthal C, Petersen AK, Spanos K (2001) End of Use and End of Life Aspects in LCA of Wood Products - Selection of Waste Management Options and LCA Integration. Life cycle assessment of forestry and forest products; achievements of COST Action E9 working group 3 'End of life: recycling, disposal and energy generation'. Joanneum, Institute of Energy Research, Graz, 4/1-4/25.

Nocetti M, Aminti G, Degl'Innocenti M, Brunetti M (2021) Geometric representation of the irregular cross-section of old timber elements: Comparison of different approaches for mechanical characterization. Construction and Building Materials, 304.

Osuna-Sequera C, F Llana D, Íñiguez-González G, Arriaga F (2020) The influence of cross-section variation on bending stiffness assessment in existing timber structures, Engineering Structures, 204.

Potting J, Hekkert M P, Worrell E, Hanemaaijer A, Hanemaaijer A (2017) Circular Economy: Measuring Innovation in the Product Chain. PBL Netherlands Environmental Assessment Agency: The Haague, The Netherlands.

Ramage M H, Burridge H, Busse-Wicher M, Fereday G and others (2017) The wood from the trees: The use of timber in construction. Renewable and Sustainable Energy Reviews, 68, 333–359.

Sirkin T, Houten M (1994) The cascade chain: A theory and tool for achieving resource sustainability with applications for product design. Resources, Conservation and Recycling, 10, 213-276.

Wagner A, Ott S (2022) Cascading Wood-based Construction Products – A Guideline for Product Development. E3S Web of Conferences, 349.

Westoby M J, Brasington J, Glasser N F, Hambrey M J, Reynolds J M (2012) 'Structure-from-Motion' photogrammetry: A low-cost, effective tool for geoscience applications. Geomorphology, 179, 300-314.

Yen Y W, Tom Svilans T (2025) A digital framework for robotic processing of reclaimed timber. In: Proceedings from the 14th World Conference on Timber Engineering, Brisbane, 3564-3573.

# Toward Sustainable Reuse and Recycling of Biocide-Treated Wood: First Results from the WoodTreat Project

**Elise Bertheau[1], César Segovia[1], Justine Moral-Boiteau[1], Nicolas Brosse[1], Arnaud Besserer[1]**

[1]Laboratoire d'Etudes et de Recherche sur le Matériau Bois (LERMaB) - Université de Lorraine, France, elise.bertheau@univ-lorraine.fr, arnaud.besserer@univ-lorraine.fr

## Background

Wood is impregnated with preservatives (fungicides and insecticides) to improve its biological durability. However, these treatments limit its recyclability, as biocides may persist through successive recycling loops. The growing use of wood, promoted by initiatives such as the New European Bauhaus (NEB), is expected to increase the amount of preservative-treated wood entering waste streams. Wood waste comprises products with varying contamination levels, requiring different management pathways. The most contaminated fraction such as highly polluted post-consumer wood (HPPCW), commonly classified as Grade C or AIII/AIV, includes preservative-treated wood and is currently incinerated or landfilled due to the environmental and health risks associated with preservation chemicals. Effective decontamination technologies are therefore needed to enable its recycling as material. The European WoodTreat project (HORIZON-JU-CBE-2024-R-01) addresses this challenge by recovering clean secondary raw materials for high-value bio-based products. Here, the first results on copper removal from treated wood by steam explosion are presented as a first step toward the reuse of HPPCW in building materials and extended carbon storage.

**Keywords:** Copper-treated wood, Decontamination, Steam explosion.

## Experimental

Wood treated with Wolmanit® CX-8WB (Wolman, Germany) commercial preservative containing bis(N-cyclohexyl-diazenium-dioxy)-copper (Cu-HDO) and copper carbonate, was ground using a disc shredder (1480 rpm). Particle size distribution was analyzed using a Camsizer *(Camsizer P4, Retsch Technology, Germany),* after which the particles were sieved into fractions and analyzed by XRF spectroscopy (*Spectrum Quant X, Thermo Fisher, France*). Klason extraction was performed, and both the solid (Klason lignin) and liquid (water-soluble lignin and carbohydrates) phases were analyzed by scanning electron microscopy coupled with energy-dispersive spectroscopy (SEM-EDX; Jeol IT200, Jeol, *Japan*). For copper removal, wood particles were impregnated with water, sodium hydroxide (NaOH, 1 M), or sulfuric acid ($H_2SO_4$, 1% w/v), prior to steam explosion (SE) at 12 bars for 10 min. Copper removal in the finest fraction (< 3 mm) was monitored by SEM-EDX.

## Results and Discussion

The particle size distribution of wood particles ground using a disc shredder showed that the majority of the particles (89%) have a thickness between 1 and 8 mm, with more than 33% having a thickness of less than 3 mm.

Copper quantification performed by XRF analysis of the sieved fractions, normalized to the respective volumes of these fractions, revealed that all the fractions have the same copper concentration.
To investigate the copper location at the chemical level and optimise its removal by the cleaning process, a Klason extraction was performed. The subsequent SEM-EDX analyses of the resulting phases indicated that copper was present in both phases, with 1.18% mass in the solid phase compared with 0.39% mass in the liquid phase, indicating that the copper present in Wolmanit® CX-8WB (Cu-HDO and copper carbonate) binds to both the lignin and the carbohydrates in the wood (Jiang, 2000).
The removal of copper using the impregnation and SE process was monitored by SEM-EDX on small particles (< 3 mm). Impregnation with NaOH and $H_2SO_4$, followed by SE, appears to be similarly effective (Figure 1) in removing copper (p-value = 0.59). Regarding the water and SE impregnation process, copper migrates to the surface as crystals (Figure 2). Ultrastructural morphology of the wood fibers was also strongly affected (Figure 1).

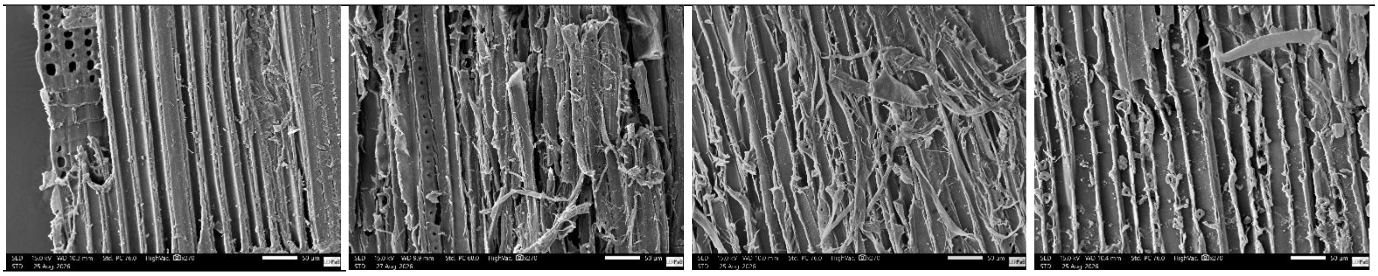

| Before SE | Water-SE | NaOH-SE | $H_2SO_4$-SE |
|---|---|---|---|
| | Copper relocation | 34% copper removal | 39% copper removal |

Figure 1. SEM-SED images of wood particles (< 3 mm) and copper removal (%Mass) after impregnation and steam explosion (SEM-EDX)

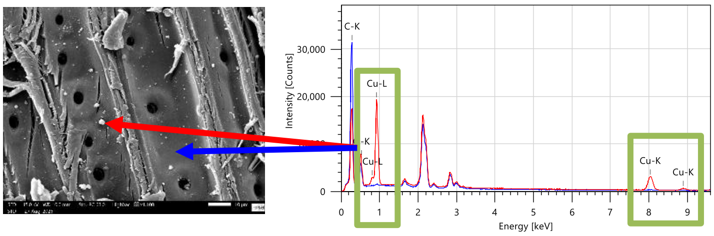


Figure 2. SEM-SED images of copper crystals and SEM-EDX spectra

## Conclusions

The process, consisting of impregnation and SE on contaminated wood particles, proved effective at removing part of the copper from the wood (up to 39%), although removal was not complete. This process could be supplemented with bioremediation using *P. placenta* (Pandharikar *et al.*, 2022) to improve copper removal efficiency.
In the WoodTreat project, particles cleaned by SE will be used to produce, among others, bio-based insulation boards. The liquid effluents from the SE process containing copper undergoes hydrothermal carbonization to capture the copper.

## Acknowledgements and fundings

The WoodTreat project (HORIZON-JU-CBE-2024-R-01) has received funding from the Circular Bio-based Europe Joint Undertaking (CBE JU) under the European Union's Horizon Europe research and innovation programme under Grant Agreement No. 101214288. Views and opinions expressed are however those of the author(s) only and do not necessarily reflect those of the European Union or the Circular Bio-based Europe Joint Undertaking. Neither the European Union nor the granting authority can be held responsible for them.

**References**

Jiang, X (2000) Fixation chemistry of amine-copper preservatives (T). University of British Columbia.

Pandharikar G, Claudien K, Rose C, Billet D, Pollier B, Deveau A, Besserer A, Morel-Rouhier M (2022) Comparative Copper Resistance Strategies of *Rhodonia placenta* and *Phanerochaete chrysosporium* in a Copper/Azole-Treated Wood Microcosm. Journal of Fungi, *8*(7), 706.

# Quantifying the Cascade: A Continuous Resource-Value Indicator for End-of-Life Wood Governance

**Stephan Ott**[1], **Jan Lüdtke**[1]

[1]Thünen Institute of Wood Research, Hamburg, Germany
stephan.ott@thuenen.de and jan.luedtke@thuenen.de

## Background

Resource allocation within the circular bioeconomy still lacks operational instruments that translate the cascading principle into a measurable quantity. Current policy treats cascading categorically — RED III Art. 3(3) "material-before-fuel", the Waste Framework Directive — with no scalar measure of how much resource value a given wood state retains. Cascading is a "lexicographic" ordering (refuse < reduce < reuse < recycle < recover), not a weighted trade-off to be optimised; applying it as a compensatory score systematically undervalues irreversible losses of material quality and function.

The field therefore lacks a continuous, conservation-aware and auditable measure of retained resource value per wood state that also encodes cascade compliance. We present the Resource Value Indicator (RVI): a continuous, dimensionless per-kilogram scalar in [0, 1] expressing the resource value of a wood-based material state relative to the system maximum (Sirkin and ten Houten 1994; Vis et al. 2016). It is designed to support policy decisions, not individual business decisions. Terms used here: cascading (above); irreversibility — an action whose consequences cannot be undone, so combustion is irreversible while reuse is not; and resource value — a composite of qualitative and value-based sub-criteria scored per criterion.

**Keywords**: resource value indicator; multi-criteria decision analysis; cascading woody biomass; RED III

## Experimental

The system boundary is one kilogram of dry matter (kg DM), tracked from harvest to final material or energy use and aligned with EN 15804 module logic, so each state can in principle be cross-checked against existing LCA data. The framework is a directed acyclic graph (DAG) of resource states and transitions, scored by a deterministic, fully scripted Python pipeline; every criterion is an explicit, inspectable rule, so any state's value is traceable to the rule that produced it. Four operational criteria are used — Material Quality (MQI), Economic Value (EVI), Environmental Value (ENVI, embedding a Cascade Compliance Index as a RED III Art. 3(3) penalty function), and Energy Content (ECI); a fifth, socio-regional criterion (RSVI) is in development and is not part of the results reported here. MQI operationalises irreversibility through purity (chemical admixture), geometry and functional integrity, referencing waste-wood classes (AltholzVO; Potting et al. 2017). The single-state RVI is a Simple Additive Weighting of the criteria (Eq. 1), with weights externalised and varied in sensitivity analysis rather than fixed. A chain-level, mass-weighted RVI is given by Eq. 2, and a Cascade Depth Score (Eq. 3) reports the mass-weighted share of premature energy use for RED III chain-level compliance.

$$RVI = w_{MQI} \cdot MQI + w_{EVI} \cdot EVI + w_{ENVI} \cdot ENVI + w_{ECI} \cdot ECI, \quad \Sigma w_i = 1 \qquad (1)$$

$$RVI_{chain} = \Sigma(m_i \cdot RVI_i) / \Sigma m_i \qquad (2)$$

$$CDS = 1 - \Sigma(m_i \cdot cascade\_remaining_i \mid level = bioenergy, cr > 0.10) / \Sigma m_i \qquad (3)$$

A non-compensatory safeguard prevents a state with high energy and low material quality from outranking a structural product through compensation: an MQI veto blocks preference increases if one state exceeds another by a set threshold in terms of MQI. Rank robustness is compared using identical criteria with TOPSIS and PROMETHEE II (Brans and Vincke 1985). The pipeline is deterministic and parameter-driven; each criterion function can already accept a distribution rather than a single point value, meaning that Monte Carlo uncertainty propagation is an integral part of the architecture. The quality reduction levels and criterion ranges used to date are placeholders defined by experts in an illustrative reference chain (from softwood harvesting to energy generation); they do not represent measured variability at batch level and are labelled as such.

**Results and Discussion**

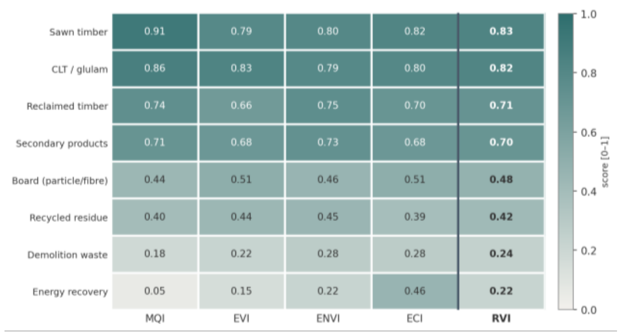


Figure 1. Sub-criterion scores (MQI, EVI, ENVI, ECI) per resource state, with the equal-weighted RVI as a separate column. Illustrative reference chain, test data, not measured

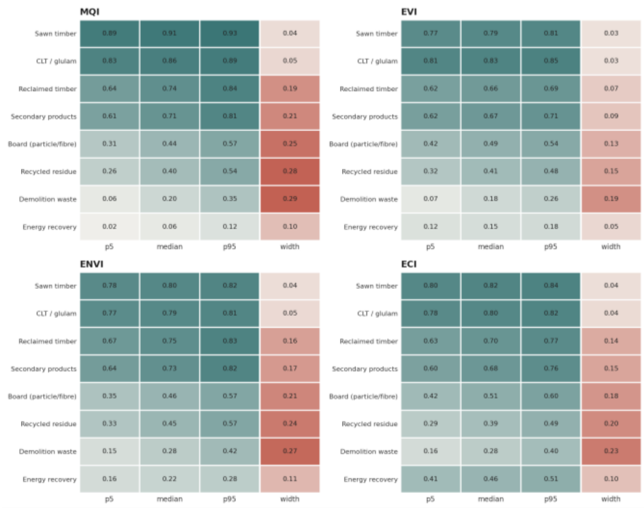


Figure 2. Per-criterion uncertainty summary (5th percentile, median, 95th percentile, and range width) across all states, shown separately for each of the four sub-indicators

Along the cascade, the material quality (MQI) declines most rapidly, whilst the ECI remains comparatively high even at the final stage of energy recovery – which is to be expected, as the ECI is based on the energy content retained rather than on material integrity. A single sub-criterion with a high value can therefore partially offset a low overall value, provided that the weightings allow for such an offset: it is precisely this scenario that the cascade conformity index and the MQI/PROMETHEE veto are designed to capture. The RVI value is a summary of the adjacent criteria and is displayed alongside them, rather than as a standalone value, to avoid giving the impression that it contains information not included in those criteria.

Uncertainty regarding the RVI is not evenly distributed; its structure matters more for decision-making than any single aggregate value. A distinction is made between three sources: (i) uncertainty regarding the condition of the material (MQI, ENVI, ECI), which is low for new sawn timber but increases significantly for recycled material, waste materials and demolition waste, where impurities and history can only be partially traced; (ii) the economic value (EVI), which remains low as it is linked to a minimum price on the energy market, but carries a one-sided downward risk if low-quality material forces an unplanned switch directly to incineration; and (iii) the state transition probability (yield) – that is, the probability that a feedstock will actually reach a high-value state – which has not yet been modelled and represents the next step in development. Until this happens, every RVI value assumes that a certain resource status has already been achieved, which limits the reliability of statements at the pathway level.

**Conclusions**

An indicator lacking conservation constraints, non-compensatory structure and correlation diagnostics still produces stable, precise, confidently reported numbers that do not mean what they appear to. Building these properties in — mass balance on a state network, acceptability screens before scoring, and reported weight provenance and criteria correlation — is what makes the CDS-number trustworthy. Because cascade choices rest on valuations that future conditions can falsify, irreversibility is best handled as an acceptability screen rather than a scored, tradable dimension: a topological property — which downstream options a step excludes, and whether material can re-enter — that needs no discount rate and no assumed future preferences (Arrow and Fisher 1974). We therefore do not add “future generations” as a further weighted dimension; an interest that cannot be measured is not repaired by assigning it a number, but respected by a structure that can refuse.

**References**

AltholzVO (2002) Verordnung über die Entsorgung von Altholz (Altholzverordnung). Bundesgesetzblatt, Germany. (“Waste wood ordinance”, national regulation).

Arrow KJ, Fisher AC (1974) Environmental preservation, uncertainty, and irreversibility. Quarterly Journal of Economics 88: 312–319.

Brans JP, Vincke P (1985) A preference ranking organisation method: the PROMETHEE method for multiple criteria decision-making. Management Science 31: 647–656.

Potting J, Hekkert M, Worrell E, Hanemaaijer A (2017) Circular Economy: Measuring Innovation in the Product Chain. PBL Netherlands Environmental Assessment Agency, The Hague.

Sirkin T, ten Houten M (1994) The cascade chain: a theory and tool for achieving resource sustainability with applications for product design. Resources, Conservation and Recycling 10: 213–276.

Vis M, Mantau U, Allen B (eds) (2016) Study on the Optimised Cascading Use of Wood. European Commission DG ENV, Brussels.

# Hydrothermal Reprocessing of Discarded Railway Sleepers and Utility Poles

**Jaka Levanič[1], Aitor Barbero-López[2], Aitana Zoco[2], Janne Jänis[2], Eemeli Eronen[2], Antti Haapala[2], Miha Humar[1]**

[1]University of Ljubljana, Department of Wood Science and Technology, Biotechnical Faculty, Ljubljana, Slovenia jaka.levanic@bf.uni-lj.si, miha.humar@bf.uni-lj.si
[2]University of Eastern Finland, Department of Chemistry and Sustainable Technology, Faculty of Science, Forestry and Technology, Joensuu, Finland aitor.barberolopez@uef.fi, aitana.zoco@uef.fi, janne.janis@uef.fi, eemeli.eronen@uef.fi, antti.haapala@uef.fi

### Background

Industrial and infrastructure applications of timber inevitably require biocidal treatment to extend service life and, more importantly, prevent critical failure during use. Once its service life ends, we are left with large amounts of biocide treated timber that needs to be disposed in a safe and environmentally acceptable way. In Europe the dominant industrial timber protection biocides are based on copper compounds. Thus, we have chosen for our experiments two ubiquitous industrial timber products; (i) railway sleepers, and (ii) utility poles. In Slovenia these are still vital infrastructure components and are exclusively protected by oil-based copper biocides or aqueous ethanolamine-based copper complexes. To reprocess these materials, we have chosen a hydrothermal liquefaction process that utilizes water as the solvent, high temperature, and pressure in an inert atmosphere. This process fractionates the material into a light aqueous fraction, heavy non-polar fraction and a solid residue (Barbero-López, López-Gómez et al. 2024). The liquefaction process causes depolymerization of the main wood constituents, and the presence of copper compounds is especially interesting in this context due to copper being a transition metal that is known to act as a catalyst in the depolymerization of organic macromolecules, like lignin (Hernández-Mañas, Martínez-Martin et al. 2024), and cellulose (Castillo, Torres-Flores et al. 2021).This opens up an interesting question, whether the presence of copper-based biocides influences the variety and yields of small molecules produced during hydrothermal liquefaction, and whether the produced bio-crude could be used as an antifungal agent in wood preservation.

**Keywords:** Antifungal, biocides, timber, hydrothermal-liquefaction, waste valorisation

### Experimental

Discarded European beech (*Fagus sylvatica*) railway sleepers treated with an oil-based preservative (Cu concentration 3600 ppm) and Scotts pine (*Pinus sylvestris*) utility poles treated with a copper-ethanolamine complex preservative (1800 ppm) were used as the treated raw materials. Untreated beech and pine were used as controls. The timber samples were milled to a fraction passing a 2 mm screen and liquefied in a Parr Instruments Series 4580 HT reactor under a nitrogen atmosphere (10 bar initial load) at 330℃ and 136 bar of pressure. Water was used as the sole solvent at a 6:1 solvent to biomass ratio. Following liquefaction, the process liquid was filtered and the solid residue extracted using ethyl acetate. The ethyl acetate soluble fraction was recovered using a rotary evaporator yielding a reddish/dark brown oil-like substance (bio-crude) which was then analysed for its chemical composition using FT-IRC-MS. The process liquid, i.e. the aqueous phase was analysed for its pH, total water content (Karl-Fischer titration), and total acid number. Furthermore, the biocrude was tested for antifungal activity using a disc diffusion method against some common wood decay fungi.

## Results and Discussion

### Properties of the aqueous phase

The aqueous phase is relatively poor in products as it is mainly water, some organic acids, and a small amount of sugars. The total non-aqueous content is also relatively low with a maximum of 3.1 %. The total acid number in the copper biocide treated specimens is also higher, this is corroborated by pH measurements. We also noted the absence of any copper ions in the aqueous phase (Table 1).

Table 1. General characteristics of the aqueous phase after hydrothermal liquefaction of biomass (values in parentheses represent standard deviation)

| Aqueous phase sample | Water content (K-F) | Total acid number (mg KOH/g sample) | pH | Copper concentration* |
|---|---|---|---|---|
| Pine | 98.3 | 7.6 (± 0.02) | 3.45 (± 0.00) | < 5 ppm |
| Utility pole | 97.4 | 8.7 (± 0.11) | 3.36 (± 0.01) | < 5 ppm |
| Beech | 97.2 | 14.96 (±1.22) | 3.61 (± 0.01) | < 5 ppm |
| Railway sleeper | 96.9 | 17.47 (± 0.56) | 3.49 (± 0.01) | < 5 ppm |

*Machine detection limit is set at 5 ppm

### Composition of the heavy oil

The composition of the heavy oil was analysed by FT-ICR-MS. In all cases the oil is rich in hydrocarbons and lignin. The most obvious difference was observed in the Beech/Sleeper specimens. The HTL processed railway sleeper shows lower relative intensities of hydrocarbons and lignin compared to neat beech wood. However, at the same time, the amount of lipids observed in the railway sleeper sample is higher. This is in accordance with expectations as the railway sleepers are treated with an oil-based preservative. It appears that in both cases where a copper-based preservative is present, the variety of chemical compounds produced also differs between them and their respective controls. Railway sleeper biocrude, for example, exhibits relatively lower amounts of high C-number and highly unsaturated compounds compared to beech HTL bio-crude, but is conversely richer in shorter chain unsaturated compounds. The total double bond equivalency of railway sleeper HTL biocrude is also lower than that of neat Beech HTL bio-crude.

### Efficacy against wood decay fungi

The cellulose discs treated with a solution of biocrude in acetone were exposed to wood decay fungi on a nutrient rich medium and the fungal response was evaluated visually. It quickly became evident that a 1:1 dilution of biocrude with acetone was the most effective in slowing down fungal growth in all tested fungi. Higher dilutions were significantly less effective. However, in most cases the biocrude did not stop the fungi from colonizing the cellulose discs after enough time. The most vulnerable were *Trametes versicolor* and *Gloeophyllum trabeum. Coniophora puteana*, on the other hand, was not affected by the presence of the HTL biocrude, regardless of the source.

Similarly, *Pleurotus ostreatus* also showed little response to the HTL biocrude. With the fungi that did exhibit a response, it was noted that the railway sleeper based HTL biocrude showed more prominent signs of inhibition compared to the others. While there was no copper present in either of the biocrude made from treated timbers, the higher potency of the railway sleeper-based crude warrants some additional research to see if any residual co-biocides (tebuconazole) might have survived the HTL process intact.

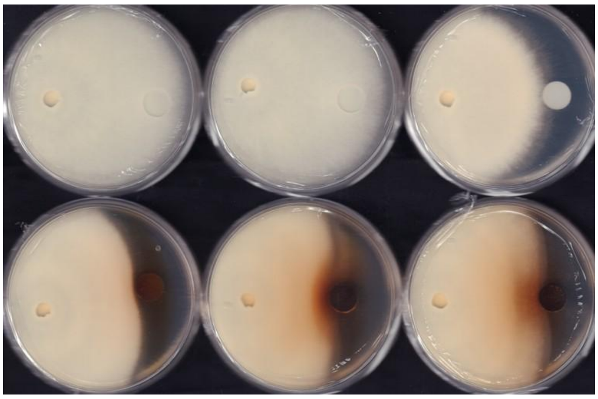

Figure 6. Railway sleeper HTL biocrude against *Trametes versicolor* after 14 days growth time

**Conclusions**

Residual biocide treated timber was successfully treated in a hydrothermal reactor and light aqueous phase and a heavy organic phase (biocrude) was obtained. The heavy organic phase is a highly complex mixture of polyphenolic degradation products stemming primarily from lignin. We could observe that the presence of biocides affects the composition of this mixture, likely due to the presence of copper and potentially also due to the presence of other biocide constituents (co-biocides, solvents…). There lies potential in valorizing this material in a circular approach to wood treatment, as the biocrude shows some signs it might prevent or slow wood decay, but further tests are needed to determine the true bioactive efficacy of this material.

**References**

Barbero-López, A., Y. M. López-Gómez, J. Carrasco, N. Jokinen, R. Lappalainen, J. Akkanen, B. Mola-Yudego and A. Haapala (2024). "Characterization and antifungal properties against wood decaying fungi of hydrothermal liquefaction liquids from spent mushroom substrate and tomato residues." Biomass and Bioenergy **181**: 107035.

Castillo, I., A. P. Torres-Flores, D. F. Abad-Aguilar, A. Berlanga-Vázquez, M. Orio and D. Martínez-Otero (2021). "Cellulose Depolymerization with LPMO-inspired Cu Complexes." ChemCatChem **13**(22): 4700-4704.

Hernández-Mañas, A., A. Martínez-Martin, J. Madignier, P. Fongarland, F. Bertaud, L. Vilcocq and L. Djakovitch (2024). "Copper catalyzed alkaline aerobic lignin depolymerization: effect of botanical origin and industrial extraction process on reactivity supported through characterization." RSC Sustainability **2**(10): 2930-2948.

# SESSION 7: MODIFICATION AND TREATMENT

# Lignin-Based Flame Retardant for Sustainable and Multifunctional Wood Protection

**Alanis Bré[1], Ander Larruscain[1], Ainara Saralegi[1], Cristina Peña-Rodriguez[1], René Herrera Díaz[1], Oihana Gordobil[1]**

[1] Materials +Technologies" Research Group (GMT), Department of Chemical and Environmental Engineering, Faculty of Engineering, Gipuzkoa, University of the Basque Country (EHU), Pza. Europa, 1, 20018 Donostia, Spain
alanis.bre@ehu.eus

## Background

Wood is increasingly used in indoor and outdoor applications due to its low density, versatility, and renewable nature (Ramage, M. H. et al., 2017). However, wood remains vulnerable to degradation caused by moisture, UV radiation, microorganisms, insects, and fire, making protective treatments essential to enhance its long-term performance (Kollmann, F. F. et al., 1968). Among existing approaches, impregnation treatments are particularly attractive because they enable functional agents to penetrate the porous structure of wood. However, conventional preservative and flame-retardant treatments often rely on synthetic or inorganic compounds, raising environmental and toxicity concerns and driving the search for renewable and multifunctional alternatives Schwarzkopf, M. J. et al. 2016; Landry, V. et al., 2023). Lignin is an attractive candidate for sustainable wood protection due to its abundance as an industrial by-product and its intrinsic antioxidant and UV-absorbing properties (Zhang, Y. et al., 2021; Gordobil, O. et al.,2017; Herrera, R. et al., 2023). Its aromatic and carbon-rich structure also provide a natural basis for char formation, making lignin a promising platform for the development of bio-based flame-retardant materials (Bagueri, M. et al., 2026). However, the intrinsic flame-retardant performance of unmodified lignin is generally limited, and chemical functionalization has therefore been investigated as a strategy to enhance its fire-protection capabilities. In particular, the incorporation of phosphorus-containing functionalities has shown potential to promote char formation and improve the thermal and flame-retardant behaviour of lignin (Xie, Y. et al., 2018).
In this context, the present work investigates chemically modified lignin as a bio-based multifunctional impregnation treatment for wood. The proposed approach aims to enhance flame retardancy while retaining the intrinsic UV-absorbing functionalities of lignin, providing a more sustainable alternative to conventional wood protection treatments.

**Keywords:** Kraft Lignin functionalization, Flame retardancy, Wood impregnation

## Experimental

### Chemical modification of lignin

Lignin, phytic acid and a bio-based crosslinker were combined in a round-bottom flask at different ratios for 3h at 120ºC. The mixture was then neutralized, purified and dried to obtain the modified lignin samples. The chemical modification was confirmed by FTIR, $^{31}$PNMR, and TGA.

### Preparation of phosphorous-containing lignin nanoparticles (P-LNPs)

Modified lignin was dissolved in THF/acetone at initial concentration of 20 mg/mL (7:3, v/v). The solution was stirred and centrifuged to remove undissolved fraction. The colloidal suspension was obtained by the addition of cold distilled water into the beaker dropwise until water occupied 80 vol% of the final liquid. Finally, the organic phase was evaporated using a rotavapor. The colloidal suspension was characterized by DLS and TEM.

**Vacuum-Pressure impregnation of wood**

Pine wood samples (3.3 mm × 1.3 cm × 4 cm) were impregnated by vacuum-pressure treatment with either the colloidal suspensions (P-LNPs) or the lignin solutions in THF/acetone (P-L), at different concentrations. Conditioned samples were subjected to −1 bar vacuum for 1 h followed by 5 bar pressure for 2 h, and subsequently vacuum-dried at 50 °C to constant mass. Impregnation efficiency was evaluated by weight percent gain (WPG) and leachability, while UV stability and flame-retardant performance (LOI) were assessed.

**Results and Discussion**

The analytical techniques confirmed the successful chemical modification of lignin with phytic acid. The FTIR spectra (Fig. 1) showed the characteristic P–O–Ar band at 1000 cm$^{-1}$, supporting the incorporation of phosphorus-containing functionalities. Thermal behaviour was further evaluated by TGA under nitrogen and oxygen atmospheres (Fig. 2). Compared with unmodified lignin, phytic acid-modified lignin showed an earlier initial mass loss, followed by a more gradual decomposition and higher char residue under nitrogen, reaching approximately 43% at 800 °C compared with 36% for unmodified lignin. Under oxygen, the modified lignin also exhibited a more progressive degradation and higher residual mass, 6% at 800 °C for the modified lignin compared to 1%, at intermediate temperatures, indicating enhanced char-forming ability and the potential of the modification to improve lignin's flame-retardant performance. The modified lignin was successfully processed into nanoparticles by nanoprecipitation, yielding particles with an average hydrodynamic diameter of approximately 250 nm. Pine wood samples were impregnated with the modified lignin as either a colloidal suspension (P-LNPs) or lignin solution (P-L) at 0.8% and 2.5% concentrations. The colloidal suspension resulted in WPG values of 0.73 and 1.4%, respectively, while higher WPG values of 2.7 and 3.9% were obtained using the lignin solution. The LOI value of the modified pine using the 0.8% P-LNPs increased compared to the unmodified wood, the slight increase is due to the low concentration. The modified species (0.8% P-LNPs) show good UV stability (Fig 3).

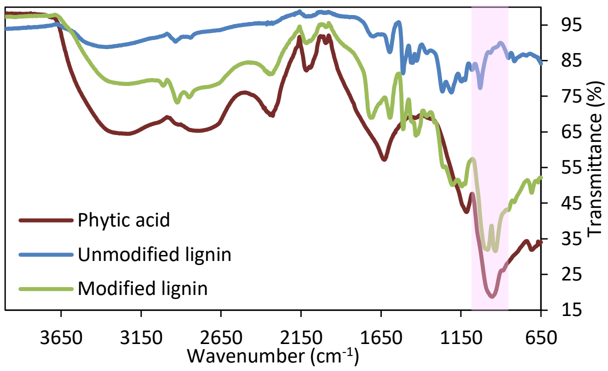


Figure 1. FTIR spectra of phytic acid, unmodified and modified lignin

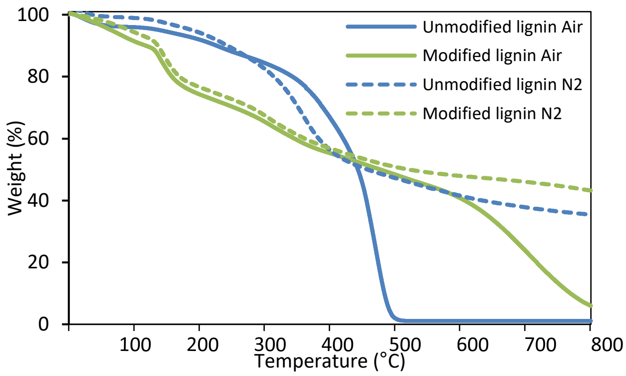


Figure 2. TGA curves of unmodified and modified lignin

| | Unmodified Pine | | Modified Pine with 0.8% P-LNPs | |
|---|---|---|---|---|
| 0h |  | LOI = 22.4% |  | LOI = 23.2% |
| 200h |  | ∆E =18.3 |  | ∆E = 7.2 |

Figure 3. Wood images, limiting oxygen index and the colour change of Unmodified and modified pine samples (0.8% P-LNPs) before and after 200h in a UV-Chamber

## Conclusions

Phytic acid-modified lignin was successfully obtained, with its chemical modification confirmed by FTIR and complementary characterization techniques. The modified lignin was successfully converted into nanoparticles, yielding a stable colloidal suspension. Treatment of pine wood resulted in improved UV stability, while only a slight improvement in flame-retardant performance was achieved, indicating the need for further optimization of the treatment. Overall, the results highlight the potential of phytic acid-modified lignin nanoparticles as a bio-based multifunctional approach for wood protection.

## References

Bagheri, Marzieh, Muhammad Farooq, Paula Nousiainen, Uula Hyväkkö, et Monika Österberg. « Engineered Phytic Acid-Lignin Networks: One-Pot Strategy toward Stable, Multifunctional Bio-Based Materials ». *Bioresource Technology* 444 (2026)

Gordobil, Oihana, René Herrera, Rodrigo Llano-Ponte, et Jalel Labidi. « Esterified Organosolv Lignin as Hydrophobic Agent for Use on Wood Products ». *Progress in Organic Coatings* 103, 143-51 (février 2017).

Herrera, Rene, Faksawat Poohphajai, Anna Sandak, et Oihana Gordobil. « Simultaneous Improvement of Surface Wettability and UV Resistance of Wood with Lignin-Based Treatments ». *Polymers* 15, nº 16, 3409 (2023).

Kollmann, F. F. et al. Principles of Wood Science and Technology. Princ. Wood Sci. Technol. (1968).

Landry, V. et al. Recent Developments and Trends in Sustainable and Functional Wood Coatings. Curr. For. Reports 9, 319–331 (2023).

Ramage, M. H. *et al.* The wood from the trees: The use of timber in construction. Renewable and Sustainable Energy Reviews, 68 (février 2017): 333-59.

Schwarzkopf, M. J. et al. Environmental Impacts of Traditional and Innovative Forest-based Bioproducts. Environ. Impacts Tradit. Innov. For. Bioprod. (2016).

Xie, Y. et al. Components Analysis of Biochar Based on Near Infrared Spectroscopy. Chinese J. Anal. Chem. 46, 609–615 (2018).

Zhang, Y. et al. A Review on Properties, and Applications as a Light-Colored UV Absorber. *ACS Sustain. Chem. Eng.* **9**, 1427–1442 (2021).

# Moisture-Induced Redistribution of Fire Retardants in Wood

**Maja Fjalland[1,2], Maria Frederiksson[3], Lisbeth Thygesen[1], Johannes Karthäuser[4], Emil Engelund Thybring[1]**

[1]University of Copenhagen, IGN, Denmark mnor@ign.ku.dk
[2]DBI Fire and Security, Denmark mkn@dbigroup.dk
[3]Lund University, Building Materials, Sweden
[4]Georg-August-University of Göttingen, Germany

## Background

While fire retardants embedded in wood materials can enable its use in broader facade applications (Lowden and Hull 2013), these fire retardants are often salt-based and risk to be redistributed within the wood and leach from the façades during weather exposure, potentially reducing their long-term fire performance (Östman and Tsantaridis 2016). While several studies have investigated chemical formulations, retention and weathering performance (Franke et al. 2026; Lin et al. 2021a, 2021b; Russell et al. 2007; Takase et al. 2024; Wu et al. 2023, 2025), less is known about how this redistribution progresses within the wood and how the resulting spatial distribution affects fire performance.

Our previous experiments with monoammonium phosphate (MAP) identified a progressive redistribution pattern during one-sided water exposure, with depletion extending from the exposed surface into the wood over time. This ongoing work builds on this observation by investigating whether similar patterns occur under different exposure conditions and with different fire retardant treatments, and how the resulting distribution relates to fire performance.

**Keywords:** Wood modification, fire retardants, leaching.

## Experimental

In the previous experiment Scots pine (*Pinus sylvestris* L.) sapwood specimens were subjected to one-sided liquid-water exposure. Moisture ingress was monitored in non-impregnated specimens using resistance-type sensors, while MAP redistribution in impregnated specimens was investigated using X-ray fluorescence (XRF) imaging and quantitative phosphorus measurements obtained by ICP-MS. MAP released to the surrounding water was also quantified. The deliquescence point of MAP was determined using dynamic vapour sorption (DVS), and the moisture sorption behaviour of non-impregnated and MAP-impregnated wood was determined gravimetrically at different relative humidities (Figure 1a).

Building on these experiments, this ongoing study uses a similar one-sided exposure setup to compare distribution of MAP with monoguanidine phosphate (MGP) in Scots pine, with and without resin impregnation. Redistribution is investigated during liquid-water exposure and subsequent drying, as well as during exposure to relative humidities below and above the deliquescence points of the salts. Following exposure, cone calorimetry will be used to investigate whether the resulting changes in fire retardant distribution affect reaction-to-fire performance.

## Results and Discussion

MAP showed a deliquescence point at approximately 95% RH. At the same RH, MAP-impregnated wood showed a pronounced increase in moisture uptake. In non-impregnated Scots pine, 95% RH corresponded to a moisture content of approximately 0.22 g $g^{-1}$ (Figure 1a), which was defined as the "critical moisture content" associated with MAP deliquescence, which could be compared to the moisture measurements done in the non-impregnated specimens. XRF and ICP-MS showed progressive MAP redistribution and depletion during water exposure. The region affected by MAP redistribution progressed with moisture ingress but remained behind the 0.22 g $g^{-1}$ moisture front measured in non-impregnated wood (Figure 1b).

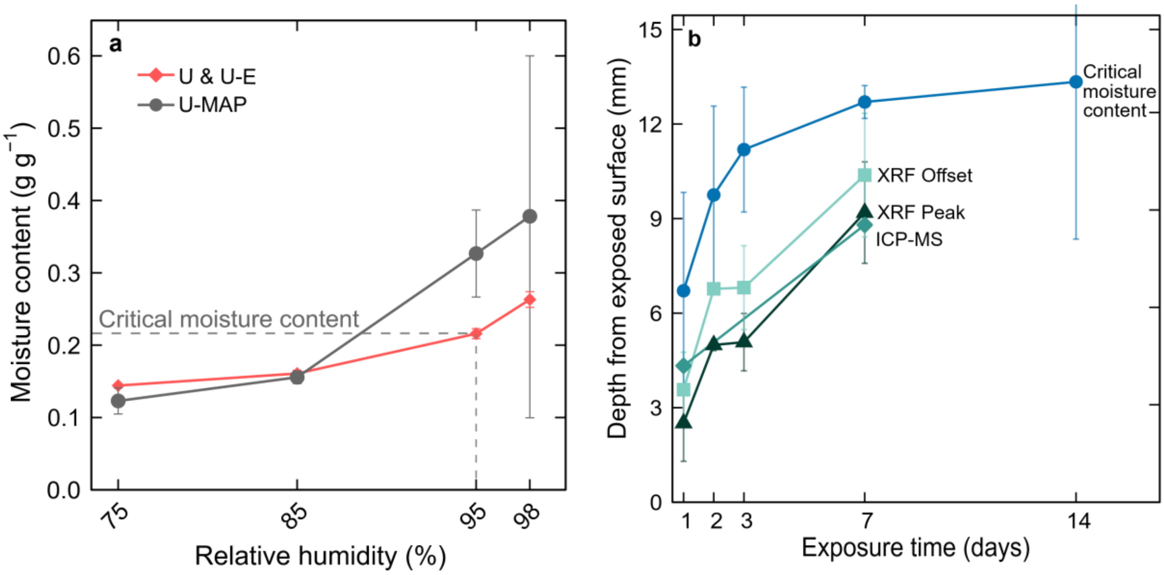


Figure 1. a) Sorption isotherm for untreated wood (U), untreated wood with moisture sensors (UE) and MAP-impregnated wood (U-MAP). b) Comparison of moisture ingress and the regions affected by MAP redistribution identified by different measurement techniques.

After one day of water exposure, MAP was greatly depleted near the exposed surface while high concentrations remained only a few millimetres further inside the wood. With continued exposure, the depleted region progressed further into the specimens while the rate of external MAP release decreased. Remaining bulk retention therefore does not necessarily reflect the fire retardant concentration at the surface. Since the surface concentration might be critical for reaction-to-fire performance, the spatial distribution of the remaining fire retardant may be as important as the total amount retained. These findings motivate the ongoing work investigating how deliquescence behaviour and resin impregnation influence redistribution of the two fire retardant salts MAP and MGP, and whether near-surface depletion and different concentration profiles within the specimens translates into changes in reaction-to-fire performance.

## Conclusions

MAP redistribution was associated with moisture ingress and the conditions associated with deliquescence, while producing substantial depletion near the exposed surface before the fire retardant was depleted from the rest of the material. Consequently, bulk retention alone may not adequately describe fire retardant performance, and the spatial distribution of the remaining fire retardant should also be considered.

**References**

Franke T, Larnøy E, Grabowski J, Volkmer T (2026) Phosphate based salts and minerals as fire retardants for wood – a critical assessment. Wood Material Science & Engineering: 1–10. https://doi.org/10.1080/17480272.2026.2614070

Lin CF, Karlsson O, Martinka J, Rantuch P, Garskaite E, Mantanis GI, Jones D, Sandberg D (2021a) Approaching highly leaching-resistant fire retardant wood by in situ polymerization with melamine formaldehyde resin. ACS Omega 6: 12733–12745. https://doi.org/10.1021/acsomega.1c01044

Lin CF, Kim I, Mantanis GI, Karlsson O, Jones D, Sandberg D (2021b) Leach-resistant fire retardant treated furfurylated wood by incorporating guanyl-urea phosphate. Wood Material Science & Engineering 16: 429–431. https://doi.org/10.1080/17480272.2021.1981998

Lowden L, Hull T (2013) Flammability behaviour of wood and a review of the methods for its reduction. Fire Science Reviews 2: 4. https://doi.org/10.1186/2193-0414-2-4

Östman B, Tsantaridis L (2016) Durability of the reaction to fire performance for fire retardant treated (FRT) wood products in exterior applications – a ten years report. MATEC Web of Conferences 46: 05005. https://doi.org/10.1051/matecconf/20164605005

Russell LJ, Marney DCO, Humphrey DG, Hunt AC, Dowling VP, Cookson LJ (2007) Combining fire retardant and preservative systems for timber products in exposed applications – state of the art review. Project No. PN04.2007. Forest and Wood Products Research and Development Corporation, Victoria.

Takase R, Ishikawa A, Kamikawa D (2024) Artificial-weathering test requirements for fire retardant-treated wood to reproduce optimal chemical retention and moisture conditions. Journal of Wood Science 70: 30. https://doi.org/10.1186/s10086-024-02143-3

Wu M, Emmerich L, Kurkowiak K, Militz H (2023) Fire resistance of pine wood treated with phenol-formaldehyde resin and phosphate-based flame retardant. Wood Material Science & Engineering 18: 1933–1939. https://doi.org/10.1080/17480272.2023.2205379

Wu M, Hötte C, Karthäuser J, Militz H (2025) Fire behavior of thermally modified pine (Pinus sylvestris) treated with DMDHEU and flame retardants: From small scale to SBI tests. Holzforschung 79: 352–357. https://doi.org/10.1515/hf-2025-0021

# Changes in Wood after Treatment with Copper-Based Preservatives

**Lotārs Olivers Vasiļjevs[1, 2], Edgars Kuka[1], Monta Druviņa[1, 2], Dace Cīrule[1]**

[1]Latvian State Institute of Wood Chemistry, Latvia,
lotars.vasiljevs@kki.lv , edgars.kuka@kki.lv ,
monta.druvina@kki.lv , dace.cirule@kki.lv
[2]University of Latvia, Latvia

## Background

Data from 2017 indicate that approximately 6.5 million m³ of pressure-treated wood is manufactured in Europe each year, of which 14% consists of utility poles (Chronopoulos et al. 2020). When the need for removing arises, the withdrawn poles are discarded in landfills (Hasanagić et al. 2026).

Softwoods are most commonly used for the production of utility poles, although the use of specific wood species depends on location and climate (Mitchell et al. 2026, Temiz et al. 2014). Nowadays, copper-based preservatives have replaced chromated copper arsenate. Quats and azoles are included in the preservatives to ensure their efficacy against copper-tolerant fungi. In addition, these systems contain ammonia and/or monoethanolamine to form water-soluble copper complexes (Lim et al. 2020). These complexes diffuse into the wood cell walls and react with cellulose and lignin to form water-insoluble complexes via ion exchange. Ion exchange is promoted by the dissociation of acidic wood groups due to the basic nature of the preservatives (pH 9–10) (Schultz et al. 2014, Lee et al. 2010). However, these chemical reactions may result in a decrease in physical performance of wood material (Simsek et al. 2010).

The present study determines the changes in wood caused by preservative treatment. This is the first step to evaluate the influence of the time factor on the wood properties of removed utility poles after different service lives.

**Keywords:** copper-based preservatives, wood impregnation, wood properties

## Experimental

Three groups of industrially produced utility poles of pine (*Pinus sylvestris* L.) were used in the study: untreated reference (REF), impregnated with ACQ (alkaline copper quat) and CA (copper azole) type preservatives. Each group was represented by 10 poles.

**Capillary water absorption (CWA)** test was carried out through radial surface of cubes measuring 20 × 20 × 20 mm, with four faces adjacent to the tested surface sealed. The increase in mass after submerging 2 mm in water for 2, 6 and 24 hours was recorded.

**Equilibrium moisture content (EMC)** was assessed using wood particles obtained from milling the outer 1 cm of the poles. The difference between wood particles mass at oven-dried and conditioned at different relative humidities was recorded.

**Impact bending strength (IB)** was determined with wood samples measuring 150 × 10 × 10 mm and annual ring orientation strictly parallel to one edge. Both the radial and tangential surfaces were exposed to the hammer strike.

## Results and Discussion

CWA of wood is influenced by many factors, including anisotropic anatomical properties, which makes it difficult to predict liquid flow (Cirule et al. 2019). CWA test results showed that REF absorbed liquid water at a higher rate than impregnated wood. Between both preservatives, CA absorbed at a higher rate than ACQ. It is known that wood treated with waterborne preservatives is susceptible to swelling, but liquid uptake can depend on the amount of precipitated copper inside the wood capillaries system (Lee et al. 2010, Wang et al. 2018). Correlation can be observed between CWA and EMC results (Figure 1a).

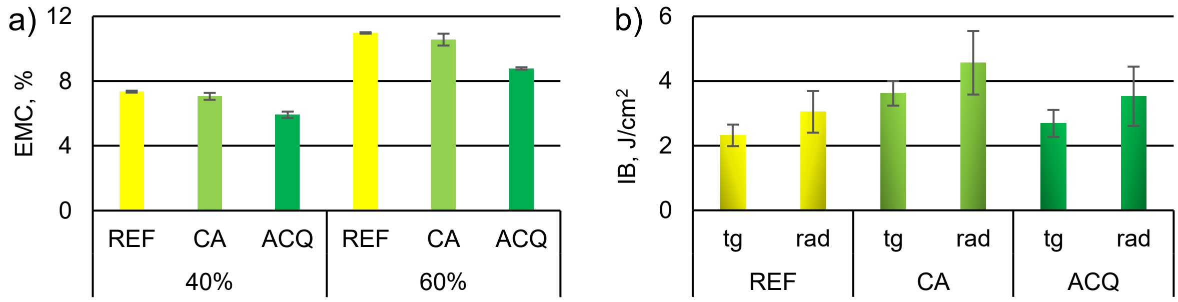


Figure 1. Wood properties a) Equilibrium moisture content (EMC) of wood conditioned at RH 40% and RH 60 %, b) Impact bending strength (IB) performed on tangential (tg) and radial (rad) surfaces; untreated wood (REF), coper azole (CA) and alkaline copper quaternary (ACQ) treated

REF had the highest EMC, which was followed by CA and ACQ. Lower EMC for treated wood can be explained by copper complexes occupying water adsorption sites, but it is also dependant on the particular preservative system, because some may even increase wood hygroscopicity (Mitchell et al. 2010). In the present study, higher copper retention (data not shown) correlated with lower EMC, which agrees with the statement of Cao and Kamdem (2004). Inconclusive results have been reported regarding the effect of preservative treatment on mechanical properties of wood (Criscuolo et al 2019, Aguayo et al 2022). IB results (Figure 1b) did not indicate a correlation between copper retention in wood and material resistance to dynamic shock. REF and ACQ samples had similar resistance, while CA samples had the highest IB, although it also had the highest deviation in results.

## Conclusions

The results of this study demonstrate that impregnation with waterborne copper preservatives can alter the physical characteristics of wood. The CWA and EMC results indicated a correlation between copper retention and the quantity of absorbed water, which is consistent with findings reported in the literature. However, the IB results did not indicate a correlation between preservative treatment and physical toughness. These findings will serve as a point of reference when the same tests and analyses are performed on weathered materials that have reached the end of their service life.

## Acknowledgement

This research was funded by the European Regional Development Fund under project No. 1.1.1.3/1/24/A/012 “Sustainable reuse of wood from removed utility poles (SuReUP)”.

## References

Aguayo MG, Erazo O, Montero C, Reyes L, Gacitua W, Gómez L, Torres H (2022) Analyses of Impregnation Quality and Mechanical Properties of Radiata Pine Wood Treated with

Copper Nanoparticle- and Micronized-Copper-Based Wood Preservatives. Forests, 13: 1636.

Cao J, Kamdem DP (2004) Moisture adsorption characteristics of copper-ethanolamine (Cu-EA) treated Southern yellow pine (Pinus spp.). Holzforschung, 58: 32-38.

Chronopoulos G, Cakmak GE, Tempany P, Klein G, Brinkmann T, Zerger B, Roudier S (2020) Best Available Techniques (BAT) Reference Document on Surface Treatment Using Organic Solvents including Preservation of Wood and Wood Products with Chemicals. Industrial Emissions Directive 2010/75/EU Integrated Pollution Prevention and Control.

Cirule D, Verovkins A, Andersone I, Kuka E, Andersons B (2020) Thermally modified birch wood interaction with liquids. Eur. J. Wood Wood Prod., 78: 849-857.

Criscuolo A, Criscuolo G, Almeida T, Christoforo A, Rocco Lah, F (2019) Influence of treatment with water-soluble CCB preservative on the physical-mechanical properties of brazilian tropical timber. Mater. Res., 22.

Hasanagić R, Japić E (2026) Wood reuse potential in the circular wood industry of Bosnia and Herzegovina. In: Proceedings IRG Annual Meeting (IRG57), Beijing, May 25-28, IRG 26-50423.

Lee MJ, Cooper P (2010) Copper monoethanolamine adsorption in wood and its relation with cation exchange capacity (CEC). Holzforschung, 64(5): 653 – 658.

Lim H, Tripathi S, Tang JD (2020) Bonding performance of adhesive systems for cross-laminated timber treated with micronized copper azole type C (MCA-C). Constr. Build. Mater., 232.

Mitchell M, Link R, Zelinka S, Glass S (2010) Water Vapor Sorption Isotherms for Southern Pine Treated with Several Waterborne Preservatives. J. Test. Eval., 38.

Mitchell P, Harris M, Strandgard M, Singh T (2026) End-of-life utility poles in Australia: Quantifying the resource and pathways for timber circularity. In: Proceedings IRG Annual Meeting (IRG57), Beijing, May 25-28, IRG 26-50422.

Schultz, TP, Goodell B, Nicholas DD (2014) Deterioration and Protection of Sustainable Biomaterials. ACS Symposium Series, 1158: 217–225.

Simsek H, Baysal E, Peker H (2010) Some mechanical properties and decay resistance of wood impregnated with environmentally-friendly borates. Constr. Build. Mater., 24(11): 2279-2284.

Temiz A, Alfredsen G, Gezer ED, Umit C (2014) Leaching and decay resistance of alder and pine wood treated with copper based wood preservatives. Maderas Ciencia y Tecnología, 16(1), 63 – 76.

Wang J, Zhong H, Ma E, Cao J (2018) Properties of wood treated with compound systems of paraffin wax emulsion and copper azole. Eur. J. Wood Wood Prod., 76(1).

# Densification of Aspen Veneer

**Silvi Treial[1], Loretta Kalju[1], Matilda Vitsut[1], Heikko Kallakas[1], Anti Rohumaa[1]**

[1]Tallinn University of Technology, Estonia
silvi.treial@taltech.ee

## Background

European aspen (Populus tremula L.) is a fast-growing pioneer species that readily colonizes areas affected by fire, windthrow and harvesting (Sibul 2025). Despite its availability, aspen is still under-utilized in higher-value applications such as veneer-based composites. One possible approach for upgrading aspen veneer is densification, which can improve density, hardness and surface quality through compression of the wood structure (Bekhta et al. 2014; Cabral et al. 2022).
Conventional densification processes may require high temperatures or chemical modification, increasing energy consumption and manufacturing costs. Moisture-assisted densification offers a lower-energy alternative because water acts as a plasticizer, increasing the deformability of wood at moderate temperatures (Navi and Sandberg 2012).
This study investigates the effects of pre-conditioning relative humidity and pressing temperature on the properties of densified aspen veneers. The objective was to determine how moderate pressing temperatures combined with controlled moisture conditions affect veneer density, surface roughness, Brinell hardness and dimensional stability without the use of chemical treatments.

**Keywords:** densification, aspen veneer, surface qualities

## Experimental

European aspen logs were rotary peeled into veneers with an initial thickness of 3.34 mm. Samples were conditioned at either 65% or 90% relative humidity at 20 °C for approximately one week. The veneers were compressed radially at 6 MPa for 20 min. Cooling was subsequently carried out for 10 min at the same position while maintaining pressure. Different pressing temperatures from 80 °C to 120 °C in 10-degree increments were investigated.
Density, compression ratio and moisture content were determined from measurements taken immediately before and after densification. Surface roughness was measured using Mitutoyo Surftest SJ-210 equipped with a 90° 5 µm stylus. Brinell hardness was evaluated according to EN 1534. Dimensional stability was measured after 24 hours of submersion in water.

## Results and Discussion

Density and compression ratio increased with temperature up to 110 °C, reaching their highest values at this temperature, but decreased at 120 °C. Veneers conditioned at 90% RH generally showed slightly higher values than those conditioned at 65% RH, although the groups overlapped considerably. Temperature significantly affected density ($p < 0.001$), whereas the effect of conditioning RH was not significant ($p = 0.074$). Overall initial density increased from an average of 443 kg/m$^3$ to an average of 838 kg/m$^3$. Densification at 120 °C was not efficient as moisture evaporated too rapidly during pressing and the plasticization effect was lost.

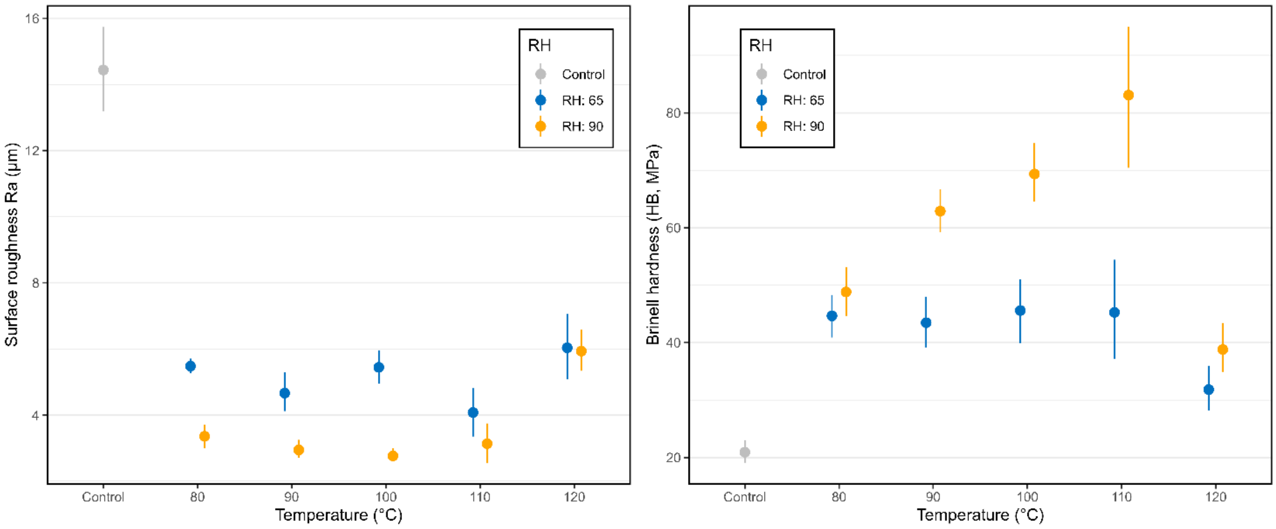


Figure 1. Effect of densification temperature and conditioning relative humidity on surface roughness (left) and Brinell hardness (right) of aspen veneers. Points represent mean values, and error bars indicate 95% confidence intervals

Densification substantially improved both surface roughness and Brinell hardness compared with the untreated control. The smoothest and hardest surfaces were generally obtained at 90–110 °C, particularly for veneers conditioned at 90% RH. Both temperature and conditioning RH significantly affected surface roughness and hardness ($p < 0.001$), although temperature explained the larger proportion of the variation.
At 65% RH, set recovery remained relatively high across the temperature range. In contrast, the 90% RH specimens showed a stronger temperature response, with the lowest set recovery (75%) obtained at 100 °C. Both temperature and conditioning RH significantly affected set recovery (p < 0.001), with RH having the stronger overall effect.

## Conclusions

Overall, the results indicate that the most favourable combination of properties was achieved using high pre-conditioning humidity and pressing temperatures between approximately 100 °C and 110 °C. These conditions provided effective densification together with improved surface smoothness, hardness and dimensional stability. These findings demonstrate that optimizing both densification temperature and moisture conditioning is essential for balancing mechanical performance with long-term dimensional stability.

**References**

Bekhta P, Proszyk S, Krystofiak T, Mamonova M, Pinkowski G, Lis B (2014) Effect of thermomechanical densification on surface roughness of wood veneers. Wood Material Science & Engineering 9(4): 233–245. DOI: 10.1080/17480272.2014.923042.

Cabral JP, Kafle B, Subhani M, Reiner J, Ashraf M (2022) Densification of timber: a review on the process, material properties, and application. Journal of Wood Science 68: 20. DOI: 10.1186/s10086-022-02028-3.

Navi P, Sandberg D (2012) *Thermo-Hydro-Mechanical Processing of Wood*. EPFL Press, Lausanne. DOI: 10.1201/b10143.

Sibul I (2025) Harilik haab – metsakujundaja ja elupaikade looja. Loodusajakiri, 30 December 2025. Available at: https://www.loodusajakiri.ee/aasta-puu-harilik-haab-metsakujundaja-ja-elupaikade-looja/

# A Matter of Location: Water Distribution in Modified Wood in the Full Moisture Range

**Maria Fredriksson[1], Muhammad Awais[2], Christoph Hötte[3], Holger Militz[3], Lauri Rautkari[2], Emil Engelund Thybring[4]**

[1]Division of Buildings Materials, Lund University, Lund, Sweden, maria.fredriksson@byggtek.lth.se,
[2]Department of Bioproducts and Biosystems, Aalto University, Espoo Finland, muhammad.awais@aalto.fi, lauri.rautkari@aalto.fi
[3]Department of Wood Biology and Wood, Georg-August-University Göttingen, Göttingen, Germany, christoph.hoette@uni-goettingen.de, holger.militz@uni-goettingen.de
[4]Bioresource Chemistry and Technology, University of Copenhagen, Frederiksberg, Denmark, eet@ign.ku.dk

## Background

Water in wood can be present both within and outside of cell walls, and water in both locations affect the degradability by wood degrading fungi. Chemical wood modification is one way to prevent fungal degradation and it most commonly alters the wood-water interactions (Zelinka et al. 2022). Designing materials where the wood-water interactions are altered differently within and outside cell walls, would facilitate studies on how the amount and location of water affect the degradability by wood degrading fungi. In addition, although fungal degradation occurs at high non-saturated moisture levels, most studies on wood-water interactions of modified wood are performed in the hygroscopic moisture range. In the present study, we explored how a range of wood modifications affect the amount and location of water. The study was performed in the full moisture range separating water within and outside of cell walls at high moisture states.

**Keywords:** moisture, sorption, moisture content, wood modification**.**

## Experimental

Mature sapwood of Norway spruce (*Picea abies* (L.) Karst.) from Vindeln experimental forests in the northern parts of Sweden (Fredriksson et al. 2016) were cut to dimensions of 15 x 10 x 4 mm$^3$ where 4 mm was in the longitudinal direction. The mass after drying in vacuum oven at 60 °C was determined. Some specimens were then left untreated while others were exposed to the following treatments. Delignification was performed by impregnation with a glacial acetic acid and hydrogen peroxide solution and then the specimens were kept at 60 °C for 270 min as described by Frey et al. (2018). Acetylation was performed by impregnation with acetic anhydride and pyridine (then kept at 80 °C for 3 h) and only acetic anhydride (then kept at 75 °C for 24 h) according to the procedure described by Digaitis et al. (2021) to achieve both uniform acetylation and acetylation of only the cell wall-lumen interface. Hexanoylation was performed by impregnation with hexanoic anhydride, and the specimens were then kept at 80 °C for 270 min. Modification with paraformaldehyde was performed as described by Awais et al. (2022) with a reaction time of 24 h at 100 °C. Modification with DMDHEU was performed by impregnation with an aqueous DMDHEU solution with magnesium nitrate ($Mg(NO_3)_2$) as a catalyst. Curing was performed in an oven with stepwise increasing temperature, ending with a final step at 120°C for 24 h.

Hygroscopic desorption and absorption isotherms were determined by an automatic sorption balance (DVS Intrinsic, Surface Measurement Systems, UK) from vacuum saturated state. In addition, specimens were conditioned by pressure plate at 99.93% relative humidity (Fredriksson and Thybring 2019). For these specimens as well as water saturated specimens, cell wall water and capillary water were separated using Differential Scanning calorimetry (DSC) similarly as in Fredriksson and Thybring (2019).

## Results and Discussion

The cell wall sorption isotherms, the moisture exclusion efficiency, and the capillary moisture content at 99.93% relative humidity are shown in Figure 1. In general, the relative humidity dependence of the moisture exclusion efficiency differed in the hygroscopic and the over-hygroscopic moisture ranges and for many modifications, moisture was excluded more efficiently from cell walls in the over-hygroscopic range. In addition, the different modifications altered the amount of capillary water differently.

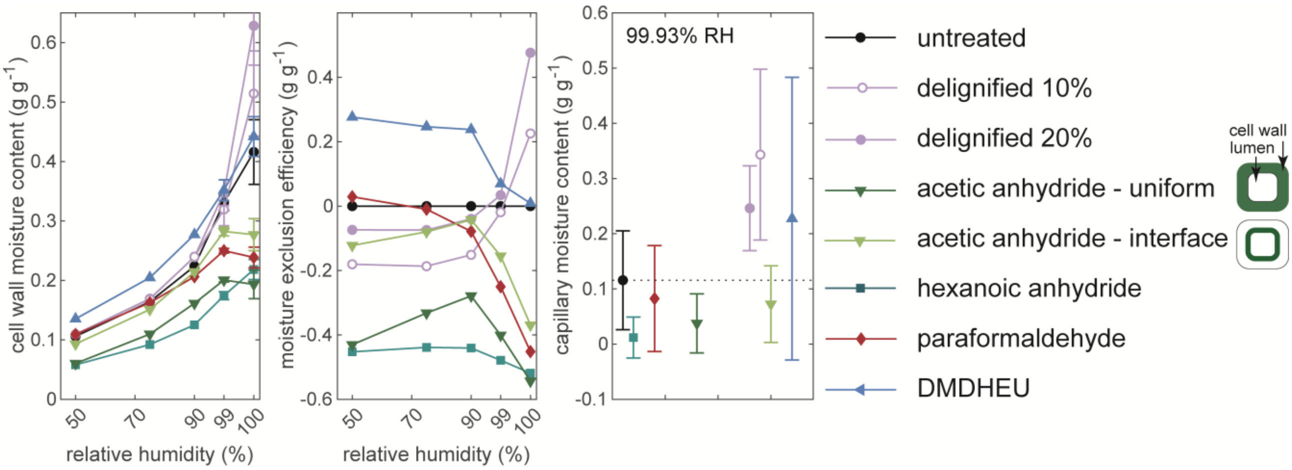


Figure 1. The cell wall sorption isotherms, moisture exclusion efficiency and capillary moisture content for the differently modified specimens and untreated controls. Note that the x-axis is cut to better visualize the data points at 99.93% and 100% relative humidity. Moisture contents were calculated based on the dry mass before modification

## Conclusions

The moisture exclusion efficiency of cell walls was generally different between the hygroscopic and the over-hygroscopic range highlighting that results from the hygroscopic range not necessarily can be extrapolated to higher moisture states. The wood-water interactions could be altered differently in different parts of the wood structure, achieving both higher and lower cell wall and capillary moisture contents compared to untreated wood. This opens up for systematic studies on how wood degradation by fungi is affected by both amount and location of water within the wood structure.

**References**

Awais, M., Altgen, M., Belt, T., Teräväinen, V., Mäkelä, M., Altgen, D., Nopens, M. and Rautkari, L. (2022). Wood–water relations affected by anhydride and formaldehyde modification of wood. ACS Omega 7: 42199-42207.

Digaitis, R., Thybring, E. E., Thygesen, L. G. and Fredriksson, M. (2021). Targeted acetylation of wood: a tool for tuning wood-water interactions. Cellulose 28: 8009-8025.

Fredriksson, M. and Thybring, E. E. (2019). On sorption hysteresis in wood: Separating hysteresis in cell wall water and capillary water in the full moisture range. PLOS ONE 14: e0225111.

Fredriksson, M., Wadsö, L., Johansson, P. and Ulvcrona, T. (2016). Microclimate and moisture content profile measurements in rain exposed Norway spruce (*Picea abies* (L.) Karst.) joints. Wood Material Science & Engineering 11: 189-200.

Frey, M., Widner, D., Segmehl, J. S., Casdorff, K., Keplinger, T. and Burgert, I. (2018). Delignified and densified cellulose bulk materials with excellent tensile properties for sustainable engineering. ACS Applied Materials & Interfaces 10: 5030-5037.

Zelinka, S. L., Altgen, M., Emmerich, L., Guigo, N., Keplinger, T., Kymäläinen, M., Thybring, E. E. and Thygesen, L. G. (2022). Review of wood modification and wood functionalization technologies. Forests 13: 1004.

# Weathering Performance and Life Cycle Impact of Biofinish Coating and Flame-Charring

**Ulrich Hundhausen**[1], **Johann Kristian Næss**[2]

[1,2]NTI (Norwegian Institute of Wood Technology),
uhun@treteknisk.no, jkn@treteknisk.no

## Background

Conventional exterior wood coatings are predominantly based on synthetic polymer binders derived from petrochemical feedstocks. Despite significant progress in the development of bio-based binders in recent years (Mann and Eschig 2025), alternative wood façade treatments with potentially lower environmental impacts are gaining interest in contemporary architecture, including flame-charring (Bahrami et al. 2023) and Biofinish (Poohphajai et al. 2024). Both treatments produce dark grey to black wood surfaces, but through fundamentally different mechanisms: charred wood relies on a carbonised surface layer (Hasburgh et al. 2021), whereas Biofinish is based on a melanised biological layer formed by the fungus *Aureobasidium pullulans* (Poohphajai et al. 2024). Both treatments, however, have different challenges: the char layer is prone to erosion (Kymäläinen et al. 2022), whereas the development of the Biofinish film is gradual and depends on fungal colonisation and growth after application. Melanin production, which contributes to the characteristic dark colour, is promoted by UV radiation (Hernandez and Evans 2015). This contrast motivated a direct comparison of their weathering stability and maintenance requirements under Norwegian exposure conditions; in addition, their life cycle impacts were compared with those of a commercial black alkyd-acrylic paint system.

**Keywords:** fungal Biofinish, Aureobasidium pullulans, flame-charring, yakisugi, shou sugi ban, wood surface treatments, weathering stability, life cycle assessment

## Experimental

The study investigated the following influences on the general appearance, flaking and colour of the surface treatments: wood species (*Picea abies* vs. *Pinus sylvestris*), surface roughness (fine sawn vs. planed), application method (brushing vs. spraying), application rate of Biofinish (1 coat vs. 2 coats), artificial UV exposure after Biofinish application (with vs. without UV), coating of the char layer to reduce erosion (no coating vs. linseed oil vs. Biofinish vs. alkyd oil), and climate conditions (mild lowland vs. high-elevation mountain climate). Specimens were exposed to natural weathering according to EN 927-3:2019 (CEN 2019) at 45° at two locations representing a mild lowland climate (180 m a.s.l.) and a high-elevation mountain climate (930 m a.s.l.). In addition, cladding boards were exposed at 90° (vertical full façade) at a third location. Artificial weathering was performed according to EN 927-6:2018 (CEN 2018). After treatment, the wood surfaces were examined by light microscopy to determine thickness and penetration of the treatments. Artificial weathering was performed for 1512 h, natural weathering at 45° for 49 weeks. Natural weathering at 90°, starting in December 2020, is still ongoing. The appearance of the specimens was assessed before exposure and after exposure applying the rating according to EN ISO 4628-

1:2016. In addition, colour analyes in the CIELAB space was done on the EN 927-3 and -6 specimens.

In the LCA, the functional unit was 1 m² black coated softwood cladding with an expected lifetime of 60 years. Five alternatives were considered: 1) linseed oil pressure impregnation + 3 coats Biofinish, 2) 1 coat linseed oil + 3 coats Biofinish, 3) 3 coats Biofinish, 4) Flame-charred, 5) 1 coat alkyd primer + 2 black hybrid (acrylic/alkyd) top coats. The following maintenance regimes were assumed for the five alternatives based on experience with the specific or similar treatments: 1), 2) and 3) 1 coat with Biofinish every 5 year; 4) 1 coat with a black waterborne alkyd-based oil every 3 year; 5) Cleaned with an anti-mould preservative every 2 year and 1 coat every 8 year. The covered modules were cradle-to-gate (A1-A3) and maintenance (B2).

## Results and Discussion

Charred cladding showed pronounced erosion in all weathering test. The post-treatments, namely linseed oil, Biofinish and alkyd oil, stabilised the char layer only to a limited extent. Compared with charred cladding, Biofinish-treated cladding was initially lighter in colour but developed a considerably more uniform appearance after weathering.

Two industrially applied coats of Biofinish produced a darker surface than a single coat, although a fully opaque black appearance was not achieved. The colour became substantially darker when an additional coat was applied to selected cladding boards after 17 months of outdoor exposure, and two maintenance coats resulted in a uniformly black appearance on both spruce and pine. On pine, however, the black Biofinish was later disturbed by resin exudation from knots and fatwood. By contrast, the latest inspection of the façade in August 2026 showed that the Biofinish on spruce still did not require repainting 51 months after the two maintenance coats had been applied.

Artifical UV treatment after Biofinish application resulted in slightly darker surfaces but no clear effect on overall performance was demonstrated. For planed surfaces, spray application rather than industrial brushing was necessary to achieve satisfactory coating quality and coverage.

In the LCA that considers the overall GWP for modules A1–A3 and B, painted cladding (alternative 5) ranks best, followed by Biofinish-treated cladding and charred cladding (Table 1). The ranking is largely explained by differences in maintenance frequency. The substantial influence of maintenance requirements on the environmental performance of exterior wood cladding has previously been demonstrated (Plesser et al. 2013). Furthermore, the results show a clear negative impact of linseed oil, which becomes especially apparent when the three Biofinish treatments are compared with each other: alternatives 1, 2 and 3.

Table 2. Carbon footprint GWP100a IOBC kg $CO_2$ eq/m$^2$ (without biogenic $CO_2$)

| Alternative | A1 to A3 | B | A1 to A3+B |
|---|---|---|---|
| 1. Linseed oil impregnation + Biofinish | 2.33 | 2.84 | 5.2 |
| 2. Linseed oil (brushed) + Biofinish | 1.80 | 2.84 | 4.6 |
| 3. Biofinish | 1.49 | 2.84 | 4.3 |
| 4. Carbonised | 1.35 | 3.93 | 5.3 |
| 5. Conventional black coating | 1.93 | 2.06 | 4.0 |

**References**

Bahrami A, Hornborg A, Persson S, Norén J, Asplin BB (2023) Evaluation of untreated and surface-treated wooden facades of buildings in Sweden. Coatings 13: 746

European Committee for Standardization. (2016). Paints and varnishes - Evaluation of degradation of coatings - Designation of quantity and size of defects, and of intensity of uniform changes in appearance - Part 1: General introduction and designation system (ISO 4628-1:2016). CEN.

European Committee for Standardization. (2018). Paints and varnishes – Coating materials and coating systems for exterior wood – Part 6: Exposure of wood coatings to artificial weathering using fluorescent UV lamps and water (EN 927-6:2018). CEN.

European Committee for Standardization. (2019). Paints and varnishes – Coating materials and coating systems for exterior wood – Part 3: Natural weathering test (EN 927-3:2019). CEN.

Hasburgh LE, Zelinka SL, Bishell AB, Kirker GT (2021) Durability and fire performance of charred wood siding (Shou Sugi Ban). Forests 12: 1262.

Hernandez VA, Evans PD (2015) Technical note: Melanization of the wood-staining fungus Aureobasidium pullulans in response to UV radiation. Wood Fiber Science 47:120–124.

Kymäläinen M, Sjökvist T, Dömény J, Rautkari L (2022) Artificial weathering of contact-charred wood - The effect of modification duration, wood species and material density. Materials 15: 3951.

Mann J, Eschig S (2025) Sustainable bio-based functional additives for adhesives and coatings – A review. Next Sustainability 6: 100151.

Plesser TSW, Kristjansdottir T, Tellnes L, Flæte PO, Gobakken LR, Alfredsen G (2013) Miljøanalyse av trefasader [Environmental analysis of wooden façades]. SINTEF Fag 5. SINTEF akademisk forlag, Oslo. ISSN 1894-1583; ISBN 978-82-536-1339-0

Poohphajai F, Gubenšek A, Černoša A, Butina Ogorelec K, Rautkari L, Sandak J, Sandak A (2024) Bioinspired living coating system for wood protection: Exploring fungal species on wood surfaces coated with Biofinish during its service life. Coatings 14: 430.

# Evaluation of Antifungal Properties of Biomass-Derived Hydrolysates as Wood Preservatives

**Jasmina Jusic[1,2], Swati Tamantini[1], Eli Krzic[3], Andreja Zagar[3], Miha Humar[3], Dominik Matt[2], Manuela Romagnoli[1]**

[1]Department of Innovation in Biological, Agro-Food and Forest Systems (DIBAF), University of Tuscia, Viterbo, 01100 Italy, jasmina.jusic@unitus.it, swati.tamantini@unitus.it
[2] Fraunhofer Italia Research Innovation Engineering Center, Bolzano 39100, Italy,
[3]University of Ljubljana, Biotechnical Faculty, Department of Wood Science and Technology, Jamnikarjeva 101, SI-1000 Ljubljana, Slovenia

## Background

Copper-based preservatives are widely used to protect wood against decay fungi, but Cu mobility and leaching can reduce long-term efficacy and increase environmental release (Richardson 1997; Humar et al. 2004**)**. Improving Cu fixation while incorporating renewable or waste-derived components could therefore contribute to more sustainable wood-protection systems. Natural extractives and phenolic-rich biomass derivatives have been investigated for their interactions with wood and metals (Vek et al. 2020), but the use of hydrolysates derived from chestnut-processing residues in Cu-based preservatives remains insufficiently explored. This study evaluated hydrolysates from detannized chestnut wood and bark as bio-based additives to $CuSO_4$ treatments of Scots pine (*Pinus sylvestris* L.). Their performance was assessed in terms of fungal decay resistance and Cu release during water leaching, with the aim of determining whether chestnut residues can enhance Cu-based preservation while providing a route for biomass valorisation.

**Keywords:** chestnut residues, lignocellulosic hydrolysates, copper fixation, wood preservation, Scots pine, decay resistance, circular bioeconomy

## Experimental

Detannized chestnut wood and bark residues were hydrolysed with 5% $H_2SO_4$ at 200 °C for 90 min. The resulting hydrolysates were combined with $CuSO_4{\cdot}5H_2O$ at 0.5, 0.75 and 1% Cu and applied to Scots pine sapwood by vacuum-pressure impregnation; $CuSO_4$ in water at the same concentrations served as controls. Decay resistance was evaluated using a modified EN 113 mini-block test (EN 113-1:2021)) against *Coniophora puteana* for 12 weeks, with oven-dry mass loss as the response variable. Cu release was determined by XRF during five sequential water-leaching cycles.

## Results and Discussion

Addition of chestnut-derived hydrolysates improved the decay resistance of Cu-treated Scots pine, although the magnitude of the effect depended on hydrolysate type and Cu concentration (Fig. 1). The clearest response was obtained with detannized wood hydrolysate (D). At 0.75% Cu, mean mass loss after 12 weeks of exposure to *Coniophora puteana* decreased from approximately 8.4% for $CuSO_4$ in water (W) to 5.9% with D ($p$adj $< 0.001$). At 1% Cu, D similarly reduced mass loss from 10.3% to 7.7% ($p$adj $= 0.004$).

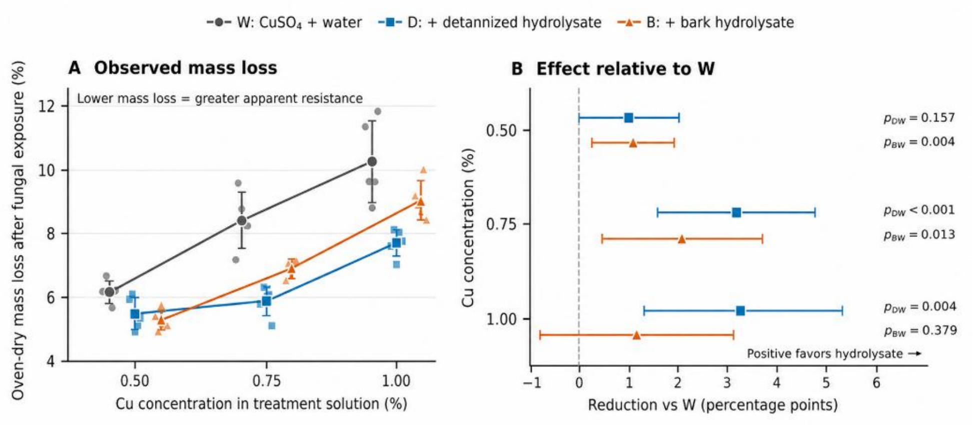


Figure 1. Effect of chestnut-derived hydrolysates on decay resistance of Cu-treated Scots pine. (A) Oven-dry mass loss after fungal exposure at different Cu concentrations. (B) Reduction in mass loss relative to the $CuSO_4$-water control

Bark hydrolysate (B) also improved resistance at 0.5 and 0.75% Cu ($p$adj = 0.004 and 0.013, respectively), whereas its effect at 1% Cu was not significant. These results show that the benefit of the hydrolysates cannot be attributed simply to increasing Cu concentration and instead depends on formulation. The decay-resistance response was accompanied by lower Cu release during water leaching at the two higher Cu concentrations (Fig. 2). After five leaching cycles, cumulative Cu release at 1% Cu decreased from 161 XRF units for W to 142 and 137 units for D and B, respectively, corresponding to reductions of approximately 12 and 15%. At 0.75% Cu, cumulative release decreased from 143 units for W to 132 for D and 119 for B. This trend was not observed at 0.5% Cu, where D showed the same cumulative release as W and B showed a higher value. Most Cu release occurred during the first leaching cycle.

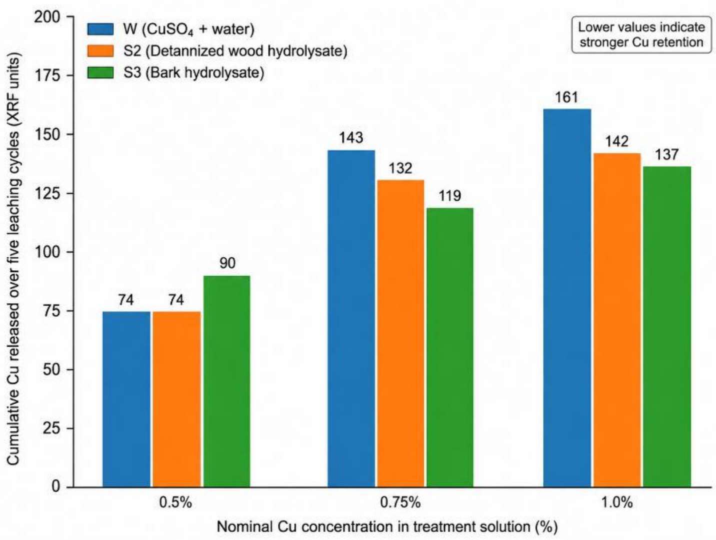


Figure 2. Cumulative Cu released from treated Scots pine during five sequential water-leaching cycles

Together, the biological and leaching results indicate that chestnut-processing hydrolysates can enhance Cu-based wood-preservation systems, with the strongest evidence provided by the reduction in fungal mass loss. Reduced Cu release at 0.75 and 1% Cu is consistent with enhanced interaction between Cu and hydrolysate-derived phenolic components (Pizzi 2008). Contact-angle measurements confirmed pronounced treatment-induced changes in surface wettability, while FTIR spectra showed treatment-associated spectral differences; however, these observations are considered secondary and require further mechanistic analysis.

## Conclusions

Chestnut-derived hydrolysates enhanced the performance of Cu-based wood treatments, with detannized wood hydrolysate showing the most consistent reduction in fungal mass loss. Both hydrolysates also reduced cumulative Cu release at 0.75 and 1% Cu, although this trend was not observed at 0.5% Cu. These findings support the potential valorisation of chestnut-processing residues as bio-based additives for wood preservation, while further replicated leaching studies are needed to confirm improved Cu fixation.

**References**

EN 113-1:2021. Durability of wood and wood-based products — Test method against wood-destroying basidiomycetes — Part 1: Assessment of biocidal efficacy of wood preservatives.

Humar M, Pohleven F, Šentjurc M (2004) Effect of oxalic, acetic acid, and ammonia on leaching of Cr and Cu from preserved wood. *Wood Science and Technology* 37: 463–473.

Pizzi A (2008) Tannins: Major sources, properties and applications. In: Belgacem MN, Gandini A (eds) *Monomers, Polymers and Composites from Renewable Resources*. Elsevier.

Richardson HW (1997) *Handbook of Copper Compounds and Applications*. CRC Press.

Vek V, Balzano A, Poljanšek I, Humar M, Oven P (2020) Improving fungal decay resistance of less durable sapwood by impregnation with Scots pine knotwood and black locust heartwood hydrophilic extractives with antifungal or antioxidant properties. *Forests* 11: 1024.

# SESSION 8: VALORISATION

# Utilization Potential of VOCs Collected During Kiln Drying of Pine and Spruce Timber

**Petri Österberg[1], Tuomas Niskanen[1], Teemu Pätsi[1], Mikko Luomaranta[1], Jasmiina Haverinen[1], Ilkka Leinonen[1], Mika Ruusunen[1]**

[1]University of Oulu, Finland, petri.osterberg@oulu.fi, tuomas.niskanen@oulu.fi, teemu.patsi@oulu.fi, mikko.luomaranta@oulu.fi, jasmiina.haverinen@oulu.fi, ilkka.leinonen@oulu.fi, mika.ruusunen@oulu.fi.

## Background

Volatile organic compounds (VOCs) are major air pollutants in many countries (Seinfeld & Pandis, 2016), and a few countries have set emission restrictions for VOCs evaporated from timber drying in sawmills (BMU, 2021). As environmental legislation tightens, e.g. in the EU, mandatory reductions in VOC emission seem likely in the future. VOCs released during timber drying have been extensively studied (Shen, 2020). However, in discussions with sawmill industry experts, the recovery of VOCs has not been considered profitable. On the other hand, commercially available wood-derived terpenoids may have high per-litre values in specialty chemical markets (Thermo Fischer Scientific, n.d.). An interesting approach that has not been so intensively studied is the utilization of VOC compounds as starting materials to produce valuable chemicals, which could increase interest in VOC recovery, and this is the core of our study described in this paper.

**Keywords:** Kiln drying, Timber VOC emissions, VOC recovery, value of timber VOCs

## Experimental

We studied VOCs emitted from sawn timber first in a laboratory oven and later from the air outlets of drying kilns of three Finnish sawmills. We built an activated carbon-based VOC recovery instrument for the laboratory oven and an improved version for the sawmill drying kilns and collected VOC samples over periods ranging from 1 to 21 hours in the laboratory oven and from 1 to 21 days at the sawmills. We tested the recovery capability of activated carbon (particle size of 3 mm) by evaporating a known amount of pure α-pinene in a glass vessel. The recovery rate of α-pinene was 80%. We analysed the VOC samples collected from the laboratory oven with gas chromatography (GC-MSD) and determined the mass of the evaporated compounds from a certain amount of sawn timber. We extrapolated this to the sawmill environment because it was only possible to collect VOC samples from a small side stream there. Consequently, a very small error in VOC masses increases with heavy extrapolation. The relative proportions of different compounds were obtained from sawmill samples using GC-MSD.

## Results and Discussion

In the analysis of the sawmill VOC samples, we found over 100 different compounds that were emitted from the timber. We examined in more detail approximately fifty compounds whose identification confidence exceeded 95% and conducted a market analysis of these compounds. We focused on finding compounds that best met the following conditions: 1) The compound already has a large existing market, and 2) The value of the compound relative to its production yield is high. This means that the price per liter of a low-yield compound must be very high to be worth considering.

Tables 1 and 2 show the value of the seven most important compounds evaporated from pine and spruce timber at a medium-sized sawmill producing 400,000 $m^3$ of sawn timber per year, if only one of the two wood species is used. As shown in Tables 1 and 2, α-pinene dominated in the analyses: It explained 77% of the value of all VOCs evaporated from pine timber and 33% from spruce timber, respectively. The next most important compound α-terpineol accounted for 11% of the value of VOCs in pine while limonene accounted for 15% in spruce respectively.

Tables 1 and 2. Annual value of the most valuable VOCs (purity > 95%) from a medium-sized sawmill if only one of the two wood species is used

| **PINE** (400 000 $m^3$) | |
|---|---|
| **Molecule** | **Turnover price per ton** |
| α-pinene | 216,000 € |
| α-terpineol | 32,000 € |
| Limonene | 15,000 € |
| β-pinene | 5,000 € |
| 3-carene | 4,000 € |
| Myrcene | 4,000 € |
| Methyl eugenol | 3,000 € |
| **Sum** | **279,000 €** |

| **SPRUCE** (400 000 $m^3$) | |
|---|---|
| **Molecule** | **Turnover price per ton** |
| α-pinene | 138,000 € |
| Limonene | 64,000 € |
| trans-Pinocarveol | 62,000 € |
| β-pinene | 54,000 € |
| α-terpineol | 39,000 € |
| Germacrene D | 33,000 € |
| Fenchol | 30,000 € |
| **Sum** | **420,000 €** |

It should be noted that not all compounds could be identified because the GC-MS library did not contain matching reference spectra for all detected compounds, even though the library included approximately 65,000 compounds. We also identified compounds for which there was no market or a very limited market where large quantities of the compounds could not be sold. However, the situation may improve in the future through new inventions and applications. The market value of these compounds may also increase if demand grows.

## Conclusions

We found that the value of the most valuable VOC compounds emitted from sawn timber is estimated at several hundred thousand euros per year for a medium-sized sawmill. However, this would increase the sawmill's revenue by less than one percent. The recovery of VOC compounds could be economically justified, at least to cover the associated costs, if VOC emissions from sawmills need to be reduced due to tightening environmental legislation. Most of the economic and environmental benefits could be achieved by focusing primarily on the recovery of α-pinene. From a technological perspective, it would be easier to separate and commercialize chemically related compounds as compounds groups.

**References**

Bundesministerium für Umwelt, BMU (2021). Technische Anleitung zur Reinhaltung der Luft (TA Luft 2021, Technical Instructions on Air Quality Control issued by the German Federal Ministry for the Environment) )

Seinfeld, J.H. & Pandis, S.N. (2016). Atmospheric Chemistry and Physics: From Air Pollution to Climate Change (3rd ed.). Wiley.

Shen, Y. et al. (2020) Study of VOCs release during drying of plantation-grown Pinus sylvestris and naturally grown Russian Pinus sylvestris. Journal of Wood Science 66, 2020: 1-13.

Thermo Fisher Scientific (n.d.) alpha-Terpineol, 96%. Fisher Scientific. Available at: https://www.fishersci.com/shop/products/alpha-terpineol-96-thermo-scientific/AA1628514 (Accessed: 12 August 2026).

# Unlocking Value from Scots Pine Side Streams

**Mikko Luomaranta[1], Jasmiina Haverinen[1], Tuomas Niskanen[1], Mika Mahosenaho[1], Jarkko Räty[1]**

[1]University of Oulu, Measurement technology unit, Kajaani, Finland, mikko.luomaranta@oulu.fi

## Background

Sustainable utilization of forest tree biomass and the development of renewable green chemicals from the biomass can help reduce reliance on fossil-fuel-derived chemicals. (Zuiderveen *et al*., 2023). One source of this biomass is residual biomass from the forest bioeconomy industry, which is particularly significant in northern European countries. This sector produces large volumes of underutilized conifer biomass side streams, which contain valuable components with potential for high-value applications. Extraction of these components before eventual energy production would derive value from the biomass and would support the circular bioeconomy and cascade use of forest tree biomass.

Due to its complex physicochemical nature, processing lignocellulosic biomass presents challenges, and extraction methods have relied on strong solvents and extensive processing. Greener alternatives, such as supercritical fluid extraction (SFE), have emerged to address environmental and product safety concerns related to traditional methods.

One of the major species with large volumes of biomass residues available in Northern Europe is Scots pine (Pinus sylvestris). The bark is known to contain a diverse range of lipophilic extractives (Barbini *et al*., 2021), while its needles are rich in terpenes and phenolic compounds (Judžentienė & Kupčinskienė, 2006; Kurtiš *et al*., 2026). The chemical profile of these tissues makes them a promising source of bioactive compounds for antimicrobial applications.

In this study, we applied supercritical fluid extraction, a more environmentally friendly extraction approach, to these underutilized residues to characterize the resulting extracts and identify potential applications, including antimicrobial activity relevant to the increasing challenge of drug-resistant microorganisms.

**Keywords:** Super critical fluid extraction, forest tree biomass, antimicrobial extracts**,** Scots pine

## Experimental

Our chemical analysis was performed using gas chromatography-mass spectrometry (GC-MS), with a method adapted from Örså and Holmbom (1994). Antifungal activity of the extracts against *Aspergillus flavus* was assessed using a Bioscreen C automated growth assay (Medina *et al*., 2012). Scots pine bark was extracted by SFE using $CO_2$ at 350 bar and 60 °C for 60–120 min, with or without ethanol as a co-solvent. The agar dilution method was adapted from Alzagameem *et al*. (2019) and Moosavy *et al*. (2008).

## Results and Discussion

GC-MS confirmed that the chemical profile of the pine bark extracts was enriched in sterols (14.59% % of total peak area) and fatty acids (8.19%), the presence of these compounds is known and shown in earlier reports (Barbini *et al*., 2021). The lack of harsh solvents would allow utilization of these extracts, which are enriched in phytosterols and sterol esters, in food industry applications to lower blood cholesterol levels or in natural cosmetics applications (Zorić *et al*., 2022; Shen *et al*., 2024).

In the pine needle extracts terpenes were the most abundant group of components (20.28%). Needles also have an epicuticular wax layer that contains long-chain alkanes, fatty acids, and primary alcohols (Kunst & Samuels, 2003), and various bioactive polyphenols (Metsämuuronen & Siren *et al*., 2019). The chemical profile of the extracts motivated us to perform antimicrobial experiments on various microorganisms utilizing the SFE extracts.

Antimicrobial properties towards bacteria E. coli and S. Aureus on solid media showed that neither extract influenced the growth of Gram-negative E. coli, while both extracts inhibited the growth of S. aureus. Against the fungi A. flavus, only needle extract showed effective inhibition (Figure 1), while bark extract showed no difference from controls. Our results indicate that these extracts could have value in targeted applications, for example in food industry packaging (Pinto *et al*., 2023).

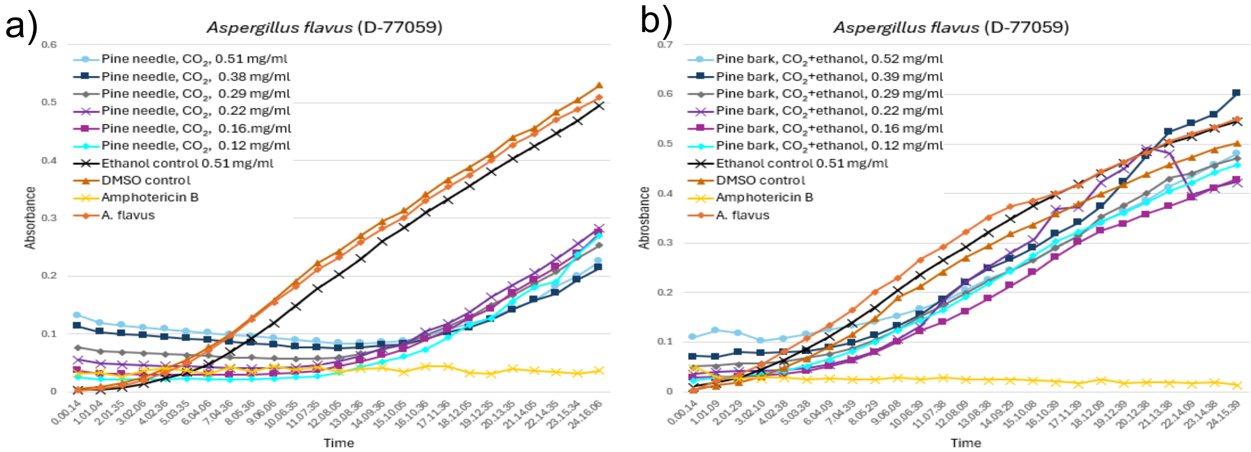


Figure 1. (a) Scots pine needle samples and (b) Scots pine bark samples analyzed using Bioscreen C, with each color representing a different sample. The y-axis display absorbance (420–580 nm) and the x-axis represents time, with measurements presented at 60-min intervals. Samples were analyzed in five replicates in 100-well honeycomb plates and incubated at 37 °C for 24 h 15 min; 1% DMSO, Amphotericin B (0.013 mg/mL), and ethanol (0.51 mg/mL) were used as controls

## Conclusions

Our results indicate that SFE, as a technology, and Scots pine biomass residues are suitable for production of antimicrobial extracts. The lack of harsh solvents allows the use of the extracts in various applications, which can be validated in cytotoxicity experiments. If the economic challenges of large-scale supercritical fluid extraction methods can be addressed, the method has the potential to be utilized to produce environmentally friendly value-added products from the side streams of forest bioeconomy while supporting the cascade use of forest biomass.

**References**

Alzagameem A, Klein SE, Bergs M, Do XT, Korte I, Dohlen S, *et al*. (2019) Antimicrobial activity of lignin and lignin-derived cellulose and chitosan composites against selected pathogenic and spoilage microorganisms. Polymers 11(4): 670.

Barbini S, Sriranganadane D, España Orozco S, Kabrelian A, Karlström K, Rosenau T, Potthast A (2021) Tools for bark biorefineries: Studies toward improved characterization of lipophilic lignocellulosic extractives by combining supercritical fluid and gas chromatography. ACS Sustainable Chemistry & Engineering 9(3): 1323–1332.

Judzentiene A, Kupcinskiene E (2008) Chemical composition on essential oils from needles of Pinus sylvestris L. grown in Northern Lithuania. Journal of Essential Oil Research 20(1): 26–29.

Kunst L, Samuels AL (2003) Biosynthesis and secretion of plant cuticular wax. Progress in Lipid Research 42(1): 51–80.

Kurtiš A, Antić-Stanković J, Bufan B, Božić DD, Krivokapić S, Damjanović-Vratnica B, Perović S (2026) Quantitative analysis of polyphenols and in vitro antioxidant, antimicrobial and toxicity assessments in needles of five Pinus species from Montenegro. Microorganisms 14(1): 170.

Moosavy MH, Basti AA, Misaghi A, Salehi TZ, Abbasifar R, Mousavi HAE, *et al*. (2008) Effect of Zataria multiflora Boiss. essential oil and nisin on Salmonella typhimurium and Staphylococcus aureus in a food model system and on the bacterial cell membranes. Food Research International 41(10): 1050–1057.

Örså F, Holmbom B (1994) A convenient method for the determination of wood extractives in papermaking process waters and effluents. Journal of Pulp and Paper Science 20(12): J361–J366.

Pinto L, Tapia-Rodríguez MR, Baruzzi F, Ayala-Zavala JF (2023) Plant antimicrobials for food quality and safety: Recent views and future challenges. Foods 12(12): 2315.

products to reduce environmental impacts. Nature Communications 14: 8521.

Shen M, Yuan L, Zhang J, Wang X, Zhang M, Li H, Jing Y, Zeng F, Xie J (2024) Phytosterols: Physiological functions and potential application. Foods 13(11): 1754.

Zorić M, Banožić M, Aladić K, Vladimir-Knežević S, Jokić S (2022) Supercritical $CO_2$ extracts in cosmetic industry: Current status and future perspectives. Sustainable Chemistry and Pharmacy 27: 100688.

Zuiderveen EAR, Kuipers KJJ, Caldeira C, Hanssen SV, van der Hulst MK, de Jonge MMJ, Vlysidis A, van Zelm R, Sala S, Huijbregts MAJ (2023) The potential of emerging bio-based

# Continuous Supercritical $CO_2$ Extraction for Extracting Valuable Compounds from Spruce and Pine Sawmill Residue

**Juuso Finne[1], Petri Österberg[1], Henri Hämäläinen[1], Tuomas Niskanen[1], Teemu Pätsi[1], Mika Ruusunen[1]**

[1]University of Oulu, Finland, Juuso.Finne@oulu.fi, Petri.Osterberg@oulu.fi, Henri.Hamalainen@oulu.fi, Tuomas.Niskanen@oulu.fi, Teemu.Patsi@oulu.fi, Mika.Ruusunen@oulu.fi

## Background

In Finland, 11,7 million $m^2$ of softwood lumber were produced in 2025. This process produces also a significant amount of wood residues, such as bark and branches, which are burned for energy at the mills (UPM Timber, 2026). There is potential to exploit the residues further by extracting high value compounds before burning. A promising extraction method for this purpose is the supercritical carbon dioxide extraction (SFE-$CO^2$), due to its clean operation, no organic solvents and no solvent residues in extract (Sookwong & Mahatheeranont, 2017).
Since the late 70's, at industrial scale the SFE-$CO^2$ has been used successfully in different areas such as food, drug, petrochemical and environment (Machado, 2013). The main drawback of the SFE-$CO^2$ is the lack of proven solutions for continuous extraction from solids, which causes the need for multiple large high-pressure reactors and that increases the initial costs for a plant. The objective of this paper was to research and develop a pilot-scale continuous SFE-$CO^2$ for solids. Also increasing the research data for further development of SFE-$CO^2$ solutions.

**Keywords:** softwood lumber residue, continuous supercritical fluid extraction, carbon dioxide**.**

## Experimental

The raw material used, was a slurry containing the solid sample and water or a water-ethanol mixture. The solid samples were spruce and pine bark from sawmills located in northern Finland (and paprika powder from local supermarket for screening the process parameters). The carbon dioxide ($CO^2$) used in the experiments was 99.9% pure and it was provided by a local supplier. The bark and paprika samples were hammer milled to a maximum particle size of 0,5 mm and then mixed to water or a water-ethanol mixture containing around 25 or 50 vol-% of ethanol to form the slurries. The object of the experiments was to raise the solid content in the slurry from 4 m-% (i.e. mass-%) to 15 m-% and run the SFE-$CO^2$ continuously at least 60 min without problems at extraction pressure of 200 bar and temperature of 40–45 ˚C.

### Continuous SFE-$CO^2$

The process starts with charging the reactor with approximately 650 g of water and raising the pressure and temperature to desired extraction conditions 200 bar and 40–45 ˚C respectively. After the extraction conditions are met, the process swaps between two phases, the extraction phase (lasting minutes) and the filling phase (lasting seconds). In the extraction phase, the $CO^2$ circulates through the process countercurrently in relation to the slurry. The desired flow rate is set by a control valve. In the filling phase, the $CO^2$ flow is halted by closing the valve between the reactor and the separator. This allows the slurry level to be controlled more accurately via the slurry pump and the exit valve at the bottom of the reactor. The slurry flow rate is controlled by adjusting the length of filling and extraction phases.

## Results and Discussion

The first experiments started with paprika slurries, because it was found to not swell that much when introduced to liquids. This aided the screening of process parameters for the bark experiments. In total seven runs lasting 60 min were conducted with solid content ranging from 4 m-% to 15 m-% mixed with water, doubling the 13 m-% and 15 m-% with two different slurry flow rates. The runs were completed without any major issues, but it was observed that some of the solid particles ended up flowing to the separator. This also resulted in accumulation of particles at the $CO^2$ flow control valve with a risk of blockage, if the valve was not open enough.

The bark experiments started with spruce. The first 60 min run was completed with solid content of 6 m-% and a water-ethanol mixture at 25 vol-%. The three subsequent runs, with solid content ranging from 8–13 m-% and a water-ethanol mixture at 50 vol-%, ran into blockage problems observed with paprika slurries. The $CO^2$ flow dropped to near zero after 33 min with 8 m-% and 13 m-% slurries and after 51 min with 10 m-% slurry. To combat this issue, a frame supporting five discs 5 cm apart with slits was designed and manufactured. The idea was to minimise the slurry from splashing, due to the $CO^2$ flowing through the slurry, towards the top of the reactor where the line to the separator is located. This structure was then placed inside the reactor, so that the discs are located at the top half of the reactor above the slurry level.

After this installation, the runs were completed without issue, apart from the slurry pump having problems pumping bark slurries reliably with solid content over 12.5 m-%. These runs include 60 min spruce bark runs with solid contents of 11 m-% and 12 m-% in water, a longer 209 min run with 10 m-% solid content in water and two pine bark runs with solid contents of 10 m-% and 12.5 m-% in water and run durations of 75 min and 94 min respectively. The longer runs were aborted due to all the prepared slurry been processed rather than any system failure.

## Conclusions

The objective of developing a fully continuous pilot-scale SFE-$CO^2$, that can process solid softwood bark material using slurries as a medium was achieved. The goal of achieving completed run with a slurry containing 15 m-% of solid material was succeeded with paprika powder. With the softwood bark, the goal was nearly achieved with spruce at 12 m-% and pine at 12.5 m-%, due to the pumping challenges brought by the swelling of the milled bark material. Based on these results, further research should focus on getting the solid content of the feed even higher still to improve efficiency and pushing the continuous SFE-$CO^2$ towards industrial scale.

**References**

Machado, B. A. S., Pereira, C. G., Nunes, S. B., Padilha, F. F., & Umsza-Guez, M. A. (2013). Supercritical Fluid Extraction Using $CO^2$: Main Applications and Future Perspectives. Separation Science and Technology, 48(18), 2741–2760.

Sookwong, P., & Mahatheeranont, S. (2017). Supercritical $CO^2$ Extraction of Rice Bran Oil –the Technology, Manufacture, and Applications. Journal of Oleo Science, 66(6), 557-564.

UPMtimber (2026) Sahateollisuus Suomessa [online article in Finnish]. Available from: https://www.upmtimber.com/fi/Artikkeleita/timber/26/sahateollisuus-suomessa/ [Accessed 7 August 2026].

# The Influence of Deep Eutectic Solvents (DES) on the Lignin Content in Pine (*Pinus* Sp.) Wood Biomass

**Jan Szadkowski**[1]

[1]Department of Wood Science and Wood Protection, Institute of Wood Sciences and Furniture, Warsaw University of Life Sciences, 166 Nowoursynowska St., 02-787 Warsaw, Poland, jan_szadkowski@sggw.edu.pl

## Background

The aim of the research was to verify the effect of deep eutectic solvents (DES) on the lignin content in pine (*Pinus* Sp.) biomass in liquid biofuel technology. One alternative energy source with a favorable $CO_2$ equivalent balance for our planet's climate is lignocellulosic biomass. This biomass is produced during plant life through photosynthesis. As plants grow, they absorb carbon dioxide from the atmosphere, using it to synthesize nutrients and building blocks used during plant growth. Synthesized raw materials such as cellulose, hemicelluloses, lignin, etc., enable the capture of one of the key greenhouse gases from the planet's atmosphere, reducing human impact on the greenhouse effect. Plants are also an attractive source of energy resources and raw materials for the chemical and pharmaceutical industries. However, the development of a sustainable economy requires the selective use of available lignocellulosic raw materials. The use of a complex biomass processing system could yield complex raw materials for industries such as the chemical industry, ensuring high quality and environmental friendliness. This approach requires the use of pretreatment of lignocellulosic biomass and green chemistry in the processing of the obtained raw materials. Deep eutectic solvents (DES) are liquids considered green chemistry. Their discovery and development occurred at the beginning of the 21st century. They constitute an environmentally friendly method of biomass digestion. By selecting the appropriate DES solution, selective digestion of biomass can be achieved, removing selected structural components from the raw material. This solution allows for the extraction of high-quality intermediates such as cellulose, lignin, and others. Obtaining high-quality raw materials from lignocellulosic biomass will translate into increased profitability in obtaining liquid biofuels from raw materials such as wood and will enable the use of raw materials currently considered waste, such as lignin. Unlike cellulose or hemicellulose, lignin is an amorphous compound. It constitutes approximately 20-30% of the dry weight of woody biomass. Unlike cellulose or hemicellulose, it is an amorphous compound. Currently, the estimated production of lignin by the pulp and paper industry is around 130 million tons.

**Keywords:** wood, pine, deep eutectic solvents DES, pretreatment**.**

## Experimental

The key element of the study was to examine changes in lignin content in pine biomass as a result of the action of a mixture of choline chloride and lactic acid in a molar ratio of 1:5. The biomass:solvent ratio was 1:10 [g/g]. For the material pretreated with eutectic mixtures (DES), classical chemical composition analyses of woody biomass were performed, focusing on determining lignin content using the TAPPI method, cellulose content using the Kürschner-Hoffer method, and holoceuosis content using the sodium chlorite method. For selected materials, pyrolysis analysis coupled to a gas chromatograph (PY/GC-MS) was performed, and porosity was measured using inverse size exclusion chromatography (ISEC).

## Results and Discussion

The change in the chemical content of pine biomass after pretreatment with deep eutectic solvents is presented in Table 1. As a result of pretreatment, changes in all chemical substances can be observed. The change in cellulose content is a result of the reduction in lignin and hemicelluloses due to DES treatment and increased temperature. Hemicelluloses are the least thermally resistant of the structural substances of lignocellulosic biomass.

Table 1. Results of the content of structural substances after DES pretreatment

| **Chemical Compounds** | **Native** | **DES 90** | **DES 130** | **DES 160** |
|---|---|---|---|---|
| Cellulose [%] | 55,6+/- 0,033 | 69,9+/- 0,022 | 71+/- 0,035 | 76,3+/- 0,053 |
| Holocellulose [%] | 78,3+/- 0,023 | 75,5+/- 0,004 | 76,1+/- 0,020 | 78,1+/- 0,021 |
| Lignin [%] | 21,0 +/- 0,025 | 18,6+/- 0,023 | 19,3+/- 0,017 | 16,1+/- 0,029 |
| Extractive [%] | 0,7 +/- 0,019 | 6,2+/- 0,007 | 7,2+/- 0,023 | 16,1+/- 0,029 |

The greatest change in lignin content was observed after pretreatment at 160°C. Observing the pretreatment results, an apparent increase in cellulose content can be observed, which increases due to a decrease in lignin content. The content of extractives, which incorporate low-molecular-weight substances resulting from the breakdown of hemicelluloses, and lignin also increased.

## Conclusions

The results indicate the high potential of using a choline chloride:lactic acid mixture for lignin removal from woody biomass. For a 1:5 choline chloride:lactic acid mixture at 90ºC and maintained at the process temperature, the lignin content in the pine test material was reduced by 5 percentage points compared to the native material. Increasing the temperature increased this effect to 12 percentage points at 130ºC, for the same process maintenance time. Extending the process time beyond 15 and 60 minutes did not significantly affect efficiency and was within the standard deviation. During the lignin removal process, a reduction in the hemicellulose content was also observed (determined from the difference in holocellulose and Kürschner-Hoffer cellulose content). The results of the pyrolytic analysis showed a decrease in the content of products derived from the thermal decomposition of lignin, such as vanillin.

**References**

Alvira P, Tomás-Pejó E, Ballesteros M, Negro MJ (2010) Pretreatment technologies for an efficient bioethanol production process based on enzymatic hydrolysis: a review. Bioresour Technol 101:4851–4861. https://doi.org/10.1016/j.biortech.2009.11.093

Betlej I, Andres B, Krajewski K, Kiełtyka-Dadsiewicz A, Boruszewski P, Szadkowska D, Zawadzki J, Radomski A, Borysiuk P, (2023) The effect of Ethanol Extracts and Essential Oils Obtained from Different Varieties of Mint on Wood Molding. Forests 2023, 14(8), 1522, DOI - 10.3390/f14081522.

Hill CAS (2007) Wood Modification: Chemical, Thermal and Other Processes. John Wiley & Sons, Southern Gate, Chichester.

Jablonský M., Šima J., (2019) Deep eutectic solvents in biomass valorization, Slovenská Technická univerzita v Bratislave

Kačik F., Solár R., (1999) Analytická Chémia Dreva, Tchnická Univerzta vo Zvolene, Zvolen

Kissoudi, M.; Samanidou, V. Recent Advances in Applications of Ionic Liquids in Miniaturized Microextraction Techniques. Molecules 2018, 23, 1437, https://doi.org/10.3390/molecules23061437

Koshijima, T., Watanabe, T. (2003). Association between lignin and carbohydrates in wood and other plant tissues. In: Springer Series in Wood Science, Timell, T.E., Ed., SpringeeVerlag: New York, NY, USA, 329

Krutul D., (2002) Ćwiczenia z chemii drewna oraz wybranych zagadnień z chemii organicznej, SGGW Warszawa.

Krutul D., Szadkowski J., Vybohová E., Kucerová V., Cabalova I., Antczak A., Szadkowska D., Drożdżek M., Zawadzki J., Effect of steam explosion pretreatment on chosen saccharides yield and cellulose structure from fast-growing poplar (Populus deltoides x maximowiczii) wood, Wood Science and Technology 2024, http://doi.org/10.1007/s00226024-01532-7

Tomás-Pejó E, Alvira P, Ballesteros M, Negro MJ (2011) Pretreatment technologies for lignocellulose to bioethanol conversion. In: Pandey A, Larroche Ch, Ricke SC, Dussap C-G, Gnansounou E (eds) Biofuels. Academic Press, Amsterdam, pp 149–176. https://doi.org/10.1016/B978-0-12-385099-7.00007-3

Trezza, L. Mahboob, A. Visibelli, M. Geminiani, A. Santucci (2025). Lignin Waste Valorization in the Bioeconomy Era: Toward Sustainable Innovation and Climate Resilience. Applied Sciences. 15(14):8038. https://doi.org/10.3390/app15148038

# Bio-Based Fire-Resistant Insulation Panels from Wood-Algae Residues for Multifunctional Building Applications

**Stephen O Amiandamhen[1], Ralf Rautenberger[2]**

[1]Department of Wood Technology, Norwegian Institute of Bioeconomy Research, Ås, Norway
stephen.amiandamhen@nibio.no
[2]Department of Biomarine Resource Valorisation, Norwegian Institute of Bioeconomy Research, Bodø, Norway
ralf.rautenberger@nibio.no

## Background

Wood-based insulation is an important renewable construction material, but its flammability remains a major limitation for wider use in building insulation. At the same time, increasing demand for circularity and resource efficiency creates opportunities to valorise secondary biomass streams, including residues from marine biomass processing. Previous observations showed that mixtures of wood and algae residues can exhibit enhanced fire resistance. However, the mechanisms responsible for this behaviour and the potential of combining these residues with cellulose nanofibrils (CNF) for multifunctional insulation materials remain insufficiently understood. This study investigates bio-based insulation panels produced from wood chips, CNF and algae processing residues. The objective was to understand the chemical, structural and thermochemical interactions within the algae–CNF system and evaluate their potential contribution to fire-resistant wood-based insulation panels. The approach provides a route for converting forest and marine biomass residues into higher-value construction products, supporting circular bioeconomy value chains and low-carbon building applications.

**Keywords:** Bio-based insulation; Marine biomass; Thermochemical interactions.

## Experimental

Algae, wood chips and CNF were locally sourced in Norway. Algae processing residues and CNF were combined in aqueous slurries at 10% solid content. Hybrid formulations were subsequently mixed with wood chips at a constant slurry-to-wood ratio and formed into panels before drying and conditioning. Chemical composition and interactions were investigated using ICP-OES and ATR-FTIR, while XRD, SEM-EDS and STA were used to examine structural, morphological and thermochemical behaviour. Panel properties were determined according to EN 310 (European Standard 1993) and compared against EN 622-4 requirements for general purpose and load bearing softboards (European Standard 2009). Sound absorption was measured according to ISO 10534-1, while reaction to fire was evaluated using a mass loss calorimeter according to ISO 5660-1.

## Results and Discussion

The enhanced fire resistance of the wood composite appears to originate from synergistic interactions between CNF and the mineral-rich algae residue. During slurry processing and drying, the algae components become integrated within the CNF network, forming a structured bio-inorganic matrix. The high concentrations of inorganics in the algae residue are believed to promote dehydration and carbonisation reactions during heating, favouring char formation over volatilisation (Fig. 1). SEM-EDS and ICP-OES analyses further support this interaction within the hybrid structure. The inorganic domains may act as local thermal barriers, thus stabilising the developing char layer. As a result, the hybrid composite exhibits greater resistance to thermal degradation than the individual components (Table 1).

Table 1. STA indicators for constituent and hybrid materials

| Material | Principal thermal features | Residual mass |
|---|---|---|
| Algae | Thermal events near 309, 485–538 and 778 °C | 55.09% stage 1; 22.5% final stage |
| CNF | DSC onset temperature at 310 °C; Final residual mass reported at 443.9 °C | 34.05% stage 1; −2.22% final stage |
| Algae–CNF hybrid | 33.72% first-stage loss at 296.7 °C; Later event at about 758.7 °C | 66.28% stage 1; 34.93% final stage |

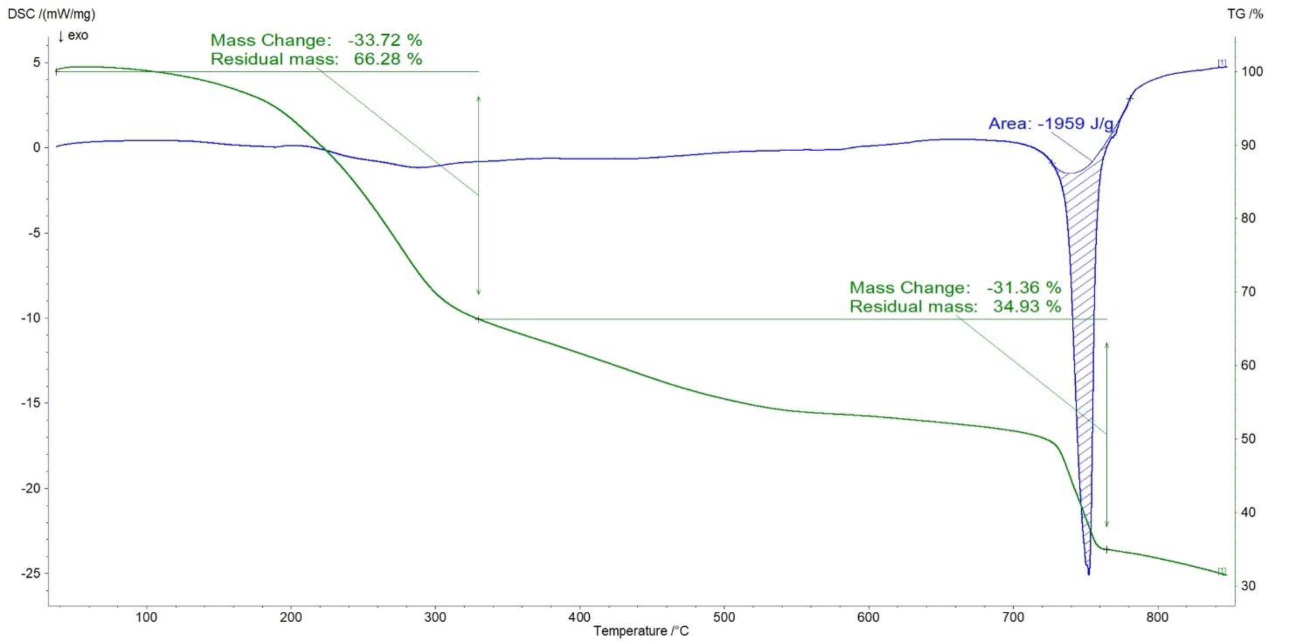


Figure 1. STA thermogram of the algae–CNF hybrid

## Conclusions

The developed bio-based insulation panels show promising potential for multifunctional building applications. The study demonstrates that the interaction of algae and CNF contributes to structural and thermochemical changes associated with enhanced char formation and fire resistance. Combined with the mechanical and acoustic properties of the porous wood-based composite, these findings support the development of lightweight, circular insulation materials from forest and marine biomass residues.

**References**

European Standard. 1993. Wood-Based Panels - Determination of Modulus of Elasticity in Bending and of Bending Strength. EN-310. London.

European Standard. 2009. Fibreboards - Specifications. Part 4: Requirements for Softboards. EN 622. 4. Brussels.

## *WSE Network*

The Northern European Network for Wood Science and Engineering started in 2004. After 21 successful meetings in 10 different partner countries, WSE has become a well-established platform for researchers from various fields of wood science and engineering. To sign up to the network's mailing list, go to this page. This network is supported by SNS Nordic Forest Research funded by the Nordic Council of Ministers.

### List of WSE meetings:

| | |
|---|---|
| 2005 | Honne (Norway) |
| 2006 | Stockholm (Sweden) |
| 2007 | Helsinki (Finland) |
| 2008 | Riga (Latvia) |
| 2009 | Copenhagen (Denmark) |
| 2010 | Tallinn (Estonia) |
| 2011 | Oslo (Norway) |
| 2012 | Kaunas (Lithuania) |
| 2013 | Hanover (Germany) |
| 2014 | Edinburgh (United Kingdom) |
| 2015 | Poznan (Poland) |
| 2016 | Riga (Latvia) |
| 2017 | Copenhagen (Denmark) |
| 2018 | Tallinn (Estonia) |
| 2019 | Lund (Sweden) |
| 2020 | Helsinki (Finland) |
| 2021 | Kaunas (Lithuania) |
| 2022 | Goettingen (Germany) |
| 2023 | Oslo (Norway) |
| 2024 | Edinburgh (Scotland) |
| 2025 | Växjö (Sweden) |
| 2026 | Riga (Latvia) |

# THANK YOU

LATVIAN STATE INSTITUTE OF WOOD CHEMISTRY

RTU

SNS Nordic Forest Research

Nordic Council of Ministers

Latvijas Finieris

ZAZA TIMBER

arxada

RIGA

KOPPERS

Latvijas koks